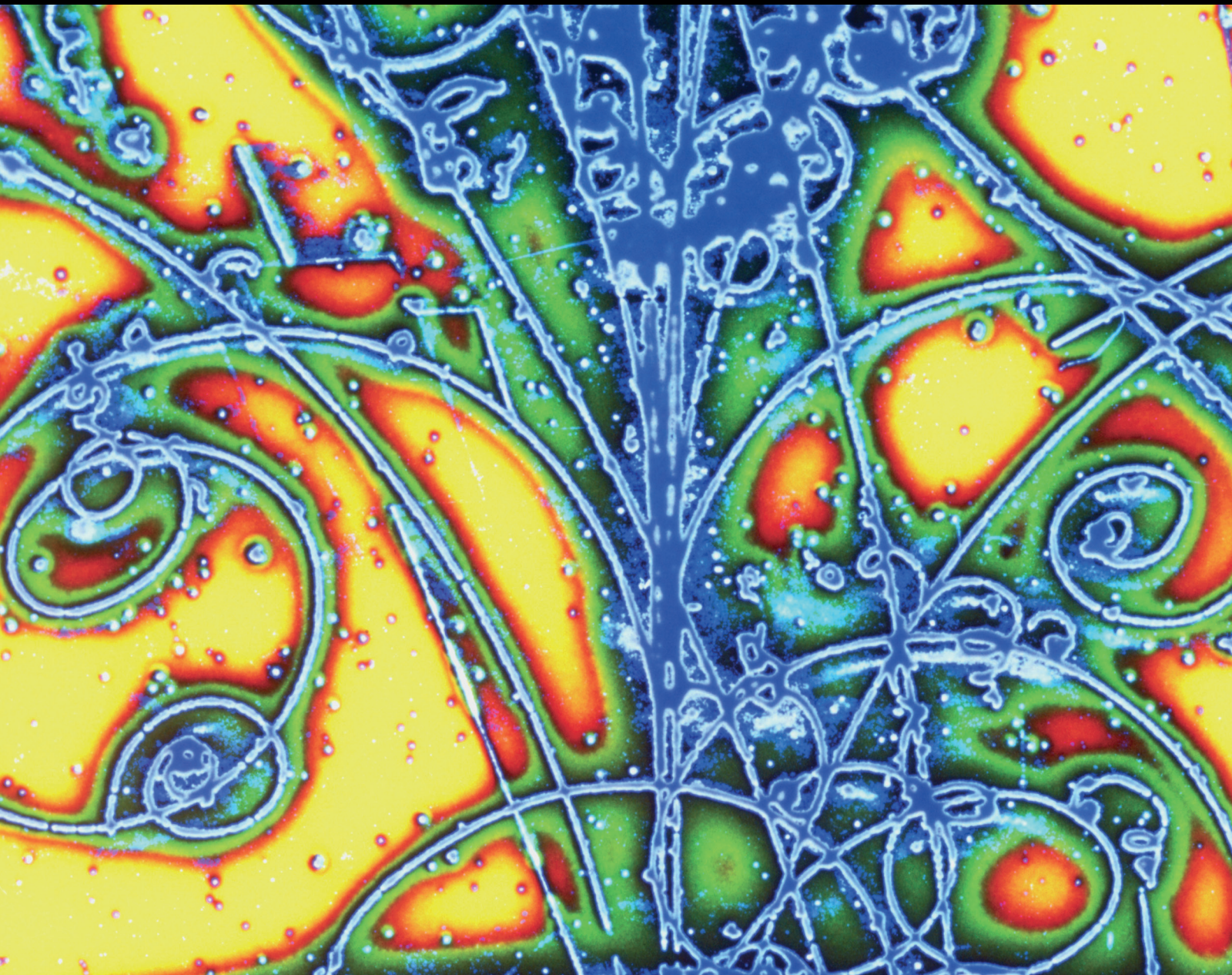# Perspectives on Decay and Time Evolution of Metastable States: From Particle Physics to Cosmology

Lead Guest Editor: Krzysztof Urbanowski
Guest Editors: Neelima G. Kelkar, Marek Nowakowski, and Marek Szydlowski

Perspectives on Decay and Time Evolution of Metastable States: From Particle Physics to Cosmology

Perspectives on Decay and Time Evolution of Metastable States: From Particle Physics to Cosmology

Lead Guest Editor: Krzysztof Urbanowski
Guest Editors: Neelima G. Kelkar, Marek Nowakowski, and Marek Szydlowski

Contents

Editorial

Perspectives on Decay and Time Evolution of Metastable States: From Particle Physics to Cosmology

K. Urbanowski [1], **N. G. Kelkar** [2], **M. Nowakowski** [2], **and M. Szydłowski** [3]

[1] *Institute of Physics, University of Zielona Góra, Prof. Z. Szafrana 4a, 65-516 Zielona Góra, Poland*
[2] *Departamento de Fisica, Universidad de los Andes, Cra 1E, 18A-10, Bogotá, Colombia*
[3] *Astronomical Observatory, Jagiellonian University, Orla 171, 30-244 Kraków, Poland*

Correspondence should be addressed to K. Urbanowski; k.urbanowski@if.uz.zgora.pl

Many, if not most of the quantum states which constitute the building blocks of nature, are unstable and decay spontaneously. As such they require a special treatment in quantum mechanics which displays new effects as compared to a classical theory. Examples of such unstable states can be found in the Standard Model of particle theory including quarks, heavy gauge bosons, leptons heavier than the electron, baryons heavier than the proton, and all mesons made up from a quark and an antiquark. In nuclear physics the word "radioactivity" is a synonym for the instability of the nuclei which either de-excite emitting a photon, decay via a cluster emission (of which the alpha decay is the most famous and the best studied example of a quantum tunneling process) or undergo the weak transition known as beta decay or inverse beta decay. In atomic physics, excited states are indeed considered as unstable and in a similar way we could treat excited molecules. Finally, the whole universe can tunnel from a false vacuum into a lower lying energy state which from the point of view of quantum mechanics is understood as a spontaneous decay. Indeed, in quantum mechanics a decay process is quite natural as any state will decay unless we have a conservation law (symmetry) which forbids it. Quantum mechanics allows also a unified treatment of the spontaneous decay which can be applied to all unstable states and exhibits new phenomena ("new" as compared to the classical "exponential decay") at short and large times. At small times the exponential decay law is replaced by a power law and is closely related to the Zeno and anti-Zeno

effect which loosely speaking states that "watched states decay differently," a fact which can be even applied in cosmology. This behavior is followed by the exponential decay law. At large times, the latter again gets replaced by a new power law preceded by a transition region in which the survival probability can grow locally. This also finds applications in cosmology. The deviations from the exponential decay are a genuine quantum effect.

The ramifications of the spontaneous decay process in understanding nature and its applications are widely spread. It is the photon emission of excited atoms which gives information of the matter far away from our sun. It is the beta decay which plays a decisive role in the nucleosynthesis of elements heavier than iron. It is the alpha decay of thorium and uranium which in part heats up the inner core of the earth, making it fluid, allowing for the continental drift and the magnetic field. It is the inverse beta decay supplying us with the positron needed in medical tomography whose one version relies on the decay of the positronium.

The present special issue consists of articles which deal with instability from a scale as small as that of elementary particles to that of the universe itself. On the way, the authors discover interesting phenomena related to the effects of relativity, violation of symmetries, and the bizarre behaviour of the universe under certain conditions. Chen and Wang, for example, consider the tunneling of the universe within the scenario of an inhomogeneous quantum vacuum and, calculating the tunneling amplitude of the universe from nothing,

they find that the inhomogeneity leads to a faster tunneling. In contrast to this approach which uses the Friedmann-Lemaitre-Robertson-Walker metric, M. Gogberashvili considers a different approach using Einstein's static universe metric and investigates the effects of the strong static gravitational field. A. Stachowski et al. bring in a new player, the metastable dark energy, in the investigation of the evolution of the universe. G. J. M. Zilioti et al. attempt to resolve some cosmological puzzles within decaying vacuum models. A completely different approach using concepts from statistical physics is introduced by Z. Haba to study the evolution of the expanding universe. Going over to smaller scales, the paper by T. V. Obikhod and I. A. Petrenko studies the properties of new particles predicted by the theories of extra dimensions. The survival probabilities of moving unstable particles are considered by E. V. Stefanovich, F. Giraldi, and F. Giacosa in three different papers. The feasibility of testing the time reversal symmetry in a purely leptonic system is reported by the Jagellonian-PET team from their pilot measurement involving the three photon decay of a positronium atom. Finally, the probability distribution of tunneling times of particles in connection with the recent laser induced tunnel ionization experiments is presented by J. T. Lunardi and L. A. Manzoni.

Conflicts of Interest

The editors declare that there are no conflicts of interest regarding the publication of this special issue.

K. Urbanowski
N. G. Kelkar
M. Nowakowski
M. Szydłowski

Research Article

Feasibility Study of the Time Reversal Symmetry Tests in Decay of Metastable Positronium Atoms with the J-PET Detector

**A. Gajos [ID],[1] C. Curceanu,[2] E. Czerwiński,[1] K. Dulski,[1] M. Gorgol,[3]
N. Gupta-Sharma,[1] B. C. Hiesmayr,[4] B. Jasińska,[3] K. Kacprzak,[1] Ł. Kapłon,[1,5]
D. Kisielewska,[1] G. Korcyl,[1] P. Kowalski,[6] T. Kozik,[1] W. Krzemień,[7] E. Kubicz,[1]
M. Mohammed,[1,8] Sz. Niedźwiecki,[1] M. Pałka,[1] M. Pawlik-Niedźwiecka,[1] L. Raczyński,[6]
J. Raj,[1] Z. Rudy,[1] S. Sharma,[1] Shivani,[1] R. Shopa,[6] M. Silarski,[1] M. Skurzok,[1]
W. Wiślicki,[6] B. Zgardzińska,[3] M. Zieliński,[1] and P. Moskal[1]**

[1]*Faculty of Physics, Astronomy and Applied Computer Science, Jagiellonian University, 30-348 Cracow, Poland*
[2]*INFN, Laboratori Nazionali di Frascati, 00044 Frascati, Italy*
[3]*Department of Nuclear Methods, Institute of Physics, Maria Curie-Skłodowska University, 20-031 Lublin, Poland*
[4]*Faculty of Physics, University of Vienna, 1090 Vienna, Austria*
[5]*Institute of Metallurgy and Materials Science of Polish Academy of Sciences, Cracow, Poland*
[6]*Świerk Department of Complex Systems, National Centre for Nuclear Research, 05-400 Otwock-Świerk, Poland*
[7]*High Energy Department, National Centre for Nuclear Research, 05-400 Otwock-Świerk, Poland*
[8]*Department of Physics, College of Education for Pure Sciences, University of Mosul, Mosul, Iraq*

Correspondence should be addressed to A. Gajos; aleksander.gajos@uj.edu.pl

This article reports on the feasibility of testing of the symmetry under reversal in time in a purely leptonic system constituted by positronium atoms using the J-PET detector. The present state of $\mathcal{T}$ symmetry tests is discussed with an emphasis on the scarcely explored sector of leptonic systems. Two possible strategies of searching for manifestations of $\mathcal{T}$ violation in nonvanishing angular correlations of final state observables in the decay of metastable triplet states of positronium available with J-PET are proposed and discussed. Results of a pilot measurement with J-PET and assessment of its performance in reconstruction of three-photon decays are shown along with an analysis of its impact on the sensitivity of the detector for the determination of $\mathcal{T}$-violation sensitive observables.

1. Introduction

The concept of symmetry of Nature under discrete transformations has been exposed to numerous experimental tests ever since its introduction by E. Wigner in 1931 [1]. The first evidence of violation of the supposed symmetries under spatial ($\mathcal{P}$) and charge ($\mathcal{C}$) parity transformations in the weak interactions has been found already in 1956 and 1958, respectively [2, 3]. However, observation of noninvariance of a physical system under reversal in time required over 50 years more and was finally performed in the system of entangled neutral B mesons in 2012 [4]. Although many experiments proved violation of the combined $\mathcal{CP}$ symmetry, leading to $\mathcal{T}$ violation expected on the ground of the $\mathcal{CPT}$ theorem, experimental evidence for noninvariance under time reversal remains scarce to date.

The Jagiellonian PET (J-PET) experiment aims at performing a test of the symmetry under reversal in time

in a purely leptonic system constituted by orthopositronium (o-Ps) with a precision unprecedented in this sector. The increased sensitivity of J-PET with respect to previous discrete symmetry tests with o-Ps⟶3γ is achieved by a large geometrical acceptance and angular resolution of the detector as well as by improved control of the positronium atoms polarization. In this work, we report on the results of feasibility studies for the planned $\mathscr{T}$ violation searches by determination of angular correlations in the o-Ps⟶3γ decay based on a test run of the J-PET detector.

This article is structured as follows: next section briefly discusses the properties of time and time reversal in quantum systems. Subsequently, Section 3 provides an overview of the present status and available techniques of testing of the symmetry under reversal in time and points out the goals of the J-PET experiment in this field. A brief description of the detector and details of the setup used for a test measurement are given in Section 4. Section 5 discusses possible strategies to test the time reversal symmetry with J-PET. Results of the feasibility studies are presented in Section 6 and their impact on the perspectives for a $\mathscr{T}$ test with J-PET is discussed in Section 7.

2. Time and Reversal of Physical Systems in Time

Although the advent of special relativity made it common equate time with spatial coordinates, time remains a distinct concept. Its treatment as an external parameter used in classical mechanics still cannot be consistently avoided in today's quantum theories [5]. As opposed to position and momentum, time lacks a corresponding operator in standard quantum mechanics and thus, countering the intuition, cannot be an observable. Moreover, a careful insight into the time evolution of unstable quantum systems reveals a number of surprising phenomena such as deviations from exponential decay law [6, 7] or emission of electromagnetic radiation at late times [8]. The decay process, inevitably involved in measurements of unstable systems is also a factor restricting possible studies of the symmetry under time reversal [9].

While efforts are taken to define a time operator, observation of $\mathscr{CP}$ violation in the decaying meson systems disproves certain approaches [10]. Alternatively, concepts of time intervals not defined through an external parameter may be considered using tunneling and dwell times [11, 12]. However, also in this case invariance under time reversal is an important factor [13].

It is important to stress that all considerations made herein are only valid if gravitational effects are not considered. In the framework of general relativity with a generic curved spacetime, the concept of inversion of time (as well as the $\mathscr{P}$ transformation) loses its interpretation specific only to the linear affine structure of spacetime [14].

The peculiar properties of time extend as well to the operation of reversing physical systems in time (the T operator), which results in grave experimental challenges limiting the possibilities of $\mathscr{T}$ violation measurements. In contrast to the unitary P and C operators, T can be shown to be antiunitary. As a consequence, no conserved quantities may be attributed to the T operation [15] excluding symmetry tests by means of, e.g., testing selection rules.

Feasibility of $\mathscr{T}$ tests based on a comparison between time evolution of a physical system in two directions, i.e., $|\psi(t)\rangle \longrightarrow |\psi(t + \delta t)\rangle$ and $|\psi(t + \delta t)\rangle \longrightarrow |\psi(t)\rangle$, is also limited as most of the processes which could be used involve a decaying state making it impractical to obtain a reverse process with the same conditions in an experiment. The only exception exploited to date is constituted by transitions of neutral mesons between their flavour-definite states and CP eigenstates [16, 17]. A comparison of such reversible transitions in a neutral B meson system with quantum entanglement of $B^0\overline{B^0}$ pairs produced in a decay of $\Upsilon(4s)$ yielded the only direct experimental evidence of violation of the symmetry under reversal in time obtained to date [4]. While a similar concept of $\mathscr{T}$ violation searches is currently pursued with the neutral kaon system [17–19], no direct tests of this symmetry have been proposed outside the systems of neutral mesons.

In the absence of conserved quantities and with the difficulties of comparing mutually reverse time evolution processes in decaying systems, manifestations of $\mathscr{T}$ violation may still be sought in nonvanishing expectation values of certain operators odd under the T transformation [20]. It follows from the antiunitarity of the T operator that for any operator $\mathscr{O}$

$$\langle\phi|\mathscr{O}|\psi\rangle = \langle\phi|T^\dagger T\mathscr{O}T^\dagger T|\psi\rangle = \langle\phi_T|\mathscr{O}_T|\psi_T\rangle^*, \quad (1)$$

where the T subscript denotes states and operators transformed by the operator of reversal in time. Therefore, an operator odd with respect to the T transformation (i.e., $\mathscr{O}_T = -\mathscr{O}$) must satisfy

$$\langle\phi|O|\psi\rangle = -\langle\phi_T|O|\psi_T\rangle^*. \quad (2)$$

For stationary states or in systems where conditions on interaction dynamics such as absence of significant final state interactions are satisfied [21], the mean value of a T-odd and Hermitian operator must therefore vanish in case of $\mathscr{T}$ invariance:

$$\langle O\rangle_T = -\langle O\rangle, \quad (3)$$

and violation of the $\mathscr{T}$ symmetry may thus be manifested as a nonzero expectation value of such an operator.

3. Status and Strategies of $\mathscr{T}$ Symmetry Testing

A number of experiments based on the property of T operator demonstrated in (1)-(3) have been conducted to date. The electric dipole moment of elementary systems, constituting a convenient T-odd operator, has been sought for neutrons and electrons in experiments reaching a precision of 10^{-26} and 10^{-28}, respectively [22, 23]. However, none of such

experiments has observed $\mathscr{T}$ violation to date despite their excellent sensitivity. In another class of experiments, a T-odd operator is constructed out of final state observables in a decay process, such as the weak decay $K^+ \longrightarrow \pi^0 \mu^+ \nu$ studied by the KEK-E246 experiment [24] in which the muon polarization transverse to the decay plane ($\mathscr{P}_T = \mathscr{P}_K \cdot (\mathbf{p}_\pi \times \mathbf{p}_\mu)/|\mathbf{p}_\pi \times \mathbf{p}_\mu|$) was determined as an observable whose nonzero mean value would manifest $\mathscr{T}$ violation. However, neither this measurement nor similar studies using decay of polarized ^{8}Li nuclei [25] and of free neutrons [26] have observed significant mean values of T-odd final state observables.

Notably, although the property of reversal in time shown in (1)-(3) is not limited to any particular system nor interaction, it has been mostly exploited to test the $\mathscr{T}$ symmetry in weak interactions. Whereas the latter is the most promising candidate due to well proven $\mathscr{CP}$ violation, evidence for $\mathscr{T}$ noninvariance may be sought in other physical systems and phenomena using the same scheme of a symmetry test. Systems constituted by purely leptonic matter are an example of a sector where experimental results related to the time reversal symmetry—and to discrete symmetries in general—remain rare. Several measurements of neutrino oscillations are being conducted by the NOνA and T2K experiments searching for $\mathscr{CP}$ violation in the $\nu_\mu \longrightarrow \nu_e$ and $\overline{\nu}_\mu \longrightarrow \overline{\nu}_e$ channels [27, 28], which may provide indirect information on the $\mathscr{T}$ symmetry. Another notable test of discrete symmetries in the leptonic sector is the search for the violation of Lorentz and $\mathscr{CPT}$ invariance based on the Standard Model Extension framework [29] and anti-CPT theorem [30] which has also been performed by T2K [31, 32]. Other possible tests of these symmetries with the positronium system include spectroscopy of the 1S-2S transition [33] and measuring the free fall acceleration of positronium [34]. However, the question of the $\mathscr{T}$, $\mathscr{CP}$, and $\mathscr{CPT}$ symmetries in the leptonic systems remains open as the aforementioned experiments have not observed a significant signal of a violation.

Few systems exist which allow for discrete symmetry tests in a purely leptonic sector. However, a candidate competitive with respect to neutrino oscillations is constituted by the electromagnetic decay of positronium atoms, exotic bound states of an electron and a positron. With a reduced mass only twice smaller than that of a hydrogen atom, positronium is characterized by a similar energy level structure. At the same time, it is a metastable state with a lifetime strongly dependent on the spin configuration. The singlet state referred to as parapositronium, may only decay into an even number of photons due to charge parity conservation, and has a lifetime (in vacuum) of 0.125 ns. The triplet state (orthopositronium, o-Ps) is limited to decay into an odd number of photons and lives in vacuum over three orders of magnitude longer than the singlet state ($\tau_{o-Ps} = 142$ ns) [35–37].

Being an eigenstate of the parity operator alike atoms, positronium is also characterized by symmetry under charge conjugation typical for particle-antiparticle systems. Positronium atoms are thus a useful system for discrete symmetry studies. Moreover, they may be copiously produced in

laboratory conditions using typical sources of β^+ radiation [38], giving positronium-based experiments a technical advantage over those using, e.g., aforementioned neutrino oscillations. However, few results on the discrete symmetries in the positronium system have been reported to date. The most precise measurements studied the angular correlation operators in the decay of orthopositronium states into three photons and determined mean values of final state operators odd under the $\mathscr{CP}$ and $\mathscr{CPT}$ conjugations, finding no violation signal at the sensitivity level of 10^{-3} [39, 40]. Although the aforementioned studies sought for violation of $\mathscr{CP}$ and $\mathscr{CPT}$, it should be emphasized that the operators used therein were odd under the T operation as well, leading to an implicit probe also for the symmetry under reversal in time.

The results obtained to date, showing no sign of violation, were limited in precision by technical factors such as detector geometrical acceptance and resolution, uncertainty of positronium polarization, and data sample size. In terms of physical restrictions, sensitivity of such discrete symmetry tests with orthopositronium decay is only limited by possible false asymmetries arising from photon-photon final state interactions at the precision level of 10^{-9} [41, 42]. The J-PET experiment thus sets its goal to explore the $\mathscr{T}$-violating observables at precision beyond the presently established 10^{-3} level [43].

4. The J-PET Detector

The J-PET (Jagiellonian Positron Emission Tomograph) is a photon detector constructed entirely with plastic scintillators. Along with constituting the first prototype of plastic scintillator-based cost-effective PET scanner with a large field of view [44, 45], it may be used to detect photons in the sub-MeV range such as products of annihilation of positronium atoms, thus allowing for a range of studies related to discrete symmetries and quantum entanglement [43].

J-PET consists of three concentric cylindrical layers of axially arranged γ detection modules based on strips of EJ-230 plastic scintillator as shown schematically in Figure 1. Each scintillator strip is 50 cm long with a rectangular cross-section of 7×19 mm^2. Within a detection module, both ends of a scintillator strip are optically coupled to photomultiplier tubes. Due to low atomic number of the elements constituting plastic scintillators, γ quanta interact mostly through Compton scattering in the strips, depositing a part of their energy dependent on the scattering angle. The lack of exact photon energy determination in J-PET is compensated by fast decay time of plastic scintillators resulting in high time resolution and allowing for use of radioactive sources with activity as high as 10 MBq. The energy deposited by photons scattered in a scintillator is converted to optical photons which travel to both ends of a strip undergoing multiple internal reflections. Consequently, the position of γ interaction along a detection module is determined using the difference between effective light propagation times to the two photomultiplier tubes
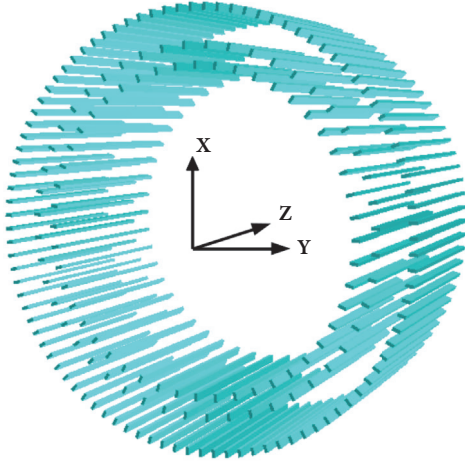
FIGURE 1: Schematic view of the J-PET detector consisting of 192 plastic scintillator strips arranged in three concentric layers with radii ranging from 42.5 cm to 57.5 cm. The strips are oriented along the Z axis of the detector barrel.

FIGURE 2: Vectors describing the final state of an o-Ps⟶3γ annihilation in the o-Ps frame of reference. $\vec{S}$ denotes orthopositronium spin and $\vec{k}_{1,2,3}$ are the momentum vectors of the annihilation photons, lying in a single plane. The operator defined in (4) is a measure of angular correlation between the positronium spin and the decay plane normal vector.

attached to a scintillator strip [46]. In the transverse plane of the detector, γ interactions are localized up to the position of a single module, resulting in an azimuthal angle resolution of about 1°.

Although the J-PET γ detection modules do not allow for a direct measurement of total photon energy, recording interactions of all photons from a 3γ annihilation allows for an indirect reconstruction of photons' momenta based on event geometry and 4-momentum conservation [47].

As J-PET is intended for a broad range of studies from medical imaging [48] through quantum entanglement [49, 50] to tests of discrete symmetries [43], its data acquisition is operating in a triggerless mode [51] in order to avoid any bias in the recorded sample of events. Electric signals produced by the photomultipliers are sampled in the time domain at four predefined voltage thresholds allowing for an estimation of the deposited energy using the time over threshold technique [52]. Further reconstruction of photon interactions as well as data preselection and handling is performed with dedicated software [53, 54]. Several extensions of the detector are presently in preparation such as improvements of the J-PET geometrical acceptance by inclusion of additional detector layers [47] as well as enhanced scintillator readout with silicon photomultipliers [55] and new front-end electronics [52].

5. Discrete Symmetry Tests with the J-PET Detector

5.1. Measurements Involving Orthopositronium Spin. The symmetry under reversal in time can be put to test in the o-Ps⟶3γ decay by using the properties of T conjugation demonstrated by (1)-(3). Spin $\vec{S}$ of the decaying orthopositronium atom and momenta of the three photons produced

in the decay $\vec{k}_{1,2,3}$ (ordered according to their descending magnitude, i.e., $|\vec{k}_1| > |\vec{k}_2| > |\vec{k}_3|$) allow for construction of an angular correlation operator odd under reversal in time:

$$C_T = \vec{S} \cdot \left(\vec{k}_1 \times \vec{k}_2 \right), \qquad (4)$$

which corresponds to an angular correlation between the positronium spin direction and the decay plane as illustrated in Figure 2.

Such an approach which requires estimation of the spin direction of decaying positronia was used by both previous discrete symmetry tests conducted with orthopositronium decay [39, 40]. These two experiments, however, adopted different techniques to control the o-Ps spin polarization. In the $\mathscr{CP}$ violation search, positronium atoms were produced in strong external magnetic field resulting in their polarization along a thus imposed direction [39]. A setup required to provide the magnetic field, however, was associated with a limitation of the geometrical acceptance of the detectors used. The second measurement, testing the $\mathscr{CPT}$ symmetry using the Gammasphere detector which covered almost a full solid angle, did not therefore rely on external magnetic field. Instead, positronium polarization was evaluated statistically by allowing for o-Ps atoms formation only in a single hemisphere around a point-like positron source, resulting in estimation of the polarization along a fixed quantization axis with an accuracy limited by a geometrical factor of 0.5 [40]. Neither of the previous experiments attempted to reconstruct the position of o-Ps⟶3γ decay, instead limiting the volume of o-Ps creation and assuming the same origin point for all annihilations.

The J-PET experiment attempts to improve on the latter approach which does not require the use of external magnetic field. The statistical knowledge of spin polarization of the positrons forming o-Ps atoms can be significantly increased with a positronium production setup depicted in Figure 3, where polarization is estimated on an event-by-event basis instead of assuming a fixed quantization axis throughout the measurement. A trilateration-based technique of recon-
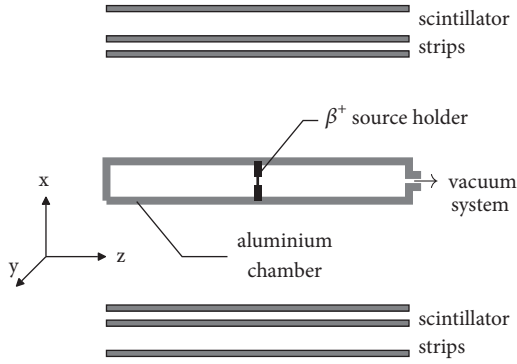
FIGURE 3: Scheme of the positronium production setup devised for positron polarization determination in J-PET experiment. Positrons are produced in a β^+ source mounted in the center of a cylindrical vacuum chamber coaxial with the detector. Positronium atoms are formed by the interaction of positrons in a porous medium covering the chamber walls. Determination of an o-Ps⟶3γ annihilation position in the cylinder provides an estimate of positron momentum direction.

FIGURE 4: Determination of positron polarization axis using its momentum direction (black arrow) estimated using the β^+ source position and reconstructed origin of the 3γ annihilation of orthopositronium in the chamber wall (dark gray band). The shaded region represents the angular uncertainty of positron flight direction resulting from achievable resolution of the 3γ annihilation point.
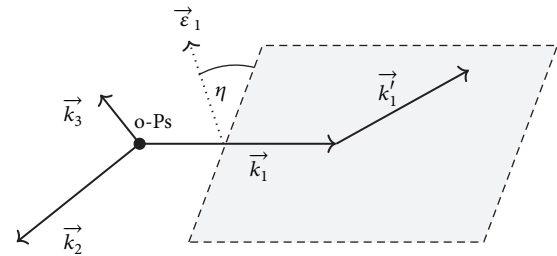
FIGURE 5: Scheme of estimation of polarization vector for a photon produced in o-Ps⟶3γ at J-PET. Photon of momentum $\vec{k}_1$ is scattered in one of the detection modules and a secondary interaction of the scattering product $\vec{k}'_1$ is recorded in a different scintillator strip. The most probable angle η between the polarization vector $\vec{\varepsilon}_1$ and the scattering plane spanned by $\vec{k}_1$ and $\vec{k}'_1$ amounts to 90°.

structing the position of o-Ps⟶3γ decay created for J-PET allows for estimation of the direction of positron propagation in a single event with a vector spanned by a point-like β^+ source location and the reconstructed orthopositronium annihilation point [56].

The dependence of average spin polarization of positrons (largely preserved during formation of orthopositronium [57]) on the angular accuracy of the polarization axis determination is given by $(1/2)(1 + \cos \alpha)$ where α is the opening angle of a cone representing the uncertainty of polarization axis direction [58]. This uncertainty in J-PET results predominantly from the resolution of determination of the 3γ annihilation point as depicted in Figure 4 and amounts to about 15° [56], resulting in a polarization decrease smaller than 2%. By contrast, in the previous measurement with Gammasphere [40] where the polarization axis was fixed, the same geometrical factor accounted for a 50% polarization loss.

5.2. Measurements Using Polarization of Photons. The scheme of measurement without external magnetic field for positronium polarization may be further simplified with modified choice of the measured T-odd operator. This novel approach of testing the $\mathscr{T}$ symmetry may be pursued by J-PET with a spin-independent operator constructed for the o-Ps⟶3γ annihilations if the polarization vector of one of the final state photons is included [43]:

$$C'_T = \vec{k}_2 \cdot \vec{\varepsilon}_1, \tag{5}$$

where $\vec{\varepsilon}_1$ denotes the electric polarization vector of the most energetic γ quantum and $\vec{k}_2$ is the momentum of the second most energetic one. Such angular correlation operators involving photon electric polarization have never been studied in the decay of orthopositronium. Geometry of

the J-PET detector enables a measurement of $\langle C'_T \rangle$ thanks to the ability to record secondary interactions of once scattered photons from the o-Ps⟶3γ annihilation as depicted in Figure 5.

6. Test Measurement with the J-PET Detector

The setup presented in Figure 3 was constructed and fully commissioned in 2017 [59]. One of the first test measurements was dedicated to evaluation of the feasibility of identification and reconstruction of three-photon events. A ^{22}Na β^+ source was mounted inside a cylindrical vacuum chamber of 14 cm radius. The positronium formation-enhancing medium, presently under elaboration, was not included in the measurement. Therefore, the test of 3γ event reconstruction was based on direct 3γ annihilation of positrons with electrons of the aluminium chamber walls, with a yield smaller by more than an order of magnitude than the rate of o-Ps⟶3γ annihilations expected in the
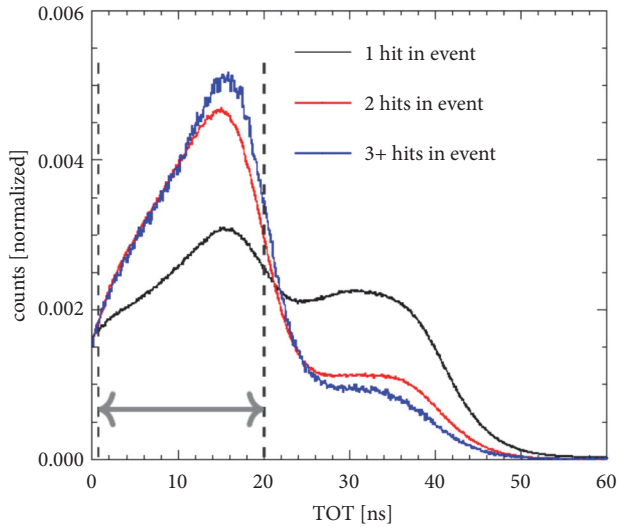
FIGURE 6: Distributions of time over threshold (TOT) values, for γ interactions observed in groups of 1, 2 and more within a coincidence time window of 2.5 ns. In the samples with increasing number of coincident photons, the contribution of γ quanta from 3γ annihilations increases with respect to other processes. Gray lines and arrow denote the region used to identify 3γ annihilation photon candidates.

final measurements with a porous medium for positronium production.

The capabilities of J-PET to select 3γ events and discriminate background arising from two-photon e^+e^- annihilations as well as from accidental coincidences are based primarily on two factors:

(i) a measure of energy deposited by a photon in Compton scattering, provided by the time over threshold (TOT) values determined by the J-PET front-end electronics,

(ii) angular dependencies between relative azimuthal angles of recorded γ interaction points, specific to topology of the event [60].

Distributions of the TOT values, after equalization of responses of each detection module, are presented in Figure 6. Separate study of TOT distributions for γ quanta observed in groups of 1, 2 and more recorded γ hits in scintillators within a short time window reveals the different composition of photons from 3γ annihilations with respect to those originating from background processes such as deexcitation of the β^+ decay products from a ^{22}Na source (1270 keV) and cosmic radiation. Two Compton edges corresponding to 511 keV and 1270 keV photons are clearly discernible in TOT distributions, allowing identifying candidates for interactions of 3γ annihilation products by TOT values located below the 511 keV Compton edge as marked with dashed lines in Figure 6.

The second event selection criterion is based on the correlations between relative azimuthal angles of photon interactions recorded in the detector in cases of three interactions observed in close time coincidence. The tests performed with Monte Carlo simulations have shown that annihilations into two and three photons can be well separated using such correlations [60]. An exemplary relative distribution of values constructed using these correlations, obtained with the test measurement, is presented in Figure 7(a). For a comparison, the same distribution obtained with a point-like annihilation medium used in another test measurement of J-PET is presented in Figure 7(b).

A sharp vertical band at $\delta\theta_2 + \delta\theta_3 \approx 180°$ seen in Figure 7(b) originates from events corresponding to annihilations into two back-to-back photons. Broadening of this 2γ band in case of the extensive chamber is a result of the increased discrepancy between relative azimuthal angles of detection module locations used for the calculation and the actual relative angles in events originating in the walls of the cylindrical chamber as depicted schematically in Figure 8.

The distributions presented in Figure 7 are in good agreement with the simulation-based expectations [60]. Selection of events with values of $\delta\theta_2 + \delta\theta_3$ significantly larger than 180° allows for identification of three-photon annihilations.

The aforementioned event selection techniques allowed to extract 1164 3γ event candidates from the two-day test measurement with a β^+ source activity of about 10 MBq placed in the center of the aluminium cylinder as depicted in Figure 3. Therefore, a quantitative estimation of the achievable resolution of three-photon event origin points and its impact on the positronium polarization control capabilities requires a measurement including a medium enhancing the positronium production.

Resolution of the detector and its field of view was validated with a benchmark analysis of the test data performed using the abundant 2γ annihilation events. Figure 9 presents the images of the annihilation chamber obtained using 2γ events whose selection and reconstruction was performed with the same techniques as applied to medical imaging tests performed with J-PET [48]. Although a large part of recorded annihilations originate already in the setup holding the β^+ source, a considerable fraction of positrons reach the chamber walls. The effective longitudinal field of view of J-PET for 2γ events which can be directly extended to 3γ annihilations due to similar geometrical constraints spans the range of approximately $|z| < 8$ cm.

7. Summary and Perspectives

The J-PET group attempts to perform the first search for signs of violation of the symmetry under reversal in time in the decay of positronium atoms. One of the available techniques is based on evaluation of mean values of final state observables constructed from photons' momenta and positronium spin in an o-Ps$\longrightarrow 3\gamma$ annihilation with a precision enhanced with respect to the previous realization of similar measurements by determination of positronium spin distinctly for each recorded event. Moreover, the J-PET detector enables a novel test by determination of a T-odd

(a)

(b)
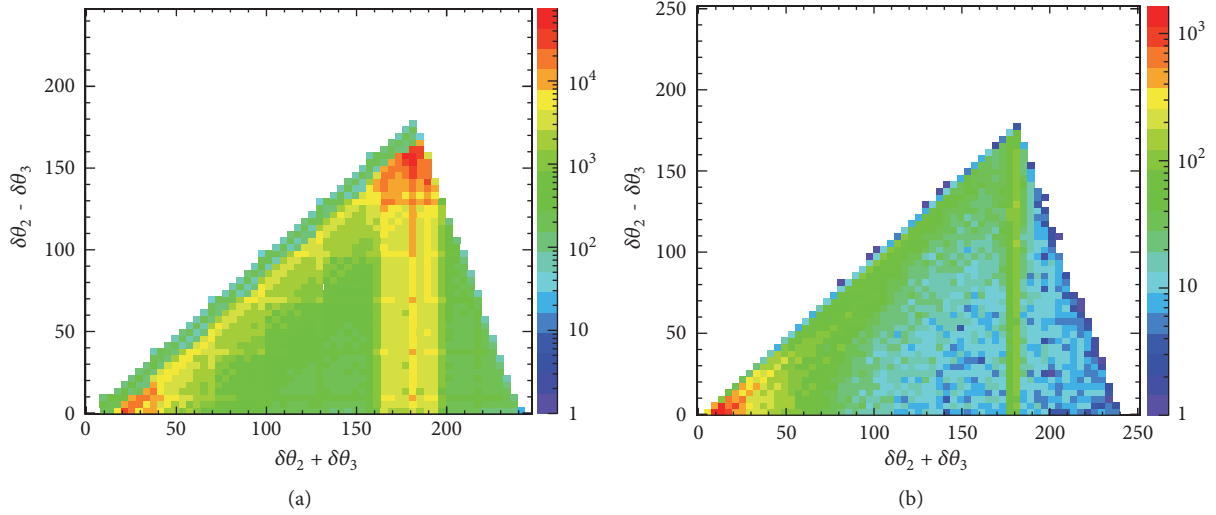
FIGURE 7: Relations between the sum and difference of two smallest relative azimuthal angles ($\delta\theta_2$ and $\delta\theta_3$, respectively) between γ interaction points in events with three recorded interactions. (a) Distribution obtained in the test measurement with the aluminium chamber presented in Figure 3. For reference, the same spectrum obtained with a point-like annihilation medium located in the detector center [59] is displayed in (b). The vertical band around $\delta\theta_2 + \delta\theta_3 \approx 180°$ arises from two-photon annihilations and is broadened in the first case due to extensive dimensions of the annihilation chamber used. 3γ annihilation events are expected in the region located at the right side of the 2γ band [60].
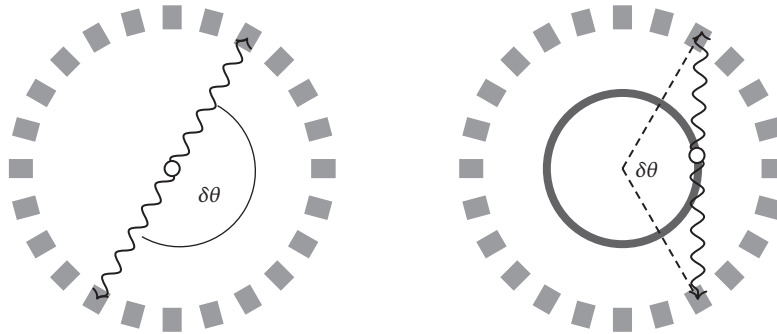
FIGURE 8: Explanation of the broadening of the 2γ annihilation band present in Figures 7(a) and 7(b) at $\delta\theta_2 + \delta\theta_3 \approx 180°$. Left: when 2γ annihilations originate in a small region in the detector center, the calculated relative azimuthal angles of detection modules which registered the photons correspond closely to actual relative angles between photons' momenta. Right: with 2γ annihilations taking place in the walls of an extensive-size annihilation chamber (gray band), the broadening of the band at $180°$ is caused by a discrepancy between the calculated and actual relative angles. The detector scheme and proportions are not preserved for clarity.

observable constructed using the momenta and polarization of photons from annihilation.

The pilot measurement conducted with the J-PET detector demonstrated the possibility of identifying candidates of annihilation photons interactions in the plastic scintillator strips by means of the time over threshold measure of deposited energy and angular dependencies between relative azimuthal angles of γ interaction points specific to event spatial topology. A preliminary selection of three-photon annihilation events yielded 1164 event candidates from a two-day test measurement with a yield reduced by more than an order of magnitude with respect to the planned experiments with a porous positronium production target and a centrally located 10 MBq source. The annihilation reconstruction resolution and performance of the setup

proposed for positron spin determination was validated with a benchmark reconstruction of two-photon annihilations. Results obtained from the test measurement confirm the feasibility of a test of symmetry under reversal in time by measurement of the angular correlation operator defined in (4) without external magnetic field once a positronium production medium is used.

Data Availability

As this article covers a feasibility study of time reversal symmetry tests with the J-PET detector in the view of the future measurements, the data with a physical relevance will only be collected in the future and the presently used data of a test measurement are mostly of technical importance only.

(a)

(b)
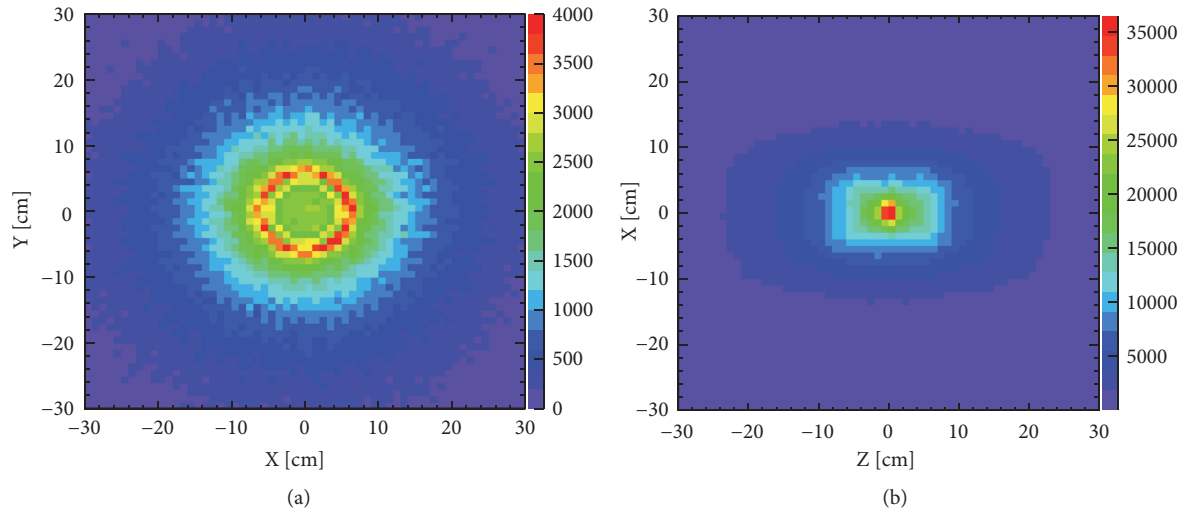
FIGURE 9: Tomographic images of the cylindrical chamber used in the test run of J-PET, obtained using reconstructed $e^+e^- \longrightarrow 2\gamma$ annihilation events. (a) Transverse view of the chamber (the central longitudinal region of $|z| < 4$ cm was excluded where the image is dominated by annihilation events originating in the setup of the β^+ source.). (b) Longitudinal view of the imaged chamber. In the central region, a strong image of the positron source and its mounting setup is visible.

Disclosure

Conflicts of Interest

The authors declare that there are no conflicts of interest regarding the publication of this paper.

Acknowledgments

References

[1] E. P. Wigner, *Group theory and its application to the quantum mechanics of atomic spectra*, Academic Press, New York, NY, USA, 1959.

[2] C. S. Wu, E. Ambler, R. W. Hayward, D. D. Hoppes, and R. P. Hudson, "Experimental test of parity conservation in beta decay," *Physical Review A: Atomic, Molecular and Optical Physics*, vol. 105, no. 4, pp. 1413–1415, 1957.

[3] P. C. Macq, K. M. Crowe, and R. P. Haddock, "Helicity of the electron and positron in muon decay," *Physical Review A: Atomic, Molecular and Optical Physics*, vol. 112, no. 6, pp. 2061–2071, 1958.

[4] J. P. Lees, V. Poireau, V. Tisserand et al., "Observation of Time Reversal Violation in the B0 Meson System," *Physical Review Letters*, vol. 109, p. 211801, 2012.

[5] J. G. Muga, R. Sala Mayato, and I. L. Egusquiza, *Time in Quantum Mechanics*, Springer-Verlag, Berlin, Germany, 2nd edition, 2008.

[6] K. Urbanowski, "Decay law of relativistic particles: quantum theory meets special relativity," *Physics Letters B*, vol. 737, pp. 346–351, 2014.

[7] F. Giacosa, "Time evolution of an unstable quantum system," *Acta Physica Polonica B*, vol. 48, no. 10, pp. 1831–1836, 2017.

[8] K. Urbanowski and K. Raczyńska, "Possible emission of cosmic X- and γ-rays by unstable particles at late times," *Physics Letters B*, vol. 731, pp. 236–241, 2014.

[9] J. Bernabeu and F. Martinez-Vidal, "Colloquium: Time-reversal violation with quantum-entangled B mesons," *Reviews of Modern Physics*, vol. 87, no. 1, pp. 165–182, 2015.

[10] T. Durt, A. Di Domenico, and B. Hiesmayr, *Falsification of a Time Operator Model based on Charge-Conjugation-Parity violation of neutral K-mesons*, 2015.

[11] N. G. Kelkar, "Electron tunneling times," *Acta Physica Polonica B*, vol. 48, no. 10, pp. 1825–1830, 2017.

[12] N. G. Kelkar, "Quantum Reflection and Dwell Times of Metastable States," *Physical Review Letters*, vol. 99, no. 21, 2007.

[13] N. G. Kelkar and M. Nowakowski, "Analysis of averaged multichannel delay times," *Physical Review A: Atomic, Molecular and Optical Physics*, vol. 78, no. 1, 2008.

[14] L. M. Sokołowski, "Discrete Lorentz symmetries in gravitational fields," *Acta Physica Polonica B*, vol. 48, no. 10, pp. 1947–1953, 2017.

[15] R. G. Sachs, *The physics of time reversal*, University of Chicago Press, Chicago, IL, USA, 1987.

[16] J. Bernabéu, F. Martínez-Vidal, and P. Villanueva-Pérez, "Time Reversal Violation from the entangled B0-B0 system," *Journal of High Energy Physics*, vol. 2012, no. 8, 2012.

[17] J. Bernabeu, A. Di Domenico, and P. Villanueva-Perez, "Direct test of time reversal symmetry in the entangled neutral kaon system at a ϕ-factory," *Nuclear Physics B*, vol. 868, no. 1, pp. 102–119, 2013.

[18] A. Gajos, "A direct test of *T* symmetry in the neutral K meson system at KLOE-2," *Journal of Physics: Conference Series*, vol. 631, p. 012018, 2015.

[19] A. Gajos, "Tests of discrete symmetries and quantum coherence with neutral kaons at the KLOE-2 experiment," *Acta Physica Polonica B*, vol. 48, no. 10, pp. 1975–1981, 2017.

[20] L. Wolfenstein, "The search for direct evidence for time reversal violation," *International Journal of Modern Physics E*, vol. 8, no. 6, pp. 501–511, 1999.

[21] H. E. Conzett, "Tests of time-reversal invariance in nuclear and particle physics," *Physical Review C: Nuclear Physics*, vol. 52, no. 2, pp. 1041–1046, 1995.

[22] J. M. Pendlebury, S. Afach, N. J. Ayres et al., "Revised experimental upper limit on the electric dipole moment of the neutron," *Physical Review D*, vol. 92, p. 092003, 2015.

[23] J. Baron, W. C. Campbell, and D. DeMille, "Order of magnitude smaller limit on the electric dipole moment of the electron," *Science*, vol. 343, no. 6168, pp. 269–272, 2014.

[24] M. Abe, M. Aoki, I. Ara et al., "Search for T-violating transverse muon polarization in the $K+\longrightarrow \pi 0\mu+\nu$ decay," *Physical Review Letters*, vol. D73, p. 072005, 2006.

[25] R. Huber, J. Lang, S. Navert et al., "Search for time-reversal violation in the β decay of polarized 8Li nuclei," *Physical Review Letters*, vol. 90, no. 20, p. 202301/4, 2003.

[26] A. Kozela, G. Ban, A. Białek et al., "Measurement of the transverse polarization of electrons emitted in free neutron decay," *Physical Review C nuclear physics*, vol. 85, no. 4, 2012.

[27] J. Bian, "The NOvA Experiment: Overview and Status," in *Proceedings of the Meeting of the APS Division of Particles and Fields (DPF 2013)*, Santa Cruz, Calif, USA, https://arxiv.org/abs/1309.7898.

[28] K. Abe, J. Amey, C. Andreopoulos et al., "T2K, Combined Analysis of Neutrino and Antineutrino Oscillations at T2K," *Physical Review Letters*, vol. 11, p. 151801, 2017.

[29] V. A. Kostelecký, "Formalism for CPT, T, and Lorentz violation in neutral meson oscillations," *Physical Review D: Particles, Fields, Gravitation and Cosmology*, vol. 64, no. 7, 2001.

[30] O. W. Greenberg, "CPT violation implies violation of Lorentz invariance," *Physical Review Letters*, vol. 89, no. 23, p. 231602/4, 2002.

[31] K. Abe, J. Amey, C. Andreopoulos et al., "Search for Lorentz and CPT violation using sidereal time dependence of neutrino flavor transitions over a short baseline," *Physical Review D*, vol. 95, p. 111101, 2017.

[32] V. A. Kostelecký and N. Russell, "Data tables for Lorentz and CPT violation," *Reviews of Modern Physics*, vol. 83, p. 11, 2011.

[33] K. Pachucki and S. G. Karshenboim, "Higher-order recoil corrections to energy levels of two-body systems," *Physical Review A: Atomic, Molecular and Optical Physics*, vol. 60, no. 4, pp. 2792–2798, 1999.

[34] V. A. Kostelecký and A. J. Vargas, "Lorentz and CPT tests with hydrogen, antihydrogen, and related systems," *Physical Review D: Particles, Fields, Gravitation and Cosmology*, vol. 92, no. 5, 2015.

[35] A. H. Al-Ramadhan and D. W. Gidley, "New precision measurement of the decay rate of singlet positronium," *Physical Review Letters*, vol. 72, no. 11, pp. 1632–1635, 1994.

[36] R. S. Vallery, P. W. Zitzewitz, and D. W. Gidley, "Resolution of the orthopositronium-lifetime puzzle," *Physical Review Letters*, vol. 90, no. 20, p. 203402/4, 2003.

[37] O. Jinnouchi, S. Asai, and T. Kobayashi, "Precision measurement of orthopositronium decay rate using SiO2 powder," *Physics Letters B*, vol. 572, no. 3-4, pp. 117–126, 2003.

[38] B. Jasińska, M. Gorgol, and M. Wiertel, "Determination of the 3γ fraction from positron annihilation in mesoporous materials for symmetry violation experiment with J-PET scanner," *Acta Physica Polonica B*, vol. 47, p. 453, 2016.

[39] T. Yamazaki, T. Namba, S. Asai, and T. Kobayashi, "Search for cp violation in positronium decay," *Physical Review Letters*, vol. 104, p. 083401, 2010.

[40] P. A. Vetter and S. J. Freedman, "Search for cpt-odd decays of positronium," *Physical Review Letters*, vol. 91, no. 26, p. 263401, 2003.

[41] B. K. Arbic, S. Hatamian, M. Skalsey, J. Van House, and W. Zheng, "Angular-correlation test of CPT in polarized positronium," *Physical Review A: Atomic, Molecular and Optical Physics*, vol. 37, no. 9, pp. 3189–3194, 1988.

[42] W. Bernreuther, U. Low, J. P. Ma, and O. Nachtmann, "How to Test CP, T and CPT Invariance in the Three Photon Decay of Polarized s Wave Triplet Positronium," *Zeitschrift für Physik C*, vol. 41, p. 143, 1988.

[43] P. Moskal, D. Alfs, T. Bednarski et al., "Potential of the J-PET detector for studies of discrete symmetries in decays of positronium atom - A purely leptonic system," *Acta Physica Polonica B*, vol. 47, no. 2, pp. 509–535, 2016.

[44] P. Moskal, *Strip device and the method for the determination of the place and response time of the gamma quanta and the application of the device for the positron emission thomography*, Patent number US2012112079, EP2454612, JP2012533734, 2010.

[45] S. Niedźwiecki, P. Białas, C. Curceanu et al., "J-PET: a new technology for the whole-body PET imaging," *Acta Physica Polonica A*, vol. 48, p. 1567, 2017.

[46] P. Moskal, S. Niedźwiecki, T. Bednarski et al., "Test of a single module of the J-PET scanner based on plastic scintillators," *Nuclear Instruments and Methods in Physics Research Section A: Accelerators, Spectrometers, Detectors and Associated Equipment*, vol. 764, pp. 317–321, 2014.

[47] D. Kamińska, A. Gajos, E. Czerwiński et al., "A feasibility study of ortho-positronium decays measurement with the J-PET scanner based on plastic scintillators," *The European Physical Journal C*, vol. 76, p. 445, 2016.

[48] M. Pawlik-Niedźwiecka, S. Niedźwiecki, D. Alfs et al., "Preliminary Studies of J-PET Detector Spatial Resolution," *Acta Physica Polonica A*, vol. 132, no. 5, pp. 1645–1649, 2017.

[49] B. C. Hiesmayr and P. Moskal, "Genuine Multipartite Entanglement in the 3-Photon Decay of Positronium," *Scientific Reports*, vol. 7, no. 1, 2017.

[50] M. Nowakowski and D. B. Fierro, "Three-photon entanglement from ortho-positronium revisited," *Acta Physica Polonica B*, vol. 48, no. 10, pp. 1955–1960, 2017.

[51] G. Korcyl, D. Alfs, T. Bednarski et al., "Sampling FEE and Trigger-less DAQ for the J-PET Scanner," *Acta Physica Polonica B*, vol. 47, no. 2, p. 491, 2016.

[52] M. Pałka, P. Strzempek, G. Korcyl et al., "Multichannel FPGA based MVT system for high precision time (20 ps RMS) and charge measurement," *Journal of Instrumentation*, vol. 12, no. 08, pp. P08001–P08001, 2017.

[53] W. Krzemień, A. Gajos, A. Gruntowski et al., "Analysis Framework for the J-PET Scanner," *Acta Physica Polonica A*, vol. 127, no. 5, pp. 1491–1494, 2015.

[54] W. Krzemień, D. Alfs, P. Białas et al., "Overview of the Software Architecture and Data Flow for the J-PET Tomography Device," *Acta Physica Polonica B*, vol. 47, no. 2, p. 561, 2016.

[55] P. Moskal, O. Rundel, D. Alfs et al., "Time resolution of the plastic scintillator strips with matrix photomultiplier readout for J-PET tomograph," *Physics in Medicine and Biology*, vol. 61, no. 5, pp. 2025–2047, 2016.

[56] A. Gajos, D. Kamińska, E. Czerwiński et al., "Trilateration-based reconstruction of ortho -positronium decays into three photons with the J-PET detector," *Nuclear Instruments and Methods in Physics Research Section A: Accelerators, Spectrometers, Detectors and Associated Equipment*, vol. 819, pp. 54–59, 2016.

[57] P. W. Zitzewitz, J. C. Van House, A. Rich, and D. W. Gidley, "Spin Polarization of Low-Energy Positron Beams," *Physical Review Letters*, vol. 43, no. 18, pp. 1281–1284, 1979.

[58] P. Coleman, *Positron Beams and Their Applications*, World Scientific, 2000.

[59] E. Czerwiński, K. Dulski, P. Białas et al., "Commissioning of the J-PET Detector for Studies of Decays of Positronium Atoms," *Acta Physica Polonica B*, vol. 48, no. 10, p. 1961, 2017.

[60] P. Kowalski, W. Wiślicki, L. Raczyński et al., "Scatter Fraction of the J-PET Tomography Scanner," *Acta Physica Polonica B*, vol. 47, no. 2, p. 549, 2016.

Research Article
From Quantum Unstable Systems to the Decaying Dark Energy: Cosmological Implications

Aleksander Stachowski [iD],[1] **Marek Szydłowski** [iD],[1,2] **and Krzysztof Urbanowski** [iD] [3]

[1]*Astronomical Observatory, Jagiellonian University, Orla 171, 30-244 Kraków, Poland*
[2]*Mark Kac Complex Systems Research Centre, Jagiellonian University, Łojasiewicza 11, 30-348 Kraków, Poland*
[3]*Institute of Physics, University of Zielona Góra, Prof. Z. Szafrana 4a, 65-516 Zielona Góra, Poland*

Correspondence should be addressed to Marek Szydłowski; marek.szydlowski@uj.edu.pl

We consider a cosmology with decaying metastable dark energy and assume that a decay process of this metastable dark energy is a quantum decay process. Such an assumption implies among others that the evolution of the Universe is irreversible and violates the time reversal symmetry. We show that if we replace the cosmological time t appearing in the equation describing the evolution of the Universe by the Hubble cosmological scale time, then we obtain time dependent $\Lambda(t)$ in the form of the series of even powers of the Hubble parameter H: $\Lambda(t) = \Lambda(H)$. Our special attention is focused on radioactive-like exponential form of the decay process of the dark energy and on the consequences of this type decay.

1. Introduction

In the explanation of the Universe, we encounter the old problem of the cosmological constant, which is related to understanding why the measured value of the vacuum energy is so small in comparison with the value calculated using quantum field theory methods [1]. Because of a cosmological origin of the cosmological constant one must also address another problem. Namely, it is connected with our understanding, with a question of not only why the vacuum energy is not only small, but also, as current Type Ia supernova observations to indicate, why the present mass density of the Universe has the same order of magnitude [2].

Both mentioned cosmological constant problems can be considered in the framework of the extension of the standard cosmological ΛCDM model in which the cosmological constant (naturally interpreted as related to the vacuum energy density) is running and its value is changing during the cosmic evolution.

Results of many recent observations lead to the conclusion that our Universe is in an accelerated expansion phase [3]. This acceleration can be explained as a result of a presence of dark energy. A detailed analysis of results of recent observations shows that there is a tension between local and primordial measurements of cosmological parameters [3]. It appears that this tension may be connected with dark energy evolving in time [4]. This paper is a contribution to the discussion of the nature of the dark energy. We consider the hypothesis that dark energy depends on time, $\rho_{\mathrm{de}} = \rho_{\mathrm{de}}(t)$, and it is metastable: We assume that it decays with the increasing time t to ρ_{bare}: $\rho_{\mathrm{de}}(t) \longrightarrow \rho_{\mathrm{bare}} \neq 0$ as $t \longrightarrow \infty$. The idea that vacuum energy decays was considered in many papers (see, e.g., [5, 6]). Shafieloo et al. [7] assumed that $\rho_{\mathrm{de}}(t)$ decays according to the radioactive exponential decay law. Unfortunately, such an assumption is not able to reflect all the subtleties of evolution in the time of the dark energy and its decay process. It is because the creation of the Universe is a quantum process. Hence the metastable dark energy can be considered as the value of the scalar field at the false vacuum state and therefore the decay of the dark energy should be considered as a quantum decay process. The radioactive exponential decay law does not reflect correctly all phases of the quantum decay process. In general, analysing quantum decay processes one can distinguish the following

phases [8, 9]: (i) the early time initial phase, (ii) the canonical or exponential phase (when the decay law has the exponential form), and (iii) the late time nonexponential phase. The first phase and the third one are missed when one considers the radioactive decay law only. Simply they are invisible to the radioactive exponential decay law. For example, the theoretical analysis of quantum decay processes shows that at late times the survival probability of the system considered in its initial state (i.e., the decay law) should tend to zero as $t \longrightarrow \infty$ much more slowly than any exponential function of time and that as a function of time it has the inverse power-like form at this regime of time [8, 10, 11]. So, all implications of the assumption that the decay process of the dark energy is a quantum decay process can be found only if we apply a quantum decay law to describe decaying metastable dark energy. This idea was used in [12], where the assumption made in [7] that $\rho_{\mathrm{de}}(t)$ decays according to the radioactive exponential decay law was improved by replacing that radioactive decay law by the survival probability $\mathscr{P}(t)$, that is, by the decay law derived assuming that the decay process is a quantum process.

This is the place where one has to emphasize that the use of the assumption that dark energy depends on time and is decaying during time evolution leads to the conclusion that such a process is irreversible and violates a time reversal symmetry. (Consequences of this effect will be analysed in next sections of this paper) Note that the picture of the evolving Universe, which results from the solutions of the Einstein equations completed with quantum corrections appearing as the effect of treating the false vacuum decay as a quantum decay process, is consistent with the observational data. The evolution starts from the early time epoch with the running $\Lambda(t)$ and then it goes to the final accelerating phase expansion of the Universe. In such a scenario the standard cosmological ΛCDM model emerges from the quantum false vacuum state of the Universe.

The paper is organised as follows: In Section 2 one finds a short introduction of formalism necessary for considering decaying dark energy as a quantum decay process. Cosmological implications of a decaying dark energy are considered in Section 3. Section 4 contains conclusions.

2. Decay of a Dark Energy as a Quantum Decay Process

In the quantum decay theory of unstable systems, properties of the survival amplitudes

$$\mathscr{A}(t) = \langle \phi | \phi(t) \rangle \tag{1}$$

are usually analysed. Here a vector $|\phi\rangle$ represents the unstable state of the system considered and $|\phi(t)\rangle$ is the solution of the Schrödinger equation

$$i\hbar \frac{\partial}{\partial t} |\phi(t)\rangle = \mathfrak{H} |\phi(t)\rangle. \tag{2}$$

The initial condition for (2) in the case considered is usually assumed to be

$$|\phi(t = t_0 \equiv 0)\rangle \overset{\text{def}}{=\!=} |\phi\rangle, \tag{3}$$

or equivalently

$$\mathscr{A}(0) = 1. \tag{4}$$

In (2) $\mathfrak{H}$ denotes the complete (full), self-adjoint Hamiltonian of the system. We have $|\phi(t)\rangle = \exp[-(i/\hbar)t\mathfrak{H}]|\phi\rangle$. It is not difficult to see that this property and hermiticity of H imply that

$$(\mathscr{A}(t))^* = \mathscr{A}(-t). \tag{5}$$

Therefore, the decay probability of an unstable state (usually called the decay law), i.e., the probability for a quantum system to remain at time t in its initial state $|\phi(0)\rangle \equiv |\phi\rangle$,

$$\mathscr{P}(t) \overset{\text{def}}{=\!=} |\mathscr{A}(t)|^2 \equiv \mathscr{A}(t)(\mathscr{A}(t))^*, \tag{6}$$

must be an even function of time [8]:

$$\mathscr{P}(t) = \mathscr{P}(-t). \tag{7}$$

This last property suggests that, in the case of the unstable states prepared at some instant t_0, say $t_0 = 0$, initial condition (3) for evolution equation (2) should be formulated more precisely. Namely, from (7), it follows that the probabilities of finding the system in the decaying state $|\phi\rangle$ at the instant, say $t = T \gg t_0 \equiv 0$, and at the instant $t = -T$ are the same. Of course, this can never occur. In almost all experiments in which the decay law of a given unstable subsystem system is investigated this particle is created at some instant of time, say t_0, and this instant of time is usually considered as the initial instant for the problem. From property (7) it follows that the instantaneous creation of the unstable subsystem system (e.g., a particle or an excited quantum level and so on) is practically impossible. For the observer, the creation of this object (i.e., the preparation of the state, $|\phi\rangle$, representing the decaying subsystem system) is practically instantaneous. What is more, using suitable detectors he/she is usually able to prove that it did not exist at times $t < t_0$. Therefore, if one looks for the solutions of Schrödinger equation (2) describing properties of the unstable states prepared at some initial instant t_0 in the system and if one requires these solutions to reflect situations described above, one should complete initial conditions (3), (4) for (2) by assuming additionally that

$$|\phi(t < t_0)\rangle = 0$$
$$\text{or } \mathscr{A}(t)(t < t_0) = 0. \tag{8}$$

Equivalently, within the problem considered, one can use initial conditions (3), (4) and assume that time t may vary from $t = t_0 > -\infty$ to $t = +\infty$ only, that is, that $t \in \mathbb{R}^+$.

Note that canonical (that is a classical radioactive) decay law $\mathscr{P}_c(t) = \exp[-t/\tau_0]$ (where τ_0 is a lifetime) does not satisfy property (7), which is valid only for the quantum decay law $\mathscr{P}(t)$. What is more, from (5) and (6) it follows that at very early times, i.e., at the Zeno times (see [8, 13]),

$$\left. \frac{\partial \mathscr{P}(t)}{\partial t} \right|_{t=0} = 0, \tag{9}$$

which implies that

$$\mathscr{P}(t) > e^{-t/\tau_0} \stackrel{\text{def}}{=\!=} \mathscr{P}_c(t) \quad \text{for } t \longrightarrow 0. \tag{10}$$

So at the Zeno time region the quantum decay process is much slower than any decay process described by the canonical (or classical) decay law $\mathscr{P}_c(t)$.

Now let us focus the attention on the survival amplitude $\mathscr{A}(t)$. An unstable state $|\phi\rangle$ can be modeled as wave packets using solutions of the following eigenvalue equation $\mathfrak{H}|E\rangle = E|E\rangle$, where $E \in \sigma_c(\mathfrak{H})$, and $\sigma_c(\mathfrak{H})$ denotes a continuum spectrum of $\mathfrak{H}$. Eigenvectors $|E\rangle$ are normalized as usual: $\langle E|E'\rangle = \delta(E - E')$. Using vectors $|E\rangle$ we can model an unstable state as the following wave-packet:

$$|\phi\rangle \equiv |\phi\rangle = \int_{E_{\min}}^{\infty} c(E)|E\rangle \, dE, \tag{11}$$

where expansion coefficients $c(E)$ are functions of the energy E and $E_{\min}$ is the lower bound of the spectrum $\sigma_c(\mathfrak{H})$ of $\mathfrak{H}$. The state $|\phi\rangle$ is normalized $\langle\phi|\phi\rangle = 1$, which means that it has to be $\int_{E_{\min}}^{\infty} |c(E)|^2 dE = 1$. Now using the definition of the survival amplitude $\mathscr{A}(t)$ and the expansion (11) we can find $\mathscr{A}(t)$, which takes the following form within the formalism considered:

$$\mathscr{A}(t) \equiv \mathscr{A}(t - t_0) = \int_{E_{\min}}^{\infty} \omega(E) e^{-iE(t-t_0)} \, dE, \tag{12}$$

where $\omega(E) \equiv |c(E)|^2 > 0$ and $\omega(E)dE$ is the probability to find the energy of the system in the state $|\phi\rangle$ between E and $E + dE$. The last relation (12) means that the survival amplitude $\mathscr{A}(t)$ is a Fourier transform of an absolute integrable function $\omega(E)$. If we apply the Riemann-Lebesgue Lemma to integral (12) then one concludes that there must be $\mathscr{A}(t) \longrightarrow 0$ as $t \longrightarrow \infty$. This property and relation (12) are an essence of the Fock–Krylov theory of unstable states [14, 15].

As it is seen from (12), the amplitude $\mathscr{A}(t)$ and thus the decay law $\mathscr{P}(t)$ of the unstable state $|\phi\rangle$ are completely determined by the density of the energy distribution $\omega(E)$ for the system in this state [14, 15] (see also [8, 10, 11, 16–21]).

In the general case the density $\omega(E)$ possesses properties analogous to the scattering amplitude; i.e., it can be decomposed into a threshold factor, a pole-function $P(E)$ with a simple pole, and a smooth form factor $F(E)$. There is $\omega(E) = \Theta(E - E_{\min})(E - E_{\min})^{\alpha_l} P(E)F(E)$, where α_l depends on angular momentum l through $\alpha_l = \alpha + l$ [8] (see equation (6.1) in [8]), $0 \le \alpha < 1$) and $\Theta(E)$ is a step function: $\Theta(E) = 0$ for $E \le 0$ and $\Theta(E) = 1$ for $E > 0$. The simplest choice is to take $\alpha = 0$, $l = 0$, $F(E) = 1$ and to assume that $P(E)$ has a Breit–Wigner (BW) form of the energy distribution density. (The mentioned Breit–Wigner distribution was found when the cross section of slow neutrons was analysed [22]) It turns out that the decay curves obtained in this simplest case are very similar in form to the curves calculated for the above described more general $\omega(E)$ (see [16] and analysis in [8]). So to find the most typical properties of the decay process it is sufficient to make the relevant calculations for $\omega(E)$ modeled by the Breit–Wigner distribution of the energy density $\omega(E) \equiv$

$\omega_{\text{BW}}(E) \stackrel{\text{def}}{=\!=} (N/2\pi)\Theta(E - E_{\min})(\Gamma_0/((E - E_0)^2 + (\Gamma_0/2)^2))$, where N is a normalization constant. The parameters E_0 and Γ_0 correspond to the energy of the system in the unstable state and its decay rate at the exponential (or canonical) regime of the decay process. $E_{\min}$ is the minimal (the lowest) energy of the system. Inserting $\omega_{\text{BW}}(E)$ into formula (12) for the amplitude $\mathscr{A}(t)$ and assuming for simplicity that $t_0 = 0$, after some algebra, one finds that

$$\mathscr{A}(t) = \frac{N}{2\pi} e^{-(i/\hbar)E_0 t} I_\beta\left(\frac{\Gamma_0 t}{\hbar}\right), \tag{13}$$

where

$$I_\beta(\tau) \stackrel{\text{def}}{=\!=} \int_{-\beta}^{\infty} \frac{1}{\eta^2 + 1/4} e^{-i\eta\tau} d\eta. \tag{14}$$

Here $\tau = \Gamma_0 t/\hbar \equiv t/\tau_0$, τ_0 is the lifetime, $\tau_0 = \hbar/\Gamma_0$, and $\beta = (E_0 - E_{\min})/\Gamma_0 > 0$. The integral $I_\beta(\tau)$ has the following structure:

$$I_\beta(\tau) = I_\beta^{\text{pole}}(\tau) + I_\beta^L(\tau), \tag{15}$$

where

$$I_\beta^{\text{pole}}(\tau) = \int_{-\infty}^{\infty} \frac{1}{\eta^2 + 1/4} e^{-i\eta\tau} d\eta \equiv 2\pi e^{-\tau/2}, \tag{16}$$

and

$$I_\beta^L(\tau) = -\int_{+\beta}^{\infty} \frac{1}{\eta^2 + 1/4} e^{+i\eta\tau} d\eta. \tag{17}$$

(The integral $I_\beta^L(\tau)$ can be expressed in terms of the integral-exponential function [23–26] (for a definition, see [27, 28])) The result (15) means that there is a natural decomposition of the survival amplitude $\mathscr{A}(t)$ into two parts:

$$\mathscr{A}(t) = \mathscr{A}_c(t) + \mathscr{A}_L(t), \tag{18}$$

where

$$\mathscr{A}_c(t) = \frac{N}{2\pi} e^{-(i/\hbar)E_0 t} I_\beta^{\text{pole}}\left(\frac{\Gamma_0 t}{\hbar}\right) \equiv N e^{-(i/\hbar)E_0 t} e^{-\Gamma_0 t/2}, \tag{19}$$

and

$$\mathscr{A}_L(t) = \frac{N}{2\pi} e^{-(i/\hbar)E_0 t} I_\beta^L\left(\frac{\Gamma_0 t}{\hbar}\right), \tag{20}$$

and $\mathscr{A}_c(t)$ is the canonical part of the amplitude $\mathscr{A}(t)$ describing the pole contribution into $\mathscr{A}(t)$ and $\mathscr{A}_L(t)$ represents the remaining part of $\mathscr{A}(t)$.

From decomposition (18) it follows that in the general case within the model considered the survival probability (6) contains the following parts:

$$\mathscr{P}(t) = |\mathscr{A}(t)|^2 \equiv |\mathscr{A}_c(t) + \mathscr{A}_L(t)|^2$$
$$= |\mathscr{A}_c(t)|^2 + 2\Re\left[\mathscr{A}_c(t)(\mathscr{A}_L(t))^*\right] + |\mathscr{A}_L(t)|^2. \tag{21}$$

This last relation is especially useful when one looks for a contribution of late time properties of the quantum unstable system to the survival amplitude.

The late time form of the integral $I_\beta^L(\tau)$ and thus the late time form of the amplitude $\mathscr{A}_L(t)$ can be relatively easy to find using analytical expression for $\mathscr{A}_L(t)$ in terms of the integral-exponential functions or simply performing the integration by parts in (17). One finds for $t \longrightarrow \infty$ (or $\tau \longrightarrow \infty$) that the leading term of the late time asymptotic expansion of the integral $I_\beta^L(\tau)$ has the following form:

$$I_\beta^L(\tau) \simeq -\frac{i}{\tau}\frac{e^{i\beta\tau}}{\beta^2 + 1/4} + \dots, \quad (\tau \longrightarrow \infty). \qquad (22)$$

Thus inserting (22) into (20) one can find late time form of $\mathscr{A}_L(t)$.

As was mentioned we consider the hypothesis that a dark energy depends on time, $\rho_{de} = \rho_{de}(t)$, and decays with the increasing time t to ρ_{bare}: $\rho_{de}(t) \longrightarrow \rho_{bare} \neq 0$ as $t \longrightarrow \infty$. We assume that it is a quantum decay process. The consequence of this assumption is that we should consider $\rho_{de}(t_0)$ (where t_0 is the initial instant) as the energy of an excited quantum level (e.g., corresponding to the false vacuum state) and the energy density ρ_{bare} as the energy corresponding to the true lowest energy state (the true vacuum) of the system considered. Our hypothesis means that $(\rho_{de}(t) - \rho_{bare}) \longrightarrow 0$ as $t \longrightarrow \infty$. As it was said we assumed that the decay process of the dark energy is a quantum decay process: From the point of view of the quantum theory of decay processes this means that $\lim_{t \to \infty}(\rho_{de}(t) - \rho_{bare}) = 0$ according to the quantum mechanical decay law. Therefore if we define

$$\widetilde{\rho}_{de}(t) \stackrel{def}{=\!=} \rho_{de}(t) - \rho_{bare}, \qquad (23)$$

our assumption means that the decay law for $\widetilde{\rho}_{de}(t)$ has the following form (see [12]):

$$\begin{aligned}\widetilde{\rho}_{de}(t) &= \widetilde{\rho}_{de}(t_0)\mathscr{P}(t) \equiv \widetilde{\rho}_{de}(t_0) \\ &\cdot \left(\left|\mathscr{A}_c(t)\right|^2 + 2\mathfrak{R}\left[\mathscr{A}_c(t)\left(\mathscr{A}_L(t)\right)^*\right] + \left|\mathscr{A}_L(t)\right|^2\right),\end{aligned} \qquad (24)$$

where $\mathscr{P}(t)$ is given by relation (6), or, equivalently, our assumption means that the decay law for $\widetilde{\rho}_{de}(t)$ has the following form (compare [12]):

$$\begin{aligned}\rho_{de}(t) &\equiv \rho_{bare} + \widetilde{\rho}_{de}(t_0) \\ &\cdot \left(\left|\mathscr{A}_c(t)\right|^2 + 2\mathfrak{R}\left[\mathscr{A}_c(t)\left(\mathscr{A}_L(t)\right)^*\right] + \left|\mathscr{A}_L(t)\right|^2\right),\end{aligned} \qquad (25)$$

where $\widetilde{\rho}_{de}(t_0) = (\rho_{de}(t_0) - \rho_{bare})$ and $\mathscr{P}(t)$ is replaced by (21). Taking into account the standard relation between ρ_{de} and the cosmological constant Λ we can write

$$\begin{aligned}\Lambda_{eff}(t) &\equiv \Lambda_{bare} + \widetilde{\Lambda}(t_0) \\ &\cdot \left(\left|\mathscr{A}_c(t)\right|^2 + 2\mathfrak{R}\left[\mathscr{A}_c(t)\left(\mathscr{A}_L(t)\right)^*\right] + \left|\mathscr{A}_L(t)\right|^2\right),\end{aligned} \qquad (26)$$

where $\widetilde{\Lambda}(t_0) \equiv \widetilde{\Lambda}_0 = (\Lambda(t_0) - \Lambda_{bare})$. Thus within the considered case using definition (6) or relation (21) we can determine changes in time of the dark energy density $\rho_{de}(t)$ (or running $\Lambda(t)$) knowing the general properties of survival amplitude $\mathscr{A}(t)$.

The above described approach is self-consistent if we identify $\rho_{de}(t_0)$ with the energy E_0 of the unstable system divided by the volume V_0 (where V_0 is the volume of the system at $t = t_0$): $\rho_{de}(t_0) \equiv \rho_{de}^{qft} \stackrel{def}{=\!=} \rho_{de}^0 = E_0/V_0$ and $\rho_{bare} = E_{min}/V_0$. Here ρ_{de}^{qft} is the vacuum energy density calculated using quantum field theory methods. In such a case

$$\beta = \frac{E_0 - E_{min}}{\Gamma_0} \equiv \frac{\rho_{de}^0 - \rho_{bare}}{\gamma_0} > 0, \qquad (27)$$

(where $\gamma_0 = \Gamma_0/V_0$), or equivalently $\Gamma_0/V_0 \equiv (\rho_{de}^0 - \rho_{bare})/\beta$.

3. Cosmological Implications of Decaying Vacuum

Let us consider cosmological implications of the parameter Λ with the time parameterized decaying part, derived in the previous section, in the form

$$\Lambda \equiv \Lambda_{eff}(t) = \Lambda_{bare} + \delta\Lambda(t), \qquad (28)$$

where $\delta\Lambda(t)$ describes quantum corrections and it is given by a series with respect to $1/t$; i.e.,

$$\delta\Lambda(t) = \sum_{n=1}^{\infty} \alpha_{2n}\left(\frac{1}{t}\right)^{2n}, \qquad (29)$$

where t is the cosmological scale time and the functions $\Lambda_{eff}(t)$ and $\delta\Lambda(t)$ have a reflection symmetry with respect to the cosmological time $\delta\Lambda(-t) = \delta\Lambda(t)$. The next step in deriving dynamical equations for the evolution of the Universe is to consider this parameter as a source of gravity which contributes to the effective energy density; i.e.,

$$3H(t)^2 = \rho_m(t) + \rho_{de}(t), \qquad (30)$$

where $\rho_{de}(t)$ is identified as the energy density of the quantum decay process of vacuum

$$\rho_{de}(t) = \Lambda_{bare} + \delta\Lambda(t). \qquad (31)$$

In this paper, we assume that $c = 8\pi G = 1$. The Einstein field equation for the FRW metric reduces to

$$\begin{aligned}\frac{dH(t)}{dt} &= -\frac{1}{2}\left(\rho_{eff}(t) + p_{eff}(t)\right) \\ &= -\frac{1}{2}\left(\rho_m(t) + 0 + \rho_{de}(t) - \rho_{de}(t)\right),\end{aligned} \qquad (32)$$

where $\rho_{eff} = \rho_m + \rho_{de}$, $p_{eff} = 0 + p_{de}$, or

$$\frac{dH(t)}{dt} = -\frac{1}{2}\rho_m(t) = -\frac{1}{2}\left(3H(t)^2 - \Lambda_{bare} - \delta\Lambda(t)\right). \qquad (33)$$

Szydlowski et al. [12] considered the radioactive-like decay of metastable dark energy. For the late time, this decay process has three consecutive phases: the phase of radioactive decay, the phase of damping oscillations, and finally the phase

of power law decaying. When $\beta > 0$ for $t > (\hbar/\Gamma_0)(2\beta/(\beta^2 + 1/4))$, dark energy can be described in the following form (see (25) and [12]):

$$\rho_{de}(t) \approx \rho_{bare} + \epsilon \left(4\pi^2 e^{-(\Gamma_0/\hbar)t} \right.$$

$$+ \frac{4\pi e^{-(\Gamma_0/2\hbar)t}\sin\left(\beta\left(\Gamma_0/\hbar\right)t\right)}{(1/4 + \beta^2)\left(\Gamma_0/\hbar\right)t} \qquad (34)$$

$$\left. + \frac{1}{\left((1/4 + \beta^2)\left(\Gamma_0/\hbar\right)t\right)^2} \right),$$

where ϵ, Γ_0, and β are model parameters. Equation (34) results directly from (25): One only needs to insert (22) into formula for $\mathscr{A}_L(t)$ and result (19) instead of $\mathscr{A}_c(t)$ into (25). In this paper, we consider the first phase of decay process, in other words, the phase of radioactive (exponential) decay.

The model with the radioactive (exponential) decay of dark energy was investigated by Shafieloo et al. [7]. During the phase of the exponential decay of the vacuum

$$\frac{d\delta\Lambda(t)}{dt} = A\delta\Lambda(t), \qquad (35)$$

where $A = \text{const} < 0$ ($\delta\Lambda(t)$ is decaying).

The set of equations (33) and (35) constitute a two-dimensional closed autonomous dynamical system in the form

$$\frac{dH(t)}{dt} = -\frac{1}{2}\left(3H(t)^2 - \Lambda_{bare} - \delta\Lambda(t)\right),$$
$$\frac{d\delta\Lambda(t)}{dt} = A\delta\Lambda(t). \qquad (36)$$

System (36) has the time dependent first integral in the form

$$\rho_m(t) = 3H(t)^2 - \Lambda_{bare} - \delta\Lambda(t). \qquad (37)$$

At the finite domain, system (36) possesses only one critical point representing the standard cosmological model (the running part of Λ vanishes, i.e., $\delta\Lambda(t) = 0$).

System (36) can be rewritten in variables

$$x = \frac{\delta\Lambda(t)}{3H_0^2},$$
$$y = \frac{H(t)}{H_0} \qquad (38)$$

where H_0 is the present value of the Hubble function. Then

$$\frac{dx}{d\sigma} = \frac{A}{H_0}x$$
$$\frac{dy}{d\sigma} = -\frac{1}{2}\left(3y^2 - 3\Omega_{\Lambda_{bare}} - 3x\right), \qquad (39)$$

where $\Omega_{\Lambda_{bare}} = \Lambda_{bare}/3H_0^2$ and $\sigma = H_0t$ are a new reparametrized time. The phase portrait of system (39) is shown in Figure 1.
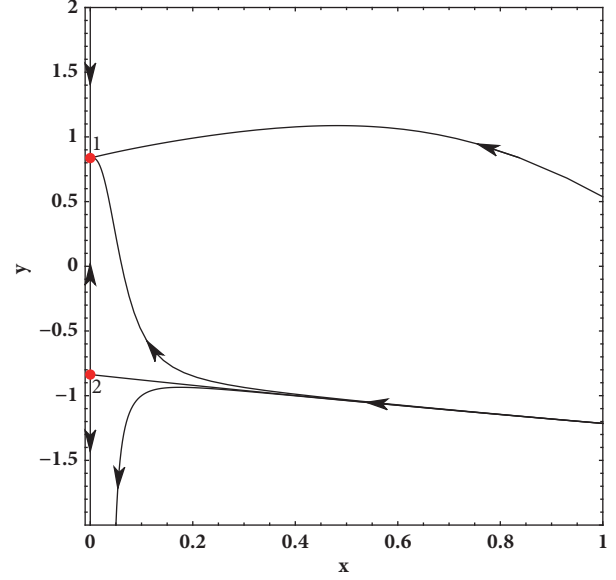
FIGURE 1: The phase portrait of system (39). Critical point 1 ($x = 0$, $y = \sqrt{\Lambda_{bare}}/\sqrt{3}H_0$) is the stable node and critical point 2 ($x = 0$, $y = -\sqrt{\Lambda_{bare}}/\sqrt{3}H_0$) is the saddle. These critical points represent the de Sitter universes. Here, H_0 is the present value of the Hubble function. The value of A is assumed as $-H_0$. Note that the phase portrait is not symmetric under reflection $H \longrightarrow -H$. While critical point 1 is a global attractor, only a unique separatrix reaches critical point 2.

Szydlowski et al. [12] demonstrated that the contribution of the energy density of the decaying quantum vacuum possesses three disjoint phases during the cosmic evolution. The phase of exponential decay like in the radioactive decay processes is long phase in the past and future evolution. Our estimation of model parameter shows that we are living in the Universe with the radioactive decay of the quantum vacuum.

It is interesting that, during this phase, the Universe violates the reflection symmetry of the time: $t \longrightarrow -t$. In cosmology and generally in physics there is a fundamental problem of the origin of irreversibility in the Universe [29]. Note that in our model irreversibility is a consequence of the radioactive decay of the quantum vacuum.

If we considered radioactivity (in which the time reversal symmetry is broken) then a direction of decaying vacuum is in accordance with the thermodynamical arrow of time. First, note that it is in some sense very natural that the dynamics of the Universe is in fact irreversible when the full quantum evolution is taken into account. Therefore, radioactive decay of vacuum irreversibility has a thermodynamic interpretation as far as the evolution of the Universe is concerned: in horizon thermodynamics the area of the cosmological horizon is interpreted as (beginning proportional to) the entropy, i.e., the Hawking entropy. In a system where Λ decays as a result of irreversible quantum processes we obtain the very natural conclusion that the entropy of the Universe grows, in many cases without an upper bound [30, 31].

In the general parameterization (29), of course, the symmetry of changing $t \longrightarrow -t$ is present and this symmetry is

also in a one-dimensional nonautonomous dynamical system describing the evolution of the Universe:

$$\frac{dH(t)}{dt} = -\frac{1}{2}\left(3H(t)^2 - \Lambda_{\text{bare}} - \sum_{n=1}^{\infty}\alpha_{2n}t^{-2n}\right). \quad (40)$$

In cosmology, especially in quantum cosmology, the analysis of the concept of time seems to be the key for the construction of an adequate quantum gravity theory, which we would like to apply to the description of early Universe.

The good approximation of (40) is to replace in it the cosmological time by the Hubble cosmological scale time

$$t_{\text{H}} = \frac{1}{H}. \quad (41)$$

In consequence, parameterization (29) can be rewritten in the new form

$$\delta\Lambda(t) = \delta\Lambda(H(t)) = \sum_{n=1}^{\infty}\alpha_{2n}H(t)^{2n}. \quad (42)$$

After putting this form into (40), we obtain dynamical system in an autonomous form with the preserved symmetry of time $t \longrightarrow -t$, $H \longrightarrow -H$. In Figure 2 presents a diagram of the evolution of the Hubble function obtained from the following one-dimensional dynamical system:

$$\frac{dH(t)}{dt} = -\frac{1}{2}\left(3H(t)^2 - \Lambda_{\text{bare}} - \sum_{n=1}^{\infty}\alpha_{2n}H(t)^{2n}\right). \quad (43)$$

For comparison, the evolution of the Hubble functions derived in the ΛCDM model, model (40), and model (43) are presented in Figure 3. For the existence of the de Sitter global attractor as $t \longrightarrow \infty$ asymptotically a contribution coming from the decaying part of $\delta\Lambda(H(t)) = \sum_{n=1}^{\infty}\alpha_{2n}H(t)^{2n}$ should be vanishing.

This condition guarantees for us a consistency of our model with astronomical observations of the accelerating phase of the Universe [3].

If all parameters α_{2n} for $n > 1$ equal zero then the Hubble parameter is described by the following formula:

$$H(a) = \pm\sqrt{\frac{\rho_{\text{m,0}}a^{\alpha_{21}-3} + \Lambda_{\text{bare}}}{3 - \alpha_{21}}}, \quad (44)$$

or

$$H(z) = \pm\sqrt{\frac{\rho_{\text{m,0}}(1+z)^{3-\alpha_{21}} + \Lambda_{\text{bare}}}{3 - \alpha_{21}}}, \quad (45)$$

where $z = a^{-1} - 1$ is redshift. From (44) we can obtain the following formula for the expanding Universe:

$$a(t)$$
$$= \left(\sqrt{\frac{\rho_{\text{m,0}}}{\Lambda_{\text{bare}}}}\sinh\left(\frac{\sqrt{(3-\alpha_{21})\Lambda_{\text{bare}}}}{2}t\right)\right)^{2/(3-\alpha_{21})}. \quad (46)$$

FIGURE 2: The diagram of the evolution of the Hubble function with respect to the cosmological time t, which is described by (43) with $\alpha_{21} \neq 0$ and $\alpha_{2n} = 0$ for every $n > 1$. For illustration, two example values of the parameter $\alpha_{21} =$ are chosen: -1 and -2. The top blue curve describes the evolution of the Hubble function in the ΛCDM model. The middle curve describes one for $\alpha_{21} = -1$ and the bottom red curve describes one for $\alpha_{21} = -2$. The Hubble function is expressed in km/s Mpc and the cosmological time t is expressed in s Mpc/km.

FIGURE 3: The diagram of the evolution of the Hubble function with respect to the cosmological time t, which is described by (40) and (43) with $\alpha_{21} \neq 0$ and $\alpha_{2n} = 0$ for every $n > 1$. For illustration, the value of the parameter $\alpha_{21} =$ is chosen as -0.3. The top blue curve describes the evolution of the Hubble function in the ΛCDM model. The middle curve describes one for (43) and the bottom red curve describes one for (40). The Hubble function is expressed in km/s Mpc and the cosmological time t is expressed in s Mpc/km. Note that these models are not qualitatively different.

Figure 4 presents the evolution of the scale factor, which is described by (46). Eq. (46) gives us the following formula:

$$H(t) = \sqrt{\frac{\Lambda_{\text{bare}}}{3 - \alpha_{21}}}\coth\left(\frac{1}{2}\sqrt{\Lambda_{\text{bare}}(3-\alpha_{21})}t\right). \quad (47)$$

In the extension of Friedmann equation (37) matter is contributed as well as dark energy. The total energy-momentum tensor $T^{\mu\nu} = T_{\text{m}}^{\mu\nu} + T_{\text{de}}^{\mu\nu}$ is of course conserved. However, between the matter and dark energy sectors exist an interaction—the energy density is transferred between
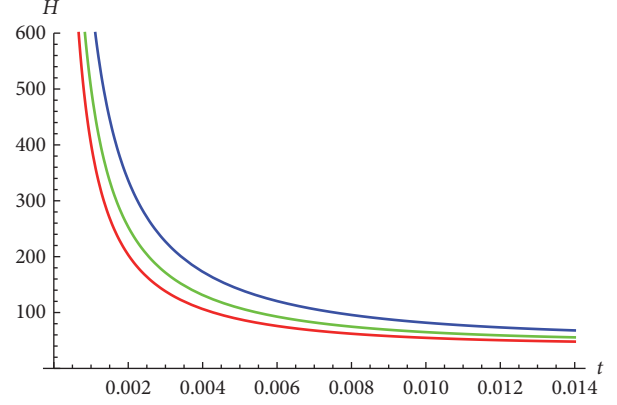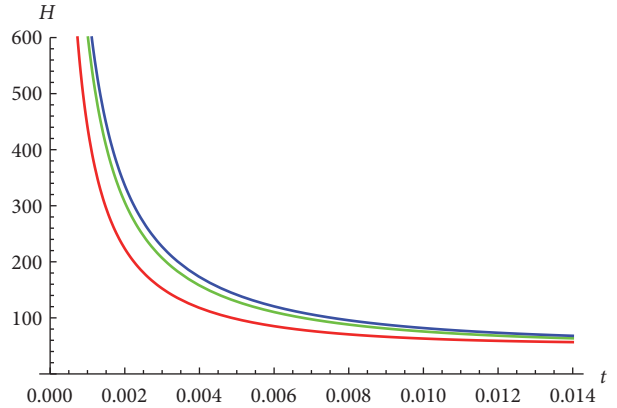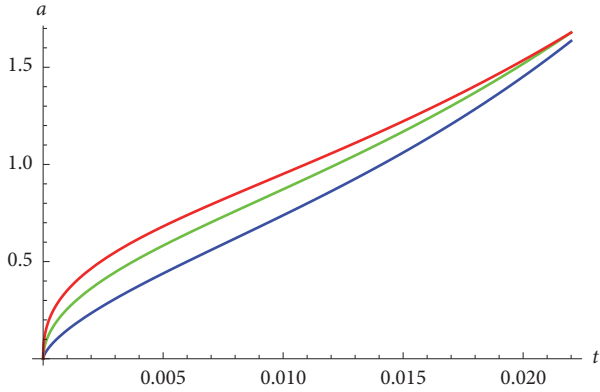
FIGURE 4: The diagram of the evolution of the scale factor with respect to the cosmological time t, which is described by (46). For illustration, two example values of the parameter α_{21} = are chosen: -1 and -2. The bottom blue curve describes the evolution of the scale factor in the ΛCDM model. The middle curve describes one for $\alpha_{21} = -1$ and the top red curve describes one for $\alpha_{21} = -2$. The cosmological time t is expressed in s Mpc/km.
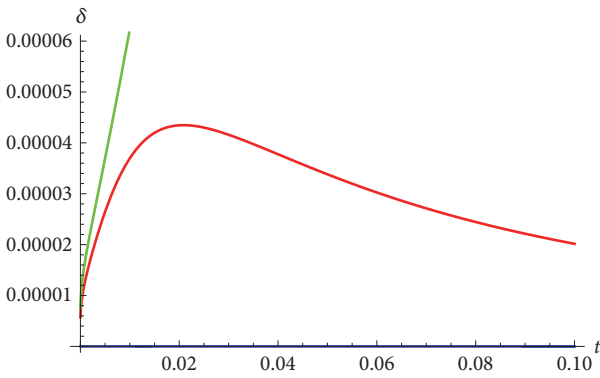
FIGURE 5: The diagram of the evolution of the parameter δ with respect to the cosmological time t. For illustration, two example values of the parameter A are chosen: $A = -100$km/s Mpc (the top green curve) and $A = -200$km/s Mpc (the middle red curve). For comparison the ΛCDM model with the parameter $\delta = 0$ is represented by the bottom blue curve. Here, the value of the parameter B is equal to 1. The cosmological time t is expressed in s Mpc/km.

these sectors. This process can be described by the system of equations

$$\frac{d\rho_{\mathrm{m}}(t)}{dt} + 3H(t)\rho_{\mathrm{m}}(t) = -\frac{d\rho_{\mathrm{de}}(t)}{dt} = -\frac{d\Lambda_{\mathrm{eff}}(t)}{dt},$$

$$\frac{d\rho_{\mathrm{de}}(t)}{dt} = \frac{d\Lambda_{\mathrm{eff}}(t)}{dt}, \qquad (48)$$

where it is assumed that pressure of matter $p_{\mathrm{m}} = 0$ and $p_{\mathrm{de}} = -\rho_{\mathrm{de}}$. The time variability of the matter and energy density of decaying vacuum are demonstrated in Figure 5.

In the special case of radioactive decay of vacuum (48) reduces to

$$\frac{d\rho_{\mathrm{m}}(t)}{dt} + 3H(t)\rho_{\mathrm{m}}(t) = -ABe^{At} = -A\delta\Lambda(t),$$

$$\frac{d\rho_{\mathrm{de}}(t)}{dt} = A\delta\Lambda(t) \qquad (49)$$

or

$$\frac{1}{a(t)^3}\frac{d}{dt}\left(a(t)^3\rho_{\mathrm{m}}(t)\right) = -ABe^{At} = -A\delta\Lambda(t) \implies$$

$$\rho_{\mathrm{m}}(t)a(t)^3 = \rho_{\mathrm{m},0}a_0^3 - \int ABe^{At}a(t)^3\,dt, \qquad (50)$$

$$\frac{d\rho_{\mathrm{de}}(t)}{dt} = A\delta\Lambda(t).$$

In the case of the interaction between matter and decaying dark energy, the natural consequence of conservation of the total energy-momentum tensor $T^{\mu\nu}$ is a modification of the standard formula for scaling matter.

Let $\rho_{\mathrm{m}}(t) = \rho_{m,0}a^{-3+\delta(t)}$, where $\delta(t)$ is a deviation from the canonical scaling of dust matter [32, 33]. Then we have

$$\delta(t) = \frac{\ln\left(\rho_{\mathrm{m}}(t)/\rho_{\mathrm{m},0}\right)}{\ln a(t)} + 3. \qquad (51)$$

4. Conclusions

From our investigation of cosmological implications of effects of the quantum decay of metastable dark energy, one can derive following results:

(i) The cosmological models with the running cosmological parameter can be included in the framework of some extension of Friedmann equation. The new ingredient in the comparison with the standard cosmological model (ΛCDM model) is that the total energy-momentum tensor is conserved and the interaction takes place between the matter and dark energy sectors. In consequence the canonical scaling law $\rho_{\mathrm{m}} \propto a^{-3}$ is modified. Because $\Lambda(t)$ is decaying ($d\Lambda/dt < 0$) energy of matter in the comoving volume $\propto a^3$ is growing with time.

(ii) We have found that the appearance of the universal exponential contribution in energy density of the decaying vacuum can explain the irreversibility of the cosmic evolution. While the reversibility $t \longrightarrow -t$ is still present in the dynamical equation describing the evolutional scenario, in the first phase of radioactive decay, this symmetry is violated.

(iii) We have also compared the time evolution of the Hubble function in the model under consideration (where $\Lambda(t)$ is parameterized by the cosmological time) with Sola et al. [34] parameterization by the Hubble function. Note that both parameterizations coincide if time t is replaced by the Hubble scale time $t_H = 1/H$. If the evolution of the Universe is invariant in the scale, i.e., the scale factor a is changing in power law, then this correspondence is exact.

Data Availability

No data were used to support this study.

Conflicts of Interest

The authors declare that they have no conflicts of interest.

Acknowledgments

References

[1] S. Weinberg, *Reviews of Modern Physics*, vol. 61, pp. 1–23, 1989.

[2] S. Weinberg, "The cosmological constant problems," in *Sources and Detection of Dark Matter and Dark Energy in the Universe*, pp. 18–26, Springer-Verlag Berlin Heidelberg, New York, NY, USA, 2001.

[3] P. A. R. Ade et al., "Planck2015 results. XIV. Dark energy and modified gravity," *Astronomy & Astrophysics*, vol. 594, no. A14, p. 31, 2016.

[4] E. Di Valentino, E. V. Linder, and A. Melchiorri, "A Vacuum Phase Transition Solves H_0 Tension," *Physical Review D*, vol. 97, p. 043528, 2018.

[5] L. M. Krauss and J. Dent, "The Late Time Behavior of False Vacuum Decay: Possible Implications for Cosmology and Metastable Inflating States," *Physical Review Letters*, vol. 100, p. 171301, 2008.

[6] L. M. Krauss, J. Dent, and G. D. Starkman, "Late Time Decay of the False Vacuum, Measurement, and Quantum Cosmology," *International Journal of Modern Physics D*, vol. 17, p. 2501, 2008.

[7] A. Shafieloo, D. K. Hazra, V. Sahni, and A. A. Starobinsky, "Metastable Dark Energy with Radioactive-like Decay," *Monthly Notices of the Royal Astronomical Society*, vol. 473, p. 2760, 2018.

[8] L. Fonda, G. C. Ghirardi, and A. Rimini, "Decay theory of unstable quantum systems," *Reports on Progress in Physics*, vol. 41, p. 587, 1978.

[9] M. Peshkin, A. Volya, and V. Zelevinsky, "Non-exponential and oscillatory decays in quantum mechanics," *Europhysics Letters*, vol. 107, no. 4, p. 40001, 2014.

[10] L. A. Khalfin, "Contribution to the decay theory of a quasistationary state," *Journal of Experimental and Theoretical Physics*, vol. 33, p. 1371, 1958.

[11] L. A. Khalfin, "Contribution to the decay theory of a quasistationary state," *Soviet Physics—JETP*, vol. 6, p. 1053, 1958.

[12] M. Szydlowski, A. Stachowski, and K. Urbanowski, "Quantum mechanical look at the radioactive-like decay of metastable dark energy," *European Physical Journal C*, vol. 77, p. 902, 2017.

[13] K. Urbanowski, "Early-time properties of quantum evolution," *Physical Review A*, vol. 50, p. 2847, 1994.

[14] N. S. Krylov and V. A. Fock, "O dvuh osnovnyh tolkovanijah sootnosenija neopredelenosti dla energii i vremeni," *Journal of Experimental and Theoretical Physics*, vol. 17, p. 93, 1947 (Russian).

[15] V. A. Fock, *Fundamentals of quantum mechanics*, Mir Publishers, Moscow, 1978.

[16] N. G. Kelkar and M. Nowakowski, "No classical limit of quantum decay for broad states," *Journal Of Physics A*, vol. 43, p. 385308, 2010.

[17] J. Martorell, J. G. Muga, and D. W. L. Sprung, "Quantum postexponential decay," in *Time in Quantum Mechanics - Vol. 2*, J. G. Muga, A. Ruschhaupt, and A. del Campo, Eds., vol. 789 of *Lecture Notes in Physics*, pp. 239–275, Springer-Verlag Berlin Heidelberg, Germany, 2009.

[18] E. Torrontegui, J. Muga, J. Martorell, and D. Sprung, "Quantum decay at long times," in *Unstable States in the Continuous Spectra, Part I: Analysis, Concepts, Methods, and Results*, C. A. Nicolaides and E. Brandas, Eds., vol. 60 of *Advances in Quantum Chemistry*, pp. 485–535, Elsevier, 2010.

[19] G. Garcia-Calderon, R. Romo, and J. Villavicencio, "Survival probability of multibarrier resonance systems: exact analytical approach," *Physical Review B*, vol. 76, p. 035340, 2007.

[20] F. Giraldi, "Logarithmic decays of unstable states," *European Physical Journal D*, vol. 69, p. 5, 2015.

[21] F. Giraldi, "Logarithmic decays of unstable states II," *European Physical Journal D*, vol. 70, p. 229, 2016.

[22] G. Breit and E. Wigner, "Capture of slow neutrons," *Physical Review*, vol. 49, p. 519, 1936.

[23] K. M. Sluis and E. A. Gislason, "Decay of a quantum-mechanical state described by a truncated Lorentzian energy distribution," *Physical Review A*, vol. 43, p. 4581, 1991.

[24] K. Urbanowski, "A quantum long time energy red shift: a contribution to varying α theories," *European Physical Journal C*, vol. 58, p. 151, 2008.

[25] K. Urbanowski, "Long time properties of the evolution of an unstable state," *Open Physics*, vol. 7, p. 696, 2009.

[26] K. Raczynska and K. Urbanowski, *Survival amplitude, instantaneous energy and decay rate of an unstable system: Analytical results*, 2018.

[27] W. J. Olver, D. W. Lozier, R. F. Boisvert, and C. W. Clark, *NIST Handbook of Mathematical Functions*, Cambridge University Press, Cambridge, USA, 2010.

[28] M. Abramowitz and I. A. Stegun, *Handbook of Mathematical Functions with Formulas, Graphs, and Mathematical Tables*, vol. 55 of *Applied Mathematics Series*, National Bureau of Standards, Washington, DC, USA, 1964.

[29] H. D. Zeh, *The Physical Basis of the Direction of Time*, Springer-Verlag Berlin Heidelberg, Germany, 5th edition, 2007.

[30] K. Freese, F. C. Adams, J. A. Frieman, and E. Mottola, "Cosmology with decaying vaccum energy," *Nuclear Physics B*, vol. 287, p. 797, 1987.

[31] T. Markkanen, "De Sitter Stability and Coarse Graining," *European Physical Journal C*, vol. 78, p. 97, 2018.

[32] I. L. Shapiro, J. Sola, C. Espana-Bonet, and P. Ruiz-Lapuente, "Variable cosmological constant as a Planck scale effect," *Physics Letters B*, vol. 574, p. 149, 2003.

[33] C. Espana-Bonet, P. Ruiz-Lapuente, I. L. Shapiro, and J. Sola, "Testing the running of the cosmological constant with Type Ia Supernovae at high z," *Journal of Cosmology and Astroparticle Physics*, vol. 402, p. 6, 2004.

[34] I. L. Shapiro and J. Sola, "On the possible running of the cosmological "constant"," *Physics Letters B*, vol. 682, p. 105, 2009.

Research Article
A Probability Distribution for Quantum Tunneling Times

José T. Lunardi [iD][1] and **Luiz A. Manzoni**[2]

[1]*Department of Mathematics & Statistics, State University of Ponta Grossa, Avenida Carlos Cavalcanti 4748,*
84030-900 Ponta Grossa, PR, Brazil
[2]*Department of Physics, Concordia College, 901 8th St. S., Moorhead, MN 56562, USA*

Correspondence should be addressed to José T. Lunardi; jttlunardi@gmail.com

We propose a general expression for the probability distribution of real-valued tunneling times of a localized particle, as measured by the Salecker-Wigner-Peres quantum clock. This general expression is used to obtain the distribution of times for the scattering of a particle through a static rectangular barrier and for the tunneling decay of an initially bound state after the sudden deformation of the potential, the latter case being relevant to understand tunneling times in recent attosecond experiments involving strong field ionization.

1. Introduction

The search for a proper definition of quantum tunneling times for massive particles, having well-behaved properties for a wide range of parameters, has remained an important and open *theoretical* problem since, essentially, the inception of quantum mechanics (see, e.g., [1, 2] and references therein). However, such tunneling times were beyond the experimental reach until recent advances in ultrafast physics have made possible measurements of time in the attosecond scale, opening up the experimental possibility of measuring electronic tunneling times through a classically forbidden region [3–6] and reigniting the discussion of tunneling times. Still, the intrinsic experimental difficulties associated with both the measurements and the interpretation of the results have, so far, prevented an elucidation of the problem and, in fact, contradictory results persist, with some experiments obtaining a finite nonzero result [3, 6] and others compatible with instantaneous tunneling [4]. It should be noticed that the similarity between Schrödinger and Helmholtz equations allows for analogies between quantum tunneling of massive particles and photons [7], and a noninstantaneous tunneling time is supported by this analogy and experiments measuring photonic tunneling times [8], as well as by many theoretical calculations based on both the Schrödinger (for reviews see, e.g., [1, 2]) and the Dirac equations (e.g., [9–16]).

The conceptual difficulty in obtaining an unambiguous and well-defined tunneling time is associated with the impossibility of obtaining a self-adjoint time operator in quantum mechanics [17], therefore leading to the need for operational definitions of time. Several such definitions exist, such as phase time [18], dwell time [19], the Larmor times [20–23], and the Salecker-Wigner-Peres (SWP) time [17, 24], and in some situations these lead to different, or even contradictory, results. This is not surprising, since by their own nature operational definitions can only describe limited aspects of the phenomena of tunneling, and it is unlikely that any one definition will be able to provide a unified description of the quantum tunneling times in a broad range of situations. Nevertheless, it remains an important task to obtain a well-defined and *real* time scale that accurately describes the recent experiments [3–6, 25–27].

It is important to notice that the time-independent approach to tunneling times (i.e., for incident particles with sharply defined energy), which comprises the vast majority of the literature, is ill-suited to accomplish the above-mentioned goal, since it ignores the essential role of localizability in defining a time scale [23, 28]; see, however, [29], which applies the time defined in [30] to investigate the half-life of α-decaying nuclei. A few works (e.g., [23, 28, 31, 32]) address the issue of localizability and, consequently, arrive at a probabilistic definition of tunneling times (that is, an

average time). In particular, in [28] the SWP clock was used to obtain an average tunneling time of transmission (reflection) for an incident wave packet, and such time was employed to investigate the Hartman effect [33] for a particle scattered off a square barrier and it was shown that it does not saturate in the opaque regime [28, 34].

The tunneling time scales considered in [23, 28, 31] involve taking an average over the spectral components of the transmitted wave packet and, thus, obscure the interpretation of the resulting average time. In this paper, we take as a starting point the real-valued average tunneling time obtained in [28], using the SWP quantum clock, and obtain a *probability distribution of transmission times*, by using a standard transformation between random variables. In addition to providing a more accurate time characterization of the tunneling process, this should provide a clearer connection with the experiments (which measure a distribution of tunneling times; see, e.g., Figure 4 in [3]). It is worth noting that some approaches using Feynman's path integrals address the problem of obtaining a probabilistic distribution of the tunneling times (see, e.g., [35]). However, these methods in general result in a complex time (or, equivalently, multiple time scales), and some *arbitrary* procedure is needed to select the physically meaningful real time *a posteriori*.

After obtaining a general formula for the distribution of tunneling times, which is the main result of this work, we apply it to two specific cases. First, to illustrate the formalism in a simple scenario, we consider the situation of a particle tunneling through a rectangular barrier. Then, we consider a slight modification of the model proposed in [36] for the tunneling decay of an initially bound state, after the sudden deformation of the binding potential by the application of a strong external field; the modification considered here allows us to investigate the whole range of possibilities for the tunneling times, without having an "upper cutoff", as is the case in the original model. Finally, some additional comments on the results are reserved for the last section.

2. The SWP Clock's Average Tunneling Time

We start by briefly reviewing the time-dependent application of the SWP clock to the scattering of a massive particle off a localized static potential barrier in one dimension (for details see [28]) which is appropriate, since it follows from the three-dimensional Schrödinger equation for this problem that the dynamics is essentially one-dimensional [3].

The SWP clock is a quantum rotor weakly coupled to the tunneling particle and that runs only when the particle is within the region in which $V(x) \neq 0$, where $V(x)$ is the potential energy. The Hamiltonian of the particle-clock system is given by (we use $\hbar = 2\mu = 1$, where μ is the particle's mass) [17]

$$H = -\frac{\partial^2}{\partial x^2} + V(x) + \mathcal{P}(x) H_c, \qquad (1)$$

where $\mathcal{P}(x) = 1$ if $V(x) \neq 0$ and zero otherwise. The clock's Hamiltonian is $H_c = -i\omega(\partial/\partial\theta)$, where the angle $\theta \in [0, 2\pi)$ is the clock's coordinate and $\omega = 2\pi/(2j+1)\vartheta$ is the clock's

angular frequency, with j being a nonnegative integer or half-integer giving the clock's total angular momentum, and ϑ is the clock's resolution. The weak coupling condition amounts to assume that ϑ is large, in such a way that the clock's energy eigenvalues, $\eta_m \equiv m\omega \, (-j < m < j)$, are very small compared to the barrier height and the particle's energy. It is assumed that, at $t = 0$, well before it reaches the barrier, the particle is well-localized far to the left of the barrier and the wave function of the system is a product state of the form

$$\Phi(\theta, x, t = 0) = \psi(x) \, v_0(\theta), \qquad (2)$$

where $\psi(x)$ is the particle's initial state, represented by a wave packet centered around an energy E_0, and the clock initial state is assumed to be "in the zero-th hour" [17]

$$v_0(\theta) = \frac{1}{\sqrt{2j+1}} \sum_{m=-j}^{j} u_m(\theta), \qquad (3)$$

where $u_m(\theta) = e^{im\theta}/\sqrt{2\pi}$ are the clock's eigenfunctions corresponding to the energy eigenvalues η_m.

The state $v_0(\theta)$ is strongly peaked at $\theta = 0$, thus allowing the interpretation of the angle θ as the clock's hand, since for a freely running clock the peak evolves to ωt_c, where t_c is the time measured by the clock [17]. Since here clock and particle are coupled according to (1), when the particle passes through the region $V(x) \neq 0$ it becomes entangled with the clock, with the wave function for the entire system given by

$$\Phi(\theta, x, t) = \frac{1}{\sqrt{2j+1}} \sum_{m=-j}^{j} \Psi^{(m)}(x, t) \, u_m(\theta),$$

$$\Psi^{(m)}(x, t) = \int_0^\infty dk A(k) \psi_k^{(m)}(x) \, e^{-iEt}, \qquad (4)$$

where E is the incident particle's energy, $k = \sqrt{E}$, and $A(k)$ is the Fourier spectral decomposition of the initial wave packet $\psi(x)$ in terms of the free particle eigenfunctions (we are assuming delta-normalized eigenfunctions). The functions $\psi_k^{(m)}(x)$ satisfy a time-independent Schrödinger equation with a constant potential η_m in the barrier region. Outside the potential barrier region and for a particle incident from the left, the (unnormalized) solution $\psi_k^{(m)}(x)$ of the time-independent Schrödinger equation is given by [28]

$$\psi_k^{(m)}(x) = \begin{cases} e^{ikx} + R^{(m)}(k) \, e^{-ikx}, & x \leq -L \\ T^{(m)}(k) \, e^{ikx}, & x \geq L, \end{cases} \qquad (5)$$

where $T^{(m)}(k) \, [R^{(m)}(k)]$ stands for the transmission (reflection) coefficient, and it is assumed, without loss of generality, that the potential is located in the region $-L < x < L$. Considering only the transmitted solution in (5) and substituting it into the time-dependent solution (4), it can be shown that for weak coupling

$$\Phi_{tr}(\theta, x, t)$$
$$= \int_0^\infty dk A(k) T(k) \, e^{i(kx - Et)} v_0 \left(\theta - \omega t_c^T(k) \right), \qquad (6)$$

where

$$t_c^T(k) = -\left(\frac{\partial \varphi_T^{(m)}}{\partial \eta_m}\right)_{\eta_m = 0} \tag{7}$$

is the stationary transmission clock time corresponding to the wave number component k [17, 37]. The transmission coefficient $T(k)$ corresponds to the stationary problem in the absence of the clock.

For *tunneling* times one is interested only in the clock's reading for the *postselected* asymptotically transmitted wave packet. Thus, tracing out the particle's degrees of freedom, the expectation value of the clock's measurement can be defined, resulting in the average tunneling time [28]

$$\left\langle t_c^T \right\rangle = \int dk\, \rho(k)\, t_c(k), \quad \rho(k) = N\, |A(k)\, T(k)|^2, \tag{8}$$

where $N = 1/\int dk |A(k)T(k)|^2$ is a normalization constant and $\rho(k)$ is the probability density of finding the component k in the transmitted wave packet. Similar expressions can be obtained for the reflection time.

3. The Tunneling Times Distribution

An important aspect of the average tunneling time considered in the previous section is that it emphasizes the *probabilistic nature of the tunneling process*. However, since the average in (8) is over the time taken by the *spectral components* of the wave packet, it does not lend itself to an easy interpretation, given the spectral components of the wave packet tunnel with different times. Thus, instead of (8), one would rather obtain an average over (*real*) times of the form

$$\left\langle t_c \right\rangle = \int_0^\infty d\tau\, \tau\, \rho_t(\tau), \tag{9}$$

where $\rho_t(\tau)$ stands for the probability density for observing a particular tunneling time τ for the asymptotically transmitted wave packet. This can easily be achieved by noticing that in probability theory (8) and (9), which must be equal, are related by a standard transformation between the two random variables k and τ through a function $t_c^T(k)$. It follows that the probability distribution of times is given by

$$\rho_t(\tau) = \int \rho(k)\, \delta\left(\tau - t_c^T(k)\right) dk \tag{10}$$

which, in essence, is the statement that all the k-components in the transmitted packet for which $t_c^T(k) = \tau$ must contribute to the value of $\rho_t(\tau)$ with a weight $\rho(k)$. Finally, using the properties of the Dirac delta function (specifically, we use the fact that $\delta(g(x)) = \sum_j (\delta(x - x_j)/|g'(x_j)|)$, where $\{x_j\}$ is the set of zeros of the function $g(x)$ and the prime indicates a derivative with respect to the independent variable), we obtain

$$\rho_t(\tau) = \sum_j \frac{\rho\left(k_j(\tau)\right)}{\left|t_c^{T\prime}\left(k_j(\tau)\right)\right|}, \tag{11}$$

where $\{k_j(\tau)\}$ is the set of zeros of the function $g(k) \equiv t_c^T(k) - \tau$ and $t_c^{T\prime}$ is the derivative of $t_c^T(k)$ with respect to k.

A similar definition of the distribution of tunneling times given in (10)-(11) can be obtained for any time scale which is probabilistic in nature, that is, of the form (8). Although several other probabilistic tunneling times exist in the literature (e.g., [23, 31, 32, 35]), the SWP clock has proven to yield well-behaved *real* times both in the time-independent [17, 37, 38] and time-dependent approaches [28, 34, 39] and it provides a simple procedure to *derive* the probabilistic expression (8). In addition, the role exerted by circularly polarized light in attoclock experiments [3, 25] seems to provide a natural possibility for interpretation in terms of the SWP clock.

As will be illustrated below, for the simple application of this formalism to the problem of a wave packet scattered off a rectangular potential barrier, the distribution of times (10)-(11) cannot, in general, be obtained analytically even for the simplest cases, except in trivial cases such as for a single Dirac delta potential barrier [40–42], in which case $t_c^T(k) = 0$ and $\rho_t(\tau) = \delta(\tau) \int dk \rho(k)$.

It should also be noticed that, despite the fact that the derivation of the previous section leading to (8) and, thus (10)-(11), assumed a scattering situation, these expressions can be shown to be valid for any situation involving preselection of an initial state localized to the left of a potential "barrier" followed by postselection of an asymptotic transmitted wave packet. This allows us to obtain the distribution of times for a model that simulates the tunneling decay of an initially bound particle by ionization induced by the sudden application of a strong external field; the model considered below is a variant of that introduced in [36].

4. The Distribution of Tunneling Times for a Rectangular Barrier

As a first illustration of the formalism developed above, let us consider a rectangular barrier of height V_0 located in the region $x \in (-L, L)$. The particle's initial state $\phi_0(x) \equiv \psi(x, t = 0)$ is assumed to be a Gaussian wave packet

$$\phi_0(x) = \frac{1}{(2\pi)^{1/4}\sqrt{\sigma}} \exp\left[ik_0 x - \frac{(x - x_0)^2}{4\sigma^2}\right], \tag{12}$$

where the parameters x_0, σ, and k_0 are chosen such that the wave packet is sharply peaked in a tunneling wave number $k_0 = \sqrt{E_0} < \sqrt{V_0}$ and is initially well-localized around $x = x_0$, far to the left of the barrier; in the calculations that follow we take $x_0 = -8\sigma$, such that at $t = 0$ the probability of finding the particle within or to the right of the barrier is negligible. The transmission coefficient $T(k)$ and the spectral function $A(k)$ are well-known and given by

$$T(k) = \frac{2ikq e^{-2ikL}}{(k^2 - q^2)\sinh(2Lq) + 2ikq\cosh(2Lq)} \tag{13}$$

$$A(k) = \left(\frac{2}{\pi}\right)^{1/4} \sqrt{\sigma} \exp\left[4k\sigma\left(k_0\sigma + 4i\right)\right. \tag{14}$$
$$\left. - \sigma\left(k + k_0\right)\left(k\sigma + k_0\sigma + 8i\right)\right],$$

where $q = \sqrt{V_0 - k^2}$. The stationary transmission clock time (7) is [22, 28]

$$t_c^T(k) = \frac{k}{q}$$
$$\cdot \frac{\left(q^2 + k^2\right)\tanh\left(2qL\right) + 2qL\left(q^2 - k^2\right)\operatorname{sech}^2\left(2qL\right)}{4q^2k^2 + \left(q^2 - k^2\right)^2\tanh^2\left(2qL\right)}, \tag{15}$$

with tunneling times corresponding to real values of q (i.e., $V_0 > k^2$). Figure 1 shows a plot for the stationary transmission times $t_c^T(k)$, the distribution of wave numbers $\rho(k)$ in the transmitted wave packet, and the distribution $|A(k)|^2$ of wave numbers (momenta) in the incident packet, for two values of the barrier width. For the chosen parameters and barrier widths both the incident and the transmitted wave packets have an energy distribution very strongly peaked in a tunneling component (in the bottom plot of Figure 1 the barrier is much more opaque than that in the top plot and we can observe that—despite being with a negligible probability for the parameters chosen for this plot—in this situation some above-the-barrier components start to appear in the distribution of the transmitted wave packet. So, in order to consider mainly transmission by tunneling we must restrict the barrier widths to not too large ones). We also observe the very well-known fact that the transmitted wave packet "speeds up" when compared to the incident particle [28]. As a general rule, the larger is the barrier width (i.e., the more opaque is the barrier), the greater is the translation of the central component towards higher momenta. In what concerns the off-resonance stationary transmission time, it initially grows with the barrier width, and saturates for very opaque barriers (the Hartman effect); on the other hand, it presents peaks at resonant wave numbers that grow and narrow with the barrier width; for a detailed discussion see [28]).

Figure 2 shows plots of the probability distribution $\rho_t(\tau)$ of the tunneling times according to (10)-(11), corresponding to both the barrier widths shown in Figure 1 [to obtain these plots we used a Monte Carlo procedure to generate a large number of k outcomes from the distribution $\rho(k)$, which afterwards were transformed into τ values by using the function $\tau = t_c^T(k)$]. The vertical grey lines in these plots correspond to the time the light takes to cross the barrier distance. It is observed that for the two distributions shown in Figure 2 the probability to observe superluminal tunneling times is negligible. It is also observed that these distributions have a shape that resembles that of the k distribution, albeit with a more pronounced skewness. This shape could be inferred from Figure 1 and from (11), since $t_c^{T\prime}(k)$ grows very smoothly in the region were $\rho(k)$ is nonvanishing. Furthermore, a comparison between the two plots in Figure 2 shows that the tunneling times do not grow linearly with the barrier width and, therefore, the distribution
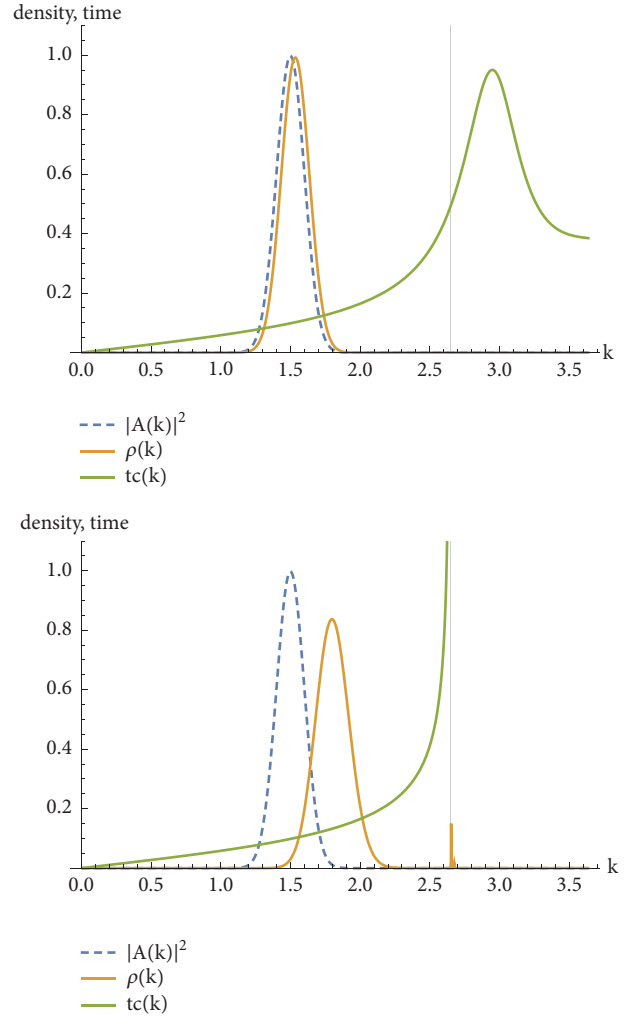
FIGURE 1: Stationary transmission clock time $t_c^T(k)$ (green) and the distributions $\rho(k)$ (orange and arbitrary scale) and $|A(k)|^2$ (blue, dashed, and arbitrary scale) for the transmitted and incident wave packets, respectively. Rydberg atomic units $\hbar = 2\mu = 1$ are used in all plots; the tunneling energies correspond to $0 < k < \sqrt{7}$, corresponding to a barrier height $V_0 = 7$ (the maximum tunneling wave number $\sqrt{7}$ is shown by a vertical grey line in the plots). In both plots the incident wave packet parameters are $k_0 = 1.5, \sigma = 5, x_0 = -8\sigma$. *Top:* barrier width $2L = 2$. *Bottom:* barrier width $2L = 16$.

in the bottom plot of Figure 2 is "closer" to the light time than the distribution shown in the top plot; [28] already observed that for intermediate values of barrier widths the average transmission time—corresponding to the mean of the distribution ρ_t—reaches a plateau.

5. Distribution of Ionization Tunneling Times

In this section we obtain a distribution for tunneling times for a particle that is initially in a bound state of a given binding potential. The potential is then suddenly deformed in such a way that the particle can escape from the initially confining region by tunneling. The model considered here is a slight modification of that proposed by Ban *et al.* [36] to simulate,
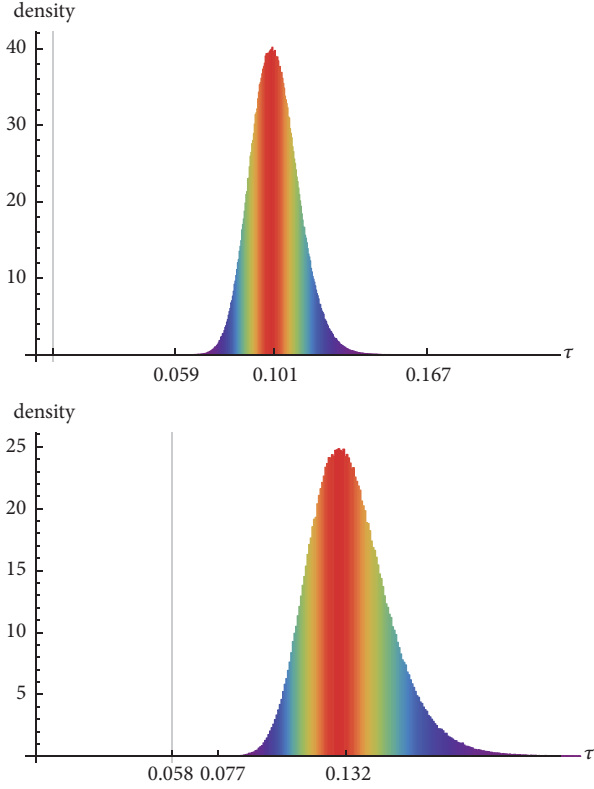
FIGURE 2: Probability distribution $\rho_t(\tau)$ for the tunneling times τ, obtained by Monte Carlo samplings of k-values from the distribution $\rho(k)$ and then transforming these to time values through $\tau = t_c^T(k)$. The parameters are the same as in the corresponding plots in Figure 1 and are all expressed in Rydberg atomic units. *Top: 2L = 2. Bottom: 2L = 16.* These plots are in the same range and scale and can be compared. The vertical grey line in both plots corresponds to the time the light takes to traverse the barrier distance. The ticks in the horizontal axes correspond to the light time, the minimum, the median and the maximum values of τ in the histogram (in the bottom plot the maximum τ is out of the plot's range).

in a simple scenario, key features of the decay of a localized state by tunneling ionization induced by the application of a strong external field with a finite duration.

In [36], for $t < 0$, the particle is in an eigenstate of a semi-infinite square-well potential $V_1(x)$,

$$V_1(x) = \begin{cases} +\infty & x < 0 \\ 0 & 0 \leq x \leq a \\ V_0 & x > a, \end{cases} \qquad (16)$$

and, therefore, it cannot decay by tunneling. At $t = 0$ the potential is suddenly deformed to $V_2(x)$,

$$V_2(x) = \begin{cases} +\infty & x < 0 \\ 0 & 0 \leq x \leq a \\ V_0 & a < x < b \\ 0 & x \geq b, \end{cases} \qquad (17)$$

such that the particle can now tunnel through the potential barrier; it is assumed that the wave function does not change during the sudden change of the potential. Finally, after a finite time t_0 the potential returns to its original configuration, $V_1(x)$, and tunneling terminates. The cutoff time t_0 mimics the natural upper bound for tunneling times measured in recent attoclock experiments (see, e.g., [3, 6] and references therein), since the opening and closing of the tunneling channel in these experiments occur in intervals of half the laser field's period.

Here, we deviate from [36] by setting $t_0 \longrightarrow \infty$; i.e., once deformed the potential does not return to its original form and, after a long enough time, the particle will be transmitted with unit probability; thus, by eliminating the cutoff (which is just an experimental limitation) we are able to explore the whole range of possibilities for the ionization tunneling time. In addition, for $t \geq 0$, the particle is assumed to be coupled to a SWP quantum clock running only in the region (a, b), so that the clock's readings for the asymptotic transmitted wave packet give the time the particle spent within the barrier after $t = 0$. Following [36], we assume that for $t < 0$ the particle is in the ground state of the potential $V_1(x)$, whose stationary wave function is given by

$$\phi_0(x) = N \begin{cases} \sin(k_0 x), & 0 < x \leq a \\ \sin k_0 e^{q_0(a-x)}, & x > a, \end{cases} \qquad (18)$$

where N is a normalization constant, $k_0 = \sqrt{E_0}$, E_0 is the ground state energy, and $q_0 = \sqrt{V_0 - k_0^2}$. It is also assumed, as in [36], that immediately after the sudden deformation of the potential from $V_1(x)$ to $V_2(x)$, at $t = 0$, the wave function does not change. However, for $t \geq 0$ the particle state, which is no longer an energy eigenstate, is given by a superposition of the energy eigenstates $\psi_k(x)$ ($k = \sqrt{E}$) of the potential $V_2(x)$, i.e., [36]

$$\psi(x, t = 0) = \phi_0(x) = \int_0^\infty S(k) \psi_k(x) \, dk, \qquad (19)$$

where

$$S(k) = \int_0^\infty \phi_0(x) \psi_k^*(x) \, dx, \qquad (20)$$

with

$$\psi_k(x) = \begin{cases} A(k)\sin(kx), & 0 < x \leq a \\ C(k)e^{qx} + D(k)e^{-qx}, & a < x \leq b \\ \sqrt{\dfrac{2}{\pi}}\cos[k(x-b) + \Omega(k)], & x > b, \end{cases} \qquad (21)$$

where $q = \sqrt{V_0 - k^2}$ and the coefficients $A(k), C(k), D(k)$ and the phase $\Omega(k)$ are determined by the usual boundary conditions at $x = a$ and $x = b$ and are such that the normalization $\langle \psi_k(x), \psi_{k'}(x) \rangle = \delta(k - k')$ holds [36]. From the above expressions it follows that, without any loss of generality, we can take $S(k)$ and all the eigenfunctions (21) to be real.

In order to consider the coupling with the SWP clock for times $t \geq 0$ we proceed as follows. At $t = 0$ the system particle+clock is described by the product state $\psi(x,0)v_0(\theta)$, where $\psi(x,0)$ is the state (19) and $v_0(\theta)$ is the initial clock state given by (3). After $t = 0$ the particle and the clock states become entangled. For the procedure of postselection of the asymptotically transmitted wave function we notice that the role of the transmission coefficient for the wave function (21) is played by $\sqrt{2/\pi}\, e^{i(-kb+\Omega^{(m)}(k))}$, where the superscript m indicates the weak coupling with the clock. The right moving *asymptotic* wave packet representing the coupled system formed by the transmitted particle and the clock is

$$\Phi_{tr}(\theta,x,t) = \int_0^\infty dk S(k)\, e^{i[k(x-b)+\Omega^{(m)}(k)-Et]} \quad (22)$$
$$\times v_0\left[\theta - \omega t_c^T(k)\right],$$

where, as before, $t_c^T(k) = -(\partial\Omega^{(m)}(k)/\partial\eta_m)_{\eta_m=0} = -(1/2q)(\partial\Omega/\partial q)$ [with quantities without the subscript "(m)" representing the limit $\eta_m \longrightarrow 0$]. By following the same steps described in [28], we trace out the clock's degree of freedom in the asymptotic transmitted wave packet in order to obtain the distribution $\rho(k)$ of the wave numbers for the asymptotically transmitted wave packet, which in this case is simply given by

$$\rho(k) = |S(k)|^2; \quad (23)$$

i.e., the probability to find a wave number k in the asymptotic transmitted wave packet is the same as in the initial state, which is as expected, since after a long enough time the initial wave packet will be transmitted with probability unit, as mentioned earlier.

The general behavior of $t_c^T(k)$ and $\rho(k)$ is illustrated in Figures 3 and 4, corresponding to two barriers with different opacities ($b - a = 2$ and 4, respectively). These plots show, as expected, that the distribution $\rho(k)$ is strongly peaked at the wave number k_0, corresponding to the energy of the initially bound state and is negligible for nontunneling components. For tunneling wave numbers ($k < \sqrt{V_0}$) the function $t_c^T(k)$ is also strongly peaked at the same wave number k_0, which corresponds to a local maximum (for nontunneling wave numbers there are several other resonance peaks). From (11) we would expect that the peaks in the tunneling times distribution $\rho_t(\tau)$ would occur for times $\tau = t_c^T(k)$ corresponding to values of k for which $t_c^{T\prime}(k) \approx 0$—which occur at points of local maxima and minima of the function $t_c^T(k)$—*and* corresponding to nonnegligible $\rho(k)$. Therefore, from the plots in Figures 3 and 4 one could expect the first peak of the tunneling time distribution $\rho_t(\tau)$ at $\tau \approx 0.105$ *a.u.* (the local minimum of $t_c^T(k)$, which is similar for both barrier widths, since nonresonant times $t_c^T(k)$ change little with the barrier width for opaque barriers, as is the case in Figures 3 and 4); a second peak in $\rho_t(\tau)$ is expected to occur around the local maximum of $t_c^T(k)$, which corresponds to $\tau \approx t_c^T(k_0)$ (this local maximum—corresponding to resonant wave numbers—changes significantly with the barrier widths; see, e.g., [28]). On the other hand, peaks in

Figure 3: *Top*: the stationary transmission clock time $t_c^T(k)$ (blue) and the wave number distribution $\rho(k) = |S(k)|^2$ (orange, dashed, and arbitrary scale), for $V_0 = 7$, $a = 1$, $b = 3$, and $k_0 \approx 2.175932$), with the initial state given by (18). *Bottom*: close view of the above plot for small times. The vertical grey lines in the plots correspond to $k = k_0$ and $k = \sqrt{V_0}$. The regions in which $t_c^{T\prime}(k) \approx 0$ (around the local maximum and minimum of $t_c^T(k)$) correspond to times $\tau \approx t_c^T(k_0)$ and $\tau \approx 0.105$ *a.u.* Rydberg atomic units were used in all the plots.

$\rho_t(\tau)$ coming from local maxima (resonances) and minima associated with nontunneling values of k are suppressed, since $\rho(k) \approx 0$ in these cases. Figure 5 confirm these claims. For both barrier widths considered, the distribution of tunneling times is "U" shaped, having peaks at the times corresponding to the local maxima and minima of the stationary time $t_c^T(k)$ inside the tunneling region. It should be observed that the larger is the barrier width, the broader is the tunneling time distribution, due to the strong increase of the resonant tunneling time with the barrier width.

Figures 6 and 7 show close views of the tunneling time distributions $\rho_t(\tau)$ for small and large tunneling times (Figure 6 corresponds to the plot at the top of Figure 5, while Figure 7 corresponds to the plot at the bottom of Figure 5). In the top plots of these Figures we can clearly observe the first peak around the local minimum of $t_c(k)$ in the tunneling
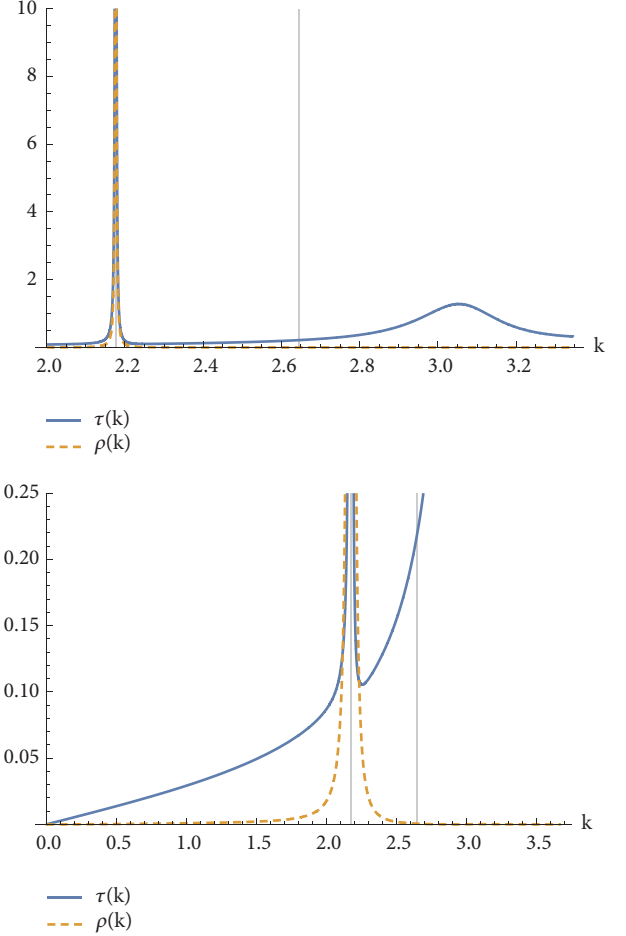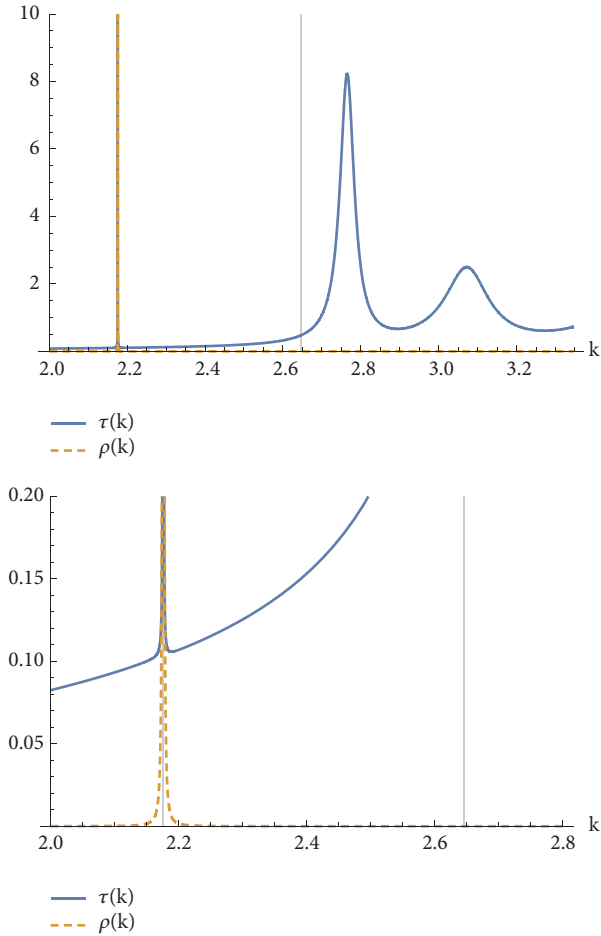
FIGURE 4: *Top*: the stationary transmission clock time $t_c^T(k)$ (blue) and the wave number distribution $\rho(k) = |S(k)|^2$ (orange, dashed, and arbitrary scale), for $V_0 = 7$, $a = 1$, $b = 5$, and $k_0 \approx 2.175932$), with the initial state given by (18). *Bottom*: close view of the above plot for small times. The vertical grey lines in the plots correspond to $k = k_0$ and $k = \sqrt{V_0}$. The region of relatively slow growth of the derivative $t^{T\prime}(k)$ correspond to times around 0.105 *a.u.* Rydberg atomic units were used in all the plots.

FIGURE 5: Distributions of tunneling decay times $\rho_t(\tau)$ through the barrier of the potential $V_2(x)$ for the initial bound state $\phi_0(x)$ given by (18). The histograms were built by using the Monte Carlo procedure described in Figure 2 and in the main text. The vertical grey lines indicate percentiles of the distribution (the first and the last correspond to 1% and 99%, the remaining ones range from 5% to 95%, in steps of 5%); the three thick vertical lines indicate the first quartile (percentile 25%), the median, and the third quartile (percentile 75%). Rydberg atomic units were used in all the plots. *Top*: barrier width $b - a = 2$ and bin length $\approx 0.0031 a.u.$ (≈ 0.15 attoseconds). *Bottom*: barrier width $b - a = 4$ and bin length $\approx 40 a.u.$ ($\approx 1,935$ attoseconds).

region, which in both plots corresponds to almost the same value $\tau \approx 0.105$ *a.u* ≈ 5.1 attoseconds. The top plot of Figure 6 shows that for the less opaque barrier there exists a (very small) probability to observe a superluminal tunneling time. Even if this possibility cannot be precluded in principle (see, e.g., [16]), in the present case the possibility of emergence of such small times was expected, since at $t = 0$ there was a significant portion of the wave packet (roughly 27%) penetrating the whole distance of the barrier, and this has an important contribution to the emergence of small times in the clock's readings associated with the transmitted particle. On the other hand, the top plot of Figure 7 shows that for the thicker barrier the probability for superluminal times is negligible; the portion of the wave packet already inside the barrier at $t = 0$ is the same (~27%), but the wave packet penetrates proportionally a smaller distance inside the barrier and, thus, it does not contribute in a significant way to the

emergence of very small times in the clock readings. We note that the introduction of the cutoff t_0, as in [36], would result in a time distribution similar to the truncated distributions shown in the top plots of Figures 6 and 7.

It is also worth observing that, for small times, the distributions obtained here resemble qualitatively those in Figure 4 of [3], except for the presence of several peaks at discrete values of the time in the latter. The considerations above, relating the peaks of the distribution of clock times $\rho_t(\tau)$ to the local maxima and minima of the stationary time $t_c^T(k)$ and the magnitude of distribution $\rho(k)$ in the neighborhood of these points, suggest a scenario in which such multiple peaks at discrete values of time can appear in the distribution $\rho_t(\tau)$ of transmission times. Indeed, if above-the-barrier wave numbers had a significant contribution to the initial wave packet, then the several local maxima and minima present in the vicinities of the resonant *nontunneling* components will also contribute in a significant way to build
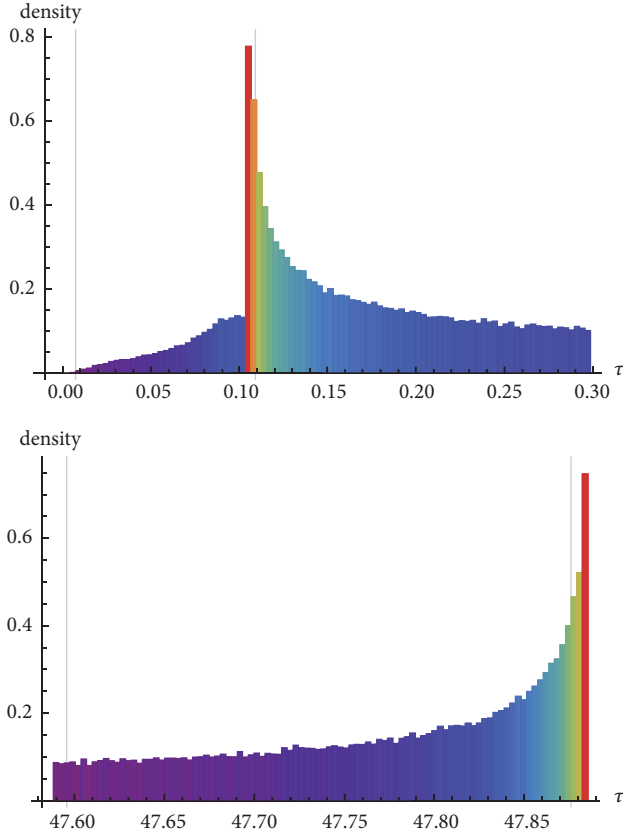
FIGURE 6: Close views of the plot at the top of Figure 5, corresponding to the barrier width $b - a = 2$, with the bin length $\approx 0.0031 a.u.$ (≈ 0.15 attoseconds). *Top*: small tunneling times. The vertical grey line in the left of this plot corresponds to the time the light takes to travel the barrier distance. The second grey vertical line corresponds to the percentile 1%. *Bottom:* large tunneling times. The vertical grey lines correspond to the percentiles 95% and 99%, respectively.

FIGURE 7: Close views of the plot at the bottom of Figure 5, corresponding to the barrier width $b - a = 4$. *Top*: small tunneling times and bin length $\approx 0.0031 a.u.$ (≈ 0.15 attoseconds). The vertical grey line in the left of this plot corresponds to the time the light takes to travel the barrier distance. The percentile 1% (corresponding to $\approx 5.1\ a.u. \approx 247$ attoseconds) is out of the range of this plot. *Bottom:* large tunneling times, with bin length $\approx 2\ a.u \approx 100$ attoseconds. The vertical grey line corresponds to the percentile 99%.

multiple peaks in the distribution of transmission times; these peaks, however, could not be associated with the tunneling process. We can consider such a scenario by choosing as the initial state a tightly localized state given by $\psi(x, 0) = \sqrt{2} \sin k_0 x$, with $k_0 = \pi$ and the barrier parameters $a = 1$, $b = 2$, and $V_0 = 11$, in Rydberg atomic units. In this situation the initial wave function is perfectly confined to the left of the barrier ($0 < x < 1$), and above-the-barrier components contribute in a significant way to build the wave packet, as can be seen from $\rho(k)$ in the top plot of Figure 8 (in this case the probability of finding a nontunneling k component in the wave packet is approximately 75%). In this plot we can also observe that all the local maxima and minima of $t_c^T(k)$ shown occur in neighborhoods of wave numbers k for which $\rho(k)$ is nonnegligible; therefore, all these local maxima and minima contribute significantly to build multiple peaks in the distribution of transmission times $\rho_t(\tau)$. The middle and the bottom plots of Figure 8 confirm this statement: all the peaks of the distribution of transmission times correspond very closely to the local maxima and minima of $t_c(k)$, as can be seen by comparing the plots in the top and the bottom of this figure (except for the first, all the other significant

peaks in the bottom plot are associated with nontunneling components).

6. Conclusions

Taking as a starting point the *probabilistic* (average) tunneling time obtained in [28] with the use of a SWP clock [17, 24, 37], we obtained a *probability distribution of times* (10)-(11). An important advantage of using the SWP clock, in addition to those already mentioned, is that by running only when the particle is inside the barrier it allows us to address the concept of *tunneling* time in a proper way, since the time spent by the particle standing in the well *before* penetrating the barrier is *not* computed. A clear advantage of having a probability distribution of transmission (tunneling) times is that, in addition to the usual expectation value, we can obtain *all* the statistical properties of this time, such as its most probable values (peaks of the distribution), the dispersion around the mean value, and the probability to observe extreme outcomes (superluminal times, for instance).

As an initial test, the distribution of times (10)-(11) was applied to the simple problem of a particle tunneling through
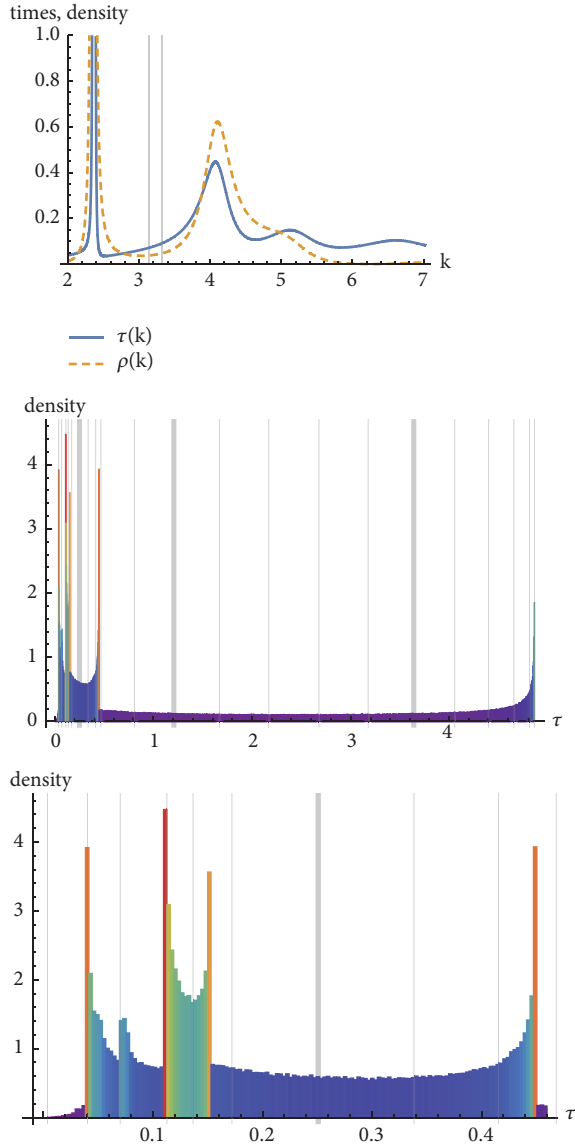
FIGURE 8: *Top*: the stationary time $t_c^T(k)$ and the wave number distribution $\rho(k)$, for $V_0 = 11$, barrier width $b - a = 36$, $k_0 = \pi$, and an initial state $\psi(x, 0) = \sqrt{2} \sin k_0 x$, with $k_0 = \pi$. The vertical lines correspond to $k = k_0$ and $k = \sqrt{V_0}$. *Middle*: distribution $\rho_t(\tau)$ for the transmission times, with the histogram built by the Monte Carlo procedure described in the text. Vertical lines indicate the percentiles, as in the Figure 5. *Bottom*: close view of the above histogram for the range of small times. The first vertical line at the left indicates the time the light takes to cross the barrier distance. In both the histograms we used a bin length ≈ 0.0031 *a.u.* ≈ 0.15 attoseconds. Rydberg atomic units were used in all these plots.

a rectangular barrier. Unsurprisingly, it revealed behavior similar to that already known from previous works using a distribution of wave numbers (momentum)—see, e.g., [28]—although, using $\rho_t(\tau)$ these conclusions are much more transparent. For example, one could answer the question about the possibility of superluminal tunneling by direct calculation from the probability distribution $\rho_t(\tau)$. In the nonstationary case—which is the correct to address this question—this problem is usually answered by considering

just the average tunneling time. But, given its probabilistic nature, an answer based only on the average time may not be satisfactory, especially if the dispersion of the distribution of tunneling times is large, which is often the case when one deals with well-localized particles, as suggested by the two situations addressed in the present work.

As a main application of (10)-(11), we considered a slight modification of the problem considered in [36] to model strong field ionization by tunneling. The modification considered here was the elimination of the cutoff time that was introduced in [36] to simulate the upper bound that arises in attoclock experiments [3, 6] due to the opening and closing of the tunneling channel, naturally associated with the oscillations in the laser field intensity. This cutoff is not a fundamental requirement, but rather it is associated with the experimental methods employed—in any case, its implementation is rather trivial, since it just truncates the distribution of times. The consideration of the full range of the distribution of times allowed us to show that an important contribution to $\rho_t(\tau)$ comes from very large times associated with the resonance peaks in the tunneling region; these very long tunneling times occur with a probability comparable to very short ones, thus having an important impact on the average tunneling times and, therefore, cause difficulties when comparing theoretical predictions based on an average time with the outcomes of experiments presenting a natural cutoff in the possible time measurements. In particular, in the attoclock experiments the relevant measure is often associated with the peak of the tunneling time, which may be promptly identified once one knows the probability distribution for all possible times. A remark is in place; the distribution of times proposed here, built on the SWP clock readings, refers to the time the particle *dwells within* the barrier, while the tunneling times often measured in recent attoclock experiments actually refer to *exit* times [43].

In sum, the approach introduced above and resulting in (10)-(11) builds upon the already (conceptually) well tested SWP clock to provide a real-valued distribution of times that, in the simple models considered here, was demonstrated to have physically sound properties and, in fact, (rough) similarities with the time distribution obtained in recent experiments [3], therefore warrantying further investigation with more realistic potentials.

Data Availability

The numerical data used in the construction of the histograms in this article were generated by a Monte Carlo procedure, whose details were described in the main text.

Conflicts of Interest

The authors declare that they have no conflicts of interest.

References

[1] H. G. Winful, "Tunneling time, the Hartman effect, and superluminality: a proposed resolution of an old paradox," *Physics Reports*, vol. 436, no. 1-2, pp. 1–69, 2006.

[2] H. G. Winful, "The meaning of group delay in barrier tunnelling: a re-examination of superluminal group velocities," *New Journal of Physics*, vol. 8, Article ID 101, 2006.

[3] A. S. Landsman, M. Weger, J. Maurer et al., "Ultrafast resolution of tunneling delay time," *Optica*, vol. 1, no. 5, pp. 343–349, 2014.

[4] L. Torlina, F. Morales, J. Kaushal et al., "Interpreting attoclock measurements of tunnelling times," *Nature Physics*, vol. 11, no. 6, pp. 503–508, 2015.

[5] O. Pedatzur, G. Orenstein, V. Serbinenko et al., "Attosecond tunnelling interferometry," *Nature Physics*, vol. 11, no. 10, pp. 815–819, 2015.

[6] T. Zimmermann, S. Mishra, B. R. Doran, D. F. Gordon, and A. S. Landsman, "Tunneling time and weak measurement in strong field ionization," *Physical Review Letters*, vol. 116, no. 23, Article ID 233603, 2016.

[7] R. Chiao, P. Kwiat, and A. Steinberg, "Analogies between electron and photon tunneling: a proposed experiment to measure photon tunneling times," *Physica B: Condensed Matter*, vol. 175, no. 1–3, pp. 257–262, 1991.

[8] A. M. Steinberg, P. G. Kwiat, and R. Y. Chiao, "Measurement of the single-photon tunneling time," *Physical Review Letters*, vol. 71, no. 5, pp. 708–711, 1993.

[9] C. R. Leavens and R. Sala Mayato, "Are predicted superluminal tunneling times an artifact of using nonrelativistic Schrödinger equation?" *Annalen der Physik*, vol. 7, no. 7-8, pp. 662–670, 1999.

[10] P. Krekora, Q. Su, and R. Grobe, "Effects of relativity on the time-resolved tunneling of electron wave packets," *Physical Review A: Atomic, Molecular and Optical Physics*, vol. 63, no. 3, Article ID 032107, 2001.

[11] C.-F. Li and X. Chen, "Traversal time for Dirac particles through a potential barrier," *Annalen der Physik*, vol. 11, no. 12, pp. 916–925, 2002.

[12] V. Petrillo and D. Janner, "Relativistic analysis of a wave packet interacting with a quantum-mechanical barrier," *Physical Review A: Atomic, Molecular and Optical Physics*, vol. 67, no. 1, Article ID 012110, 2003.

[13] X. Chen and C. Li, "Negative group delay for Dirac particles traveling through a potential well," *Physical Review A: Atomic, Molecular and Optical Physics*, vol. 68, no. 6, Article ID 052105, 2003.

[14] S. De Leo and P. Rotelli, "Dirac equation studies in the tunneling energy zone," *The European Physical Journal C*, vol. 51, no. 1, pp. 241–247, 2007.

[15] J. T. Lunardi and L. A. Manzoni, "Relativistic tunneling through two successive barriers," *Physical Review A: Atomic, Molecular and Optical Physics*, vol. 76, no. 4, Article ID 042111, 2007.

[16] J. T. Lunardi, L. A. Manzoni, A. T. Nystrom, and B. M. Perreault, "Average transmission times for the tunneling of wave packets," *Journal of Russian Laser Research*, vol. 32, no. 5, pp. 431–438, 2011.

[17] A. Peres, "Measurement of time by quantum clocks," *American Journal of Physics*, vol. 48, no. 7, pp. 552–557, 1980.

[18] E. P. Wigner, "Lower limit for the energy derivative of the scattering phase shift," *Physical Review*, vol. 98, no. 1, p. 145, 1955.

[19] F. T. Smith, "Lifetime matrix in collision theory," *Physical Review*, vol. 118, no. 1, p. 349, 1960.

[20] A. I. Baz', "Lifetime of intermediate states," *Soviet Journal of Nuclear Physics*, vol. 4, p. 182, 1967.

[21] V. F. Rybachenko, "Time penetration of a particle through a potential barrier," *Soviet Journal of Nuclear Physics*, vol. 5, p. 635, 1967.

[22] M. Büttiker, "Larmor precession and the traversal time for tunneling," *Physical Review B*, vol. 27, no. 10, p. 6178, 1983.

[23] J. P. Falck and E. H. Hauge, "Larmor clock reexamined," *Physical Review B: Condensed Matter and Materials Physics*, vol. 38, no. 5, pp. 3287–3297, 1988.

[24] H. Salecker and E. P. Wigner, "Quantum limitations of the measurement of space-time distances," *Physical Review*, vol. 109, pp. 571–577, 1958.

[25] P. Eckle, A. N. Pfeiffer, C. Cirelli et al., "Attosecond ionization and tunneling delay time measurements in helium," *Science*, vol. 322, no. 5907, pp. 1525–1529, 2008.

[26] G. Orlando, C. R. McDonald, N. H. Protik, G. Vampa, and T. Brabec, "Tunnelling time, what does it mean?" *Journal of Physics B: Atomic, Molecular and Optical Physics*, vol. 47, no. 20, Article ID 204002, 2014.

[27] A. S. Landsman and U. Keller, "Attosecond science and the tunnelling time problem," *Physics Reports*, vol. 547, pp. 1–24, 2015.

[28] J. T. Lunardi, L. A. Manzoni, and A. T. Nystrom, "Salecker–Wigner–Peres clock and average tunneling times," *Physics Letters A*, vol. 375, no. 3, pp. 415–421, 2011.

[29] N. G. Kelkar, H. M. Castañeda, and M. Nowakowski, "Quantum time scales in alpha tunneling," *Europhysics Letters*, vol. 85, no. 2, Article ID 20006, 2009.

[30] M. Goto, H. Iwamoto, V. De Aquino, V. C. Aguilera-Navarro, and D. H. Kobe, "Relationship between dwell, transmission and reflection tunnelling times," *Journal of Physics A: Mathematical and General*, vol. 37, no. 11, pp. 3599–3606, 2004.

[31] S. Brouard, R. Sala, and J. G. Muga, "Systematic approach to define and classify quantum transmission and reflection times," *Physical Review A: Atomic, Molecular and Optical Physics*, vol. 49, no. 6, pp. 4312–4325, 1994.

[32] V. Petrillo and V. S. Olkhovsky, "Time asymptotic expansion of the tunneled wave function for a double-barrier potential," *Europhysics Letters*, vol. 74, no. 2, p. 327, 2006.

[33] T. E. Hartman, "Tunneling of a wave packet," *Journal of Applied Physics*, vol. 33, pp. 3427–3433, 1962.

[34] B. A. Frentz, J. T. Lunardi, and L. A. Manzoni, "Average clock times for scattering through asymmetric barriers," *European Physical Journal Plus*, vol. 129, no. 1, Article ID 5, 2014.

[35] N. Turok, "On quantum tunneling in real time," *New Journal of Physics*, vol. 16, Article ID 063006, 2014.

[36] Y. Ban, E. Y. Sherman, J. G. Muga, and M. Büttiker, "Time scales of tunneling decay of a localized state," *Physical Review A: Atomic, Molecular and Optical Physics*, vol. 82, no. 6, Article ID 062121, 2010.

[37] M. Calçada, J. T. Lunardi, and L. A. Manzoni, "Salecker-Wigner-Peres clock and double-barrier tunneling," *Physical Review A: Atomic, Molecular and Optical Physics*, vol. 79, no. 1, Article ID 012110, 2009.

[38] C.-S. Park, "Transmission time of a particle in the reflectionless Sech-squared potential: quantum clock approach," *Physics Letters A*, vol. 375, no. 38, pp. 3348–3354, 2011.

[39] C.-S. Park, "Barrier interaction time and the Salecker-Wigner quantum clock: wave-packet approach," *Physical Review A*, vol. 80, no. 1, Article ID 012111, 2009.

[40] Y. Aharonov, N. Erez, and B. Reznik, "Superoscillations and tunneling times," *Physical Review A: Atomic, Molecular and Optical Physics*, vol. 65, no. 5, Article ID 052124, 2002.

[41] Y. Aharonov, N. Erez, and B. Reznik, "Superluminal tunnelling times as weak values," *Journal of Modern Optics*, vol. 50, no. 7, pp. 1139–1149, 2003.

[42] M. A. Lee, J. T. Lunardi, L. A. Manzoni, and E. A. Nyquist, "Double General Point Interactions: Symmetry and Tunneling Times," *Frontiers in Physics*, vol. 4, Article ID 10, 2016.

[43] N. Teeny, E. Yakaboylu, H. Bauke, and C. H. Keitel, "Ionization time and exit momentum in strong-field tunnel ionization," *Physical Review Letters*, vol. 116, no. 6, Article ID 063003, 2016.

Research Article

From de Sitter to de Sitter: Decaying Vacuum Models as a Possible Solution to the Main Cosmological Problems

G. J. M. Zilioti,[1] **R. C. Santos,**[2] **and J. A. S. Lima** [iD][3]

[1]*Universidade Federal do ABC (UFABC), Santo André, 09210-580 São Paulo, Brazil*
[2]*Departamento de Física, Universidade Federal de São Paulo (UNIFESP), 09972-270 Diadema, SP, Brazil*
[3]*Departamento de Astronomia, Universidade de São Paulo (IAGUSP), Rua do Matão 1226, 05508-900 São Paulo, Brazil*

Correspondence should be addressed to J. A. S. Lima; jas.lima@iag.usp.br

Decaying vacuum cosmological models evolving smoothly between two extreme (very early and late time) de Sitter phases are able to solve or at least to alleviate some cosmological puzzles; among them we have (i) the singularity, (ii) horizon, (iii) graceful-exit from inflation, and (iv) the baryogenesis problem. Our basic aim here is to discuss how the coincidence problem based on a large class of running vacuum cosmologies evolving from de Sitter to de Sitter can also be mollified. It is also argued that even the cosmological constant problem becomes less severe provided that the characteristic scales of the two limiting de Sitter manifolds are predicted from first principles.

1. Introduction

The present astronomical observations are being successfully explained by the so-called cosmic concordance model or Λ_0CDM cosmology [1]. However, such a scenario can hardly provide by itself a definite explanation for the complete cosmic evolution involving two unconnected accelerating inflationary regimes separated by many aeons. Unsolved mysteries include the predicted existence of a space-time singularity in the very beginning of the Universe, the "graceful-exit" from primordial inflation, the baryogenesis problem, that is, the matter-antimatter asymmetry, and the cosmic coincidence problem. Last but not least, the scenario is also plagued with the so-called cosmological constant problem [2].

One possibility for solving such evolutionary puzzles is to incorporate energy transfer among the cosmic components, as what happens in decaying or running vacuum models or, more generally, in the interacting dark energy cosmologies. Here we are interested in the first class of models because the idea of a time-varying vacuum energy density or $\Lambda(t)$-models ($\rho_\Lambda \equiv \Lambda(t)/8\pi G$) in the expanding Universe is physically

more plausible than the current view of a strict constant Λ [3–13].

The cosmic concordance model suggests strongly that we live in a flat, accelerating Universe composed of $\sim 1/3$ of matter (baryons + dark matter) and $\sim 2/3$ of a constant vacuum energy density. The current accelerating period ($\ddot{a} > 0$) started at a redshift $z_a \sim 0.69$ or equivalently when $2\rho_\Lambda = \rho_m$. Thus, it is remarkable that the constant vacuum and the time-varying matter-energy density are of the same order of magnitude just by now thereby suggesting that we live in a very special moment of the cosmic history. This puzzle ("why now"?) has been dubbed by the cosmic coincidence problem (CCP) because of the present ratio $\Omega_m/\Omega_\Lambda \sim \mathcal{O}(1)$, but it was almost infinite at early times [14, 15]. There are many attempts in the literature to solve such a mystery, some of them closely related to interacting dark energy models [16–18].

Recently, a large class of flat nonsingular FRW type cosmologies, where the vacuum energy density evolves like a truncated power-series in the Hubble parameter H, has been discussed in the literature [19–22] (its dominant term behaves like $\rho_\Lambda(H) \propto H^{n+2}, n > 0$). Such models has some interesting features; among them, there are (i) a new

mechanism for inflation with no "graceful-exit" problem, (ii) the late time expansion history which is very close to the cosmic concordance model, and (iii) a smooth link between the initial and final de Sitter stages through the radiation and matter dominated phases.

In this article we will show in detail how the coincidence problem is also alleviated in the context of this class of decaying vacuum models. In addition, partially based on previous works, we also advocate here that a generic running vacuum cosmology providing a complete cosmic history evolving between two extreme de Sitter phases is potentially able to mitigate several cosmological problems.

2. The Model: Basic Equations

The Einstein equations, $G^{\mu\nu} = 8\pi G \ [T_{(\Lambda)}^{\mu\nu} + T_{(T)}^{\mu\nu}]$, for an interacting vacuum-matter mixture in the FRW geometry read [19, 20]

$$8\pi G \ \rho_T + \Lambda (H) = 3H^2, \tag{1}$$

$$8\pi G \ p_T - \Lambda (H) = -2\dot{H} - 3H^2, \tag{2}$$

where $\rho_T = \rho_M + \rho_R$ and $p = p_M + p_R$ are the total energy density and pressure of the material medium formed by nonrelativistic matter and radiation. Note that the bare Λ appearing in the geometric side was absorbed on the matter-energy side in order to describe the effective vacuum with energy density $\rho_\Lambda = -p_\Lambda \equiv \Lambda(H)/8\pi G$. Naturally, the time dependence of Λ is provoked by the vacuum energy transfer to the fluid component. In this context, the total energy conservation law, $u_\mu [T_{(\Lambda)}^{\mu\nu} + T_{(T)}^{\mu\nu}]_{;\nu} = 0$, assumes the following form:

$$\dot{\rho}_T + 3H (\rho_T + p_T) = -\dot{\rho}_\Lambda \equiv -\frac{\dot{\Lambda}}{8\pi G}. \tag{3}$$

What about the behavior of $\dot{\Lambda}$? Assuming that the created particles have zero chemical potential and that the vacuum fluid behaves like a condensate carrying no entropy, as what happens in the Landau-Tisza two-fluid description employed in helium superfluid dynamics[23], it has been shown that $\dot{\Lambda} < 0$ as a consequence of the second law of thermodynamics [10], that is, the vacuum energy density diminishes in the course of the evolution. Therefore, in what follows we consider that the coupled vacuum is continuously transferring energy to the dominant component (radiation or nonrelativistic matter components). Such a property defines precisely the physical meaning of decaying or running vacuum cosmologies in this work.

Now, by combining the above field equation it is readily checked that

$$\dot{H} + \frac{3 (1 + \omega)}{2} H^2 - \frac{1 + \omega}{2} \Lambda (H) = 0, \tag{4}$$

where the equation of state $p_T = \omega \rho_T \ (\omega \geq 0)$ was used. The above equations are solvable only if we know the functional form of $\Lambda(H)$.

The decaying vacuum law adopted here was first proposed based on phenomenological grounds [7–9, 11] and later on

suggested by the renormalization group approach techniques applied to quantum field theories in curved space-time [24]. It is given by

$$\Lambda (H) \equiv 8\pi G\rho_\Lambda = c_0 + 3\nu H^2 + \alpha \frac{H^{n+2}}{H_I{}^n}, \tag{5}$$

where H_I is an arbitrary time scale describing the primordial de Sitter era (the upper limit of the Hubble parameter), ν and α are dimensionless constants, and c_0 is a constant with dimension of $[H]^2$.

In a point of fact, the constant α above does not represent a new degree of freedom. It can be determined with the proviso that, for large values of H, the model starts from a de Sitter phase with $\rho = 0$ and $\Lambda_I = 3H_I^2$. In this case, from (5) one finds $\alpha = 3(1 - \nu)$ because the first two terms there are negligible in this limit [see Eq. (1) in [9] for the case $n = 1$ and [11] for a general n]. The constant c_0 can be fixed by the time scale of the final de Sitter phase. For $H << H_I$ we also see from (4) that $c_0 = 3(1-\nu)H_F^2$, where H_F characterizes the final de Sitter stage (see (6) and (8)). Hence, the phenomenological law (5) assumes the final form:

$$\Lambda (H) = 3 (1 - \nu) H_F^2 + 3\nu H^2 + 3 (1 - \nu) \frac{H^{n+2}}{H_I{}^n}. \tag{6}$$

This is an interesting 3-parameter phenomenological expression. It depends on the arbitrary dimensionless constant ν and also the two extreme Hubble parameters (H_I, H_F) describing the primordial and late time inflationary phases, respectively. Current observations imply that the value of ν is very small, $|\nu| \sim 10^{-6} - 10^{-3}$ [25, 26]. More interestingly, the analytical results discussed below remain valid even for $\nu = 0$. In this case, we obtain a sort of minimal model defined only by a pair of physical time scales, H_I and H_F, determining the entire evolution of the Universe. As we shall see, the possible existence of these two extreme de Sitter regimes suggests a different perspective to the cosmological constant problem.

By inserting the above expression into (3) we obtain the equation of motion:

$$\dot{H} + \frac{3 (1 + \omega) (1 - \nu)}{2} H^2 \left[1 - \frac{H_F^2}{H^2} - \frac{H^n}{H_I{}^n} \right] = 0. \tag{7}$$

In principle, all possible de Sitter phases here are simply characterized by a constant Hubble parameter (H_C) satisfying the conditions $\dot{H} = \rho = p = 0$ and $\Lambda = 3H_C^2$. For all physically relevant values of ν and ω in the present context, we see that the condition $\dot{H} = 0$ is satisfied whether the possible values of H_C are constrained by the algebraic equation involving the arbitrary (initial and final) de Sitter vacuum scales H_I and H_F:

$$H_C^{n+2} - H_I^n H_C^2 + H_F^2 H_I^n = 0. \tag{8}$$

In particular, for $n = 2$, the value preferred from the covariance of the action, the exact solution is given by

$$H_C^2 = \frac{H_I^2}{2} \pm \frac{H_I^2}{2} \sqrt{1 - \frac{4H_F^2}{H_I^2}}, \tag{9}$$

and since $H_F << H_I$ we see that the two extreme scaling solutions for $n = 2$ are $H_{1C} = H_I$ and $H_{2C} = H_F$. However, we also see directly from (8) that the condition $H_F << H_I$, also guarantees that such solutions are valid regardless of the values of n. In certain sense, since H_0 is only the present day expansion rate, characterizing a quite casual stage of the recent evolving Universe, probably, it is not the interesting scale to be a priori predicted. In what follows we consider that the pair of extreme de Sitter scales (H_I, H_F) are the physically relevant quantities. This occurs because different from H_0, the expanding de Sitter rates are associated with very specific limiting manifolds. For instance, it is widely known that de Sitter spaces are static when written in a suitable coordinate system. Besides the discussion on the coincidence problem (see next section), a new idea to be advocated here is that the prediction of such scales, at least in principle, should be an interesting theoretical target. Their first principles prediction would open a new and interesting route to investigate the cosmological constant problem.

The solutions for the Hubble parameter describing analytically the transitions vacuum-radiation ($\omega = 1/3$) and matter-vacuum ($\omega = 0$) can be expressed in terms of the scale factor, the couple of scales (H_I, H_F), and free parameters (ν, n):

$$H = \frac{H_I}{\left[1 + Ca^{2n(1-\nu)}\right]^{1/n}}, \tag{10}$$

$$H = H_F\left[Da^{-3(1-\nu)} + 1\right]^{1/2}. \tag{11}$$

We remark that the transition radiation-matter is like that in the standard cosmic concordance model. The only difference is due to the small ν parameter that can be fixed to be zero (minimal model). Indeed, if one fixes $\nu = 0$, the matter-vacuum transition is exactly the same one appearing in the flat ΛCDM model. As we shall see below, the final scale H_F can be expressed as a simple function of H_0, ν, and Ω_Λ. Naturally, the existence of such an expression is needed in order to compare with the present observations. However, it cannot be used to hide the special meaning played by H_F in a possible solution of the cosmological constant problem.

3. Alleviating the Coincidence Problem

The so-called coincidence problem is very well known. It comes from the fact that the matter-energy density of the nonrelativistic components (baryons + dark matter) decreases as the Universe expands while the vacuum energy density (ρ_{Λ_0}) is always constant in the cosmic concordance model (Λ_0CDM). This happens also because the energy densities of the radiation ρ_γ (CMB photons) and neutrinos (ρ_ν) are negligible today. Thus, in a broader perspective, one may also say that the ratio $(\rho_M + \rho_R)/\rho_{\Lambda_0}$, where $\rho_R = \rho_\gamma + \rho_\nu$, was almost infinite at early times, but it is nearly of the order unity today.

The current fine-tuning behind the coincidence problem can also be readily defined in terms of the corresponding density parameters, since ($\Omega_{\Lambda_0} \sim 0.7$ and $\Omega_M + \Omega_R \sim 0.3$), so that the ratio is of the order unity some 14 billion years later.
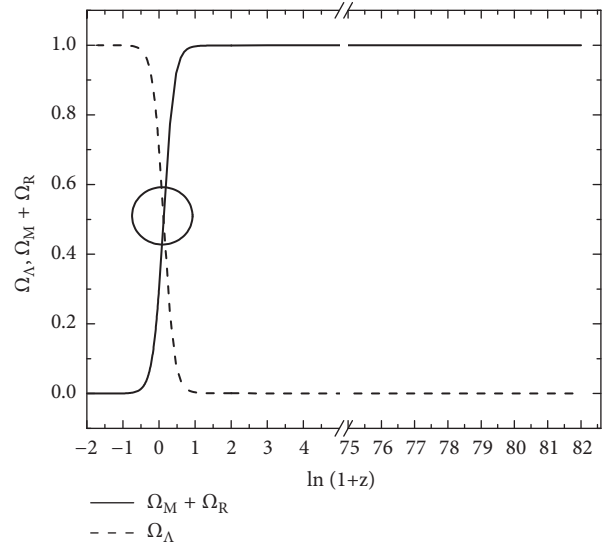
FIGURE 1: Standard coincidence problem in the cosmic concordance model (Λ_0CDM). Solid and dashed lines represent the evolution of the vacuum (Ω_{Λ_0}) and total matter-radiation ($\Omega_M + \Omega_R$) density parameters. The circle marks the low (and unique!) redshift presenting the extreme coincidence between the density parameter of the vacuum and material medium. Note that the model discussed here is fully equivalent to Λ_0CDM when the time dependent corrections in the decay $\Lambda(t)$ expression are neglected [see (5)].

In Figure 1 we display the standard view of the coincidence problem in terms of the corresponding density parameters: $\Omega_M = \Omega_b + \Omega_{cdm}$ (baryons + cold dark matter) and $\Omega_R = \Omega_\gamma + \Omega_\nu$ (CMB photons + relic neutrinos). As one may conclude from the figure, the ratio was practically infinite at very high redshifts, that is, at the early Universe (say, roughly at the Planck time). However, both densities are nearly coincident at present. The ratio $(\Omega_R + \Omega_M)/\Omega_{\Lambda_0} \sim 1)$ is at low redshifts. Note also that, in the far future, that is, very deep in the de Sitter stage, the ratio approaches zero or equivalently the inverse ratio is almost infinite because the vacuum component becomes fully dominant.

A natural way to solve this puzzle is to assume that the vacuum energy density must vary in the course of the expansion. As shown in the previous section, the characteristic scales of the $\Lambda(t)$ model specify the evolution during the extreme de Sitter phases: the primordial vacuum solution with $Ca^{2n(1-\nu)} << 1$ and $H = H_I$ behaves like a "repeller" in the distant past, while the final vacuum solution for $a >> 1$, that is, $Da^{3(1-\nu)} \longmapsto 0$ and $H = H_F$, is an attractor in the distant future.

The arbitrary integration constants C and D are also easily determined. The constant C can be fixed by the end of the primordial inflation ($\ddot{a} = 0$) or equivalently $\rho_\Lambda = \rho_R$. This means that $C = a_{(eq)}^{-2n(1-\nu)}/(1 - 2\nu)$ [$a_{(eq)}$ corresponds to the value of the scale factor at vacuum-radiation equality]. In terms of the present day observable quantities we also find $D = \Omega_{M0}/(\Omega_{\Lambda0} - \nu)$ and $H_F = H_0\sqrt{\Omega_{\Lambda0} - \nu}/\sqrt{1 - \nu}$. For $\nu = 0$ and $\Omega_{\Lambda0} \sim 0.7$ one finds $H_F \sim 0.83H_0$, as expected a little smaller than H_0. The small observable parameter

$\nu < 10^{-3}$ quantifies the difference between the late time decaying vacuum model and the cosmic concordance cosmology; namely,

$$H = \frac{H_0}{\sqrt{1-\nu}} \left[\Omega_{M0} a^{-3(1-\nu)} + 1 - \Omega_{M0} - \nu \right]^{1/2}. \qquad (12)$$

As remarked above, the $H(a)$ expression of the standard ΛCDM model is fully recovered for $\nu = 0$.

The solution of the coincidence problem in the present framework can be demonstrated as follows. The density parameters of the vacuum and material medium are given by

$$\Omega_\Lambda \equiv \frac{\Lambda(H)}{3H^2} = \nu + (1-\nu)\frac{H_F^2}{H^2} + (1-\nu)\frac{H^n}{H_I^n}, \qquad (13)$$

$$\Omega_T \equiv 1 - \Omega_\Lambda = 1 - \nu - (1-\nu)\frac{H_F^2}{H^2} - (1-\nu)\frac{H^n}{H_I^n}. \qquad (14)$$

Such results are a simple consequence of expression (6) for $\Lambda(H)$ and constraint Friedman equation (1). Note that $\Omega_T \equiv \Omega_M + \Omega_R$ is always describing the dominant component, either the nonrelativistic matter ($\omega = 0$) or radiation ($\omega = 1/3$).

The density parameters of the vacuum and material medium are equal in two different epochs specifying the dynamic transition between the distinct dominant components. These specific moments of time will be characterized here by Hubble parameters H_1^{eq} and H_2^{eq}. The first equality (vacuum-radiation, $\rho_\Lambda = \rho_R$) occurs just at the end of the first accelerating stage ($\ddot{a} = 0$), that is, when $H_1^{eq} = [(1 - 2\nu)/2(1-\nu)]^{1/n}H_I$, while the second one is at low redshifts when $H_2^{eq} = [2(1-\nu)/(1-2\nu)]^{1/2}H_F$. Note that such results are also valid for the minimal model by taking $\nu = 0$. In particular, inserting $\nu = 0$ in the first expression above we find $H_1^{eq} = H_I/2^{1/n}$. The scale H_2^{eq} can also be determined in terms of H_0. By adding the result $H_F \sim 0.83H_0$ we find for $\nu = 0$ that $H_2^{eq} \sim 1.18H_0$, which is higher than H_0, as should be expected for the matter-vacuum transition.

Naturally, the existence of two subsequent equalities on the density parameter suggests a solution to the coincidence problem. Neglecting terms of the order of 10^{-120} and 10^{-60n} in above expressions, it is easy to demonstrate the following results:

(1) $\lim_{H \to H_I} \Omega_\Lambda = 1$ and $\lim_{H \to H_I} \Omega_T = 0$,

(2) $\lim_{H \to H_F} \Omega_\Lambda = 1$ and $\lim_{H \to H_F} \Omega_T = 0$.

The meaning of the above results is quite clear. The density parameters of the vacuum and material components (radiation + matter) perform a cycle, that is, Ω_Λ, and $\Omega_M + \Omega_R$ are periodic in the long run.

In Figure 2, we show the complete evolution of the vacuum and matter-energy density parameters for this class of decaying vacuum model. Different from Figure 1 we observe that the values of Ω_Λ and $\Omega_M + \Omega_R$ are cyclic in the long run.

These parameters start and finish the evolution satisfying the above limits. The physical meaning of such evolution is also remarkable. For any value of $n > 0$, the model starts as
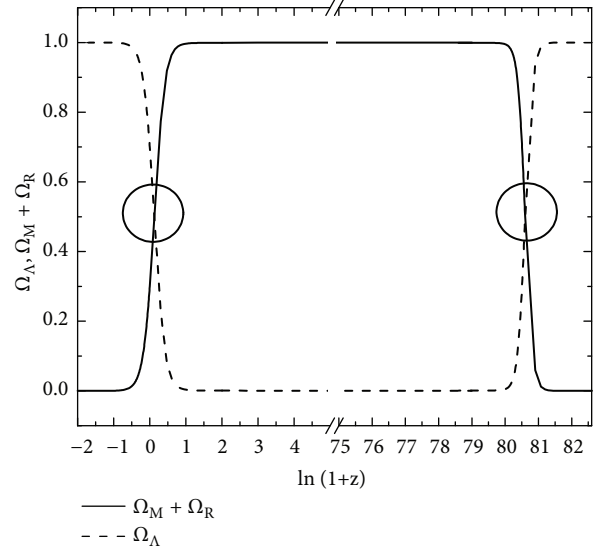
FIGURE 2: Solution of the coincidence problem in running vacuum cosmologies. The right graphic is our model; the left is ΛCDM. Solid and dashed lines represent the evolution of the vacuum (Ω_Λ) and total matter-radiation ($\Omega_M + \Omega_R$) density parameters for n=2, $\nu = 10^{-3}$, and $H_I/H_0 = 10^{60}$. The late time coincidence between the density parameter of the vacuum and material medium (left circle) has already occurred at very early times (right circle). Note also that the values 5 and 75 in the horizontal axis were glued in order to show the complete evolution (the suppressed part presents exactly the same behavior). Different values of n change slightly the value of the redshift for which $\Omega_\Lambda = \Omega_M + \Omega_R$ at the very early Universe (see also discussion in the text).

a pure unstable vacuum de Sitter phase with $H = H_I$ (in the beginning there is no matter or radiation, $\Omega_\Lambda = 1, \Omega_M + \Omega_R = 0$). The vacuum decays and the model evolves smoothly to a quasi-radiation phase parametrized by the small ν-parameter.

The circles show the redshifts for which $\Omega_\Lambda = \Omega_M + \Omega_R$. Of course, the existence of two equality solutions alleviates the cosmic coincidence problem.

The robustness of the solution must also be commented on. It holds not only for any value of $n > 0$ but also for $\nu = 0$. In the latter case, the primordial nonsingular vacuum state deflates directly to the standard FRW radiation phase. Later on, the transition from radiation to matter-vacuum dominated phase also occurs, thereby reproducing exactly the matter-vacuum transition of the standard Λ_0CDM model.

The "irreversible entropic cycle" from initial Sitter (H_I) to the late time de Sitter stage is completed when the Hubble parameter approaches its small final value ($H \mapsto H_F$). The de Sitter space-time that was a "repeller" (unstable solution) at very early times ($z \to \infty$) becomes an attractor in the distant future ($z \to -1$) driven by the incredibly low energy scale H_F which is associated with the late time vacuum energy density, $\rho_M \to 0, \rho_{\Lambda F} \propto H_F^2$.

Like the above solution to the coincidence problem, some cosmological puzzles can also be resolved along the same lines because the time behavior of the present scenario even fixing $\alpha = 1 - \nu$ has been proven here to be exactly the one discussed in [20] (see also [9] for the case $n = 1$).

4. Final Comments and Conclusion

As we have seen, the phenomenological $\Lambda(t)$-term provided a possible solution to the coincidence problem because the ratio Ω_M/Ω_Λ is periodic in long run (see Figure 2). In other words, the coincidence is not a novelty exclusive of the current epoch (low redshifts) since it also happened in the very early Universe at extremely high redshifts. In this framework, such a result seems to be robust because it is not altered even to the minimal model, that is, for $\nu = 0$.

It should also be stressed that the alternative complete cosmological scenario (from de Sitter to de Sitter) is not a singular attribute of decaying vacuum models. For instance, it was recently proved that at the background level such models are equivalent to gravitationally induced particle production cosmologies [27, 28] by identifying $\Lambda(t) \equiv \rho\Gamma/3H$, where Γ is the gravitational particle production rate. In a series of papers [29, 30], the dynamical equivalence of such scenario at late times with the cosmic concordance model was also discussed. It is also interesting that such a reduction of the dark sector can mimic the cosmic concordance model (Λ_0CDM) at both the background and perturbative levels [31, 32]. In principle, this means that alternative scenarios evolving smoothly between two extreme de Sitter phases are also potentially able to provide viable solutions of the main cosmological puzzles. However, different from $\Lambda(t)$-cosmologies, such alternatives are unable to explain the cosmological constant problem with this extreme puzzle becoming restricted to the realm of quantum field theory.

At this point, in order to compare our results with alternative models also evolving between two extreme de Sitter stages, it is interesting to review briefly how the main cosmological problems are solved (or alleviated) within this class of models driven by a pure decaying vacuum initial state:

(i) *Singularity:* the space-time in the distant past is a nonsingular de Sitter geometry with an arbitrary energy scale H_I. In order to agree with the semiclassical description of gravity, the arbitrary scale H_I must be constrained by the upper limit $H_I \leq 10^{19}$ GeV (Planck energy) in natural units or equivalently based on general relativity is valid only for times greater than the Plank time, $H_I^{-1} \geq 10^{-43}$ sec.

(ii) *Horizon problem:* the ansatz (6) can mathematically be considered as the simplest decaying vacuum law which destabilizes the initial de Sitter configuration. Actually, in such a model the Universe begins as a steady-state cosmology, $R \sim e^{H_I t}$. Since the model is nonsingular, it is easy to show that the horizon problem is naturally solved in this context (see, for instance, [22]).

(iii) *"Graceful-Exit" from inflation:* the transition from the early de Sitter to the radiation phase is smooth and driven by (10). The first coincidence of density parameters happens for $H = H_1^{eq}, \rho_\Lambda = \rho_R$, and $\ddot{a} = 0$, that is, when the first inflationary period ends (see Figure 2). All the radiation entropy ($S_0 \sim 10^{88}$, in dimensionless units) and matter-radiation content now observed were generated during the early

decaying vacuum process (see [21] for the entropy produced in the case $n = 2$). For an arbitrary $n > 0$, the exit of inflation and the entropy production had also already been discussed [22]. Some possible curvature effects were also analyzed [33].

(iv) *Baryogenesis problem:* recently, it was shown that the matter-antimatter asymmetry can also be induced by a derivative coupling between the running vacuum and a nonconserving baryon current [34, 35]. Such an ingredient breaks dynamically CPT thereby triggering baryogenesis through an effective chemical potential (for a different but related approach see [36]). Naturally, baryogenesis induced by a running vacuum process has at least two interesting features: (i) the variable vacuum energy density is the same ingredient driving the early accelerating phase of the Universe and it also controls the baryogenesis process; (ii) the running vacuum is always accompanied by particle production and entropy generation [8, 10, 22]. This nonisentropic process is an extra source of T-violation (beyond the freeze-out of the B-operator) which as first emphasized by Sakharov [37] is a basic ingredient for successful baryogenesis. In particular, for $\nu = 0$ it was found that the observed B-asymmetry ordinarily quantified by the η parameter

$$5.7 \times 10^{-10} < \eta < 6.7 \times 10^{-10} \qquad (15)$$

can be obtained for a large range of the relevant parameters (H_I, n) of the present model [34, 35]. Thus, as remarked before, the proposed running vacuum cosmology may also provide a successful baryogenesis mechanism.

(v) *de Sitter Instability and the future of the Universe:* another interesting aspect associated with the presence of two extreme Sitter phases as discussed here is the intrinsic instability of such space-time. Long time ago, Hawking showed that the space-time of a static black hole is thermodynamically unstable to macroscopic fluctuation in the temperature of the horizon [38]. Later on, it was also demonstrated by Mottola [39] based on the validity of the generalized second law of thermodynamics that the same arguments used by Hawking in the case of black holes remain valid for the de Sitter space-time. In the case of the primordial de Sitter phase, described here by the characteristic scale H_I, such an instability is dynamically described by solution (10) for $H(a)$. As we know, it behaves like a "repeller" driving the model to the radiation phase. However, the instability result in principle must also be valid to the final de Sitter stage which behaves like an attractor. In this way, once the final de Sitter phase is reached, the space-time would evolve to an energy scale smaller than H_F thereby starting a new evolutionary "cycle" in the long run.

(vi) *Cosmological constant problem:* it is known that phenomenological decaying vacuum models are unable to solve this conundrum [22, 34]. The basic reason

seems to be related to the clear impossibility to predict the present day value of the vacuum energy density (or equivalently the value of H_0) from first principles. However, the present phenomenological approach can provide a new line of inquiry in the search for alternative (first principle) solutions for this remarkable puzzle. In this concern, we notice that the minimal model discussed here depends only on two relevant physical scales (H_F, H_I) which are associated with the extreme de Sitter phases. The existence of such scales implies that the ratio between the late and very early vacuum energy densities $\rho_{\Lambda F}/\rho_{\Lambda I} = (H_F/H_I)^2$ does not depend explicitly on the Planck mass. Indeed, the gravitational constant (in natural units, $G = M_{Planck}^{-2}$) arising in the expressions of the early and late time vacuum energy densities cancels out in the above ratio. Since $H_F \sim 10^{-42}$GeV, by assuming that $H_I \sim 10^{19}$GeV (the cutoff of classical theory of gravity), one finds that the ratio $\rho_{\Lambda F}/\rho_{\Lambda I} \sim 10^{-122}$, as suggested by some estimates based on quantum field theory, a result already obtained in some nonsingular decaying vacuum models [19]. In this context, the open new perspective is related to the search for a covariant action principle where both scales arise naturally. One possibility is related to models whose theoretical foundations are based on modified gravity theories like $F(R), F(R, T), etc$ [see, for instance, [40, 41]].

The results outlined above suggest that decaying vacuum models phenomenologically described by $\Lambda(t)$-cosmologies may be considered an interesting alternative to the mixing scenario formed by the standard ΛCDM plus inflation. However, although justified from different viewpoints, the main difficulty of such models seems to be a clear-cut covariant Lagrangian description.

Data Availability

The data used to support the findings of this study are available from the corresponding author upon request.

Conflicts of Interest

The authors declare that there are no conflicts of interest regarding the publication of this paper.

Acknowledgments

References

[1] P. A. R. Ade et al., *Planck Collaboration A&A*, vol. 594, pp. 1502–1589, 2016.

[2] S. Weinberg, "The cosmological constant problem," *Reviews of Modern Physics*, vol. 61, no. 1, pp. 1–23, 1989.

[3] M. Bronstein, "On the expanding universe," *Physikalische Zeitschrift der Sowjetunion*, vol. 3, pp. 73–82, 1933.

[4] M. Özer and M. Taha, "A possible solution to the main cosmological problems," *Physics Letters B*, vol. 171, no. 4, pp. 363–365, 1986.

[5] M. Ozer and M. O. Taha, "A model of the universe free of cosmological problems," *Nuclear Physics*, vol. 287, p. 776, 1987.

[6] K. Freese, F. C. Adams, J. A. Frieman, and E. Mottola, "Cosmology with decaying vacuum energy," *Nuclear Physics A*, vol. 287, p. 797, 1987.

[7] J. C. Carvalho, J. A. Lima, and I. Waga, " Cosmological consequences of a time-dependent ," *Physical Review D: Particles, Fields, Gravitation and Cosmology*, vol. 46, no. 6, pp. 2404–2407, 1992.

[8] I. Waga, "Decaying vacuum flat cosmological models - Expressions for some observable quantities and their properties," *The Astrophysical Journal*, vol. 414, p. 436, 1993.

[9] J. A. Lima and J. M. Maia, "Deflationary cosmology with decaying vacuum energy density," *Physical Review D: Particles, Fields, Gravitation and Cosmology*, vol. 49, no. 10, pp. 5597–5600, 1994.

[10] J. A. Lima, "Thermodynamics of decaying vacuum cosmologies," *Physical Review D: Particles, Fields, Gravitation and Cosmology*, vol. 54, no. 4, pp. 2571–2577, 1996.

[11] J. M. F. Maia, *Some Applications of Scalar Fields in Cosmology [Ph.D. thesis]*, University of São Paulo, Brazil, 2000.

[12] M. Szydlowski, A. Stachowski, and K. Urbanowski, "Cosmology with a Decaying Vacuum Energy Parametrization Derived from Quantum Mechanics," *Journal of Physics: Conference Series*, vol. 626, no. 1, 2015.

[13] M. Szydłowski, A. Stachowski, and K. Urbanowski, "Quantum mechanical look at the radioactive-like decay of metastable dark energy," *The European Physical Journal C*, vol. 77, no. 12, 2017.

[14] P. J. Steinhardt, L. Wang, and I. Zlatev, "Cosmological tracking solutions," *Physical Review D: Particles, Fields, Gravitation and Cosmology*, vol. 59, no. 12, Article ID 123504, 1999.

[15] P. J. Steinhardt, *Critical Problems in Physics*, V. L. Fitch and D. R. Marlow, Eds., Princeton University Press, Princeton, N. J, 1999.

[16] S. Dodelson, M. Kaplinghat, and E. Stewart, "Solving the Coincidence Problem: Tracking Oscillating Energy," *Physical Review Letters*, vol. 85, no. 25, pp. 5276–5279, 2000.

[17] W. Zimdahl, D. Pavón, and L. P. Chimento, "Interacting quintessence," *Physics Letters B*, vol. 521, no. 3-4, pp. 133–138, 2001.

[18] A. Barreira and P. P. Avelino, *Physical Review D: Particles, Fields, Gravitation and Cosmology*, vol. 84, no. 8, 2011.

[19] J. A. S. Lima, S. Basilakos, and J. Solá, "Expansion History with Decaying Vacuum: A Complete Cosmological Scenario," *Monthly Notices of the Royal Astronomical Society*, vol. 431, p. 923, 2013.

[20] E. L. D. Perico, J. A. S. Lima, S. Basilakos, and J. Solà, "Complete cosmic history with a dynamical $\Lambda = \Lambda(H)$ term," *Physical Review D: Particles, Fields, Gravitation and Cosmology*, vol. 88, Article ID 063531, 2013.

[21] J. A. Lima, S. Basilakos, and J. Solà, "Nonsingular decaying vacuum cosmology and entropy production," *General Relativity and Gravitation*, vol. 47, no. 4, article 40, 2015.

[22] J. A. S. Lima, S. Basilakos, and J. Solà, "Thermodynamical aspects of running vacuum models," *The European Physical Journal C*, vol. 76, no. 4, article 228, 2016.

[23] L. Landau and E. Lifshitz, *Journal of Fluid Mechanics*, Pergamon Press, 1959.

[24] I. L. Shapiro and J. Solà, "Scaling behavior of the cosmological constant and the possible existence of new forces and new light degrees of freedom," *Physics Letters B*, vol. 475, no. 3-4, pp. 236–246, 2000.

[25] S. Basilakos, D. Polarski, and J. Solà, "Generalizing the running vacuum energy model and comparing with the entropic-force models," *Physical Review D: Particles, Fields, Gravitation and Cosmology*, vol. 86, Article ID 043010, 2012.

[26] A. Gomez-Valent and J. Solà, "Vacuum models with a linear and a quadratic term in H: structure formation and number counts analysis," *Monthly Notices of the Royal Astronomical Society*, vol. 448, p. 2810, 2015.

[27] I. Prigogine, J. Geheniau, E. Gunzig, and P. Nardone, "Thermodynamics and cosmology," *General Relativity and Gravitation*, vol. 21, p. 767, 1989.

[28] M. O. Calvão, J. A. S. Lima, and I. Waga, "On the thermodynamics of matter creation in cosmology," *Physics Letters A*, vol. 162, no. 3, pp. 223–226, 1992.

[29] J. A. S. Lima, J. F. Jesus, and F. A. Oliveira, "CDM accelerating cosmology as an alternative to ΛCDM model," *Journal of Cosmology and Astroparticle Physics*, vol. 11, article 027, 2010.

[30] J. A. S. Lima, S. Basilakos, and F. E. M. Costa, "New cosmic accelerating scenario without dark energy," *Physical Review D: Particles, Fields, Gravitation and Cosmology*, vol. 86, Article ID 103534, 2012.

[31] R. O. Ramos, M. Vargas dos Santos, and I. Waga, "Matter creation and cosmic acceleration," *Physical Review D: Particles, Fields, Gravitation and Cosmology*, vol. 89, no. 8, Article ID 083524, 2014.

[32] R. O. Ramos, M. Vargas dos Santos, and I. Waga, "Degeneracy between CCDM and ΛCDM cosmologies," *Physical Review D*, vol. 90, Article ID 127301, 2014.

[33] P. Pedram, M. Amirfakhrian, and H. Shababi, "On the (2+1)-dimensional Dirac equation in a constant magnetic field with a minimal length uncertainty," *International Journal of Modern Physics D*, vol. 24, no. 2, Article ID 1550016, 8 pages, 2015.

[34] J. A. S. Lima and D. Singleton, "Matter-Antimatter Asymmetry Induced by a Running Vacuum Coupling," *The European Physical Journal C*, vol. 77, p. 855, 2017.

[35] J. A. S. Lima and D. Singleton, "Matter-antimatter asymmetry and other cosmological puzzles via running vacuum cosmologies," *International Journal of Modern Physics D*, 2018.

[36] V. K. Oikonomou, S. Pan, and R. C. Nunes, "Gravitational Baryogenesis in Running Vacuum models," *International Journal of Modern Physics A*, vol. 32, no. 22, Article ID 1750129, 2017.

[37] A. Sakharov, "Violation of CP invariance, C asymmetry, and baryon asymmetry of the universe," *JETP Letters*, vol. 5, p. 24, 1967.

[38] S. W. Hawking, "Black holes and thermodynamics," *Physical Review D: Particles, Fields, Gravitation and Cosmology*, vol. 13, no. 2, pp. 191–197, 1976.

[39] E. Mottola, "Thermodynamic instability of de Sitter space," *Physical Review D: Particles, Fields, Gravitation and Cosmology*, vol. 33, no. 6, pp. 1616–1621, 1986.

[40] T. P. Sotiriou and V. Faraoni, "*f(R)* theories of gravity," *Reviews of Modern Physics*, vol. 82, no. 1, article 451, 2010.

[41] T. Harko, F. S. N. Lobo, S. Nojiri, and S. D. Odintsov, "*F(R, T)* gravity," *Physical Review D: Particles, Fields, Gravitation and Cosmology*, vol. 84, no. 2, Article ID 024020, 2011.

Research Article

Statistical Physics of the Inflaton Decaying in an Inhomogeneous Random Environment

Z. Haba [ID]

Institute of Theoretical Physics, University of Wroclaw, 50-204 Wroclaw, Plac Maxa Borna 9, Poland

Correspondence should be addressed to Z. Haba; zhab@ift.uni.wroc.pl

We derive a stochastic wave equation for an inflaton in an environment of an infinite number of fields. We study solutions of the linearized stochastic evolution equation in an expanding universe. The Fokker-Planck equation for the inflaton probability distribution is derived. The relative entropy (free energy) of the stochastic wave is defined. The second law of thermodynamics for the diffusive system is obtained. Gaussian probability distributions are studied in detail.

1. Introduction

The ΛCDM model became the standard cosmological model since the discovery of the universe acceleration [1, 2]. It describes very well the large-scale structure of the universe. The formation of an early universe is explained by the inflationary models involving scalar fields (inflatons) [3, 4]. Such models raise the questions concerning the dynamics from their early stages till the present day. The origin of the cosmological constant as a manifestation of "dark energy" could also be explored. In models of the dark sector we hope to explain the "coincidence problem": why the densities of the dark matter and the dark energy are of the same order today as well as "the cosmological constant problem" [5]; why the cosmological constant is so small. We assume that the dark matter and dark energy consist of some unknown particles and fields. They interact in an unknown way with baryons and the inflaton. The result of the interaction could be seen in a dissipative and diffusive behaviour of the observed luminous matter. The diffusion approximation does not depend on the details of the interaction but only on its strength and "short memory" (Markovian approximation). In this paper we follow an approach appearing in many papers (see [6–10] and references quoted there) describing the dark matter and the fields responsible for inflation (inflatons) by scalar fields. In the ΛCDM model the universe originates from

the quantum Big Bang. The quantum fluctuations expand forming the observed galactic structure. The transition to classicality requires a decoherence. The decoherence can be obtained through an interaction with an environment. The environment may consist of any unobservable degrees of freedom. In [11, 12] these unobservable variables are the high energy modes of the fields present in the initial theory. We assume that the environment consists of an infinite set of scalar fields interacting with the inflaton. The model is built in close analogy to the well-known infinite oscillator model [13–16] of Brownian motion. As the model involves an infinite set of unobservable degrees of freedom the statistical description is unavoidable. We have an environment of an infinite set of scalar χ fields which have an arbitrary initial distributions. We begin their evolution from an equilibrium thermal state. In such a case we obtain a random physical system driven by thermal fluctuations of the environment. We could also take into account quantum fluctuations extracting them as high momentum modes of the inflaton as is done in the Starobinsky stochastic inflation [17]. In such a framework a description of a quantum random evolution is reduced to a classical stochastic process. We can apply the thermodynamic formalism to the study of evolution of stochastic systems. In such a framework we can calculate the probability of a transition from one state to another. In particular, a vacuum decay can be treated

as a stochastic process leading to a production of radiation [18].

The plan of this paper is the following. In Section 2 we derive the stochastic wave equation for an inflaton interacting with an infinite set of scalar fields in a homogeneous expanding metric. In Section 3 we briefly discuss a generalization to inhomogeneous perturbations of the metric satisfying Einstein-Klein-Gordon equations. In Section 4 we approximate the nonlinear system by a linear inhomogeneous stochastic wave equation with a space-time-dependent mass. The Fokker-Planck equation for the probability distribution of the inflaton is derived. A solution of the Fokker-Planck equation in the form of a Gibbs state with a time-dependent temperature is obtained. In Section 5 a general linear system is discussed. In Section 6 we obtain partial differential equations for the correlation functions of this system. In Section 7 Gaussian solutions of the Fokker-Planck equation and their relation to the equations for correlation functions are studied. In Section 8 we discuss thermodynamics of time-dependent (nonequilibrium) diffusive systems based on the notion of the relative entropy (free energy). In the Appendix we treat a simple system of stochastic oscillators in order to show that the formalism works well for this system.

2. Scalar Fields Interacting Linearly with an Environment

The CMB observations show that the universe was once in an equilibrium state. The Hamiltonian dynamics of scalar fields usually discussed in the model of inflation do not equilibrate. We can achieve an equilibration if the scalar field interacts with an environment. We suggest a field theoretic model which is an extension of the well-known oscillator model discussed in [13–16]. We consider the Lagrangian

$$\mathcal{L} = R\sqrt{g} + \frac{1}{2}\partial_\mu\phi\partial^\mu\phi - V(\phi) + \sum_b \left(\frac{1}{2}\partial_\mu\chi^b\partial^\mu\chi^b - \frac{1}{2}m_b^2\chi^b\chi^b - \lambda_b\phi\chi^b - U_b(\chi^b)\right). \tag{1}$$

Equations of motion for the scalar fields read

$$g^{-1/2}\partial_\mu\left(g^{1/2}\partial^\mu\right)\phi = -V' - \sum_b \lambda_b\chi^b, \tag{2}$$

$$g^{-1/2}\partial_\mu\left(g^{1/2}\partial^\mu\right)\chi^b + m_b^2\chi^b = -\lambda_b\phi - \frac{\partial U_b}{\partial\chi^b}, \tag{3}$$

where $g_{\mu\nu}$ is the metric tensor and $g = |\det[g_{\mu\nu}]|$.

We consider the flat expanding metric:

$$ds^2 = dt^2 - a^2 d\mathbf{x}^2, \tag{4}$$

In the metric (4), (3) reads

$$\partial_t^2\chi^b + 3H\partial_t\chi^b - a^{-2}\triangle\chi^b + m_b^2\chi^b = -\lambda_b\phi - \frac{\partial U_b}{\partial\chi^b}. \tag{5}$$

We may choose

$$U_b\left(\chi^b\right) = \kappa_b\left(\chi_b^2 - v_b^2\right)^2. \tag{6}$$

We write

$$\chi = v + a^{-3/2}\widetilde{\chi}. \tag{7}$$

Then

$$\partial_t^2\widetilde{\chi}^b - a^{-2}\triangle\widetilde{\chi}^b + \omega_b^2\widetilde{\chi}^b = -\lambda_b a^{3/2}\phi + a^{-3/2}o\left(\widetilde{\chi}^2\right) \tag{8}$$

where

$$\omega_b^2 = m_b^2 + 8\kappa_b v_b^2 - \frac{3}{2}\partial_t H - \frac{9}{4}H^2. \tag{9}$$

We consider large $a \to \infty$ so that for a large time we may neglect a^{-2} term. Moreover, we assume that $\omega_b^2 > 0$ and that ω_b is approximately constant (this is exactly so for the de Sitter space and approximate for power-law expansion when the H dependent term decays as t^{-2}). Then, the solution of (8) is

$$\widetilde{\chi}^b = \cos\left(\omega_b t\right)\widetilde{\chi}_0^b + \sin\left(\omega_b t\right)\omega_b^{-1}\widetilde{\pi}_0^b$$
$$- \lambda_b\int_{t_0}^t \sin\left(\omega_b(t-s)\right)\omega_b^{-1}a(s)^{3/2}\phi_s\,ds. \tag{10}$$

Inserting the solution of (3) in (2) we obtain an equation of the following form:

$$g^{-1/2}\partial_\mu\left(g^{1/2}\partial^\mu\right)\phi + V'(\phi)$$
$$= \int_{t_0}^t \mathcal{K}\left(t,t'\right)\phi\left(t'\right)dt' + a^{-3/2}\eta\left(\chi(0),\widetilde{\pi}\right), \tag{11}$$

where

$$\mathcal{K}(t,s) = a(t)^{-3/2}\sum_b \lambda_b^2\sin\left(\omega_b(t-s)\right)\omega_b^{-1}a(s)^{3/2} \tag{12}$$

and the noise η depends linearly on the initial conditions $(\widetilde{\chi}(0), \widetilde{\pi}(0))$:

$$\eta_t = -\sum_b \lambda_b\cos\left(\omega_b t\right)\widetilde{\chi}_0^b + \lambda_b\sin\left(\omega_b t\right)\omega_b^{-1}\widetilde{\pi}_0^b. \tag{13}$$

If the correlation function of the noise is to be stationary (depend on time difference) then we need

$$\left\langle\widetilde{\chi}_0^b\widetilde{\chi}_0^b\right\rangle = \left\langle\omega_b^{-2}\widetilde{\pi}_0^b\widetilde{\pi}_0^b\right\rangle. \tag{14}$$

Then, (assuming that $\langle\widetilde{\chi}\widetilde{\pi}\rangle = 0$, true in the classical Gibbs state) we get

$$\left\langle\eta_t(\mathbf{x})\eta_s(\mathbf{y})\right\rangle$$
$$= a^{-3}\sum_b \lambda_b^2\left\langle\left(\omega_b^{-2}\cos\left(\omega_b(t-s)\right)\widetilde{\pi}_0^b(\mathbf{x}),\widetilde{\pi}_0^b(\mathbf{y})\right)\right\rangle. \tag{15}$$

We assume a certain probability distribution for initial values. Relation (14) is satisfied for classical as well as quantum Gibbs distribution with the Hamiltonian $\widetilde{H}_b = (1/2)(\widetilde{\pi}^2 + \omega_b^2\widetilde{\chi}_b^2)$. In the classical field theory in the Gibbs state the covariance of the fields in (14) is $(-a^{-2}\triangle + \omega_b^2)^{-1}$. If $a^{-2}\triangle = 0$ then this covariance is approximated by [19] $\beta^{-1}\omega_b^{-2}\delta(\mathbf{x}-\mathbf{y})$. We choose

$$\lambda_b \simeq \sqrt{\beta}\gamma\pi^{-1/2}\omega_b \tag{16}$$

Under assumption (16) and a continuous spectrum of ω_b in (11) we shall have

$$
\begin{aligned}
\int_{t_0}^{t} & ds \mathcal{K}(t, s) \phi(s) \\
&= -\gamma^2 \partial_t \phi(t) - \frac{3}{2} \gamma^2 H(t) \phi(t) + \gamma^2 \delta(0) \phi(t) \\
&\quad - \gamma^2 \delta(t - t_0) \phi(t_0) a(t)^{-3/2} a(t_0)^{3/2}
\end{aligned} \tag{17}
$$

Here, $\delta(t)$ comes from $\beta^{-1} \sum_b \lambda_b^2 \omega_b^{-2} \cos(\omega_b t)$; the $\delta(0)$ term is (an infinite) mass renormalization which appears already in the Caldeira-Leggett model [15]; it could be included in m^2. The last term can be neglected when t_0 tends to $-\infty$. We shall omit these terms in further discussion.

In an expanding metric, (11) takes the following form:

$$
\begin{aligned}
\partial_t^2 \phi - a^{-2} \triangle \phi + \left(3H + \gamma^2\right) \partial_t \phi + \frac{3}{2} \gamma^2 H \phi + V'(\phi) \\
= \gamma a^{-3/2} \eta,
\end{aligned} \tag{18}
$$

where

$$
\left\langle \eta(t, \mathbf{x}) \eta(t', \mathbf{x}') \right\rangle = \delta(t - t') K_t(\mathbf{x}, \mathbf{x}'). \tag{19}
$$

Here, $K(\mathbf{x}, \mathbf{x}') = \delta(\mathbf{x} - \mathbf{x}')$ comes from the expectation value of the initial values $\tilde{\chi}$ and $\tilde{\pi}$ with the neglect of $a^{-2} \triangle$. If we do not neglect $a^{-2} \triangle$ in (8) then the form of (19) would be much more complicated (we would obtain a nonlocal equation). We make the approximation (19) which preserves the Markov property and provides stochastic fields which are regular functions of $\mathbf{x}$ (it can be considered as a cutoff ignoring high momenta components of ϕ). Equation (18) has been derived earlier in [19]. It is applied in the model of warm inflation [20].

3. Stochastic Equations in a Perturbed Inhomogeneous Metric

We did not write yet equations for the metric which result from Lagrangian (1). The power spectrum of inflaton perturbations depends on the metric [3, 4, 21–23]. In general, the equations for the metric are difficult to solve. They are solved in perturbation theory. We consider only scalar perturbations of the homogenous metric using the scalar fields A, B, E, ψ. Then, the metric is expressed in the following form [3, 23]:

$$
\begin{aligned}
ds^2 == & -(1 + 2A) dt^2 + 2a \partial_j B dx^j dt \\
& + a^2 \left((1 - 2\psi) \delta_{ij} + 2\partial_i \partial_j E\right) dx^i dx^j
\end{aligned} \tag{20}
$$

Inserting the metric in (2)-(3) we obtain

$$
\begin{aligned}
\partial_t^2 \phi + (3H + \Gamma) \partial_t \phi - a^{-2} \triangle \phi + V'(\phi)(1 + 2A) \\
= -\sum_b \lambda_b \chi_b (1 + 2A)
\end{aligned} \tag{21}
$$

and

$$
\begin{aligned}
\partial_t^2 \chi_b + (3H + \Gamma) \partial_t \chi_b - a^{-2} \triangle \chi_b + m_b^2 \chi_b (1 + 2A) \\
= -\lambda_b \phi (1 + 2A) - \frac{\partial U_b}{\partial \chi_b} (1 + 2A)
\end{aligned} \tag{22}
$$

where

$$
-\Gamma = \partial_t A + 3 \partial_t \psi - a^{-2} \triangle \left(a^2 \partial_t E - aB\right) \tag{23}
$$

Let

$$
\chi_b = \exp(\sigma) \tilde{\chi}_b + \nu_b \tag{24}
$$

with

$$
\partial_t \sigma = -\frac{1}{2} (3H + \Gamma) \tag{25}
$$

Then, in the approximation neglecting higher powers of $\tilde{\chi}$ in U

$$
\partial_t^2 \tilde{\chi}_b - a^{-2} \triangle \tilde{\chi}_b + \Omega_b^2 \chi_b = -\lambda_b \exp(-\sigma)(1 + 2A) \phi \tag{26}
$$

where

$$
\begin{aligned}
\Omega_b^2 = & \left(m_b^2 + 8\nu_b^2 \kappa_b\right)(1 + 2A) - \frac{1}{4}(3H + \Gamma)^2 \\
& - \frac{1}{2} \partial_t (3H + \Gamma)
\end{aligned} \tag{27}
$$

We again assume that $\Omega^2 \simeq m_b^2 + 8\nu_b^2 \kappa_b$. Then, in the derivation of (18) for ϕ the only change comes from the differentiation of $\exp(\sigma)$ inside the integral (11) and the factor $(1 + 2A)$ multiplying the fields. So,

$$
\frac{3}{2} \gamma^2 H \phi \longrightarrow \frac{1}{2} \gamma^2 (3H + \Gamma) \phi (1 + 2A)^2 \tag{28}
$$

and

$$
\gamma^2 \partial_t \phi \longrightarrow \gamma^2 (1 + 2A) \partial_t \left((1 + 2A) \phi\right) \tag{29}
$$

Hence, our final equation is (for a general theory of a stochastic wave equation on a Riemannian manifold see [24] and references cited there)

$$
\begin{aligned}
\partial_t^2 \phi + \left(3H + \gamma^2 + \Gamma\right) \partial_t \phi - a^{-2} \triangle \phi + \frac{1}{2} \gamma^2 (3H + \Gamma) \phi \\
+ 6\gamma^2 A H \phi + 2\gamma^2 \partial_t A \phi + 4\gamma^2 A \partial_t \phi \\
+ V'(\phi)(1 + 2A) = \gamma (1 + 2A) a^{-3/2} \eta
\end{aligned} \tag{30}
$$

4. A Simplified System of a Decaying Inflaton

The metric (A, B, ψ, E) can be expressed by ϕ from Einstein equations resulting from the Lagrangian (1). We expand inflaton equation with a potential V around the classical solution of Klein-Gordon-Einstein equation. The linearized version of the equation for fluctuations takes the form of the

Klein-Gordon equation with a space-time-dependent mass [3, 4, 23, 25, 26]:

$$\partial_t \phi = \Pi$$

$$d\Pi + \left(3H + \gamma^2\right)\Pi dt + \frac{3}{2}\gamma^2 H\phi dt + \nu\phi dt + a^{-2}\triangle\phi dt \quad (31)$$

$$= \gamma a^{-3/2} dB$$

where we write $\eta = dB/dt$ and treat (31) as Ito stochastic differential equation [27]. The function ν depends on the potential V in (18) and on the choice of coordinates (t, x) (the choice of gauge [28]). We do not discuss ν in this paper. We consider in this section the simplified version of (31) without ϕ terms:

$$d\Pi + \left(3H + \gamma^2\right)\Pi dt = \gamma a^{-3/2} dB \quad (32)$$

We define the energy density:

$$\rho = \frac{1}{2}\Pi^2 \quad (33)$$

Then, from (32) applying the stochastic calculus [27, 29] and (32), we obtain

$$d\Pi^2 = 2\Pi d\Pi + d\Pi d\Pi$$

$$= -2\left(3H + \gamma^2\right)\Pi^2 dt + 2\gamma a^{-3/2}\Pi dB \quad (34)$$

$$+ \gamma^2 a^{-3} K(x, x)\, dt$$

We may first integrate this equation and use $\left\langle \int_0^t f dB \right\rangle = 0$ for the Ito integral. Differentiating the expectation value over t we obtain

$$d\langle\rho\rangle + 6H\langle\rho\rangle dt = -2\gamma^2\langle\rho\rangle dt$$

$$+ \frac{1}{2}\gamma^2 K(x, x)\, a^{-3} dt \quad (35)$$

Equation (35) describes the inflaton density with $w = \rho/p = 1$ and a cosmological term varying with the speed a^{-3}. The term $-2\gamma^2\langle\rho\rangle$ violates the energy conservation of the inflaton. It describes a decay of the inflaton into the χ fields. If we couple the χ fields to radiation then if χ fields are invisible the observable effect will be detected as a production of radiation from the decay of the inflaton [18, 30].

For the stochastic system (32) the Fokker-Planck equation reads

$$\partial_t P = \frac{\gamma^2}{2}\int d\mathbf{x}d\mathbf{x}' \mathcal{G}_t\left(\mathbf{x}, \mathbf{x}'\right)\frac{\delta^2}{\delta\Pi(\mathbf{x})\,\delta\Pi(\mathbf{x}')}P$$

$$+ \int d\mathbf{x}\frac{\delta}{\delta\Pi(\mathbf{x})}\left(3H + \gamma^2\right)\Pi P. \quad (36)$$

Then, the Gaussian solution is

$$P = L\exp\left(-\frac{1}{2}\int\sqrt{g}\Pi\beta\Pi\right) \quad (37)$$

where $\sqrt{g} = a^3$. It can be checked that

$$\beta = \exp\left(2\gamma^2 t\right)a^3\left(R + \gamma^2\int_0^t dsa(s)^3\exp\left(2\gamma^2 s\right)\right)^{-1} \quad (38)$$

and

$$L^{-1}\partial_t L = -\frac{1}{2}\gamma^2 a^{-3}Tr(K\beta) + \left(3H + \gamma^2\right)\delta(0)\int d\mathbf{x}. \quad (39)$$

This normalization factor is infinite (needs renormalization) but the value of L does not appear in the expectation values $\langle F \rangle = \left(\int P\right)^{-1}\int PF$.

β has the meaning of the inverse temperature. The dependence (38) of the temperature of the diffusing system on the scale factor a has been derived (for $\gamma = 0$ and arbitrary w) in [31–33] for any system with $w = 1$ and the a^{-3} correction (35) to the cosmological term (in eq. (38) $w = 1$) (for time-dependent cosmological term see [5, 34, 35]).

5. The Linearized Wave Equation

We can rewrite (4)-(5) in a way that they do not contain first-order time derivatives of fields. Let

$$\phi = a^{-3/2}\exp\left(-\frac{1}{2}\gamma^2 t\right)\Phi \quad (40)$$

Then, the linearized version of the inflaton equation expanded around the classical solution (with an account of metric perturbations) reads

$$\partial_t \Phi = \Pi \quad (41)$$

$$\partial_t \Pi + K^2\Phi - \frac{3}{2}\partial_t H\Phi - \frac{9}{4}H^2\Phi - \frac{1}{4}\gamma^2\Phi + \nu\Phi$$

$$= \partial_t \Pi + K^2\Phi + \tilde{\nu}\Phi = \gamma a^{3/2}\exp\left(\frac{1}{2}\gamma^2 t\right)\eta \quad (42)$$

where

$$K^2 = -a^{-2}\triangle + m^2 \quad (43)$$

For the stochastic system (42) the Fokker-Planck equation reads

$$\partial_t P = \frac{\gamma^2}{2}\int d\mathbf{x}d\mathbf{x}' \mathcal{G}_t\left(\mathbf{x}, \mathbf{x}'\right)\frac{\delta^2}{\delta\Pi(\mathbf{x})\,\delta\Pi(\mathbf{x}')}P$$

$$+ \int d\mathbf{x}\left(K^2\Phi + \tilde{\nu}\Phi\right)\frac{\delta}{\delta\Pi(\mathbf{x})}P \quad (44)$$

$$- \int d\mathbf{x}\Pi(\mathbf{x})\frac{\delta}{\delta\Phi(\mathbf{x})}P \equiv \mathscr{A}P.$$

where

$$\mathcal{G}_t\left(\mathbf{x}, \mathbf{x}'\right) = a^3\exp\left(\gamma^2 t\right)K_t\left(\mathbf{x}, \mathbf{x}'\right) \quad (45)$$

and ν depends on the classical solution in the potential V [23, 25].

We may write the noise in the Fourier momentum space:

$$\left\langle \eta(t, \mathbf{k})\eta\left(t', \mathbf{k}'\right)\right\rangle = \mathcal{G}_t(\mathbf{k})\delta\left(\mathbf{k} + \mathbf{k}'\right)\delta\left(t - t'\right) \quad (46)$$

Then, (42) is rewritten as an ordinary (instead of partial) differential equation.

6. A Differential Equation for Correlations

Let us consider (42) expressed in the following form:

$$\partial_t \Phi = \Pi \tag{47}$$

$$\partial_t \Pi = A\Phi + \gamma a^{3/2} \exp\left(\frac{1}{2}\gamma^2 t\right)\eta \tag{48}$$

where

$$-A = K^2 + \tilde{\nu} = -a^{-2}\Delta + m^2 + \tilde{\nu} \tag{49}$$

Let us denote

$$\langle \Phi_t(\mathbf{x}) \Phi_t(\mathbf{y})\rangle = C_t(\mathbf{x},\mathbf{y}) \tag{50}$$

$$\langle \Phi_t(\mathbf{x}) \Pi_t(\mathbf{y})\rangle = E_t(\mathbf{x},\mathbf{y}) \tag{51}$$

$$\langle \Pi_t(\mathbf{x}) \Pi_t(\mathbf{y})\rangle = D_t(\mathbf{x},\mathbf{y}) \tag{52}$$

Using the stochastic calculus [27, 29] and taking the expectation value we get a system of differential equations for the correlation functions:

$$\partial_t C_t(\mathbf{x},\mathbf{y}) = E_t(\mathbf{x},\mathbf{y}) + E_t(\mathbf{y},\mathbf{x}) \tag{53}$$

$$\partial_t D_t(\mathbf{x},\mathbf{y}) = A_x E_t(\mathbf{x},\mathbf{y}) + A_y E_t(\mathbf{y},\mathbf{x}) + \gamma^2 \mathscr{G}_t(\mathbf{x},\mathbf{y}) \tag{54}$$

$$\partial_t E_t(\mathbf{y},\mathbf{x}) = A_x C_t(\mathbf{x},\mathbf{y}) + D_t(\mathbf{x},\mathbf{y}) \tag{55}$$

If the system is translation invariant then we can Fourier transform these equations obtaining a system of ordinary differential equations for Fourier transforms:

$$\partial_t C_t(k) = E_t(k) + E_t(-k) \tag{56}$$

$$\partial_t D_t(k) = -\left(a^{-2}k^2 + m^2 + \tilde{\nu}\right)\left(E_t(k) + E_t(-k)\right) \\ + \gamma^2 \mathscr{G}_t(k) \tag{57}$$

$$\partial_t E_t(k) = -\left(a^{-2}k^2 + m^2 + \tilde{\nu}\right)C_t(k) + D_t(k) \tag{58}$$

where $\mathscr{G}_t(k)$ is defined in (46).

7. Gaussian Solutions of the Fokker-Planck Equation

We look for a solution of the Fokker-Planck equation (44) in the following form:

$$P_t^I = L(t)\exp\left(-\gamma^{-2}\int d\mathbf{x}d\mathbf{x}'\left(\frac{1}{2}\Pi\beta_1(t,\mathbf{x},\mathbf{x}')\Pi + \Pi\beta_2(t,\mathbf{x},\mathbf{x}')\Phi + \frac{1}{2}\Phi\beta_3(t,\mathbf{x},\mathbf{x}')\Phi\right) + \int d\mathbf{x}M\Phi + \int d\mathbf{x}N\Pi\right). \tag{59}$$

or in the momentum space

$$P_t^I = L(t)\exp\left(-\gamma^{-2}\int d\mathbf{k}\left(\frac{1}{2}\Pi\beta_1(t,\mathbf{k})\Pi + \Pi\beta_2(t,\mathbf{k})\Phi + \frac{1}{2}\Phi\beta_3(t,\mathbf{k})\Phi\right) + \int d\mathbf{k}M(\mathbf{k})\Phi(-\mathbf{k}) + \int d\mathbf{k}N(\mathbf{k})\Pi(-\mathbf{k})\right). \tag{60}$$

In the configuration space β is an operator and in the momentum space a function of $\mathbf{k}$. $L(t)$ is determined by normalization or directly from the Fokker-Planck equation:

$$L^{-1}\partial_t L = -\frac{1}{2}\int d\mathbf{x}d\mathbf{x}'\mathscr{G}_t(\mathbf{x},\mathbf{x}')\beta_1(\mathbf{x},\mathbf{x}') \tag{61}$$

The equations for β read

$$\partial_t\beta_1 = -\beta_1\mathscr{G}_t\beta_1 - 2\beta_2 \tag{62}$$

$$\partial_t\beta_2 = -\beta_2\mathscr{G}_t\beta_1 + \omega^2\beta_1 - \beta_3 \tag{63}$$

$$\partial_t\beta_3 = -\beta_2\mathscr{G}_t\beta_2 + 2\omega^2\beta_2 \tag{64}$$

where

$$\omega^2 = a^{-2}k^2 + m^2 + \tilde{\nu} \tag{65}$$

We skip the equations for M and N.

It is useful to introduce instead of β_j the variables (defined by Fourier transforms of β):

$$X = \beta_3 - \frac{\beta_2^2}{\beta_1} \tag{66}$$

$$Y = \frac{\beta_2}{\beta_1} \tag{67}$$

$$Z = \frac{\beta_3}{\beta_1} \tag{68}$$

We can invert these relations:

$$\beta_1 = \frac{X}{Z - Y^2} \tag{69}$$

$$\beta_2 = \frac{XY}{Z - Y^2} \tag{70}$$

$$\beta_3 = \frac{ZX}{Z - Y^2} \tag{71}$$

P_t^I can be expressed as

$$P_t^I = L(t) \exp\left(-\int d\mathbf{x} d\mathbf{x}' \right.$$
$$\left. \cdot \frac{1}{2} \gamma^{-2} \left((\Pi + Y\Phi) \beta_1 (\Pi + Y\Phi) + \Phi X \Phi \right)\right). \quad (72)$$

From (72) it can be seen that the probability distribution is diagonal in the variables Φ and $\Pi + Y\Phi$. So, we obtain the expectation value $\langle (\Pi + Y\Phi)(\mathbf{x})(\Pi + Y\Phi)(\mathbf{x}') \rangle = \gamma^2 \beta_1^{-1}(\mathbf{x}, \mathbf{x}')$.

Assume that we calculate the expectation values at time t:

$$D = \langle \Pi_t^2 \rangle = \gamma^2 \beta_3 \left(\beta_1 \beta_3 - \beta_2^2\right)^{-1} = \gamma^2 ZX^{-1} \quad (73)$$

$$C = \langle \Phi_t^2 \rangle = \gamma^2 \beta_1 \left(\beta_1 \beta_3 - \beta_2^2\right)^{-1} = \gamma^2 X^{-1} \quad (74)$$

$$E = \langle \Phi_t \Pi_t \rangle = -\gamma^2 \beta_2 \left(\beta_1 \beta_3 - \beta_2^2\right)^{-1} = -\gamma^2 YX^{-1} \quad (75)$$

X, Y, Z can be expressed by D, C, E as

$$Z = DC^{-1} \quad (76)$$

$$Y = -EC^{-1} \quad (77)$$

$$X = \gamma^2 C^{-1} \quad (78)$$

If we know D, E, C then we can express

$$\beta_1 = C \left(DC - E^2\right)^{-1} \quad (79)$$

$$\beta_2 = -E \left(DC - E^2\right)^{-1} \quad (80)$$

$$\beta_3 = D \left(DC - E^2\right)^{-1} \quad (81)$$

Note that $\beta_2(t = 0) = 0$ means $E(t = 0) = 0$.

The relations (67)-(81) allow relating the solutions of the stochastic equation (42) with the solutions of the differential equations (62)-(64) and the solution of the Fokker-Planck equation (44). In fact, the solution P^I can be expressed by the Fokker-Planck transition function P_t (which is defined by the solution of the stochastic equation (42) [27]) as follows:

$$P_t^I(\phi, \Pi) = \int d\phi' d\Pi' P_0^I(\phi', \Pi') P_t(\phi', \Pi'; \phi, \Pi) \quad (82)$$

The expectation values of the solution of the stochastic equation with the initial condition (ϕ', Π') is

$$\langle F\left(\phi_t(\phi', \Pi'), \Pi_t(\phi', \Pi')\right) \rangle$$
$$= \int d\phi d\Pi P_t(\phi', \Pi'; \phi, \Pi) F(\phi, \Pi) \quad (83)$$

Hence,

$$\int d\phi' d\Pi' P_0^I(\phi', \Pi') \langle F\left(\phi_t(\phi', \Pi'), \Pi_t(\phi', \Pi')\right) \rangle$$
$$= \int d\phi' d\Pi' P_0^I(\phi', \Pi') \int d\phi d\Pi P_t(\phi', \Pi'; \phi, \Pi) \quad (84)$$
$$\cdot F(\phi, \Pi) = \int d\phi d\Pi P_t^I(\phi, \Pi) F(\phi, \Pi)$$

Note that the initial value P_0^I in (84) according to (59) is determined by the initial values of β_j. A possible choice for the initial value is the thermal Gibbs distribution:

$$P_0^I = \exp\left(-\frac{1}{2T} \int d\mathbf{x} \left(\Pi^2 + (\nabla \phi)^2 + m^2 \phi^2\right)\right) \quad (85)$$

which corresponds to the initial condition $\beta_2(t = 0) = 0$, $\beta_1(t = 0, \mathbf{x}, \mathbf{x}') = (1/T)\delta(\mathbf{x} - \mathbf{x}')$ and $\beta_3(t = 0, \mathbf{x}, \mathbf{x}') = (1/T)\triangle\delta(\mathbf{x} - \mathbf{x}')$. We could also consider the initial probability distribution:

$$P_0^I = \exp\left(-\frac{1}{2\sigma^2} \int d\mathbf{x} \left(\phi(\mathbf{x}) - v\right)^2\right) \quad (86)$$

describing the field concentrated at v. Then, in (59) $M(t = 0, \mathbf{x}) = \sigma^{-2} v$. In such a case, the probability distribution (59) describes the probability of the transition from v to ϕ (see [36] for such calculations in quantum mechanics).

8. The Relative Entropy

Assume we have a functional equation of the form (like (44)):

$$\partial_t P = \frac{1}{2} \int d\mathbf{x} d\mathbf{x}' \mathcal{D}_t(\mathbf{x}, \mathbf{x}') \frac{\delta^2}{\delta \Pi(\mathbf{x}) \delta \Pi(\mathbf{x}')} P$$
$$+ \int d\mathbf{x} \frac{\delta}{\delta \Pi(\mathbf{x})} D_1(\phi(\mathbf{x}), \Pi(\mathbf{x})) P \quad (87)$$
$$+ \int d\mathbf{x} \frac{\delta}{\delta \Phi(\mathbf{x})} D_2(\Phi(\mathbf{x}), \Pi(\mathbf{x})) P \equiv \mathscr{A} P$$

Let us assume that we have two solutions P_1 and P_2 of this equation. Define the relative entropy

$$F = \int d\Phi d\Pi Z_1^{-1} P_1 \ln\left(Z_2 Z_1^{-1} P_1 P_2^{-1}\right) \quad (88)$$

where

$$Z_1 = \int d\Phi d\Pi P_1 \quad (89)$$

$$Z_2 = \int d\Phi d\Pi P_2 \quad (90)$$

From the definition of F it follows that [37]

$$F \geq 0 \quad (91)$$

Calculation of the time derivative of F gives

$$\partial_t F = -\frac{1}{2} \int d\phi d\Pi P_1 \left(P_2 P_1^{-1}\right)^2 d\mathbf{x} d\mathbf{x}' \mathscr{D}_t \left(\mathbf{x}, \mathbf{x}'\right) \frac{\delta}{\delta \Pi(\mathbf{x})} \left(P_1 P_2^{-1}\right) \frac{\delta}{\delta \Pi(\mathbf{x}')} \left(P_1 P_2^{-1}\right) \leq 0 \tag{92}$$

We choose $P_2 = P^I$ (then $Z_2 = 1$ because $L(t)$ is the normalization factor). Then, we define the entropy (the entropy of inflaton and gravitational perturbations has been discussed earlier in [38, 39]):

$$S = -Z^{-1} \int d\Phi d\Pi P \ln \left(Z^{-1} P\right) \tag{93}$$

Using (87) we calculate the time derivative:

$$\partial_t S = -Z^{-1} \int d\Phi d\Pi \mathscr{A} P \ln P - Z^{-1} \int d\Phi d\Pi \mathscr{A} P \tag{94}$$

The second term is zero, whereas the first term is equal to

$$\partial_t S$$

$$= \frac{1}{2} \int d\Phi d\Pi P^{-1} d\mathbf{x} d\mathbf{x}' \mathscr{D}_t \left(\mathbf{x}, \mathbf{x}'\right) \frac{\delta}{\delta \Pi(\mathbf{x})} P \frac{\delta}{\delta \Pi(\mathbf{x}')} P \tag{95}$$

$$+ \int d\phi d\Pi \int d\mathbf{x} \left(D_1 \frac{\delta P}{\delta \Pi(\mathbf{x})} + D_2 \frac{\delta P}{\delta \Phi(\mathbf{x})}\right)$$

In (95) the first term is positive whereas the second term depends on the dynamics (it is vanishing for Hamiltonian dynamics). Using formula (59) for $P_2 = P^I$ we obtain

$$F + S = Z^{-1} \int d\Phi d\Pi P \left(\frac{1}{2} \gamma^{-2} \Pi \beta_1 \Pi + \gamma^{-2} \Phi \beta_2 \Pi \right.$$

$$\left. + \frac{1}{2} \gamma^{-2} \Phi \beta_3 \Phi\right) - \ln L(t) \tag{96}$$

Formula (96) has a thermodynamic meaning relating the sum of free energy F and entropy S to the internal energy expressed by the rhs of (96). At the initial time (with the initial conditions discussed at the end of Section 7) the rhs of (96) is the mean value of the energy

$$U_0 = \frac{1}{2} \int d\mathbf{x} \left(\Pi^2 + (\nabla \Phi)^2 + m^2 \Phi^2\right) \tag{97}$$

In the static universe we would have an equilibrium distribution as P_2. In such a case the thermodynamic relation (95) would describe the standard version of the second law of thermodynamics of diffusing systems. F with $\partial_t F \leq 0$ in (92) would show the approach to equilibrium. In the expanding universe the relation (96) can serve for a comparison of various probability measures starting from different initial conditions.

9. Summary

The main source of observational data [1, 2] comes from measurements of the cosmic microwave background (CMB) and observations of galaxies evolution (including galaxies distribution). The CMB spectrum and its fluctuations are the test ground for models involving quantum and thermal fluctuations. A simplified description of an interaction of a relativistic system with an environment leads to a stochastic wave equation for an inflaton generating the expansion (inflation) of the universe. We considered a linearization of the wave equation. We discussed the Fokker-Planck equation for the probability distribution of the inflaton. Gaussian solutions of the Fokker-Planck equation for linearized systems can be treated as Gibbs states with a time-dependent temperature. The model leads to a formula for density and temperature evolution. We have derived the density evolution law in (35) and the temperature evolution in (38) in a simplified model. In order to obtain the results in the complete model we would have to solve (numerically) equations of Section 7. The comparison of density evolution (38) with observations is discussed in [32] and in similar models with the decaying vacuum (see [34, 35] and references cited there). The model allows calculating (and compare with observations) the power spectrum resulting from thermal fluctuations which may go beyond the approximations applied in the warm inflation of [20]. We have introduced a thermodynamic description of the expanding diffusive systems in terms of the relative entropy (free energy) and entropy. The state of a stochastic system can be identified with its probability distribution. The relative entropy allows comparing the evolution of the probability distributions with different initial conditions. In this sense relative entropy can be treated as a quantitative measure of a decay of one state into another state (as an alternative to a quantum description of vacuum decay in cosmology [40, 41]).

Appendix

A. Statistical Physics of a Static Finite Dimensional Model

A finite dimensional analog of the wave equation is ($\mathbf{x} \in R^n$):

$$\frac{dx^k}{dt} = p^k \tag{A.1}$$

$$\frac{dp^k}{dt} = -\Gamma p^k - \omega^2 x^k + \gamma \eta^k \tag{A.2}$$

The Fokker-Planck equation reads

$$\partial_t P = -p^k \frac{\partial}{\partial x^k} + \frac{\partial}{\partial p^k} \left(\Gamma p^k + \omega^2 x^k\right) P + \frac{\gamma^2}{2} \frac{\partial^2 P}{\partial p^k \partial p^k} \tag{A.3}$$

The stationary solution is

$$P_\infty = \exp\left(-\frac{\Gamma}{\gamma^2}\left(\mathbf{p}^2 + \omega^2\mathbf{x}^2\right)\right) = \exp\left(-\frac{\mathscr{E}}{T}\right) \quad (A.4)$$

where $\mathscr{E}$ is the energy of the oscillator. It describes a Gibbs state with the temperature

$$T = \frac{\gamma^2}{2\Gamma} \quad (A.5)$$

We look for a solution of (A.3) in the following form:

$$P_t = L(t)\exp\left(-\frac{1}{2}\alpha_1\mathbf{p}^2 - \alpha_2\mathbf{xp} - \frac{1}{2}\alpha_3\mathbf{x}^2\right) \quad (A.6)$$

Then

$$L^{-1}\partial_t L = -\frac{n}{2}\gamma^2\alpha_1 + \Gamma n \quad (A.7)$$

$$\partial_t\alpha_1 = -2\alpha_2 - \gamma^2\alpha_1^2 + 2\Gamma\alpha_1 \quad (A.8)$$

$$\partial_t\alpha_2 = -\alpha_3 - \gamma^2\alpha_1\alpha_2 + \Gamma\alpha_2 + \omega^2\alpha_1 \quad (A.9)$$

$$\partial_t\alpha_3 = -\gamma^2\alpha_2^2 + 2\omega^2\alpha_2 \quad (A.10)$$

Let us write

$$x^k = \exp\left(-\frac{\Gamma}{2}t\right)y^k \quad (A.11)$$

Then, the stochastic equation for y reads

$$\frac{d^2y^k}{dt^2} = -\Omega^2 y^k + \gamma\exp\left(\frac{\Gamma}{2}t\right)\eta^k \quad (A.12)$$

where

$$\Omega^2 = \omega^2 - \frac{\Gamma^2}{4} \quad (A.13)$$

The solution of (A.12) is

$$y^k(t)$$
$$= \cos(\Omega t)\,y^k(0) + \sin(\Omega t)\,\Omega^{-1}\partial_t y^k(0) \quad (A.14)$$
$$+ \gamma\int_0^t \sin(\Omega(t-s))\,\Omega^{-1}\exp\left(\frac{\Gamma}{2}s\right)w(s)\,ds$$

We can easily calculate the correlation functions of $x^k(s)$ and $p^k(s)$ in two ways: either from the stochastic equations or using the probability distribution P_t resulting from the solution of the differential equations (A.8)-(A.10).

Data Availability

The data used to support the findings of this study are available from the corresponding author upon request.

Conflicts of Interest

The author declares that there are no conflicts of interest.

References

[1] P. A. R. Ade, N. Aghanim, M. Arnaud et al., https://arxiv.org/abs/1502.01589.

[2] K. T. Story, C. L. Reichardt, Z. Hou et al., "A measurement of the cosmic microwave background damping tail from the 2500-square-degree SPT-SZ survey," *The Astrophysical Journal*, vol. 779, no. 1, p. 86, 2013.

[3] V. F. Mukhanov and G. V. Chibisov, "Quantum fluctuations and a non-singular universe," *JETP Letters*, vol. 33, p. 532, 1981.

[4] M. Sasaki, "Large scale quantum fluctuations in the inflationary universe," *Progress of Theoretical and Experimental Physics*, vol. 76, p. 1036, 1986.

[5] S. Weinberg, "The cosmological constant problem," *Reviews of Modern Physics*, vol. 61, no. 1, pp. 1–23, 1989.

[6] P. J. E. Peebles and A. Vilenkin, "Noninteracting dark matter," *Physical Review D: Particles, Fields, Gravitation and Cosmology*, vol. 60, no. 10, Article ID 103506, 1999.

[7] P. J. E. Peebles and B. Ratra, "Cosmology with a time-variable cosmological 'constant'," *Astrophysical Journal*, vol. 325, p. L17, 1988.

[8] Y. L. Bolotin, A. Kostenko, O. A. Lemets, and A. D. Yerokhin, "Cosmological evolution with interaction between dark energy and dark matter," *International Journal of Modern Physics D*, vol. 24, Article ID 1530007, 2014.

[9] M. C. Bento, O. Bertolami, and N. C. Santos, "A two-field quintessence model," *Physical Review D: Particles, Fields, Gravitation and Cosmology*, vol. 65, no. 6, 2002.

[10] F. Bezrukov, D. Gorbunov, and M. Shaposhnikov, "On initial conditions for the hot big bang," *Journal of Cosmology and Astroparticle Physics*, vol. 2009, no. 06, pp. 029-029, 2009.

[11] E. Calzetta and B. L. Hu, "Quantum fluctuations, decoherence of the mean field, and structure formation in the early Universe," *Physical Review D: Particles, Fields, Gravitation and Cosmology*, vol. 52, p. 6770, 1995.

[12] D. Polarski and A. A. Starobinsky, "Semiclassicality and decoherence of cosmological perturbations," *Classical and Quantum Gravity*, vol. 13, no. 3, pp. 377–391, 1996.

[13] G. W. Ford, J. T. Lewis, and R. F. O'Connell, "Quantum Langevin equation," *Physical Review A: Atomic, Molecular and Optical Physics*, vol. 37, no. 11, pp. 4419–4428, 1988.

[14] G. W. Ford and M. Kac, "On the quantum Langevin equation," *Journal of Statistical Physics*, vol. 46, no. 5-6, pp. 803–810, 1987.

[15] A. O. Caldeira and A. J. Leggett, "Path integral approach to quantum Brownian motion," *Physica A*, vol. 121, p. 587, 1983.

[16] H. Kleinert and S. V. Shabanov, "Quantum Langevin equation from forward-backward path integral," *Physics Letters A*, vol. 200, Article ID 9503004, p. 171, 1995.

[17] A. A. Starobinsky, "Stochastic de Sitter (inflationary) stage in the early universe," in *Current Topics in Field Theory,Quantum Gravity and Strings*, H. J. Vega and N. Sanchez, Eds., vol. 246 of *Lecture Notes in Physics*, pp. 107–126, Springer, 1986.

[18] P. J. Steinhardt and M. S. Turner, "Prescription for successful new inflation," *Physical Review D: Particles, Fields, Gravitation and Cosmology*, vol. 29, no. 10, pp. 2162–2171, 1984.

[19] A. Berera, "Thermal properties of an inflationary universe," *Physical Review D: Particles, Fields, Gravitation and Cosmology*, vol. 54, no. 4, pp. 2519–2534, 1996.

[20] A. Berera, I. G. Moss, and R. O. Ramos, "Warm inflation and its microphysical basis," *Reports on Progress in Physics*, vol. 72, Article ID 026901, 2009.

[21] V. F. Mukhanov, "Quantum theory of gauge invariant cosmological perturbations," *Soviet Physics—JETP*, vol. 67, p. 1297, 1988.

[22] A. A. Starobinsky, "Dynamics of phase transition in the new inflationary universe scenario and generation of perturbations," *Physics Letters B*, vol. 117, no. 3-4, pp. 175–178, 1982.

[23] B. A. Bassett, S. Tsujikawa, and D. Wands, "Inflation dynamics and reheating," *Reviews of Modern Physics*, vol. 78, no. 2, pp. 537–589, 2006.

[24] Z. Brzezniak and M. Ondrejat, "Strong solutions to stochastic wave equations with values in Riemannian manifolds," *Journal of Functional Analysis*, vol. 253, no. 2, pp. 449–481, 2007.

[25] J. Hwang, "Curved space quantum scalar field theory with accompanying metric fluctuations," *Physical Review D: Particles, Fields, Gravitation and Cosmology*, vol. 48, no. 8, pp. 3544–3556, 1993.

[26] J. E. Lidsey, A. R. Liddle, E. W. Kolb, E. J. Copeland, T. Barreiro, and M. Abney, "Reconstructing the inflaton potential—an overview," *Reviews of Modern Physics*, vol. 69, no. 2, pp. 373–410, 1997.

[27] N. Ikeda and S. Watanabe, *Stochastic Differential Equations and Diffusion Processes*, North-Holland, Amsterdam, The Netherlands, 1981.

[28] J. M. Bardeen, P. J. Steinhardt, and M. S. Turner, "Spontaneous creation of almost scale free density perturbations in an inflationary universe," *Physical Review D: Particles, Fields, Gravitation and Cosmology*, vol. 28, no. 4, p. 678, 1985.

[29] B. Simon, *Functional Integration and Quantum Mechaics*, Academic Press, New York, 1979.

[30] A. Berera and L.-Z. Fang, "Thermally induced density perturbations in the inflation era," *Physical Review Letters*, vol. 74, no. 11, pp. 1912–1915, 1995.

[31] Z. Haba, "A relation between diffusion, temperature and the cosmological constant," *Modern Physics Letters A*, vol. 31, no. 24, p. 1650146, 2016.

[32] Z. Haba, A. Stachowski, and M. Szydłowski, "Dynamics of the diffusive DM-DE interaction—Dynamical system approach," *Journal of Cosmology and Astroparticle Physics*, vol. 2016, no. 07, pp. 024-024, 2016.

[33] Z. Haba, "Thermodynamics of diffusive DM/DE systems," *General Relativity and Gravitation*, vol. 49, no. 4, Art. 58, 21 pages, 2017.

[34] J. M. Overduin and F. I. Cooperstock, "Evolution of the scale factor with a variable cosmological term," *Physical Review D: Particles, Fields, Gravitation and Cosmology*, vol. 58, no. 4, 1998.

[35] M. Szydłowski and A. Stachowski, "Cosmology with decaying cosmological constant—exact solutions and model testing," *Journal of Cosmology and Astroparticle Physics*, vol. 2015, no. 10, pp. 066-066, 2015.

[36] A. H. Guth and S. Pi, "Fluctuations in the new inflationary universe," *Physical Review Letters*, vol. 49, no. 15, pp. 1110–1113, 1982.

[37] H. Risken, *The FokkerPlanck Equation: Method of Solution and Applications*, Springer, Berlin, Germany, 1989.

[38] R. Brandenberger, V. Mukhanov, and T. Prokopec, "Entropy of a classical stochastic field and cosmological perturbations," *Physical Review Letters*, vol. 69, no. 25, pp. 3606–3609, 1992.

[39] R. Brandenberger, V. Mukhanov, and T. Prokopec, "Entropy of the gravitational field," *Physical Review D: Particles, Fields, Gravitation and Cosmology*, vol. 48, no. 6, pp. 2443–2455, 1993.

[40] L. M. Krauss and J. Dent, "Late time behavior of false vacuum decay: possible implications for cosmology and metastable inflating states," *Physical Review Letters*, vol. 100, no. 17, Article ID 171301, 4 pages, 2008.

[41] A. Stachowski, M. Szydlowski, and K. Urbanowski, "Cosmological implications of the transition from the false vacuum to the true vacuum state," *The European Physical Journal C*, vol. 77, p. 357, 2017.

Research Article

QFT Derivation of the Decay Law of an Unstable Particle with Nonzero Momentum

Francesco Giacosa [iD] [1,2]

[1]*Institute of Physics, Jan-Kochanowski University, Ul. Swietokrzyska 15, 25-406 Kielce, Poland*
[2]*Institute for Theoretical Physics, J. W. Goethe University, Max-von-Laue-Str. 1, 60438 Frankfurt, Germany*

Correspondence should be addressed to Francesco Giacosa; fgiacosa@ujk.edu.pl

We present a quantum field theoretical derivation of the nondecay probability of an unstable particle with nonzero three-momentum $\mathbf{p}$. To this end, we use the (fully resummed) propagator of the unstable particle, denoted as S, to obtain the energy probability distribution, called $d_S^{\mathbf{p}}(E)$, as the imaginary part of the propagator. The nondecay probability amplitude of the particle S with momentum $\mathbf{p}$ turns out to be, as usual, its Fourier transform: $a_S^{\mathbf{p}}(t) = \int_{\sqrt{m_{th}^2+\mathbf{p}^2}}^{\infty} dE d_S^{\mathbf{p}}(E) e^{-iEt}$ (m_{th} is the lowest energy threshold in the rest frame of S and corresponds to the sum of masses of the decay products). Upon a variable transformation, one can rewrite it as $a_S^{\mathbf{p}}(t) = \int_{m_{th}}^{\infty} dm d_S^{\mathbf{0}}(m) e^{-i\sqrt{m_{th}^2+\mathbf{p}^2}\,t}$ [here, $d_S^{\mathbf{0}}(m) \equiv d_S(m)$ is the usual spectral function (or mass distribution) in the rest frame]. Hence, the latter expression, previously obtained by different approaches, is here confirmed in an independent and, most importantly, covariant QFT-based approach. Its consequences are not yet fully explored but appear to be quite surprising (such as the fact that the usual time-dilatation formula does not apply); thus its firm understanding and investigation can be a fruitful subject of future research.

1. Introduction

The study of the decay law is a fundamental part of quantum mechanics (QM). It is now theoretically [1–9] and experimentally [10, 11] established that deviations from the exponential decay exist, but they are usually small. Such deviations are also present in quantum field theory (QFT) [9, 12].

An interesting question addresses the decay of an unstable particle with nonzero momentum $\mathbf{p}$. In [13–17], it was shown—by using QM-based approaches enlarged to include special relativity—that the nondecay probability of an unstable particle S with momentum $\mathbf{p}$ is given by (in natural units)

$$P_S^{\mathbf{p}}(t) = \left| a_S^{\mathbf{p}}(t) \right|^2$$
$$\text{with } a_S^{\mathbf{p}}(t) = \int_{m_{th}}^{\infty} dm d_S(m) e^{-i\sqrt{m^2+\mathbf{p}^2}\,t}, \quad (1)$$

where $d_S(m)$ is the energy (or mass) distribution of S in its rest frame [$dm d_S(m)$ is the probability that the unstable state S has

energy (or mass) between m and $m + dm$]. A review of the derivation is presented in Section 2. Quite remarkably, there are many interesting properties linked to this equation, which include deviations from the standard dilatation formula; see below.

The purpose of this work is straightforward: we derive (1) in a QFT framework (see Section 3). We thus confirm its validity and, as a consequence, its peculiar features. For definiteness, an underlying Lagrangian involving scalar fields is introduced, but our discussion is valid for any spin of the unstable particle and of the decay products. A central quantity of our study is the relativistic propagator of the unstable particle S: the mass distribution $d_S(m)$ is then obtained by the imaginary part of the propagator.

In this Introduction, we recall some basic and striking features connected to (1). The normalization

$$\int_{m_{th}}^{\infty} dm d_S(m) = 1 \quad (2)$$

is a crucial feature of the spectral function, implying that $a_S^{\mathbf{p}}(0) = 1$. It must be valid both in QM and in QFT. Here, without loss of generality, we set the lower limit of the integral to $m_{th} \geq 0$. In fact, a minimal energy m_{th} is present in each physical system; in particular, for a (relevant for us) relativistic system, it is given by the sum of the rest masses of the produced particles ($m_{th} = m_1 + m_2 + \cdots \geq 0$). Clearly, for $\mathbf{p} = \mathbf{0}$, (1) reduces to the usual expression

$$P_S^{rest}(t) = P_S^{\mathbf{0}}(t) = \left| a_S^{\mathbf{0}}(t) \right|^2 = \left| \int_{m_{th}}^{\infty} \mathrm{d}m \, d_S(m) \, e^{-imt} \right|^2. \quad (3)$$

A detailed study of (1) shows that the usual time dilatation does not hold:

$$P_S^{\mathbf{p}}(t) \neq P_S^{rest}\left(t \frac{M}{\sqrt{M^2 + \mathbf{p}^2}} \right), \quad (4)$$

where M is the mass of the state S defined, for instance, as the position of the peak of the distribution $d_S(m)$; in general, however, other definitions are possible, such as the real part of the pole of the propagator; see Section 3. The point is that, no matter which definition one takes, expression (4) remains an inequality.

It is always instructive to investigate the exponential limit, in which the spectral function of the state S reads [18, 19]

$$d_S^{BW}(m) = \frac{\Gamma}{2\pi} \left[(m - M)^2 + \frac{\Gamma^2}{4} \right]^{-1}, \quad (5)$$

where M is the "mass of the unstable state" corresponding to the peak. Even if the spectral function $d_S^{BW}(m)$ is clearly unphysical because there is no minimal energy ($m_{th} \to -\infty$), in many physical cases it is a good approximation for a quite broad energy range. Here, the decay amplitude and the decay law in the rest frame of the decaying particle notoriously read

$$a_S^{BW,\mathbf{0}}(t) = e^{-iMt - \Gamma t/2} \longrightarrow$$
$$P_S^{BW,rest}(t) = e^{-\Gamma t}. \quad (6)$$

When a nonzero momentum is considered, the nondecay probability is still an exponential given by

$$P_S^{BW,\mathbf{p}}(t) = e^{-\Gamma_{\mathbf{p}} t} \quad (7)$$

where the width is [17]

$$\Gamma_{\mathbf{p}}$$
$$= \sqrt{2} \sqrt{\left[\left(M^2 - \frac{\Gamma^2}{4} + \mathbf{p}^2 \right)^2 + M^2 \Gamma^2 \right]^{1/2} - \left(M^2 - \frac{\Gamma^2}{4} + \mathbf{p}^2 \right)}. \quad (8)$$

Clearly, $\Gamma_{\mathbf{p}=\mathbf{0}} = \Gamma$. One realizes, however, that $\Gamma_{\mathbf{p}}$ *differs* from the naively expected standard time-dilatation formula, according to which the decay width of an unstable state with momentum $\mathbf{p}$ should simply be

$$\frac{\Gamma M}{\sqrt{\mathbf{p}^2 + M^2}} = \gamma \Gamma. \quad (9)$$

Namely, the quantity $\gamma = \sqrt{\mathbf{p}^2 + M^2}/M = 1/\sqrt{1 - \mathbf{v}^2}$ is the usual dilatation factor for a state with (definite) energy M. Deviations between (8) and (9) are very small, as the numerical discussion in [17] shows. Although not measurable by current experiments [20], the very fact that deviations exist is very interesting and deserves further study.

As a last point, it should be stressed that in this work we consider unstable states with a definite momentum $\mathbf{p}$. This is a subtle point: while for a state with definite energy, a boost and a momentum translation are equivalent, this is not so for an unstable state, since it is not an energy eigenstate. Even more surprisingly, a boost of an unstable state is a quantum state whose nondecay probability is actually zero: it is already decayed (on the contrary, its survival probability presents a peculiar time contraction [21]). In other words, a boosted muon consists of an electron and two neutrinos [15, 17]. In this sense, the boost mixes the Hilbert subspace of the undecayed states with the subspace of the decay products; see [17] for details. There, it is also discussed why the basis of unstable states contains states with definite three-momentum. Indeed, the investigation of this paper also confirms this aspect: unstable states with definite momentum naturally follow from the study of its propagator in QFT.

The paper is organized in this way: in Section 2 we recall the QM derivation of (1), while in Section 3—the key part of this paper—we present this derivation in a QFT context. In the end, in Section 4 we describe our conclusions.

2. Recall of the QM-Based Derivation of (1)

For completeness, we report here the "standard" derivation of (1). To this end, we use the arguments presented in [17], but similar ones can be found in [13–16].

We consider a system described by the Hamiltonian H, whose eigenstates are denoted as

$$|m, \mathbf{p}\rangle = U_{\mathbf{p}} |m, \mathbf{0}\rangle, \quad (10)$$

where $U_{\mathbf{p}}$ is the unitary operator associated with the translation in momentum space. Standard normalization expressions are assumed:

$$\langle m_1, \mathbf{p}_1 \mid m_2, \mathbf{p}_2 \rangle = \delta(m_1 - m_2) \delta(\mathbf{p}_1 - \mathbf{p}_2). \quad (11)$$

The state $|m, \mathbf{p}\rangle$ has definite energy,

$$H |m, \mathbf{p}\rangle = \sqrt{\mathbf{p}^2 + m^2} |m, \mathbf{p}\rangle, \quad (12)$$

definite momentum,

$$\mathbf{P} |m, \mathbf{p}\rangle = \mathbf{p} |m, \mathbf{p}\rangle, \quad (13)$$

and definite velocity $\mathbf{p}/\sqrt{\mathbf{p}^2 + m^2}$. Note, assuming that the energy of $|m, \mathbf{p}\rangle$ is $\sqrt{\mathbf{p}^2 + m^2}$, we have a relativistic spectrum.

Formally, the Hamiltonian can be written as

$$H = \int \mathrm{d}^3\mathrm{p} \int_{m_{th}}^{\infty} dm \sqrt{\mathbf{p}^2 + m^2} |m, \mathbf{p}\rangle \langle m, \mathbf{p}|$$
$$= \int \mathrm{d}^3\mathrm{p} H_{\mathbf{p}} \quad (14)$$

where

$$H_{\mathbf{p}} = \int_{m_{th}}^{\infty} dm \sqrt{\mathbf{p}^2 + m^2} \, |m, \mathbf{p}\rangle \, \langle m, \mathbf{p}| \qquad (15)$$

is the effective Hamiltonian in the subspace of states with definite momentum $\mathbf{p}$.

Let us now consider an unstable state S in its rest frame. The corresponding quantum state at rest is assumed to be

$$|S, \mathbf{0}\rangle = \int_{m_{th}}^{\infty} dm \alpha_S(m) |m, \mathbf{0}\rangle, \qquad (16)$$

where $\alpha_S(m)$ is the probability amplitude that the state S has energy m. Hence, it is natural that the quantity $d_S(m) = |\alpha_S(m)|^2$ is the mass distribution: $d_S(m)dm$ is the probability that the unstable particle S has a mass between m and $m + dm$. As a consequence, $\int_0^{\infty} dm d_S(m) = 1$, as already discussed in the Introduction.

For the states of zero momentum, the Hamiltonian $H_{\mathbf{p}=0}$ can be expressed in terms of the undecayed state $|S, \mathbf{0}\rangle$ and its decay products in the form of a Lee Hamiltonian [22] (similar effective Hamiltonians are used also in quantum mechanics [6, 19] and quantum field theory [9, 23]):

$$H_{\mathbf{p}=0} = \int_{m_{th}}^{\infty} dm\, m\, |m, \mathbf{0}\rangle \, \langle m, \mathbf{0}|$$
$$= M_0 |S, \mathbf{0}\rangle \, \langle S, \mathbf{0}| + \int d^3k\, \omega(\mathbf{k}) |\mathbf{k}, \mathbf{0}\rangle \, \langle \mathbf{k}, \mathbf{0}| \qquad (17)$$
$$+ \int \frac{d^3k}{(2\pi)^{3/2}} g f(\mathbf{k}) \left[|S, \mathbf{0}\rangle \, \langle \mathbf{k}, \mathbf{0}| + |\mathbf{k}, \mathbf{0}\rangle \, \langle S, \mathbf{0}| \right],$$

where $|\mathbf{k}, \mathbf{0}\rangle$ represents a decay product with vanishing total momentum: in the two-body decay case, $|\mathbf{k}, \mathbf{0}\rangle$ describes two particles, the first with momentum $\mathbf{k}$ and the second with momentum $-\mathbf{k}$, hence

$$\omega(\mathbf{k}) = \sqrt{\mathbf{k}^2 + m_1^2} + \sqrt{\mathbf{k}^2 + m_2^2}. \qquad (18)$$

The last term in (17) represents the "mixing" between $|S, \mathbf{0}\rangle$ and $|\mathbf{k}, \mathbf{0}\rangle$, which causes the decay of the former into the latter. Moreover, g is a coupling constant and $f(\mathbf{k})$ encodes the dependence of the mixing on the momentum of the produced particles. The explicit expressions connecting the states $|\mathbf{k}, \mathbf{0}\rangle$ to $|m, \mathbf{0}\rangle$ formally read

$$|\mathbf{k}, \mathbf{0}\rangle = \int_{m_{th}}^{\infty} dm \beta_{\mathbf{k}}(m) |m, \mathbf{0}\rangle \qquad (19)$$

where $\beta_{\mathbf{k}}(m)$ can be found by diagonalizing the Hamiltonian (17).

Let us now consider an unstable state with definite momentum $\mathbf{p}$, which is denoted as $|S, \mathbf{p}\rangle$:

$$|S, \mathbf{p}\rangle = U_{\mathbf{p}} |S, \mathbf{0}\rangle = \int_{m_{th}}^{\infty} dm \alpha_S(m) |m, \mathbf{p}\rangle. \qquad (20)$$

The normalization

$$\langle S, \mathbf{p}_1 | S, \mathbf{p}_2 \rangle = \delta(\mathbf{p}_1 - \mathbf{p}_2) \qquad (21)$$

follows. Note that (20) is *not* a state with definite velocity. This is due to the fact that each state $|m, \mathbf{p}\rangle$ in the superposition has a different velocity $\mathbf{p}/\sqrt{\mathbf{p}^2 + m^2}$. The subset of Hilbert space given by $\{|S, \mathbf{p}\rangle \forall \mathbf{p} \subset R^2\}$ represents the set of all undecayed quantum states of the system under study.

The form of the Hamiltonian $H_{\mathbf{p}}$ in terms of the states $|S, \mathbf{p}\rangle$ and $U_{\mathbf{p}}|\mathbf{k}, \mathbf{0}\rangle = |\mathbf{k}, \mathbf{p}\rangle$ can be in principle derived by using the expressions above. Together with (20), one shall also take (19) and apply $U_{\mathbf{p}}$ in order to get

$$U_{\mathbf{p}} |\mathbf{k}, \mathbf{0}\rangle = |\mathbf{k}, \mathbf{p}\rangle = \int_{m_{th}}^{\infty} dm \beta_{\mathbf{k}}(m) |m, \mathbf{p}\rangle. \qquad (22)$$

Then, one should invert (20) and (22) and insert it into $H_{\mathbf{p}}$ of (15). However, its explicit expression is definitely not trivial but, fortunately, also not needed in the present work. Hence, we do not attempt to write it down here.

We now turn to the nondecay amplitude of the state S. In its rest frame ($\mathbf{p} = \mathbf{0}$), upon starting from a properly normalized state with zero momentum, $|S, \mathbf{0}\rangle/\sqrt{\delta(0)}$, one obtains the usual expression

$$a_S^{\mathbf{0}}(t) = \frac{1}{\delta(0)} \langle S, \mathbf{0} | e^{-iHt} | S, \mathbf{0} \rangle$$
$$= \frac{1}{\delta(0)} \int_{m_{th}}^{\infty} dm_1 dm_2 \langle m_1, \mathbf{0} | e^{-iHt} | m_2, \mathbf{0} \rangle \qquad (23)$$
$$= \int_{m_{th}}^{\infty} dm d_S(m) e^{-imt},$$

in agreement with (3). The theory of decay is discussed in great detail for the case $\mathbf{p} = \mathbf{0}$ in [4, 6, 7, 9] and references therein. Note here the nondecay probability coincides with the survival probability (that is, the probability that the state did not change), but in general this is not the case [17].

Next, we consider a normalized unstable state S with nonzero momentum: $|S, \mathbf{p}\rangle/\sqrt{\delta(\mathbf{0})}$. The resulting nondecay probability amplitude

$$a_S^{\mathbf{p}}(t) = \frac{1}{\delta(0)} \langle S, \mathbf{p} | e^{-iHt} | S, \mathbf{p} \rangle$$
$$= \frac{1}{\delta(0)} \int_{m_{th}}^{\infty} dm_1 dm_2 \langle m_1, \mathbf{p} | e^{-iHt} | m_2, \mathbf{p} \rangle \qquad (24)$$
$$= \int_{m_{th}}^{\infty} dm d_S(m) e^{-i\sqrt{m^2 + \mathbf{p}^2} t}$$

coincides with (1), hence concluding our derivation.

In principle, one could also start from the Hamiltonian $H_{\mathbf{p}}$ and obtain the energy distribution associated with this state, denoted as $d_S^{\mathbf{p}}(E)$. Then, $a_S^{\mathbf{p}}(t)$ should also emerge as the Fourier transform of the latter. This is hard to do here, since the explicit expression of $H_{\mathbf{p}}$ in terms of $|S, \mathbf{p}\rangle$ and $|\mathbf{k}, \mathbf{p}\rangle$ was not written down (as mentioned previously, this is not an easy task). Quite interestingly, in the framework of QFT, the function $d_S^{\mathbf{p}}(E)$ can be easily determined; see Section 3.

As a last comment of this section, we recall that the general nondecay probability of an arbitrary state $|\Psi\rangle$ reads

$$P_{|\Psi\rangle}(t) = \int d^3 p \left| \langle S, \mathbf{p} | e^{-iHt} | \Psi \rangle \right|^2, \qquad (25)$$

whose interpretation is straightforward: we project $|\Psi\rangle$ onto the basis of undecayed states. In general, $P_{|\Psi\rangle}(0)$ is not unity. Notice also that $P_{|\Psi\rangle}(t)$ is *not* the survival probability of the state $|\Psi\rangle$ (a state can change with time but still be undecayed if it is a different superposition of $|S, \mathbf{p}\rangle$).

When a boost $U_{\mathbf{v}}$ on the state with zero momentum (and hence with zero velocity) $|S, \mathbf{0}\rangle$ is considered, the resulting state reads [17]

$$\begin{aligned} |\varphi_{\mathbf{v}}\rangle &= U_{\mathbf{v}} |S, \mathbf{0}\rangle \\ &= \int_{m_{th}}^{\infty} dm \alpha_S(m) \sqrt{m} \gamma^{3/2} |m, m\gamma\mathbf{v}\rangle, \end{aligned} \qquad (26)$$

where $\gamma = (1 - \mathbf{v}^2)^{-1/2}$. In fact, each element of the superposition, $|m, m\gamma\mathbf{v}\rangle$, has velocity $\mathbf{v}$. Of course, $|\varphi_{\mathbf{v}}\rangle$ is not an eigenstate of momentum, since each element in (26) has a different momentum $\mathbf{p} = m\gamma\mathbf{v}$. In this respect, the state $|S, \mathbf{0}\rangle$ is special: it is the only state which has at the same time definite momentum and definite velocity (both of them vanishing). As mentioned in the Introduction, the nondecay probability associated with $|\varphi_{\mathbf{v}}\rangle$ vanishes:

$$P_{|\varphi_{\mathbf{v}}\rangle}(t) = 0 \quad \forall \mathbf{v} \neq \mathbf{0}. \qquad (27)$$

As soon as a nonzero velocity is considered, the state has decayed. This result is quite surprising but also rather "delicate": when a wave packet is considered, $P_{nd}^{|\varphi_{\mathbf{v}}\rangle}(t)$ is nonzero (even if it is not 1 for $t = 0$) [17].

3. Covariant QFT Derivation of (1)

Let us consider an unstable particle described by the scalar field $S(x) \equiv S(t, \mathbf{x})$. For an illustrative example, one can couple S with bare mass M_0 to two scalar fields φ_1 (with mass m_1) and φ_2 (with mass m_2) via the interaction term $gS\varphi_1\varphi_2$, leading to the QFT Lagrangian

$$\begin{aligned} \mathcal{L} &= \frac{1}{2} \left[(\partial_\mu \varphi_1)^2 - m_1^2 \varphi_1^2 \right] + \frac{1}{2} \left[(\partial_\mu \varphi_2)^2 - m_2^2 \varphi_2^2 \right] \\ &+ \frac{1}{2} \left[(\partial_\mu S)^2 - M_0^2 S^2 \right] + gS\varphi_1\varphi_2. \end{aligned} \qquad (28)$$

This is the QFT counterpart of the QM system of the previous section. Note we use scalar fields for simplicity, but our discussion is in no way limited to it.

The (full) propagator of the state S (details in [24]) reads

$$\Delta_S(p^2) = \frac{1}{p^2 - M_0^2 + \Pi(p^2) + i\varepsilon} \qquad (29)$$
$$\text{with } p^2 = E^2 - \mathbf{p}^2,$$

where $E = p^0$ is the energy and $\mathbf{p}$ the three-momentum. Because of covariance, $\Delta_S(p^2)$ depends only on p^2. The

quantity $\Pi(p^2)$ is the one-particle irreducible diagram. Its calculation is of course nontrivial (it requires a proper regularization), but it is not needed for our purposes. The imaginary part is

$$\begin{aligned} \text{Im}\Pi(p^2) &= \sqrt{p^2} \Gamma\left(\sqrt{p^2}\right) \\ &= \frac{|\mathbf{k}|}{8\pi\sqrt{p^2}} g^2 f_\Lambda^2(|\mathbf{k}|) + \cdots, \end{aligned} \qquad (30)$$

where dots refer to higher orders, which are however typically very small [25]. Once $\text{Im}\Pi(p^2)$ is fixed, $\text{Re}\Pi(p^2)$ can be determined by dispersion relations (for an example of this technique, see, e.g., [26]). The quantity $\Gamma^{tl} = \Gamma(\sqrt{p^2} = M)$ is the usual tree-level decay width; hence in the exponential limit the decay law $P_S(t) = e^{-\Gamma^{tl}t}$ must be reobtained. As mentioned in the Introduction, an unstable state has not a definite mass: this is why different definitions for M (which is not the bare mass M_0 entering in (29)) are possible: $\text{Re}\Delta_S^{-1}(p^2 = M^2) = 0$ (zero of the real part of the denominator), or $\text{Re}[\sqrt{s_{pole}}]$, with $\Delta_S^{-1}(s_{pole}) = 0$ (real part of the pole), or the maximum of the spectral function defined below.

We also recall that

$$|\mathbf{k}| = \sqrt{\frac{p^4 + (m_1^2 - m_2^2)^2 - 2p^2(m_1^2 + m_2^2)}{4p^2}} \qquad (31)$$

coincides, for the on-shell decay, with the modulus of the three-momentum of one of the outgoing particles. The vertex function $f_\Lambda(|\mathbf{k}|)$ is a proper regularization which fulfills the condition $f_\Lambda(|\mathbf{k}| \to 0) = 1$ and describes the high-energy behavior of the theory (its UV completion); hence the parameter Λ is some high-energy scale; $f_\Lambda(|\mathbf{k}|)$ is formally not present in (28) since it appears in the regularization procedure, but it can be included directly in the Lagrangian by rendering it nonlocal [27] in a way that fulfills covariance [28]. In a renormalizable theory (such as the one of (28)), the dependence on Λ disappears in the low-energy limit.

The properties outlined above, although in general very important in specific calculations, turn out to be actually secondary to the proof that we present below, where only the formal expression of the propagator of (29) is relevant. Moreover, even when the unstable particle is not a scalar, one can always define a scalar part of the propagator which looks just as in (29), then the outlined properties apply, *mutatis mutandis*, to each QFT Lagrangian.

As a next step, upon introducing the Mandelstam variable $s = p^2$, the function $F(s)$ defined as

$$F(s) = \frac{1}{\pi} \text{Im}\left[\Delta_S(p^2 = s)\right] \qquad (32)$$

fulfills the normalization condition:

$$\int_{s_{th}}^{\infty} ds F(s) = 1, \qquad (33)$$

where $s_{th} = m_{th}^2$ is the minimal squared energy. For the case of (28), one has obviously $s_{th} = (m_1 + m_2)^2$. The normalization (33) is a consequence of the Källén–Lehmann representation [29]

$$\Delta_S\left(p^2\right) = \int_{s_{th}}^{\infty} ds \frac{F(s)}{p^2 - s + i\varepsilon}, \tag{34}$$

in which the propagator $\Delta_S(p^2)$ has been rewritten as the "sum" of free propagators $[p^2 - s + i\varepsilon]^{-1}$, each one of them weighted by $F(s)$: $dsF(s)$ is the probability that the squared mass lies between s and $s + ds$. Of course, the normalization (33) is a very important feature of our approach. For a detailed proof of its validity, we refer to [30]. Here we recall a simple version of it, which is obtained by assuming the rather strong requirement $\Pi(p^2) = 0$ for $p^2 > \Lambda^2$, where Λ is a high-energy scale (no matter how large). Under this assumption

$$\Delta_S\left(p^2\right) = \frac{1}{p^2 - M_0^2 + \Pi\left(p^2\right) + i\varepsilon}$$
$$= \int_{s_{th}}^{\Lambda^2} ds \frac{F(s)}{p^2 - s + i\varepsilon}. \tag{35}$$

Then, upon taking a certain value $p^2 \gg \Lambda^2$, the previous equation reduces to

$$\frac{1}{p^2} = \int_{s_{th}}^{\Lambda^2} ds \frac{F(s)}{p^2} \longrightarrow$$
$$\int_{s_{th}}^{\Lambda^2} ds F(s) = 1 \tag{36}$$

The general case in which $\Pi(p^2 \to \infty) = 0$ smoothly requires more steps, but the final result of (33) still holds [30].

Let us now consider the rest frame of the decaying particle: $\mathbf{p} = \mathbf{0}$, $s = p^2 = E^2 = m^2$. Here, upon a simple variable change ($m = \sqrt{s}$), we obtain the mass distribution (or spectral function) $d_S^{\mathbf{p}=\mathbf{0}}(m)$ through the equation

$$dm d_S^{\mathbf{p}=\mathbf{0}}(m) = ds F(s), \tag{37}$$

out of which

$$d_S(m) = d_S^{\mathbf{p}=\mathbf{0}}(m) = 2mF\left(s = m^2\right). \tag{38}$$

As already mentioned, $dm d_S(m)$ is the probability that the particle S has a mass between m and $m + dm$ [24, 31]. In this context, the normalization

$$\int_{m_{th}}^{\infty} dm d_S(m) = 1 \tag{39}$$

follows from (33). Once the function $d_S(m)$ is identified as the mass distribution of the undecayed quantum state, the nondecay probability's amplitude $a_S^0(t)$ can be obtained by repeating the steps of Section 2. The result coincides, as expected, with (3). Yet, it should be stressed that the unstable quantum state $|S, \mathbf{0}\rangle$ characterized by the distribution $d_S(m)$

is not simply given by $a_{\mathbf{0}}^{\dagger}|0_{PT}\rangle$, where $|0_{PT}\rangle$ is the perturbative vacuum and $a_{\mathbf{p}}^{\dagger}$ the creator operator of the noninteracting field S. The case of neutrino oscillations shows a similar situation: the state corresponding to a certain flavour, such as the neutrino ν_e, must be constructed with due care by making use of Bogolyubov transformations [32]. Along this line, the exact and formal determination of the state $|S, \mathbf{0}\rangle$, corresponding to the mass distribution $d_S(m)$, in the context of QFT requires a generalization of Bogolyubov transformations and was, to our knowledge, not yet explicitly done (it is left for the future). Nevertheless, it is not needed for the purpose of this paper.

Let us now consider the particle S moving with a certain momentum $\mathbf{p}$. Upon using $s = E^2 - \mathbf{p}^2$, the energy distribution—as function of E—is obtained by

$$dE d_S^{\mathbf{p}}(E) = ds F(s), \tag{40}$$

leading to

$$d_S^{\mathbf{p}}(E) = 2EF\left(s = E^2 - \mathbf{p}^2\right)$$
$$= \frac{E}{\sqrt{E^2 - \mathbf{p}^2}} d_S\left(\sqrt{E^2 - \mathbf{p}^2}\right). \tag{41}$$

The quantity $dE d_S^{\mathbf{p}}(E)$ is the probability that the particle S with definite momentum $\mathbf{p}$ has an energy between E and $E + dE$ (clearly, $d_S^{\mathbf{p}=\mathbf{0}}(E) = d_S(m = E)$). Also in this case, the normalization

$$\int_{\sqrt{m_{th}^2 + \mathbf{p}^2}}^{\infty} dE d_S^{\mathbf{p}}(E) = 1 \tag{42}$$

is a consequence of (33). When $d_S(m)$ has a maximum at M, then $d_S^{\mathbf{p}}(E)$ has a maximum at $\sim \sqrt{M^2 + \mathbf{p}^2}$. Note the very fact that the propagator depends on $p^2 = E^2 - \mathbf{p}^2$ allows to determine the spectral function $d_S^{\mathbf{p}}(E)$ for a definite momentum $\mathbf{p}$, that corresponds to the state $|S, \mathbf{p}\rangle$ of Section 2.

The nondecay probability's amplitude for a state S moving with momentum $\mathbf{p}$ is then given by

$$a_S^{\mathbf{p}}(t) = \int_{\sqrt{m_{th}^2 + \mathbf{p}^2}}^{\infty} dE d_S^{\mathbf{p}}(E) e^{-iEt}, \tag{43}$$

where we have taken into account that the minimal energy is now given by $\sqrt{m_{th}^2 + \mathbf{p}^2}$.

This expression can be manipulated by using (41) and via a change of variable:

$$a_S^{\mathbf{p}}(t) = \int_{\sqrt{m_{th}^2 + \mathbf{p}^2}}^{\infty} dE d_S^{\mathbf{p}}(E) e^{-iEt}$$
$$= \int_{\sqrt{m_{th}^2 + \mathbf{p}^2}}^{\infty} dE \frac{E}{\sqrt{E^2 - \mathbf{p}^2}} d_S\left(\sqrt{E^2 - \mathbf{p}^2}\right) e^{-iEt} \tag{44}$$
$$= \int_{m_{th}}^{\infty} dm d_S(m) e^{-i\sqrt{m^2 + \mathbf{p}^2} t},$$

which coincides *exactly* with (1), as we wanted to demonstrate. Thus, we confirm the validity of (1) in a covariant QFT-based framework.

4. Conclusions

The decay law of a moving unstable particle is an interesting subject that connects special relativity to QM and QFT. An important aspect is the validity of (1), which expresses the nondecay probability of a state with nonzero momentum and whose standard derivation is reviewed in Section 2.

The main contribution of this paper has been the derivation of a quantum field theoretical proof of (1). To this end, we started from the (scalar part of the) propagator of an unstable quantum field, denoted as S. Then, we have determined the energy distribution of the state S with definite momentum **p**, out of which the survival's probability amplitude is calculated.

As discussed in the Introduction, there are interesting and peculiar consequences of (1). Future studies are definitely needed to further understand the properties of a decay of a moving unstable particle and to look for feasible experimental tests.

Data Availability

There is no external data. Theoretical result is based on the author's research.

Conflicts of Interest

The author declares that there are no conflicts of interest regarding the publication of this paper.

Acknowledgments

References

[1] L. A. Khalfin, "Zhurnal Eksperimentalnoi i Teoreticheskoi Fiziki," *Journal for Experimental and Theoretical Physics*, vol. 6, p. 1053, 1371, (Engl. trans. Sov. Phys. JETP 6 1053).

[2] B. Misra and E. C. Sudarshan, "The Zeno's paradox in quantum theory," *Journal of Mathematical Physics*, vol. 18, no. 4, pp. 756–763, 1977.

[3] A. Degasperis, L. Fonda, and G. C. Ghirardi, "Does the Lifetime of an Unstable System Depend on the Measuring Apparatus?" *Nuovo Cim*, vol. 21, no. 3, pp. 471–484, 1973.

[4] L. Fonda, G. C. Ghirardi, and A. Rimini, "Decay theory of unstable quantum systems," *Reports on Progress in Physics*, vol. 41, no. 4, p. 587, 1978.

[5] P. Facchi, H. Nakazato, and S. Pascazio, "From the Quantum Zeno to the Inverse Quantum Zeno Effect," *Physical Review Letters*, vol. 86, no. 13, pp. 2699–2703, 2001.

[6] P. Facchi and S. Pascazio, "Spontaneous emission and lifetime modification caused by an intense electromagnetic field," *Physical Review A*, vol. 62, article 023804, 2000.

[7] K. Urbanowski and K. Raczyńska, "Possible emission of cosmic X- and γ-rays by unstable particles at late times," *Physics Letters B*, vol. 731, pp. 236–241, 2014.

[8] M. Peshkin, A. Volya, and V. Zelevinsky, "Non-exponential and oscillatory decays in quantum mechanics," *EPL (Europhysics Letters)*, vol. 107, no. 4, p. 40001, 2014.

[9] F. Giacosa, "Non-exponential decay in quantum field theory and in quantum mechanics: the case of two (or more) decay channels," *Foundations of Physics*, vol. 42, no. 10, pp. 1262–1299, 2012.

[10] S. R. Wilkinson, C. F. Bharucha, M. C. Fischer et al., "Experimental evidence for non-exponential decay in quantum tunnelling," *Nature*, vol. 387, no. 6633, pp. 575–577, 1997.

[11] C. Rothe, S. I. Hintschich, and A. P. Monkman, "Violation of the Exponential-Decay Law at Long Times," *Physical Review Letters*, vol. 96, no. 16, 2006.

[12] F. Giacosa and G. Pagliara, "Deviation from the exponential decay law in relativistic quantum field theory: the example of strongly decaying particles," *Modern Physics Letters A*, vol. 26, no. 30, pp. 2247–2259, 2011.

[13] L. A. Khalfin, "Quantum Theory of unstable particles and relativity," *PDMI Pewprint*, 1997.

[14] M. I. Shirokov, "Decay law of moving unstable particle," *International Journal of Theoretical Physics*, vol. 43, no. 6, pp. 1541–1553, 2004.

[15] E. V. Stefanovich, "Quantum effects in relativistic decays," *International Journal of Theoretical Physics*, vol. 35, no. 12, pp. 2539–2554, 1996.

[16] K. Urbanowski, "Decay law of relativistic particles: quantum theory meets special relativity," *Physics Letters B*, vol. 737, pp. 346–351, 2014.

[17] F. Giacosa, "Decay law and time dilatation," *Acta Physica Polonica B*, vol. 47, no. 9, pp. 2135–2150, 2016.

[18] V. Weisskopf, E. P. Wigner, and Z. Phys, "Berechnung der natürlichen Linienbreite auf Grund der Diracschen Lichttheorie," *Zeitschrift für Physik*, vol. 63, no. 1-2, pp. 54–73, 1930.

[19] M. O. Scully and M. S. Zubairy, *Quantum Optics*, Cambridge University Press, Cambridge, UK, 1997.

[20] J. Bailey et al., "Measurements of relativistic time dilatation for positive and negative muons in a circular orbit," *Nature*, vol. 26, pp. 301–305, 1977.

[21] S. A. Alavi and C. Giunti, "Which is the quantum decay law of relativistic particles?" *EPL (Europhysics Letters)*, vol. 109, no. 6, 2015.

[22] T. D. Lee, "Some Special Examples in Renormalizable Field TheoryT. D. Lee," *Physical Review*, vol. 95, no. 5, p. 1329, 1954.

[23] Z. Liu, W. Kamleh, D. B. Leinweber, F. M. Stokes, A. W. Thomas, and J. Wu, " Hamiltonian Effective Field Theory Study of the ," *Physical Review Letters*, vol. 116, no. 8, 2016.

[24] F. Giacosa and G. Pagliara, "Spectral functions of scalar mesons," *Physical Review C: Nuclear Physics*, vol. 76, no. 6, 2007.

[25] J. Schneitzer, T. Wolkanowski, and F. Giacosa, "The role of the next-to-leading order triangle-shaped diagram in two-body hadronic decays," *Nuclear Physics. B. Theoretical, Phenomenological, and Experimental High Energy Physics. Quantum Field Theory and Statistical Systems*, vol. 888, pp. 287–299, 2014.

[26] T. Wolkanowski, F. Giacosa, and D. H. Rischke, *Physical Review D: Particles, Fields, Gravitation and Cosmology*, vol. 93, no. 1, 2016.

[27] J. Terning, "Gauging nonlocal Lagrangians," *Physical Review D*, vol. 44, p. 887, 1991.

[28] M. Soltysiak and F. Giacosa, "A covariant nonlocal Lagrangian for the description of the scalar kaonic sector," *Acta Physica Polonica B*, 9, 2016, https://arxiv.org/abs/1607.01593.

[29] M. E. Peskin and D. V. Schroeder, *An Introduction to Quantum Field Theory*, Addison-Wesley, Reading, Mass, USA, 1995.

[30] F. Giacosa and G. Pagliara, "Spectral function of a scalar boson coupled to fermions," *Physical Review D: Particles, Fields, Gravitation and Cosmology*, vol. 88, no. 2, 2013.

[31] P. T. Matthews and A. Salam, "Relativistic theory of unstable particles," *Physical Review*, vol. 112, p. 283, 1958.

[32] M. Blasone, A. Capolupo, O. Romei, and G. Vitiello, "Quantum field theory of boson mixing," *Physical Review D: Particles, Fields, Gravitation and Cosmology*, vol. 63, no. 12, Article ID 125015, 2001.

Research Article
Time Dilation in Relativistic Quantum Decay Laws of Moving Unstable Particles

Filippo Giraldi ⬤

School of Chemistry and Physics, University of KwaZulu-Natal and National Institute for Theoretical Physics (NITheP), Westville Campus, Durban 4001, South Africa

Correspondence should be addressed to Filippo Giraldi; giraldi.filippo@gmail.com

The relativistic quantum decay laws of moving unstable particles are analyzed for a general class of mass distribution densities which behave as power laws near the (nonvanishing) lower bound μ_0 of the mass spectrum. The survival probability $\mathscr{P}_p(t)$, the instantaneous mass $M_p(t)$, and the instantaneous decay rate $\Gamma_p(t)$ of the moving unstable particle are evaluated over short and long times for an arbitrary value p of the (constant) linear momentum. The ultrarelativistic and nonrelativistic limits are studied. Over long times, the survival probability $\mathscr{P}_p(t)$ is approximately related to the survival probability at rest $\mathscr{P}_0(t)$ by a scaling law. The scaling law can be interpreted as the effect of the relativistic time dilation if the asymptotic value $M_p(\infty)$ of the instantaneous mass is considered as the effective mass of the unstable particle over long times. The effective mass has magnitude μ_0 at rest and moves with linear momentum p or, equivalently, with constant velocity $1/\sqrt{1 + \mu_0^2/p^2}$. The instantaneous decay rate $\Gamma_p(t)$ is approximately independent of the linear momentum p, over long times, and, consequently, is approximately invariant by changing reference frame.

1. Introduction

The description of the decay laws of unstable particles via quantum theory has been a central topic of research for decades [1, 2]. Many unstable particles which are generated in astrophysical phenomena or high-energy accelerator experiments are moving in the laboratory frame of the observer at relativistic or ultrarelativistic velocity. For this reason, plenty of studies have been devoted to formulate the decay laws in terms of relativistic quantum theory. See [1, 3–6], to name but a few.

A fundamental subject in the description of the relativistic decays of moving unstable particles is the way the decay laws transform by changing the reference frame. Naturally, it is essential to understand how the decay laws, holding in the rest reference frame of the moving particle, are transformed in the laboratory frame of an observer. The nondecay or survival probability of an unstable particle has been evaluated in [7, 8] for nonvanishing and vanishing values of the linear momentum in terms of the mass distribution density (MDD). The condition of vanishing linear momentum, $p = 0$,

provides the survival probability in the reference frame where the particle is at rest, while the condition of nonvanishing linear momentum, $p > 0$, can be referred to the laboratory frame of an observer where the particles move with linear momentum p. The effects of the relativistic time dilation in quantum decay laws of moving unstable particles remain a matter of central interest. See [7–17], to name but a few.

As a continuation of the scenario described above, here, we evaluate the survival probability, the instantaneous energy, and the instantaneous decay rate of a moving unstable particle over short and long times for a wide variety of MDDs and for an arbitrary value of the (constant) linear momentum. In light of the short-time transformations of the survival probability according to the relativistic time dilation, we search for further scaling relations in the decay laws which can relate the conditions of nonvanishing and vanishing linear momentum. In this way, we aim to find further descriptions of the ways the decay laws of moving unstable particle transform by changing reference frame.

The paper is organized as follows. Section 2 is devoted to the relativistic quantum decay laws of a general moving

unstable particle. In Section 3, the survival probability is evaluated over short and long times for an arbitrary value of the linear momentum and a general class of MDD. In Section 4, the transformation of the long-time survival probability is described via a scaling law. Section 5 is devoted to the evaluation of the instantaneous mass and instantaneous decay rate over short and long times. In Section 6, the scaling law, describing the transformation of the survival probability, is interpreted in terms of the relativistic time dilation and of the instantaneous mass of the moving unstable particle. Summary and conclusions are reported in Section 7.

2. Relativistic Quantum Decay Laws

An extended and detailed description of the relativistic quantum decay laws of moving unstable particles has been recently provided in [14, 17]. Following these references, a brief summary of unstable quantum states, of the survival probability, and of the instantaneous energy and decay rate is reported below for the sake of clarity, by adopting the system of units where $\hbar = c = 1$. The motion is assumed to be one-dimensional, due to the conservation of the linear momentum [1, 7, 8, 14–17].

In the Hilbert space $\mathscr{H}$ of the quantum states which describe the unstable particle, let the state kets $|m, p\rangle$ be the common eigenstates of the linear momentum P operator and the Hamiltonian H self-adjoint operator, $P|m, p\rangle = p|m, p\rangle$ and $H|m, p\rangle = E(m, p)|m, p\rangle$, for every value of the mass parameter m and of the linear momentum p. The mass parameter m belongs to the spectrum of the Hamiltonian which is supposed to be continuous with lower bound μ_0, which means $m \geq \mu_0$. In the rest reference frame of the moving particle the linear momentum vanishes and the mentioned state kets become $|m, 0\rangle$, while the eigenstates of the Hamiltonian are $E(m, 0) = m$. Let $|\phi\rangle$ be the ket of the Hilbert space $\mathscr{H}$ which describes the quantum state of the unstable particle. Such state can be expressed in terms of the eigenstates $|m, 0\rangle$ of the Hamiltonian as $|\phi\rangle = \int_{\mu_0}^{\infty} f(m)|m, 0\rangle dm$, via the expansion function $f(m)$. The survival amplitude $A_0(t)$ is defined in the rest reference frame of the moving unstable particle as $A_0(t) = \langle\phi|e^{-\imath Ht}|\phi\rangle$ and is given by the integral expression

$$A_0(t) = \int_{\mu_0}^{\infty} \omega(m) e^{-\imath m t} dm, \tag{1}$$

where $\imath$ is the imaginary unit. The function $\omega(m)$ represents the MDD and reads $\omega(m) = |f(m)|^2$. The probability $\mathscr{P}_0(t)$ that the decaying particle is in the initial state at the time t, i.e., the survival probability, is given by the following form, $\mathscr{P}_0(t) = |A_0(t)|^2$, in the rest reference frame of the moving unstable particle.

Let Λ be the Lorentz transformation which relates the reference frame where the unstable moving particle is at rest, to the one with velocity $v = p/(m\gamma_L)$, where γ_L is the corresponding relativistic Lorentz factor. Let $U(\Lambda)$ be an unitary representation of the transformation Λ acting on the Hilbert space $\mathscr{H}$ such that $|m, p\rangle = U(\Lambda)|m, 0\rangle$ for every value of the mass parameter m in the Hamiltonian spectrum.

The state ket $|\phi, p\rangle$ describes the moving unstable particle with nonvanishing linear momentum p. Such state is related to the state ket $|\phi\rangle$ as follows: $|\phi, p\rangle = U(\Lambda)|\phi\rangle$. The form $E(m, p) = m\gamma_L = \sqrt{p^2 + m^2}$ is obtained by considering the energy-momentum 4-vector and the Lorentz invariance [6, 18]. The quantity $A_p(t)$ is defined as $A_p(t) = \langle p, \phi|e^{-\imath Ht}|\phi, p\rangle$ and represents the survival amplitude in the reference frame where the particle has linear momentum p. The approach described above leads to the following integral expression of the survival amplitude:

$$A_p(t) = \int_{\mu_0}^{\infty} \omega(m) e^{-\imath\sqrt{p^2+m^2}t} dm. \tag{2}$$

The quantity $\mathscr{P}_p(t)$ represents the survival probability that the decaying particle is in the initial state at the time t in the reference frame where the unstable particle has linear momentum p and is given by the square modulus of the survival amplitude, $\mathscr{P}_p(t) = |A_p(t)|^2$. See [7, 8, 17] for details.

The decay laws of the unstable particles are obtained from the MDD via (1) and (2). In literature, the MDD is usually represented via the Breit-Wigner function [19]:

$$\omega_{\mathrm{BW}}(m) = \frac{\Theta(m - \mu_0)\lambda_{\mathrm{BW}}\overline{\Gamma}/(2\pi)}{(m - m_0)^2 + \overline{\Gamma}^2/4}, \tag{3}$$

where λ_{BW} is a normalization factor, $\Theta(m)$ is the Heaviside unit step function, m_0 is the rest mass of the particle, and $\overline{\Gamma}$ is the decay rate at rest. A detailed analysis of the survival amplitude of a moving unstable particle has been performed in [8] by considering the Breit-Wigner form of the MDD [7]. The long-time behavior of the survival amplitude results in dominant inverse power laws, besides additional decaying exponential terms. Refer to [8] for details. In [17, 20, 21] general forms of MDD are considered with power-law behaviors near the lower bound of the mass spectrum. The long-time decay of the survival amplitude $A_0(t)$ is described by inverse power laws which are determined by the low-mass profile of the MDD [20, 21]. Additional removable logarithmic singularities in the low-mass form of the MDD lead to logarithmic-like relaxations of the survival amplitude at rest $A_0(t)$ which can be arbitrarily slower or faster than inverse power laws [22, 23].

Since the unstable particle decays, the initial state is not an eigenstate of the Hamiltonian and the instantaneous mass (energy) is not defined during the time evolution. For this reason, instantaneous mass (energy) and decay rate are defined in the rest reference frame of the moving particle in terms of an effective Hamiltonian. Such operator acts on the subspace of the Hilbert space $\mathscr{H}$ which is spanned by the initial state. Refer to [14, 17, 20, 21, 24] for details. In the same way, the instantaneous mass (energy) and decay rate $\Gamma_p(t)$ of the moving unstable particle are defined in the frame system where the particle has linear momentum p. For both vanishing and nonvanishing values of the linear momentum p, the instantaneous mass $M_p(t)$ and decay rate $\Gamma_p(t)$ are

obtained from the survival amplitude $A_p(t)$ via the following forms [14, 17, 20–23]:

$$M_p(t) = -\operatorname{Im}\left\{\frac{\dot{A}_p(t)}{A_p(t)}\right\} \qquad (4)$$

$$\Gamma_p(t) = -2\operatorname{Re}\left\{\frac{\dot{A}_p(t)}{A_p(t)}\right\}. \qquad (5)$$

The long-time behavior of the instantaneous mass $M_p(t)$ and decay rate $\Gamma_p(t)$ has been evaluated in [14, 15] for the Breit-Wigner form of the MDD.

2.1. Relativistic Time Dilation. The interpretation of decay processes via the theory of special relativity suggests that the lifetime which is detected in the rest reference frame of the unstable particle increases in the reference frame where the particle is moving. The increase is due to the relativistic dilation of times and is determined by the relativistic Lorentz factor [25].

The appearance of the relativistic time dilation in quantum decays is a matter of great interest and fruitful discussions. See [7–17], to name but a few. A broadly shared opinion is that the relativistic time dilation influences the survival probability uniquely in the short-time exponential decay. Briefly, this means that the survival probability $\mathscr{P}_p(t)$ and the survival probability at rest $\mathscr{P}_0(t)$ are given by the exponential forms $\mathscr{P}_p(t) \sim e^{-t/\tau_p}$ and $\mathscr{P}_0(t) \sim e^{-t/\tau_0}$, over short times. Under this assumption, the survival probability obeys the scaling law

$$\mathscr{P}_p(t) \sim \mathscr{P}_0\left(\frac{t}{\gamma_L}\right), \qquad (6)$$

over short times. The parameter τ_0 represents the lifetime of the particle at rest, while τ_p is the lifetime which is detected in the reference frame where the particle is moving with linear momentum p. According to the relativistic time dilation, the lifetimes are related as follows: $\tau_p = \tau_0\gamma_L$, where γ_L is the corresponding relativistic Lorentz factor. Refer to [7, 8, 12–17] for an extended explanation. In this context, we intend to study the survival probability $\mathscr{P}_p(t)$ and the survival probability at rest $\mathscr{P}_0(t)$ over short and long times for a wide variety of MDDs. We search for further ways to describe the transformations of the decay laws which occur by changing reference frame.

3. Survival Probability versus Linear Momentum

In the present section the short- and long-time behaviors of the survival probability are studied for a general value p of the constant linear momentum of the moving unstable particle. The analysis performed in the whole paper is based entirely on form (2) of the survival amplitude [7, 12]. For the sake of convenience, the survival amplitude is expressed via the dimensionless variables τ, ξ, ρ, and η. These variables are defined in terms of a generic scale mass m_s as follows:

$\tau = m_s t$, $\xi = m/m_s$, $\rho = p/m_s$, and $\eta = \sqrt{\rho^2 + \xi^2}$. The MDD is expressed in terms of the auxiliary function $\Omega(\xi)$ via the scaling law $\omega(m_s\xi) = \Omega(\xi)/m_s$, for every $\xi \geq \xi_0$, where $\xi_0 = \mu_0/m_s$. In this way, the survival amplitude $A_p(t)$ results in the expression below:

$$A_p(t) = \int_{\xi_0}^{\infty} \Omega(\xi)\, e^{-i\eta\tau} d\xi. \qquad (7)$$

The MDDs under study are defined over the infinite support $[\mu_0, \infty)$ by auxiliary functions $\Omega(\xi)$ of the following form:

$$\Omega(\xi) = (\xi - \xi_0)^{\alpha}\, \Omega_0(\xi). \qquad (8)$$

In order to study the long-time behavior of the decay laws of the moving unstable particle, the MDDs are requested to obey the conditions below. The lower bound of the mass spectrum is chosen to be nonvanishing, $\xi_0 > 0$. The constraints $\alpha \geq 0$ and $\Omega_0(\xi_0) > 0$ are also requested. The function $\Omega_0(\xi)$ and the derivatives $\Omega_0^{(j)}(\xi)$ are required to be summable, for every $j = 1,\ldots,\lfloor\alpha\rfloor+4$, and continuously differentiable in the whole support $[\mu_0, \infty)$, for every $j = 1,\ldots,\lfloor\alpha\rfloor + 3$. Consequently, the limits $\lim_{\xi\to\xi_0^+}\Omega_0^{(j)}(\xi)$ must exist as finite and be $\Omega_0^{(j)}(\xi_0)$ for every $j = 0,\ldots,\lfloor\alpha\rfloor + 4$. The functions $\Omega_0^{(j)}(\xi)$ have to decay sufficiently fast as $\xi \to +\infty$, so that the auxiliary function $\Omega(\xi)$ and the derivatives $\Omega^{(j)}(\xi)$ vanish as $\xi \to +\infty$, for every $j = 0,\ldots,\lfloor\alpha\rfloor$.

As far as the short-time behavior of the survival amplitude is concerned, let the auxiliary function decay as follows: $\Omega(\xi) = \mathcal{O}(\xi^{-1-l_0})$ for $\xi \to +\infty$, with $l_0 > 5$. Under this condition, the survival amplitude evolves algebraically over short times:

$$A_p(t) \sim 1 - i a_0 t - a_1 t^2 + i a_2 t^3, \qquad (9)$$

for $t \ll 1/m_s$. The constants a_0, a_1, and a_2 are given by the expressions below:

$$\begin{aligned} a_0 &= \int_{\mu_0}^{\infty} \omega(m)\sqrt{p^2 + m^2}\, dm, \\ a_1 &= \frac{1}{2}\int_{\mu_0}^{\infty} \omega(m)\left(p^2 + m^2\right) dm, \\ a_2 &= \frac{1}{6}\int_{\mu_0}^{\infty} \omega(m)\left(p^2 + m^2\right)^{3/2} dm. \end{aligned} \qquad (10)$$

The short-time evolution of the survival probability is derived from (7) and (9) and is algebraic:

$$\mathscr{P}_p(t) \sim 1 - \pi_0 t^2, \qquad (11)$$

for $t \ll 1/m_s$, where $\pi_0 = 2a_1 - a_0^2$.

The long-time behavior of the survival amplitude is obtained from (7) and from the following equivalent form:

$$A_p(t) = \int_{\eta_0}^{\infty} \frac{\eta\,\Omega\left(\sqrt{\eta^2 - \rho^2}\right)}{\sqrt{\eta^2 - \rho^2}} e^{-i\eta\tau} d\eta, \qquad (12)$$

where $\eta_0 = \sqrt{\rho^2 + \xi_0^2}$. Notice that the constraint of non-vanishing lower bound of the mass spectrum, $\xi_0 > 0$, is fundamental for the equivalence of expressions (7) and (12) of the survival amplitude. The asymptotic analysis [26, 27] of the integral form, appearing in (12) for $\tau \gg 1$, provides the expression of the survival amplitude over long times:

$$A_p(t) \sim c_0 e^{-\iota((\pi/2)(1+\alpha)+\sqrt{\mu_0^2+p^2}t)} \left(\frac{\chi_p}{m_s t} \right)^{1+\alpha}, \quad (13)$$

for $t \gg 1/m_s$, where $c_0 = \Gamma(1+\alpha)\Omega_0(\xi_0)$, and

$$\chi_p = \sqrt{1 + \frac{p^2}{\mu_0^2}}. \quad (14)$$

Asymptotic form (13) of the survival amplitude holds for every value of the linear momentum p, nonvanishing, arbitrarily large or small, or vanishing; for the variety of MDDs under study; for every $\alpha \geq 0$; and for every value μ_0 of the lower bound of the mass spectrum such that $\mu_0/m_s > 0$. The last condition is crucial and will be interpreted in the next section in terms of the instantaneous mass at rest of the moving unstable particle. The square modulus of asymptotic expression (13) approximates the survival probability over long times:

$$\mathcal{P}_p(t) \sim c_0^2 \left(\frac{\chi_p}{m_s t} \right)^{2(1+\alpha)}, \quad (15)$$

for $t \gg 1/m_s$. Notice that the time scale $1/m_s$ and, consequently, the short or long times, $t \ll 1/m_s$ or $t \gg 1/m_s$, are independent of the auxiliary function $\Omega(\xi)$ and are determined uniquely by the MDD.

4. Scaling Law for the Survival Probability

Expression (15) of the survival probability holds for every value of the constant linear momentum p. Such arbitrariness allows evaluating the survival probability in the nonrelativistic and ultrarelativistic limits. For vanishing value of the linear momentum, $p = 0$, or, equivalently, in the rest reference frame of the unstable particle, the survival probability is approximated over long times as follows:

$$\mathcal{P}_0(t) \sim \frac{c_0^2}{(m_s t)^{2(1+\alpha)}}, \quad (16)$$

for $t \gg 1/m_s$. Instead, consider large values of the linear momentum, $p \gg \mu_0$. In such condition the survival probability is approximated over long times as follows:

$$\mathcal{P}_p(t) \sim c_0^2 \left(\frac{p}{\mu_0 m_s t} \right)^{2(1+\alpha)}, \quad (17)$$

for $t \gg 1/m_s$. By comparing (15) and (16), we observe that, for the MDDs under study, the survival probability obeys, approximately over long times, the following scaling law:

$$\mathcal{P}_p(t) \sim \mathcal{P}_0 \left(\frac{t}{\chi_p} \right), \quad (18)$$
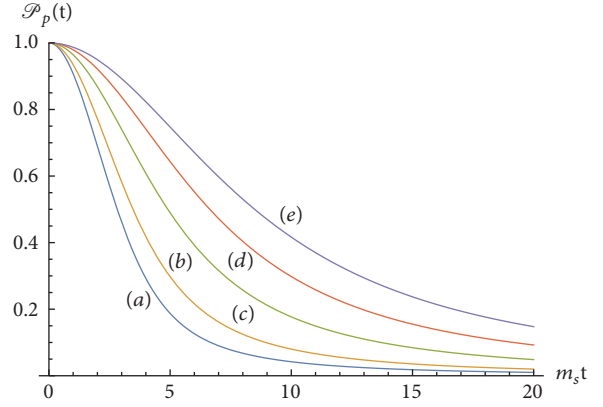

FIGURE 1: (Color online) the survival probability $\mathcal{P}_p(t)$ versus $(m_s t)$ for $0 \leq m_s t \leq 20$, MDDs given by (21), $\alpha = 0$, $\mu_0 = m_s$, and different values of the linear momentum p. Curve (a) corresponds to $p = 0 m_s$; (b) corresponds to $p = m_s$; (c) corresponds to $p = 2 m_s$; (d) corresponds to $p = 3 m_s$; (e) corresponds to $p = 4 m_s$.

for $t \gg 1/m_s$. This is the main result of the paper. In fact, the above scaling law describes how the survival probability at rest transforms, approximately over long times, in the reference frame where the particle moves with constant linear momentum p. The transformation can be interpreted, approximately, as the effect of a time dilation which is determined by the scaling factor χ_p. Notice that the scaling factor, given by (14), diverges in the limit $\mu_0 \to 0^+$. In Section 6, the scaling law (18) is interpreted, via the special relativity, as the effect of the relativistic time dilation. This interpretation holds if the asymptotic value of the instantaneous mass is considered as the effective mass of the moving unstable particle over long times.

The correction to the scaling law (18) can be estimated via the expression $(\mathcal{P}_p(t) - \mathcal{P}_0(t/\chi_p))/\mathcal{P}_0(t/\chi_p)$. For the MDDs under study, such correction vanishes inversely quadratically over long times:

$$\frac{\mathcal{P}_p(t) - \mathcal{P}_0(t/\chi_p)}{\mathcal{P}_0(t/\chi_p)} \sim \frac{\kappa_p}{(m_s t)^2}, \quad (19)$$

for $t \gg 1/m_s$, where

$$\kappa_p = \frac{(1+\alpha)(2+\alpha)m_s p^2}{\mu_0^3} \left(2 \frac{\Omega_0'(\mu_0/m_s)}{\Omega_0(\mu_0/m_s)} - \frac{m_s}{\mu_0 \chi_p^2} \right)$$

$$\times \left(3 + \alpha + \left(\frac{5}{2} + \alpha \right) \frac{p^2}{\mu_0^2} \right). \quad (20)$$

Numerical analysis of the survival probability $\mathcal{P}_p(t)$ has been displayed in Figures 1, 2, 3, 4, and 5. The computed MDDs are given by the following toy form of the auxiliary function:

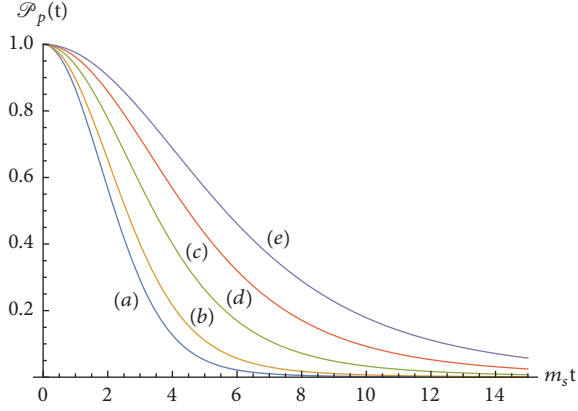$$\Omega(\xi) = w_\alpha \xi \left(\xi^2 - \xi_0^2 \right)^\alpha e^{-\xi^2}, \quad (21)$$

FIGURE 2: (Color online) the survival probability $\mathscr{P}_p(t)$ versus $(m_s t)$ for $0 \le m_s t \le 15$, MDDs given by (21), $\alpha = 1$, $\mu_0 = m_s$, and different values of the linear momentum p. Curve (a) corresponds to $p = 0 m_s$; (b) corresponds to $p = m_s$; (c) corresponds to $p = 2m_s$; (d) corresponds to $p = 3m_s$; (e) corresponds to $p = 4m_s$.

FIGURE 4: (Color online) ratio $\mathscr{P}_p(t)/\mathscr{P}_0(t)$ versus $(m_s t)$ for $0 \le m_s t \le 50$, MDDs given by (21), $\mu_0 = m_s$, $\alpha = 0$, and different values of the linear momentum p. Curve (a) corresponds to $p = m_s$; (b) corresponds to $p = 2m_s$; (c) corresponds to $p = 3m_s$; (d) corresponds to $p = 4m_s$; (e) corresponds to $p = 5m_s$.
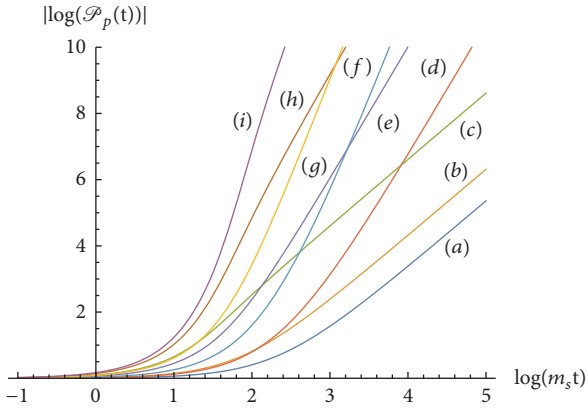

FIGURE 3: (Color online) quantity $|\log(\mathscr{P}_p(t))|$ versus $\log(m_s t)$ for $e^{-1} \le m_s t \le e^5$, MDDs given by (21), $\mu_0 = m_s$, and different values of the parameter α and of the linear momentum p. Curve (a) corresponds to $\alpha = 0$ and $p = 5m_s$; (b) corresponds to $\alpha = 0$ and $p = 3m_s$; (c) corresponds to $\alpha = 0$ and $p = 0$; (d) corresponds to $\alpha = 1$ and $p = 5m_s$; (e) corresponds to $\alpha = 1$ and $p = 2m_s$; (f) corresponds to $\alpha = 2$ and $p = 4m_s$; (g) corresponds to $\alpha = 2$ and $p = 2m_s$; (h) corresponds to $\alpha = 1$ and $p = 0m_s$; (i) corresponds to $\alpha = 2$ and $p = 0$.

FIGURE 5: (Color online) ratio $\mathscr{P}_p(t)/\mathscr{P}_0(t)$ versus $(m_s t)$ for $0 \le m_s t \le 50$, MDDs given by (21), $\mu_0 = m_s$, and different values of the parameter α and of the linear momentum p. Curve (a) corresponds to $\alpha = 1$ and $p = 2m_s$; (b) corresponds to $\alpha = 1$ and $p = 3m_s$; (c) corresponds to $\alpha = 2$ and $p = 2m_s$; (d) corresponds to $\alpha = 1$ and $p = 4m_s$.

5. Instantaneous Mass and Decay Rate versus Linear Momentum

In the present section the instantaneous mass and decay rate are analyzed over short and long times for every value of the constant linear momentum p of the particle, which is detected in the laboratory frame of the observer. The instantaneous mass and decay rate are evaluated from the survival amplitude via (4) and (5).

Again, let the auxiliary function decay as $\Omega(\xi) = \mathcal{O}(\xi^{-1-l_0})$ for $\xi \to +\infty$, with $l_0 > 5$. The short-time evolution of the instantaneous mass and decay rate are obtained from behavior (9) of the survival amplitude and from (4) and (5). In this way, the following algebraic evolution results over short times:

where w_α is a normalization factor and reads $w_\alpha = 2e^{\xi_0^2}/\Gamma(1 + \alpha)$. Different values of the nonnegative power α and linear momentum p are considered. The corresponding MDDs belong to the class under study which is defined in Section 3 via (8). The asymptotic lines appearing in Figure 3 agree with the long-time inverse-power-law decays of the survival probability, given by (15). The ordinates of the asymptotic horizontal lines of Figures 4 and 5 are in accordance with form (14) of the scaling factor χ_p. The long-time dilation in the survival probability, given by the scaling law (18), is confirmed by the common horizontal asymptotic line, at ordinate 1, which appears in Figures 6 and 7.
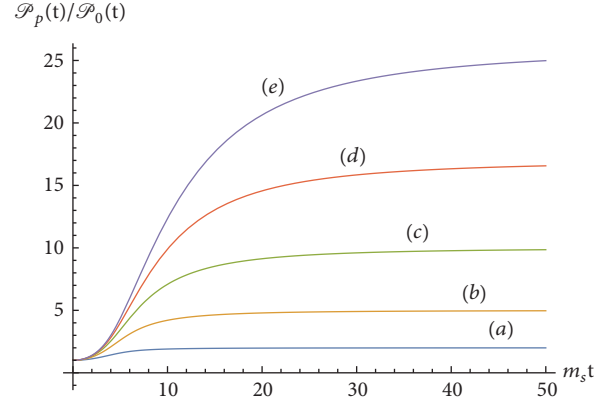
$\mathscr{P}_p(t)/\mathscr{P}_0(t/\chi_p)$

FIGURE 6: (Color online) ratio $\mathscr{P}_p(t)/\mathscr{P}_0(t/\chi_p)$ versus $(m_s t)$ for $0 \leq m_s t \leq 50$, MDDs given by (21), $\mu_0 = m_s$, $\alpha = 0$, and different values of the linear momentum p. Curve (a) corresponds to $p = 5m_s$; (b) corresponds to $p = 4m_s$; (c) corresponds to $p = 3m_s$; (d) corresponds to $p = 2m_s$; (e) corresponds to $p = m_s$.
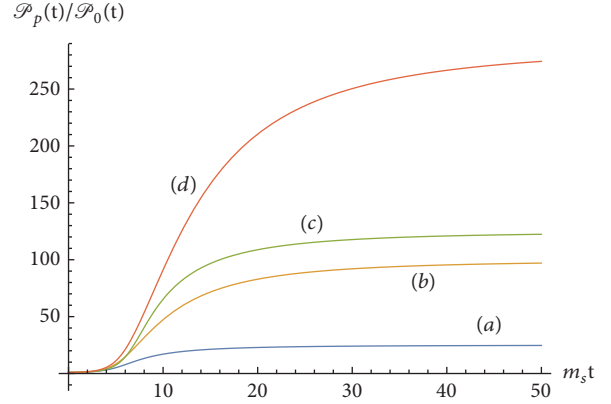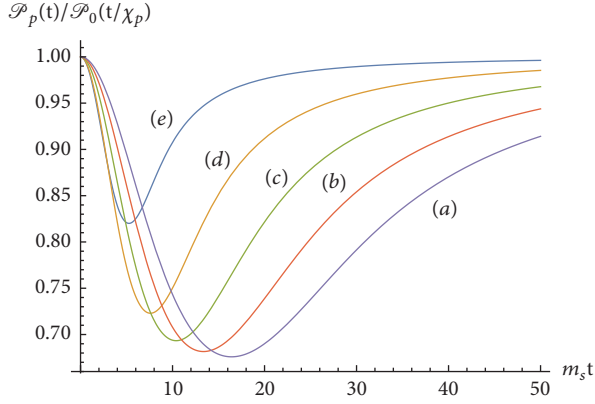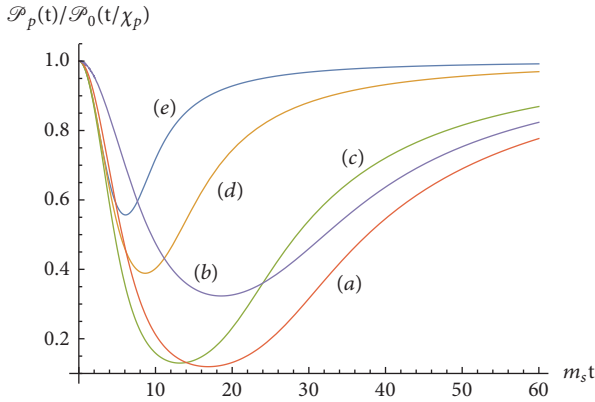
$\mathscr{P}_p(t)/\mathscr{P}_0(t/\chi_p)$

FIGURE 7: (Color online) ratio $\mathscr{P}_p(t)/\mathscr{P}_0(t/\chi_p)$ for $0 \leq m_s t \leq 60$, MDDs given by (21), $\mu_0 = m_s$, and different values of the parameter α and of the linear momentum p. Curve (a) corresponds to $\alpha = 2$ and $p = 4m_s$; (b) corresponds to $\alpha = 1$ and $p = 5m_s$; (c) corresponds to $\alpha = 2$ and $p = 3m_s$; (d) corresponds to $\alpha = 1$ and $p = 2m_s$; (e) corresponds to $\alpha = 1$ and $p = m_s$.

$$M_p(t) \sim a_0 - \pi_1 t^2,$$
$$\Gamma_p(t) \sim \pi_2 t, \tag{22}$$

for $t \ll 1/m_s$, where $\pi_1 = a_0^3 + 3(a_2 - a_0 a_1)$ and $\pi_2 = 2(2a_1 - a_0^2)$.

The long-time behavior of the instantaneous mass and decay rate are studied in case that the MDD fulfills the constraints which are reported in the second paragraph of Section 3. In addition, the functions $\xi \Omega_0(\xi)$ and $\xi \Omega(\xi)$ are required to obey the conditions which are requested in the same paragraph for the function $\Omega_0(\xi)$ and the auxiliary function $\Omega(\xi)$, respectively. The asymptotic analysis [26, 27] of the instantaneous mass or the instantaneous decay rate is obtained from the results of Section 3 and from (4) or (5), respectively.

The instantaneous mass tends over long times, $t \gg 1/m_s$, to the asymptotic value $M_p(\infty)$, given by

$$M_p(\infty) = \sqrt{\mu_0^2 + p^2}, \tag{23}$$

according to the following dominant algebraic decay:

$$M_p(t) \sim M_p(\infty)\left(1 + \zeta_p(m_s t)^{-2}\right). \tag{24}$$

The constant ζ_p is defined as

$$\zeta_p = (1 + \alpha)$$
$$\cdot \frac{m_s}{\mu_0}\left(\left(1 + \frac{\alpha}{2}\right)\frac{m_s}{\mu_0}\frac{p^2}{\mu_0^2 + p^2} - \frac{\Omega_0'(\mu_0/m_s)}{\Omega_0(\mu_0/m_s)}\right). \tag{25}$$

For large values of the linear momentum, $p \gg \mu_0$, the instantaneous mass decays over long times, $t \gg 1/m_s$, as follows:

$$M_p(t) \sim p\left(1 + \bar{\zeta}_p(m_s t)^{-2}\right), \tag{26}$$

where

$$\bar{\zeta}_p = (1 + \alpha)\frac{m_s}{\mu_0}\left(\left(1 + \frac{\alpha}{2}\right)\frac{m_s}{\mu_0} - \frac{\Omega_0'(\mu_0/m_s)}{\Omega_0(\mu_0/m_s)}\right). \tag{27}$$

If the linear momentum vanishes, $p = 0$, the instantaneous mass (at rest) tends over long times, $t \gg 1/m_s$, to the minimum value of the mass spectrum:

$$M_0(\infty) = \mu_0, \tag{28}$$

with the following dominant algebraic decay:

$$M_0(t) \sim M_0(\infty)\left(1 + \zeta_0(m_s t)^{-2}\right), \tag{29}$$

where

$$\zeta_0 = -(1 + \alpha)\frac{m_s}{\mu_0}\frac{\Omega_0'(\mu_0/m_s)}{\Omega_0(\mu_0/m_s)}. \tag{30}$$

The instantaneous decay rate $\Gamma_p(t)$ vanishes over long times, $t \gg 1/m_s$, according to the following dominant algebraic decay:

$$\Gamma_p(t) \sim \frac{2(1 + \alpha)}{t}. \tag{31}$$

Differently from the survival probability and from the instantaneous mass, the dominant asymptotic form of the instantaneous decay rate is independent of the linear momentum p. Consequently, the instantaneous decay rate at rest remains approximately unchanged over long times in the reference frame where the unstable particle moves with linear momentum p. Notice that decay laws (29) and (31) are in accordance with the ones which are obtained in [23] for a wider class of MDDs.

FIGURE 8: (Color online) quantity $M_p(t)/m_s$ versus $(m_s t)$ for $0 \leq m_s t \leq 15$, MDDs given by (21), $\mu_0 = m_s$, $\alpha = 1$, and different values of the linear momentum p. Curve (a) corresponds to $p = 0m_s$; (b) corresponds to $p = m_s$; (c) corresponds to corresponds to $p = 2m_s$; (d) corresponds to $p = 3m_s$; (e) corresponds to $p = 4m_s$.

FIGURE 10: (Color online) quantity $\Gamma_p(t)/m_s$ versus $(m_s t)$ for $0 \leq m_s t \leq 30$, MDDs given by (21), $\mu_0 = m_s$, $\alpha = 1$, and different values of the linear momentum p. Curve (a) corresponds to $p = 4m_s$; (b) corresponds to $p = 3m_s$; (c) corresponds to $p = 2m_s$; (d) corresponds to $p = 1m_s$; (e) corresponds to $p = 0m_s$.
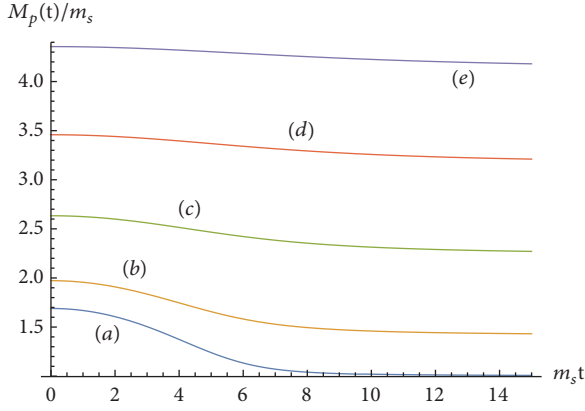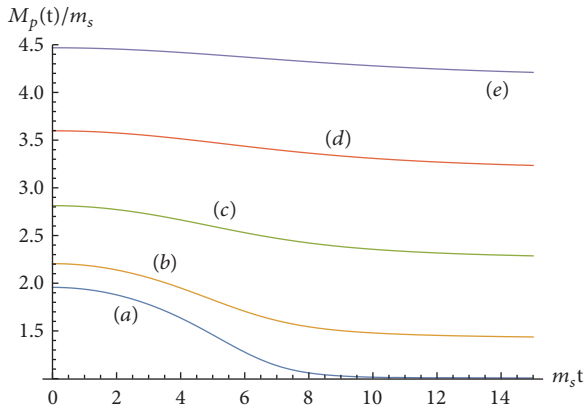

FIGURE 9: (Color online) quantity $M_p(t)/m_s$ versus $(m_s t)$ for $0 \leq m_s t \leq 15$, MDDs given by (21), $\mu_0 = m_s$, $\alpha = 2$, and different values of the linear momentum p. Curve (a) corresponds to $p = 0m_s$; (b) corresponds to $p = m_s$; (c) corresponds to corresponds to $p = 2m_s$; (d) corresponds to $p = 3m_s$; (e) corresponds to $p = 4m_s$.
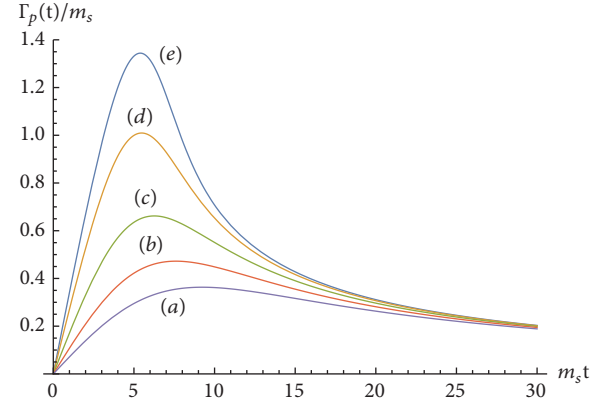
FIGURE 11: (Color online) quantity $\Gamma_p(t)/m_s$ versus $(m_s t)$ for $0 \leq m_s t \leq 30$, MDDs given by (21), $\mu_0 = m_s$, $\alpha = 2$, and different values of the linear momentum p. Curve (a) corresponds to $p = 4m_s$; (b) corresponds to $p = 3m_s$; (c) corresponds to $p = 2m_s$; (d) corresponds to $p = 1m_s$; (e) corresponds to $p = 0m_s$.

Numerical analysis of the instantaneous mass or the instantaneous decay rate is displayed in Figures 8, 9, 12, and 13 or Figures 10, 11, 14, and 15, respectively. The computed MDDs are given by the toy form (21) of the auxiliary function for different values of the nonnegative power α and of the linear momentum p. The asymptotic lines of Figure 12 and the asymptotic horizontal lines of Figure 13 are in accordance with the long-time inverse-power-law decays of the instantaneous mass, given by (24) and (29). The asymptotic horizontal lines of Figure 13 agree with (32) and with expression (14) of the scaling factor. The asymptotic lines appearing in Figure 14 and the asymptotic horizontal lines of Figure 15, at ordinate 1, agree with the long-time inverse-power-law behavior of the instantaneous decay rate, given by (31).

6. Relativistic Time Dilation and Survival Probability

In Section 2.1 how the survival probability at rest, $\mathcal{P}_0(t)$, transforms, due to the relativistic time dilation, in the reference frame where the unstable particle moves with constant linear momentum p is reported. The transformed survival probability, $\mathcal{P}_p(t)$, is related to the survival probability at rest, $\mathcal{P}_0(t)$, by the scaling law (6). The scaling factor consists in the corresponding relativistic Lorentz factor γ_L.

The analysis performed in Section 3 shows that, for the class of MDDs under study, the survival probability $\mathcal{P}_p(t)$ and the survival probability at rest $\mathcal{P}_0(t)$ are related by the scaling law (18) over long times. The corresponding scaling factor χ_p is given by (14). It is worth noticing that the scaling factor χ_p coincides with the ratio of the asymptotic form of the instantaneous mass $M_p(t)$ and the asymptotic

FIGURE 12: (Color online) quantity $|\log(|M_p(t)/\sqrt{p^2 + \mu_0^2} - 1|)|$ versus $\log(m_s t)$ for $e \leq m_s t \leq e^{3.3}$, MDDs given by (21), $\mu_0 = m_s$, and different values of the parameter α and of the linear momentum p. Curve (a) corresponds to $\alpha = 2$ and $p = 4m_s$; (b) corresponds to $\alpha = 2$ and $p = 2m_s$; (c) corresponds to $\alpha = 1$ and $p = 2m_s$; (d) corresponds to $\alpha = 2$ and $p = m_s$; (e) corresponds to $\alpha = 0$ and $p = 3m_s$; (f) corresponds to $\alpha = 0$ and $p = 5m_s$.
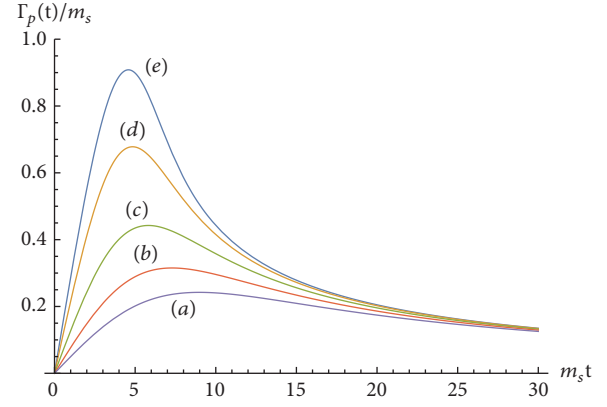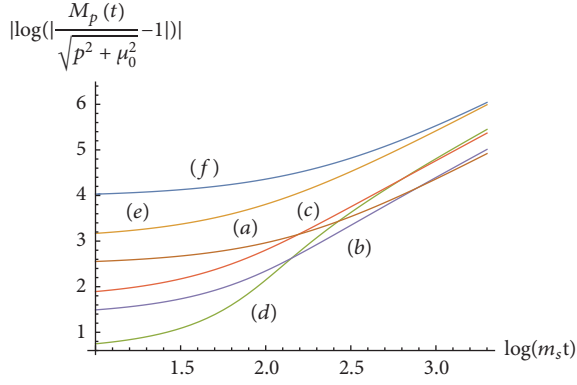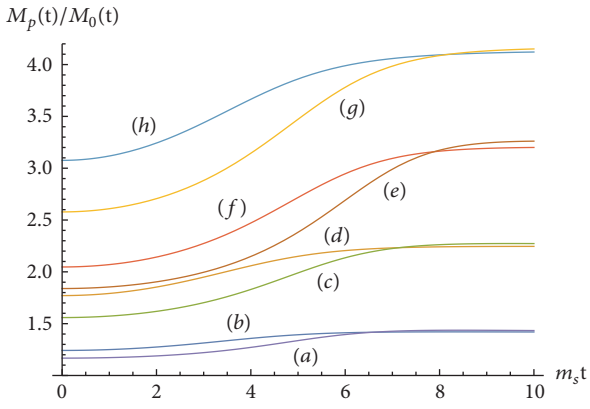

FIGURE 13: (Color online) ratio $M_p(t)/M_0(t)$ versus $(m_s t)$ for $0 \leq m_s t \leq 10$, MDDs given by (21), $\mu_0 = m_s$, and different values of the parameter α and of the linear momentum p. Curve (a) corresponds to $\alpha = 1$ and $p = m_s$; (b) corresponds to $\alpha = 0$ and $p = m_s$; (c) corresponds to $\alpha = 1$ and $p = 2m_s$; (d) corresponds to $\alpha = 0$ and $p = 2m_s$; (e) corresponds to $\alpha = 2$ and $p = 3m_s$; (f) corresponds to $\alpha = 1$ and $p = 3m_s$; (g) corresponds to $\alpha = 1$ and $p = 4m_s$; (h) corresponds to $\alpha = 0$ and $p = 4m_s$.

FIGURE 14: (Color online) quantity $|\log(\Gamma_p(t)/m_s)|$ versus $\log(m_s t)$ for $e^{1.5} \leq m_s t \leq e^{3.8}$, MDDs given by (21), $\mu_0 = m_s$, and different values of the parameter α and of the linear momentum p. Curve (a) corresponds to $\alpha = 2$ and $p = 0m_s$; (b) corresponds to $\alpha = 2$ and $p = 2m_s$; (c) corresponds to $\alpha = 1$ and $p = 0m_s$; (d) corresponds to $\alpha = 1$ and $p = 2m_s$; (e) corresponds to $\alpha = 1$ and $p = 2m_s$; (f) corresponds to $\alpha = 1$ and $p = 5m_s$; (g) corresponds to $\alpha = 0$ and $p = 0m_s$; (h) corresponds to $\alpha = 0$ and $p = 3m_s$; (i) corresponds to $\alpha = 0$ and $p = 5m_s$.
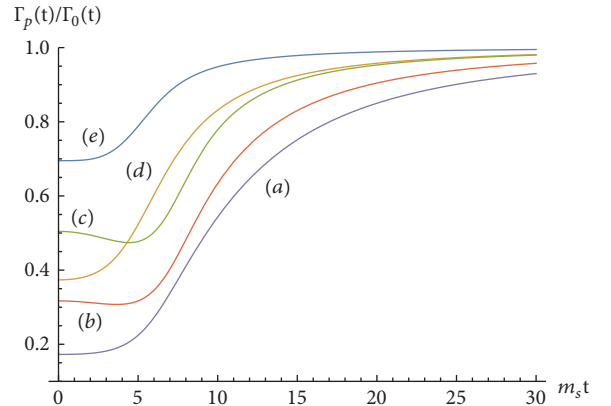
FIGURE 15: (Color online) ratio $\Gamma_p(t)/\Gamma_0(t)$ versus $(m_s t)$ for $0 \leq m_s t \leq 30$, MDDs given by (21), $\mu_0 = m_s$, and different values of the parameter α and of the linear momentum p. Curve (a) corresponds to $\alpha = 1$ and $p = 4m_s$; (b) corresponds to $\alpha = 2$ and $p = 3m_s$; (c) corresponds to $\alpha = 2$ and $p = 2m_s$; (d) corresponds to $\alpha = 0$ and $p = 2m_s$; (e) corresponds to $\alpha = 0$ and $p = m_s$.

expression of the instantaneous mass at rest $M_0(t)$ of the moving unstable particle:

$$\chi_p = \frac{M_p(\infty)}{M_0(\infty)}. \tag{32}$$

At this stage, consider the reference frame $\mathfrak{S}$ where a mass at rest which is equal to the asymptotic value $M_0(\infty)$ becomes $M_p(\infty)$ due to the relativistic transformation of the mass. According to (32), in the reference frame $\mathfrak{S}$ the corresponding relativistic Lorentz factor coincides with the scaling factor χ_p. We remind that, initially, the unstable quantum system is not in an eigenstate of the Hamiltonian. Consequently, in the present model the mass of the unstable

particle is not defined. On the contrary, the instantaneous mass is properly defined in terms of the survival amplitude. See [14, 16, 17] for details.

In light of the above observations, the long-time scaling law (18) can be interpreted as an effect of the relativistic time dilation if the asymptotic value $M_p(\infty)$ of the instantaneous mass is considered to be the effective mass of the unstable particle over long times. In fact, in the reference frame $\mathfrak{S}$ the mass at rest $M_0(\infty)$, which is equal to the value μ_0, moves with linear momentum p, or, equivalently, with constant velocity $1/\sqrt{1 + \mu_0^2/p^2}$, and becomes the relativistic mass $M_p(\infty)$, which is equal to the value $\sqrt{\mu_0^2 + p^2}$. Concurrently,

in the reference frame $\mathfrak{S}$ the survival probability at rest $\mathscr{P}_0(t)$ transforms, according to the relativistic time dilation, in the survival probability $\mathscr{P}_p(t)$ and obeys the scaling law (6), or, equivalently, (18), over long times. In this context, the crucial condition of nonvanishing lower bound of the mass spectrum, $\mu_0/m_s > 0$, suggests that the long-time relativistic dilation and the scaling law (6), or, equivalently, (18), hold uniquely for an unstable moving particle with nonvanishing effective mass, $M_0(\infty) > 0$.

7. Summary and Conclusions

The relativistic quantum decay laws of a moving unstable particle have been analyzed over short and long times for an arbitrary value p of the (constant) linear momentum. The MDDs under study exhibit power-law behaviors near the (nonvanishing) lower bound μ_0 of the mass spectrum. Due to the arbitrariness of the linear momentum, the ultrarelativistic and nonrelativistic limits have been obtained as particular cases.

The survival probability, which is detected in the rest reference frame of the unstable particle, transforms in the reference frame where the unstable particle moves with linear momentum p, approximately according to a scaling law, over long times. The scaling factor is determined by the lower bound μ_0 of the mass spectrum and by the linear momentum p of the particle. The scaling law can be interpreted as the effect of the relativistic time dilation if the asymptotic form of the instantaneous mass $M_p(t)$ is considered as the effective mass of the moving unstable particle over long times. In fact, consider the reference frame $\mathfrak{S}$ where a mass at rest of magnitude μ_0 moves with velocity $1/\sqrt{1 + \mu_0^2/p^2}$, or, equivalently, with linear momentum p. The mass at rest μ_0 coincides with the asymptotic value of the instantaneous mass at rest, $M_0(\infty)$, of the moving unstable particle. In the reference frame $\mathfrak{S}$ the transformed mass, which is equal to the value $\sqrt{\mu_0^2 + p^2}$, coincides with the asymptotic value $M_p(\infty)$ of the instantaneous mass of the particle. Simultaneously, in the reference frame $\mathfrak{S}$ the dilation of times, which is suggested by the special relativity, transforms the survival probability at rest according to the mentioned scaling law. The above description indicates the value $1/\sqrt{1 + \mu_0^2/p^2}$ as the asymptotic velocity of the moving unstable particle.

We stress that the present interpretation is an attempt to ascribe the transformation laws of the long-time survival probability to the dilation of times which is provided by the theory of special relativity. However, a clear scaling transformation of the survival probability at rest holds, approximately over long times, if the decay is observed in the reference frame where the unstable particle moves with constant linear momentum. The scaling law can still be interpreted as the effect of a time dilation which appears by changing reference frame. The dilation is determined uniquely by the scaling factor which depends on the mass spectrum and on the dynamics of the unstable particle. The theoretical results are confirmed by the numerical analysis.

While the instantaneous mass transforms by changing reference frame, no transformation is found, approximately, for the instantaneous decay rate over long times. In fact, the instantaneous decay rate vanishes, over long times, approximately independently of the linear momentum of the moving particle. Consequently, the long-time instantaneous decay rate is approximately invariant by changing reference frame.

In conclusion, the present analysis shows further ways to describe the long-time transformations of the decay laws of moving unstable particles in terms of model-independent properties of the mass spectrum. The role of the (nonvanishing) mass at rest in the relativistic transformation is assumed in the present description by the (nonvanishing) lower bound of the mass spectrum.

Data Availability

The results of this article are entirely theoretical and analytical. For each result, the main steps of the corresponding demonstration are reported in the text. The article is fully consistent without the support of any additional data.

Conflicts of Interest

The author declares that there are no conflicts of interest regarding the publication of this paper.

References

[1] L. A. Khalfin, "Quantum Theory of Unstable Particles and Relativity," Tech. Rep. PDMI PREPRINT-6/1997, St. Petersburg Department of Stelkov Mathematical Institute, St. Ptersburg, Russia, 1997.

[2] L. Fonda, G. C. Ghirardi, and A. Rimini, "Decay theory of unstable quantum systems," *Reports on Progress in Physics*, vol. 41, no. 4, pp. 587–631, 1978.

[3] B. Bakamjian, "Relativistic particle dynamics," *Physical Review A: Atomic, Molecular and Optical Physics*, vol. 121, no. 6, pp. 1849–1851, 1961.

[4] F. Coester and W. N. Polyzou, "Relativistic quantum mechanics of particles with direct interactions," *Physical Review D: Particles, Fields, Gravitation and Cosmology*, vol. 26, no. 6, pp. 1348–1367, 1982.

[5] P. Exner, "Representations of the Poincaré group associated with unstable particles," *Physical Review D: Particles, Fields, Gravitation and Cosmology*, vol. 28, no. 10, pp. 2621–2627, 1983.

[6] E. V. Stefanovich, *Relativistic Quantum Theory of Particles*, vol. 1 and 2, Lambert Academic, 2015.

[7] E. V. Stefanovich, "Quantum effects in relativistic decays," *International Journal of Theoretical Physics*, vol. 35, no. 12, pp. 2539–2554, 1996.

[8] M. Shirokov, "Decay law of moving unstable particle," *International Journal of Theoretical Physics*, vol. 43, no. 6, pp. 1541–1553, 2004.

[9] D. H. Frisch and J. H. Smith, "Measurement of the relativistic time dilation using μ-mesons," *American Journal of Physics*, vol. 31, no. 5, article 342, 1963.

[10] J. Bailey, K. Borer, F. Combley et al., "Measurements of relativistic time dilatation for positive and negative muons in a circular orbit," *Nature*, vol. 268, no. 5618, pp. 301–305, 1977.

[11] F. J. M. Farley, "The CERN (g-2) measurements," *Zeitschrift für Physik C Particles and Fields*, vol. 56, supplement 1, pp. S88–S96, 1992.

[12] M. I. Shirokov, "Evolution in time of moving unstable systems," *Concepts of Physics*, vol. 3, pp. 193–205, 2006.

[13] M. I. Shirokov, "Moving system with speeded-up evolution," *Physics of Particles and Nuclei Letters*, vol. 6, no. 1, pp. 14–17, 2009.

[14] K. Urbanowski, "Decay law of relativistic particles: quantum theory meets special relativity," *Physics Letters. B. Particle Physics, Nuclear Physics and Cosmology*, vol. 737, pp. 346–351, 2014.

[15] F. Giacosa, "Decay law and time dilatation," *Acta Physica Polonica B*, vol. 47, no. 9, pp. 2135–2150, 2016.

[16] K. Urbanowski, "On the velocity of moving relativistic unstable quantum systems," *Advances in High Energy Physics*, vol. 2015, Article ID 461987, 2015.

[17] K. Urbanowski, "Non-classical behavior of moving relativistic unstable particles," *Jagellonian University. Institute of Physics. Acta Physica Polonica B*, vol. 48, no. 8, pp. 1411–1432, 2017.

[18] W. M. Gibson and B. R. Pollard, *Symmetry Principles in Elementary Particle Physics*, Cambridge, UK, 1976.

[19] M. L. Goldberger and K. M. Watson, *Collision Theory*, Wiley, New York, NY, USA, 1964.

[20] K. Urbanowski, "General properties of the evolution of unstable states at long times," *The European Physical Journal D*, vol. 54, no. 1, pp. 25–29, 2009.

[21] K. Urbanowski, "Long time properties of the evolution of an unstable state," *Open Physics*, vol. 7, no. 4, pp. 696–703, 2009.

[22] F. Giraldi, "Logarithmic decays of unstable states," *The European Physical Journal D*, vol. 69, no. 1, 2015.

[23] F. Giraldi, "Logarithmic decays of unstable states II," *The European Physical Journal D*, vol. 70, no. 11, article no. 229, 2016.

[24] K. Urbanowski, "Early-time properties of quantum evolution," *Physical Review A: Atomic, Molecular and Optical Physics*, vol. 50, pp. 2847–2853, 1994.

[25] C. Møller, *The theory of relativity*, Clarendon Press, Oxford, UK, 1972.

[26] A. Erdélyi, *Asymptotic Expansions*, Dover, New York, NY, USA, 1956.

[27] R. Wong, *Asymptotic Approximations of Integrals*, Academic Press, Boston, Mass, USA, 1989.

Research Article

A New Inflationary Universe Scenario with Inhomogeneous Quantum Vacuum

Yilin Chen [1] and Jin Wang [1,2,3]

[1]*College of Physics, Jilin University, Changchun, Jilin 130021, China*
[2]*Department of Chemistry and Physics, State University of New York, Stony Brook, NY 11794, USA*
[3]*State Key Laboratory of Electroanalytical Chemistry, Changchun Institute of Applied Chemistry, Changchun, Jilin 130022, China*

Correspondence should be addressed to Yilin Chen; chenyilin19960823@gmail.com and Jin Wang; jin.wang.1@stonybrook.edu

We investigate the quantum vacuum and find that the fluctuations can lead to the inhomogeneous quantum vacuum. We find that the vacuum fluctuations can significantly influence the cosmological inhomogeneity, which is different from what was previously expected. By introducing the modified Green's function, we reach a new inflationary scenario which can explain why the Universe is still expanding without slowing down. We also calculate the tunneling amplitude of the Universe based on the inhomogeneous vacuum. We find that the inhomogeneity can lead to the penetration of the Universe over the potential barrier faster than previously thought.

1. Introduction

Gravity governs the evolution of the Universe. A great breakthrough in gravitational research in the last century is the discovery of general relativity (GR). After Einstein laid down the relationship between the space-time geometry through the curvature and the matter through energy momentum, the general relativity theory has been applied to many fields, especially in astrophysics and cosmology. Another great achievement of modern physics is quantum mechanics. Based on that, quantum field theory (QFT) emerged, which has been tested in many experiments. Due to the success of relativity in the macroscopic world and quantum mechanics in the microscopic world, it is natural to ask how we can combine them together. In cosmology, this issue becomes more apparent after the birth of the theory of inflationary Universe [1, 2] and successful in solving the horizon and flatness problems and eventually quantifying the seeds in terms of the density fluctuations for large scale structure formation and inhomogeneity for the microwave background radiation. In this theory, at the very early history, the Universe expanded exponentially, and the expansion was sustained by the vacuum energy. Despite the success, one issue remains on how the Universe quits this stage. Many proposals were suggested to resolve this issue [3, 4]. It turns out rather difficult to complete and have a graceful exit for the old inflationary scenario with multiple bubbles coalescing in a Universe suggested by Guth [1]. Chaotic inflationary scenario has been suggested with essentially one bubble for a Universe but forever evolving to avoid the exiting issue.

The idea of the inflationary scenario is to combine the quantum vacuum energy for describing the matter and the Einstein's equation for describing the space-time evolution together. Based on the equivalence principle of GR, each form of the energy influences the space-time in the same way. Quantum vacuum brings a new source of energy. Naively, one can study how the quantum vacuum influences the space-time evolution by simply put the energy-momentum tensor for the quantum vacuum on the right hand side and the Einstein space-time curvature tensor on the left hand side of the Einstein equation of GR.

Unfortunately, there is an issue once one naively puts these two theories of general relativity and quantum mechanics together. This is because there is currently no applicable

method for quantizing GR or space-time. This indicates that quantum mechanics and GR are at totally different footing and do not match each other. Therefore, many existing theories suggested certain approximate equations relating these two theories. However, these approaches often show great ambiguity. Firstly, let us look at Einstein's field equation:

$$R_{\mu\nu} - \frac{1}{2}Rg_{\mu\nu} = kT_{\mu\nu}. \tag{1}$$

This equation in the current form would not make sense if $T_{\mu\nu}$ represents the quantum (such as vacuum here) rather than classical matter. This is because the energy-momentum tensor is an operator in quantum world. In quantum mechanics, once we attempt to observe something about a system, the expected observed values correspond to the average values of the corresponding operator for the observable. Therefore, it seems natural to modify the Einstein equation by changing the energy-momentum operator for the average value of it:

$$R_{\mu\nu} - \frac{1}{2}Rg_{\mu\nu} = k\left\langle T_{\mu\nu}\right\rangle. \tag{2}$$

This describes, at the average level, how the quantum matter influences the space-time evolution. For quantum matter, we know that fluctuations are unavoidable. This is even true for the quantum vacuum. One natural question to ask is how the quantum matter fluctuations influence the space-time evolution. Another way to modify the Einstein equation for taking the fluctuations into account is to take the square of both sides of the Einstein equation and then take the average value on the right hand side:

$$\left(R_{\mu\nu} - \frac{1}{2}Rg_{\mu\nu}\right)^2 = k\left\langle T_{\mu\nu}^{\,2}\right\rangle. \tag{3}$$

In fact, (2) and (3) are equivalent only if the fluctuation of energy-momentum tensor is zero, but this of course is not the case since the energy-momentum tensor even for quantum vacuum is not zero.

This example illustrates that before we "totally" understand quantum gravity, there could be many ways of combining the general relativity and quantum field theory, which are not equivalent at the semiclassical level. Furthermore, these differences in semiclassical treatments are caused by the fluctuations of the quantum field vacuum. The cosmological constant problem [5] is a good example to demonstrate this issue, where the vacuum energy density predicted by quantum field theory is much larger than the cosmological constant from the observations. A natural question one can ask is whether taking the fluctuation into account can be an effective way to improve the quantitative descriptions of the cosmological evolution driven by the quantum vacuum energy [6]. The idea of considering the quantum vacuum fluctuations was suggested [6] to solve the cosmological constant problem at present. However, quantum fluctuations exist not only in the current Universe with approximately flat space-time but also in the very early history of the Universe. Therefore, it is also important to consider the impacts of quantum vacuum fluctuations on the evolution of the Universe, in particular the early Universe.

In this study, by improving the method developed in [6], we suggest going one step further beyond the conventional semiclassical method for combining the GR and the QFT by taking into account the vacuum fluctuations and, based on that, reaching a new inflationary scenario. In this new scenario, the cosmological constant issue, which arises when trying to combine GR and QFT, can be resolved.

This paper is organized as follows: in Section 2, we illustrate that the quantum vacuum is not homogeneous, but inhomogeneous, due to quantum fluctuation. In Section 3, by introducing the modified Green's function, we build up a model to quantify the fluctuations of the quantum vacuum. We study the influence of the quantum vacuum fluctuations and its physical interpretation. In Section 4, we consider a simple case and solve the corresponding Einstein's field equation. In Section 5, by introducing finite temperature field theory, we take into account the temperature, which is a key element in cosmological evolution. In Section 6, based on our solutions to the cases in Sections 4 and 5, we propose a new inflationary scenario, which can help to resolve the cosmological constant problem. In Section 7, we analyze the influence of the inhomogeneous vacuum on the tunneling amplitude of the Universe from nothing.

The units and metric signature are set to be $c = \hbar = 1$ and $(+, -, -, -)$ throughout. And in this paper, 4-vectors are denoted by light italic type, and 3-vectors are denoted by boldface type.

2. The Quantum Fluctuation and Inhomogeneous Vacuum

Vacuum energy plays an very important role in the inflationary theory. In this theory, at the very early time, the Universe expanded exponentially. In this period, vacuum energy dominated the expansion of the Universe. Usually, the vacuum energy density is treated as a constant; for example, just as in (2), the average value of T_{00} is

$$\left\langle T_{00}\right\rangle \sim \frac{\Lambda^4}{16\pi^2}, \tag{4}$$

where $T_{00} = (1/2)(\dot{\phi}^2 + (\nabla\phi)^2 + m^2\phi^2)$ is the energy density of a free scalar field, and the high energy cutoff Λ is much greater than the mass in the free scalar field.

By recalling the example in the introduction section, the vacuum fluctuations are not zero. This is because the vacuum $|0\rangle$ is not the eigen state of T_{00}, but the eigenstate of Hamiltonian $H = \int T_{00}d^3x$ (for the detailed discussions, see [6]). Therefore, the fluctuations in energy density should be considered. Due to the vacuum fluctuations, the conventional assumption of homogeneous Universe is only approximately correct. When fluctuations are taken into account, the vacuum is not homogeneous. Thus, a more suitable theory should include the effects of the fluctuations in energy density. To achieve this goal, the strategy we adopt is to modify both sides of the field equation, in order to have the fine structures which are compatible with the fluctuations.

2.1. Generalizing the FLRW Metric. To describe a homogeneous, isotropic expanding Universe, we introduce Friedmann–Lemaître–Robertson–Walker (FLRW) metric [7]:

$$ds^2 = dt^2 - a^2(t)\left(\frac{dr^2}{1-kr^2} + r^2 d\theta^2 + r^2 \sin^2\theta d\varphi^2\right), \quad (5)$$

where k can be -1, 0, or $+1$, which indicates the 3-dimensional space is elliptical space (closed), Euclidean space (flat), or hyperbolic space (open), respectively. The factor $a(t)$, known as the scale factor, depends only on t. Although the FLRW metric can naturally describe an expanding Universe, it cannot describe the inhomogeneous Universe where the inhomogeneity is caused by the vacuum fluctuations. The corresponding resolution is to allow the scale factor $a(t)$ to have spatial dependence.

$$ds^2 = dt^2$$
$$- a^2(t,r)\left(\frac{dr^2}{1-kr^2} + r^2 d\theta^2 + r^2 \sin^2\theta d\varphi^2\right). \quad (6)$$

To simplify our model, we only assume that the scale factor has only radius r dependence, so the rotational symmetry is preserved. For the spatial part, $k = 1$ is chosen (the reason will be explained in Section 5). Now, the Ricci tensor for the metric becomes

$$R_{00} = -\frac{3\ddot{a}}{a},$$

$$R_{01} = R_{10} = \frac{2\left(\dot{a}a' - a\dot{a}'\right)}{a^2},$$

$$R_{11} = \frac{2\left(1-2r^2\right)a'}{r\left(r^2-1\right)a} + \frac{2a'^2}{a^2} - \frac{2a''}{a} - \frac{2\left(\dot{a}^2+1\right)+\ddot{a}a}{r^2-1}, \quad (7)$$

$$R_{22} = \frac{R_{33}}{\sin^2\theta}$$
$$= \frac{r\left[\left(4r^2-3\right)a' + r\left(r^2-1\right)a'' + r\ddot{a}a^2 + 2r\left(\dot{a}^2+1\right)a\right]}{a},$$

where the dot represents the derivative with respect to t, and the prime represents the derivative with the respect to r. Then the Ricci tensor can be substituted into the Einstein's field equation:

$$R_{\mu\nu} = 8\pi G S_{\mu\nu}, \quad (8)$$

where $S_{\mu\nu}$ is given by the energy-momentum tensor:

$$S_{\mu\nu} = T_{\mu\nu} - \frac{1}{2}g_{\mu\nu}T, \quad (9)$$

where T is the trace of the energy-momentum tensor $T_{\mu\nu}$.

2.2. Quantification of the Inhomogeneous Vacuum. After transforming the left hand side of (8), now we can focus on the right hand side. Following the description of the introduction section, the $S_{\mu\nu}$ which is often taken as the average

value (expectation value) of the tensor over the entire spacetime should not be taken as a constant due to the vacuum fluctuations. By only taking the expectation values of the energy-momentum tensor, some fine structures which come from the fluctuations are lost. Here, our main task is to find a correct $S_{\mu\nu}$ for (8), which describes the inhomogeneity of the vacuum fluctuations.

$$\langle 0 |S_{\mu\nu}| 0 \rangle = S_{\mu\nu}(\mathbf{x}, t). \quad (10)$$

Before studying how to find the suitable $S_{\mu\nu}$, we introduce the scalar field to describe the matter field in our toy model. For simplicity, ϕ-4 theory is adopted:

$$\mathcal{L} = \frac{1}{2}g^{\mu\nu}\partial_\mu\phi\partial_\nu\phi - \frac{1}{2}m^2\phi^2 - \frac{1}{4!}\lambda\phi^4 - \frac{3m^4}{2\lambda}, \quad (11)$$

where $m^2 = -\mu^2 < 0$. Due to the Higgs mechanism, the symmetry is broken spontaneously at low temperatures. The effective potential becomes

$$V(\phi) = -\frac{\mu^2}{2}\phi^2 + \frac{\lambda}{4!}\phi^4 + \frac{3\mu^4}{2\lambda} > 0. \quad (12)$$

To be compatible with the modification of the FLRW metric, we reduce a number of degrees of freedom of the field $\phi(t,r)$ and preserve the rotational symmetries just as what we did before.

According to Noether's theorem, the energy-momentum tensor for this field is given as

$$T_{\mu\nu} = \partial_\mu\phi\partial_\nu\phi$$
$$- \frac{g_{\mu\nu}}{2}\left(\partial^\rho\phi\partial_\rho\phi - \mu^2\phi^2 - \frac{1}{12}\lambda\phi^4 - \frac{3\mu^4}{2\lambda}\right). \quad (13)$$

Substituting (13) in (9), we reach

$$S_{00} = \partial_t\phi\partial_t\phi - V(\phi),$$

$$S_{11} = -\frac{1-r^2}{a^2(t,r)}\partial_r\phi\partial_r\phi - V(\phi), \quad (14)$$

$$S_{22} = S_{33} = -V(\phi).$$

Now, we are ready to substitute S into Einstein's equations. At first, let us look at one of the Einstein equations:

$$R_{00} = -\frac{3\ddot{a}}{a} = 8\pi G S_{00}(r,t)$$
$$= 8\pi G\left(\langle\dot{\phi}\dot{\phi}\rangle - \langle V(\phi)\rangle\right). \quad (15)$$

Next, the main challenge becomes the evaluations of $\langle V(\phi)\rangle$ and $\langle\dot{\phi}\dot{\phi}\rangle$. However, it is impossible to obtain the correct $\langle V(\phi)\rangle$ and $\langle\dot{\phi}\dot{\phi}\rangle$ in conventional methods. The key to obtain the correct expectation values of the potential is to first find out $\langle 0|\phi\phi|0\rangle$. In general, this expectation value is given as

$$\langle 0 |\phi(x)\phi(x)| 0 \rangle = \lim_{x'\to x}\langle 0 |\phi(x')\phi(x)| 0 \rangle$$
$$= \lim_{x'\to x} G(x',x), \quad (16)$$

where $G(x', x)$ is the full Green's propagator. To gain insights, the free propagator should be derived at first following the perturbation theory. Due to the spontaneous symmetry breaking, the free propagator cannot be obtained directly. To resolve this issue, we make a shift of the variable, $\phi \to \phi + \phi_0$, where $\phi_0^2 = 6\mu^2/\lambda$. Then we have

$$\begin{aligned} \mathscr{L} = {} & \frac{1}{2} g^{\mu\nu} \partial_\mu \phi \partial_\nu \phi - \frac{1}{2} \left(\frac{\lambda \phi_0^2}{2} - \mu^2 \right) \phi^2 - \frac{\lambda}{4!} \phi^4 - \frac{3\mu^4}{2\lambda} \\ & + \left(\mu^2 - \frac{\lambda \phi_0^2}{6} \right) \phi_0 \phi - \frac{\lambda}{6} \phi_0 \phi^3 \\ & + \left(\frac{\mu^2}{2} - \frac{\lambda}{4!} \phi_0^2 \right) \phi_0^2. \end{aligned} \tag{17}$$

Now it is easy to see that the square of the effective mass of the new field ϕ is

$$m_{\text{eff}}^2 = \frac{\lambda}{2} \phi_0^2 - \mu^2 = 2\mu^2. \tag{18}$$

After shifting the variables, we can derive the solution for ϕ and return back to the original variable:

$$\phi = \phi_0 + (2\pi)^{-3} \int \frac{d^3k}{\sqrt{2\omega}} \left[a_k^\dagger \psi(x,t) + a_k \psi^*(x,t) \right], \tag{19}$$

where ψ satisfies the equation of motion for the free scalar field. For example, in the flat space-time, $\psi(x) = \exp(ikx)$, and in this case, the Green's function is

$$\begin{aligned} G\left(x', x \right) & = \phi_0^2 + \phi_0 \langle \phi \rangle + \phi_0 \langle \phi' \rangle + \langle \phi \phi' \rangle \\ & = \phi_0^2 + \int \frac{d^3k}{(2\pi)^3 \, 2\omega} e^{ik(x-x')}, \end{aligned} \tag{20}$$

where $\omega = \sqrt{k^2 + m_{\text{eff}}^2} = \sqrt{k^2 + 4\mu^2}$. In the curved space, the propagator is not as simple as it is in the flat space. Following [8], by introducing Riemann normal coordinates and expanding the metric, the propagator in the curved space can also be obtained in momentum space:

$$\begin{aligned} G\left(x, x' \right) = {} & \frac{i\Delta^{1/2}\left(x, x' \right)}{(4\pi)^{n/2}} \int \frac{d^n k}{(2\pi)^n} e^{ik(x-x')} \\ & \cdot \left[1 + f_1\left(x, x' \right) \left(-\frac{\partial}{\partial m^2} \right) + f_2\left(x, x' \right) \left(\frac{\partial}{\partial m^2} \right)^2 \right] \\ & \cdot \frac{1}{k^2 + m^2}, \end{aligned} \tag{21}$$

where $f_1(x, x')$ and $f_2(x, x')$ are certain functions which are related to the curvature tensor. If the curvature is not quite large, the second and third terms in (21) would be much smaller than the first term. In that case, we can establish a perturbative propagator in the curved space-time. For our toy model, we omit $f_1(x, x')$ and $f_2(x, x')$ terms and just preserve the leading term for the approximate flat space-time

(because when the scale factor a is large, the Ricci scalar for FLRW metric is proportional to a^{-1}, so the curvature, especially after inflation, is very small). Meanwhile, the van Vleck determinant $\Delta(x, x')$ should also be one in this case. Thus, the approximate propagator in the curved space-time becomes

$$G\left(x, x' \right) = \int \frac{d^3k}{(2\pi)^3} \frac{1}{2\omega} e^{-i(\omega\Delta t + \mathbf{k}\cdot\Delta\mathbf{x})}, \tag{22}$$

where the Δt and $\Delta \mathbf{x}$ are geodesic distances. After that, we can calculate the full propagator. For simplicity, the tree level propagator is considered, and higher order corrections are neglected.

3. Modifications of the Green's Function

In this section, we aim to explore the fluctuations of the vacuum and take this into account in our model by modifying the propagator; then we can establish an effective field theory taking into account of the effects of the fluctuations by introducing the modified Green's function.

3.1. Another Approach to Obtaining the Propagator. Following the previous section, the free propagator for the scalar field is given as

$$G\left(x, x' \right) = \int \frac{d^3k}{(2\pi)^3 \, 2\omega} e^{ikx}. \tag{23}$$

Usually, in quantum field theory, the free propagator can be derived by calculating the Green's function in momentum space and then integrating over t with a suitable contour. However, the two-point correlation function obtained by this way is not the expectation value, $\langle 0|\phi\phi|0\rangle(x)$, which we expect for the energy-momentum tensor. This is because certain hidden structures inside the correlation functions which can cause the fluctuations are ignored. To show the fine structures of the expectation values for the energy-momentum tensor, here we introduce another approach to obtaining the Green's function. We will write down the explicit solution of ϕ and then calculate the correlation directly.

Here, we represent the solution of ϕ in terms of the creation and annihilation operators a and $a^\dagger$ for the scalar field without interactions:

$$\phi(\mathbf{x}, t) = \int \frac{d^3k}{(2\pi)^3 \, \sqrt{2\omega}} \left(a_k e^{-ikx} + a_k^\dagger e^{ikx} \right). \tag{24}$$

Then the multiplication of the two ϕs becomes

$$\begin{aligned} \phi(\mathbf{x}, t) \phi\left(\mathbf{x}', t' \right) = {} & \int \frac{d^3k \, d^3k'}{(2\pi)^6} \frac{1}{2\sqrt{\omega\omega'}} \\ & \cdot \left[a_k a_{k'} e^{-i(kx+k'x')} + a_k^\dagger a_{k'}^\dagger e^{i(kx+k'x')} \right. \\ & \left. + a_k a_{k'}^\dagger e^{-i(kx-k'x')} + a_k^\dagger a_{k'} e^{i(kx-k'x')} \right]. \end{aligned} \tag{25}$$

Conventionally, in (25), the first two terms do not give contributions to the propagator. This is because their vacuum

expectation values are zero. When we take the expectation value of (25), $\langle 0|\phi(x)\phi(x')|0\rangle$, there would be no difference in the result in (23). However, the crucial thing to consider is how to evaluate the first two terms. To see the significance of the first two terms, here by setting $x' \to x$ and rewriting (25), we have

$$
\begin{aligned}
\phi^2(\mathbf{x}, t) = \int \frac{d^3k d^3k'}{(2\pi)^6} \frac{1}{2\sqrt{\omega\omega'}} \\
\cdot \Big[\left(a_k a_{k'} + a_k^\dagger a_{k'}^\dagger \right) \cos\left(k + k'\right) x \\
+ i \left(a_k^\dagger a_{k'}^\dagger - a_k a_{k'} \right) \sin\left(k + k'\right) x \\
+ \left(a_k a_{k'}^\dagger + a_k^\dagger a_{k'} \right) \cos\left(k - k'\right) x \\
+ i \left(a_k^\dagger a_{k'} - a_k a_{k'}^\dagger \right) \sin\left(k - k'\right) x \Big].
\end{aligned}
\tag{26}
$$

Similarly, the last two terms indicate zero point energy, and the first two terms are zero when they are taken vacuum expectation value. However, the first two terms are the parts in (26) where the fluctuations emerge

$$
\begin{aligned}
A(\mathbf{x}, t) \\
= \int \frac{d^3k d^3k'}{2(2\pi)^6 \sqrt{\omega\omega'}} \left(a_k a_{k'} + a_k^\dagger a_{k'}^\dagger \right) \cos\left(k + k'\right) x, \\
B(\mathbf{x}, t) \\
= \int \frac{i d^3k d^3k'}{2(2\pi)^6 \sqrt{\omega\omega'}} \left(a_k^\dagger a_{k'}^\dagger - a_k a_{k'} \right) \sin\left(k + k'\right) x.
\end{aligned}
\tag{27}
$$

Obviously, $\langle A(x, t)\rangle = \langle B(x, t)\rangle = 0$. However, $\langle A^2(x, t)\rangle$ and $\langle B^2(x, t)\rangle$ are not zero. In fact, they are the reason why the vacuum state is not the eigen state of the energy density. In this case, $A(x, t)$ and $B(x, t)$ are the key elements to show the "hidden" structure of $\langle\phi\phi\rangle$. Here, we have

$$
\begin{aligned}
\langle |A|^2 \rangle = \int \frac{d^3k' d^3k}{(2\pi)^6} \frac{1}{2\omega'\omega} \cos^2\left(k + k'\right) x, \\
\langle |B|^2 \rangle = \int \frac{d^3k' d^3k}{(2\pi)^6} \frac{1}{2\omega'\omega} \sin^2\left(k + k'\right) x.
\end{aligned}
\tag{28}
$$

A simplest way to preserve the part which quantifies the fluctuation is given as

$$
G(\mathbf{x}, t) = \frac{\Lambda^2}{8\pi^2} + \sqrt{\langle |A|^2(\mathbf{x}, t)\rangle} + \sqrt{\langle |B|^2(\mathbf{x}, t)\rangle}.
\tag{29}
$$

Here, we simply preserve the latest nonzero order of $\langle |A(\mathbf{x}, t)|^n\rangle$ and $\langle |B(x, t)|^n\rangle$, so as to leave all the parts in (26) "survived" after taking the expectation value. Fortunately, $G(\mathbf{x}, t)$ is convergent when $\mathbf{x}$ and t go to infinity and

$$
\lim_{\mathbf{x}, t \to \infty} G(\mathbf{x}, t) \sim \Lambda^2
$$
$$
G(0, 0) \sim \Lambda^2
\tag{30}
$$

$G(0, 0)$ is related to Λ^2. In order to be independent of the high momentum cutoff, we can rewrite this result by subtracting $G(0, 0) = G_0$, so

$$
\begin{aligned}
G_R(\mathbf{x}, t) = G(\mathbf{x}, t) - G_0 \\
= \sqrt{\langle A^2(\mathbf{x}, t)\rangle} + \sqrt{\langle B^2(\mathbf{x}, t)\rangle} \\
- \sqrt{\langle A^2(0, 0)\rangle} - \sqrt{\langle B^2(0, 0)\rangle}.
\end{aligned}
\tag{31}
$$

Now, the new Green's function is totally composed of the terms of the fluctuations $A(\mathbf{x}, t)$ and $B(\mathbf{x}, t)$ and starts at zero. Meanwhile, the large constant which is proportional to Λ^2 is eliminated. This constant is the vacuum energy which is nonobservable, due to the QFT.

3.2. The Interpretation of Modified Green's Function.

To gain the modified Green's function, (28) should be computed. However, the integration is not simple. Here is a way which can be used to estimate the integrals for $\langle |A(\mathbf{x}, t)|^2\rangle$ and $\langle |B(\mathbf{x}, t)|^2\rangle$. At first, divide the interval of the integration:

$$
\begin{aligned}
\langle |A|^2(\mathbf{x}, t)\rangle \\
= \left(\int_{\Lambda_0}^{\Lambda} + \int_0^{\Lambda_0} \right) \frac{d^3k d^3k'}{(2\pi)^6} \frac{1}{2\omega\omega'} \cos^2\left(k + k'\right) x, \\
\langle |B|^2(\mathbf{x}, t)\rangle \\
= \left(\int_{\Lambda_0}^{\Lambda} + \int_0^{\Lambda_0} \right) \frac{d^3k d^3k'}{(2\pi)^6} \frac{1}{2\omega\omega'} \sin^2\left(k + k'\right) x.
\end{aligned}
\tag{32}
$$

For the first part of integrals, because $\Lambda \gg 2\mu$, we have

$$
\omega = \sqrt{2\mu^2 + k^2} \approx k.
\tag{33}
$$

In this case, the integrals become

$$
\begin{aligned}
\langle A_1^2 \rangle = \int_{\Lambda_0}^{\Lambda} \frac{d^3k d^3k'}{(2\pi)^6} \frac{1}{2\omega\omega'} \cos^2\left(k + k'\right) x \\
\approx \int_0^{2\pi} d\varphi\, d\varphi' \int_0^{\pi} \sin\theta \sin\theta'\, d\theta\, d\theta' \\
\cdot \int_{\Lambda_0}^{\Lambda} \frac{kk'\, dk\, dk'}{2(2\pi)^6} \cos^2\left(k + k'\right) x, \\
\langle B_1^2 \rangle = \int_{\Lambda_0}^{\Lambda} \frac{d^3k d^3k'}{(2\pi)^6} \frac{1}{2\omega\omega'} \sin^2\left(k + k'\right) x \\
\approx \int_0^{2\pi} d\varphi\, d\varphi' \int_0^{\pi} \sin\theta \sin\theta'\, d\theta\, d\theta' \int_{\Lambda_0}^{\Lambda} \frac{kk'\, dk\, dk'}{2(2\pi)^6} \\
\cdot \sin^2\left(k + k'\right) x.
\end{aligned}
\tag{34}
$$

To see the result of integrals in (34) more clearly, we set $\mathbf{x} = 0$ and keep $\langle A_1^2 \rangle$ and $\langle B_1^2 \rangle$ as functions only with variable t. Here we have

$$
\begin{aligned}
\left\langle A_1^2 (0, t) \right\rangle = \frac{1}{32t^4} \Big[& 4t^4 \left(\Lambda^2 - \Lambda_0^2 \right)^2 \\
& + \left(1 - 4\Lambda_0^2 t^2 \right) \cos (4\Lambda_0 t) + \left(1 - 4\Lambda^2 t^2 \right) \cos (4\Lambda t) \\
& + 2 \left(4\Lambda_0 \Lambda t^2 - 1 \right) \cos (2t (\Lambda_0 + \Lambda)) \\
& - 4 (\Lambda_0 + \Lambda) t \sin (2t (\Lambda_0 + \Lambda)) \\
& + 4\Lambda_0 t \sin (4\Lambda_0 t) + 4\Lambda t \sin (4\Lambda t) \Big],
\end{aligned}
$$

(35)

$$
\begin{aligned}
\left\langle B_1^2 (0, t) \right\rangle = \frac{1}{32t^4} \Big[& 4t^4 \left(\Lambda^2 - \Lambda_0^2 \right)^2 \\
& + \left(4\Lambda_0^2 t^2 - 1 \right) \cos (4\Lambda_0 t) + \left(4\Lambda^2 t^2 - 1 \right) \cos (4\Lambda t) \\
& + 2 \left(1 - 4\Lambda_0 \Lambda t^2 \right) \cos (2t (\Lambda_0 + \Lambda)) \\
& + 4 (\Lambda_0 + \Lambda) t \sin (2t (\Lambda_0 + \Lambda)) \\
& - 4\Lambda_0 t \sin (4\Lambda_0 t) - 4t\Lambda \sin (4\Lambda t) \Big].
\end{aligned}
$$

After direct calculations, $\langle A_1^2 \rangle$ and $\langle B_1^2 \rangle$ have limits where

$$
\lim_{t \to \infty} \left\langle A_1^2 \right\rangle = \lim_{t \to \infty} \left\langle A_2^2 \right\rangle = \frac{\left(\Lambda^2 - \Lambda_0^2 \right)^2}{64\pi^4}.
$$

(36)

At the origin, we also have

$$
\left\langle A_1^2 (0, 0) \right\rangle = \frac{\left(\Lambda^2 - \Lambda_0^2 \right)^2}{32\pi^4},
$$

$$
\left\langle B_1^2 (0, 0) \right\rangle = 0.
$$

(37)

Then, think about the next part of integrals. In the next part of integrals, because $\Lambda_0 \ll \mu$,

$$
\omega = \sqrt{2\mu^2 + k^2} \approx \sqrt{2}\mu.
$$

(38)

Similarly, we have

$$
\begin{aligned}
\left\langle A_2^2 \right\rangle &= \int_0^{\Lambda_0} \frac{d^3k d^3k'}{(2\pi)^6} \frac{1}{2\omega\omega'} \cos^2 \left(k + k' \right) x \\
&\approx \int_0^{2\pi} d\varphi \, d\varphi' \int_0^{\pi} \sin\theta \sin\theta' \, d\theta \, d\theta' \\
&\quad \cdot \int_0^{\Lambda_0} \frac{k^2 k'^2 dk \, dk'}{4 (2\pi)^6 \mu^2} \cos^2 \left(k + k' \right) x, \\
\left\langle B_2^2 \right\rangle &= \int_0^{\Lambda_0} \frac{d^3k d^3k'}{(2\pi)^6} \frac{1}{2\omega\omega'} \sin^2 \left(k + k' \right) x \\
&\approx \int_0^{2\pi} d\varphi \, d\varphi' \int_0^{\pi} \sin\theta \sin\theta' \, d\theta \, d\theta' \\
&\quad \cdot \int_0^{\Lambda_0} \frac{k^2 k'^2 dk \, dk'}{4 (2\pi)^6 \mu^2} \sin^2 \left(k + k' \right) x.
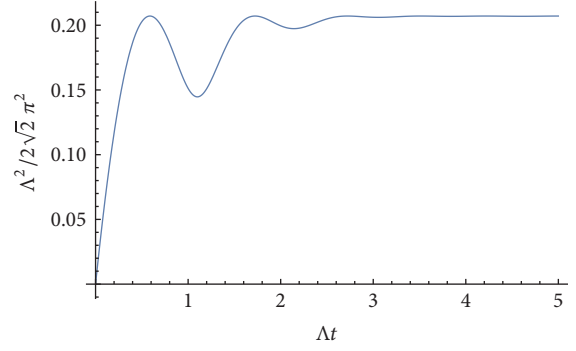\end{aligned}
$$

(39)

FIGURE 1: Approximate $G_R(0, t)$ in (41).
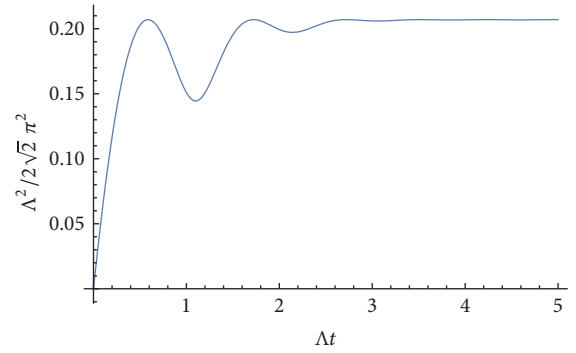
FIGURE 2: $G_R(0, t)$ derived by numerical calculation.

For simplicity, setting $x = 0$, we can easily evaluate (39) directly:

$$
\left\langle A_2^2 (0, t) \right\rangle = \frac{1}{288\pi^4} \frac{\Lambda_0^6}{\mu^2} \cos^2 \left(2\sqrt{2}\mu t \right),
$$

$$
\left\langle B_2^2 (0, t) \right\rangle = \frac{1}{288\pi^4} \frac{\Lambda_0^6}{\mu^2} \sin^2 \left(2\sqrt{2}\mu t \right).
$$

(40)

Combining (36) and (40), the modified Green's function $G_R(0, t)$ is obtained. Because $\Lambda \gg \mu \gg \Lambda_0$, the approximate result is given as

$$
G_R (0, t) \approx \sqrt{\left\langle A_1^2 (0, t) \right\rangle} + \sqrt{\left\langle B_1^2 (0, t) \right\rangle} - \frac{\Lambda^2}{4\sqrt{2}\pi^2}.
$$

(41)

In this case, the limit when time goes infinity becomes

$$
\lim_{t \to \infty} G_R \approx \frac{\left(2 - \sqrt{2} \right) \Lambda^2}{8\pi^2}.
$$

(42)

To check the validity of the approximate modified Green's function derived here, we calculate $G_R(0, t)$ numerically.

In Figure 2, the numerical result is seen to be close to the result in Figure 1 which is plotted with the approximate Green's function. The amplitude of the oscillation of $G_R(0, t)$ remains nearly a constant in Figure 1 at initial times; however, when the time becomes very long, the amplitude of the oscillations of our approximate result approaches zero.

FIGURE 3: $G_R(0, t)$ derived by numerical calculation when t goes larger. The oscillation of $G_R(0, t)$ can be seen clearly when t is large.
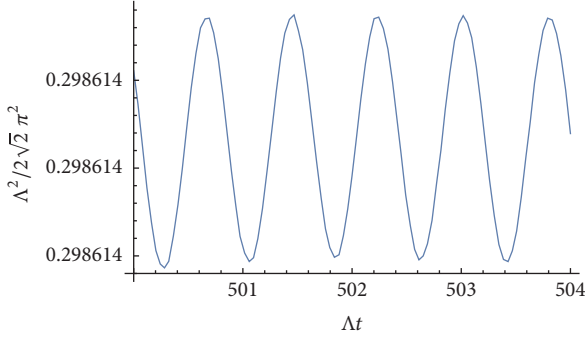
The maximal values of the two results derived by different methods are slightly different. In fact, this is not hard to explain. In (41), we drop the $\langle A_2^2(0, t) \rangle$ and $\langle B_2^2(0, t) \rangle$ terms, which influence the amplitude and the value of peak. Roughly speaking, comparing to the value of the Green's function's limit when $t \to \infty$, the oscillation's amplitude is much smaller compared to the overall value. Therefore, it can be omitted. The oscillation of the Green's function is shown in Figure 3 by computing the Green's function numerically.

Now, a problem arises naturally: how to interpret this result. In Figures 1 and 2, the modified Green's function starts at the origin and finally reaches the peak. Meanwhile after reaching the peak, the function oscillates with a small amplitude. To make a correspondence to the evolution of ϕ, we notice that when $t = 0$, the scalar field $\phi = 0$ and then ϕ evolves with time. However, ϕ cannot always increase. This is because once it starts evolving not at the true vacuum, the global minimal point of the potential, there is always a tendency towards getting back to the stable true vacuum. Taking this thought into account, $G_R(0, 0) = 0$ indicates that the scalar field ϕ starts at the origin and reaches the true vacuum periodically. Because the energy for driving the inflation of the Universe is gradually dissipated, the amplitude of ϕ becomes smaller and smaller. Finally, ϕ oscillates around the global minimal point with a small amplitude. This idea can be true only when we admit such a postulation:

$$\text{the maximum of } G_R \approx \frac{(2 - \sqrt{2})\Lambda^2}{8\pi^2} = \nu = \frac{6\mu^2}{\lambda}. \tag{43}$$

Therefore, we obtained a correlation of the ultraviolet cutoff Λ and the global minimal of the potential. This kind of relationship does not appear in QFT. This is because, in QFT, the ultraviolet cutoff is set by an exterior constant which is there just for regularization. However, for this case, we hope to establish an effective field theory which takes into consideration the quantum vacuum fluctuations. In this case, the key question is how the energy density of this effective field drives the Universe to expand. As a result, there is an exterior constraint on the cosmological background and we cannot treat it as the usual QFT in fixed background.

4. Toy Model: How the Inhomogeneous Vacuum Influences the Evolution of the Universe

After deriving the modified Green's function, now we are able to explore how the inhomogeneous vacuum influences the evolution of the Universe. Recalling Einstein's equation in Section 2 (15), adopting the approximation in (41), and substituting it into (15), we have [9]

$$-\frac{3\ddot{a}}{a} = 8\pi G \left(\langle \dot{\phi}\dot{\phi} \rangle + \frac{\mu^2}{2} G_R + \frac{\lambda}{4!} G_R^2 + \frac{3\mu^2}{2\lambda} \right). \tag{44}$$

However, here, a new issue emerges, that is, how to calculate $\langle \dot{\phi}\dot{\phi} \rangle$. As a matter of fact, we have such a relation between $\langle \dot{\phi}\dot{\phi} \rangle$ and the modified Green's function:

$$\langle \dot{\phi}\dot{\phi} \rangle (x) = \lim_{x \to x'} \langle \dot{\phi}(x) \dot{\phi}(x') \rangle$$
$$= \lim_{x \to x'} \partial_t \partial_t' \langle \phi(x) \phi(x') \rangle. \tag{45}$$

In analogy to the method that we use to derive the modified Green's function for $\langle \phi\phi \rangle$ in the previous section, functions $A(\mathbf{x}, t)$ and $B(\mathbf{x}, t)$ can also be introduced, and due to (45), the new $A(\mathbf{x}, t)$ and $B(\mathbf{x}, t)$ are given as

$$A'(\mathbf{x}, t)$$
$$= \int \frac{d^3k d^3k'}{(2\pi)^6} \frac{\sqrt{\omega\omega'}}{2} \left(a_k a_{k'} + a_k^\dagger a_{k'}^\dagger \right) \cos\left(k + k' \right) x,$$
$$B'(\mathbf{x}, t) \tag{46}$$
$$= \int \frac{d^3k d^3k'}{(2\pi)^6} \frac{\sqrt{\omega\omega'}}{2} \left(a_k^\dagger a_{k'}^\dagger - a_k a_{k'} \right) \sin\left(k + k' \right) x.$$

After the direct calculations, results in (46) are quite similar to that of the G_R. Therefore, the regulation is also necessary for $\langle \dot{\phi}\dot{\phi} \rangle$. However, unlike the method we used for the modified Green's function, the final version of $\langle \dot{\phi}\dot{\phi} \rangle$ after regulation becomes

$$\langle \dot{\phi}\dot{\phi} \rangle = \sqrt{\langle A'^2(\mathbf{x}, t) \rangle} + \sqrt{\langle B'^2(\mathbf{x}, t) \rangle}$$
$$- \lim_{t \to \infty} \left(\sqrt{\langle A'^2(\mathbf{x}, t) \rangle} + \sqrt{\langle B'^2(\mathbf{x}, t) \rangle} \right). \tag{47}$$

The reason that this type of regulation is adopted, which is different from what we used for G_R, is not hard to explain. It is clear that the scalar field ϕ finally decays to the true vacuum which is the minimal of the potential energy. Equivalently, recalling the interpretation for G_R in the previous section, we can discuss the correspondence to the evolution of ϕ. We notice that when t grows larger and larger, ϕ will be stable at the minimal point. Meanwhile, all the derivatives of ϕ should be approximately zero at this stage in order to preserve the stability. The numerical result of $\langle \dot{\phi}\dot{\phi} \rangle$ is shown in Figure 4. The evolution of this correlation function is similar to the evolution of the modified Green's functions.
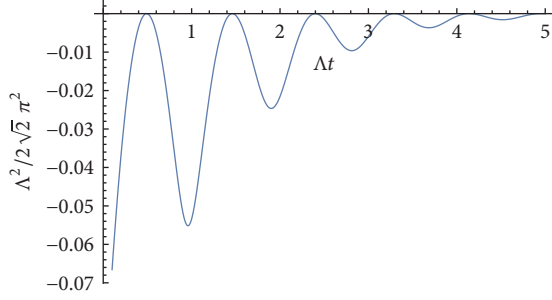
FIGURE 4: The correlation function $\langle \dot{\phi}\dot{\phi}\rangle$ after regulation in (47).
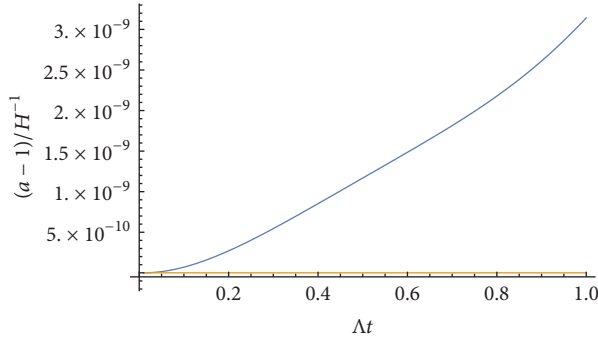

FIGURE 5: Scale factors at the beginning. The blue curve is for our toy model, and the orange one is for standard scenario. To illustrate the behavior of scale factors clearly, the vertical axis is rescaled as $(a-1)/H^{-1}$, where $H = \sqrt{8\pi GV(0)/\lambda}$.

Substituting (47) into (44), we are able to solve the equation for the evolution of the scale factor a. After numerical calculation, two figures are plotted for the scale factor $a(0,t)$ compared to the standard scenario.

In Figures 5 and 6, it is not hard to see that at the beginning, the scale factor in our toy model grows much faster that the scale factor in the standard scenario. However, when the time becomes larger, the scale factor in our toy model grows slower and finally $a \propto t$. This is because when t is large, the scalar field ϕ falls down from the top of the potential and oscillates around the global minimal point. In this case, the right hand side of (44) is approximately zero, so $\dot{a}$ is also approximately zero [9].

5. More Elaborated Model: When Temperature Is Involved

Once the temperature is introduced in our model, there are significant changes. Based on the finite temperature quantum field theory, correlation functions should satisfy Kubo–Martin–Schwinger relations [10]

$$\left\langle \chi(t)\chi(t')\right\rangle_\beta = \left\langle \chi(t')\chi(t+i\beta)\right\rangle_\beta. \tag{48}$$

Here, time t is also extended to the complex plane and β in (48) is the reciprocal for the temperature, $\beta = T^{-1}$. Not only the background becomes more complicated, but also
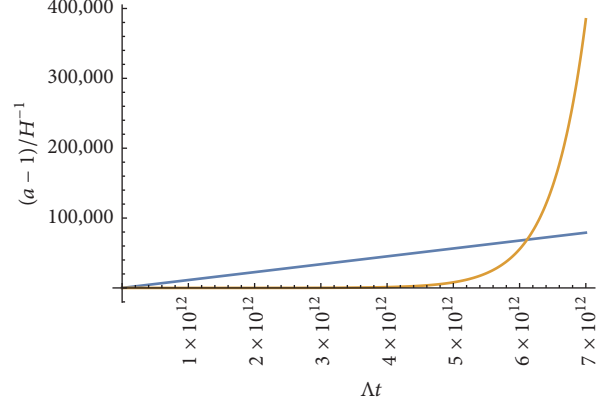

FIGURE 6: Scale factors when time is large. The blue curve is for our toy model, and the orange one is for standard scenario. Like Figure 5, the vertical axis is also rescaled.

the Lagrangian changes. If the field is not at zero Kelvin, the effective mass becomes

$$\mu^2 \longrightarrow \mu^2 - \frac{\lambda}{4!}T^2. \tag{49}$$

Thus, the Lagrangian becomes

$$\mathcal{L} = \frac{1}{2}g^{\mu\nu}\partial_\mu\phi\partial_\nu\phi + \frac{1}{2}\left(\mu^2 - \frac{\lambda}{4!}T^2\right)\phi^2 - \frac{\lambda}{4!}\phi^4 - \frac{3\mu^4}{2\lambda}, \tag{50}$$

and in this case, the minimal position of the potential is no longer at $v = 6\mu^2/\lambda$, but at

$$v(T) = \frac{6\mu^2(T)}{\lambda} = \frac{6}{\lambda}\left(\mu^2 - \frac{\lambda}{4!}T^2\right) = v(0) - \frac{T^2}{4}. \tag{51}$$

Recalling the postulation in (43), the ultraviolet cutoff now in finite temperature field theory is related to the temperature $\Lambda = \Lambda(T)$. But what would happen when the temperature is higher than the critical point $T > T_c = \sqrt{24\mu^2/\lambda}$? In this case, $v(T) = 0$, and the spontaneous symmetry breaking no longer exists. Meanwhile, due to the postulation in (43), the ultraviolet cutoff should be zero. However, the behavior of G_R when time becomes long gives us hint that ϕ should oscillate around the origin at the minimal of the potential. For more details, the modified Green's function should be discussed, which involves temperature. Similarly to the zero temperature approach, we start with $A(\mathbf{x},t)$ and $B(\mathbf{x},t)$. Replacing $t \to t + i\beta$, we reach [11]

$$A(\mathbf{x},t) = \int \frac{d^3k d^3k'}{2(2\pi)^6 \sqrt{\omega\omega'}}\left(a_k a_{k'}e^\beta + a_k^\dagger a_{k'}^\dagger e^{-\beta}\right)$$
$$\cdot \cos\left(k+k'\right)x,$$
$$B(\mathbf{x},t) = \int \frac{id^3k d^3k'}{2(2\pi)^6 \sqrt{\omega\omega'}}\left(a_k^\dagger a_{k'}^\dagger e^{-\beta} - a_k a_{k'}e^\beta\right)$$
$$\cdot \sin\left(k+k'\right)x. \tag{52}$$

Notice here that the square of the effective mass in ω is $m_{\text{eff}}^2 = \lambda T^2/4! - \mu^2$. Following the process in previous section, $\sqrt{|A(\mathbf{x},t)|^2}$ and $\sqrt{|B(\mathbf{x},t)|^2}$ need to be calculated. Nevertheless, the term which depends on β is canceled out. Therefore, finally, the modified Green's function here is not different from the previous one. To find the explicit form when T is very high, considering the approximation in (39) and $\Lambda \ll \lambda T^2$, we reach

$$G_R(0,t) \approx \frac{\sqrt{2}}{12\pi^2} \frac{\Lambda^3}{m_e} \left(|\cos 2m_e t| + |\sin 2m_e t| - 1 \right), \quad (53)$$

where $m_e^2 = \lambda T^2/4! - \mu^2 \approx \lambda T^2/4!$. It is easy to find out that $G_R(0,t)$ oscillates at the origin and the amplitude is small.

Before solving the Einstein's field equation for the scale factor, we notice that the term $\langle \dot{\phi}\dot{\phi} \rangle$ in (15) is still unknown. Similarly to the previous described approach with zero temperature, introducing $A'(\mathbf{x},t)$ and $B'(\mathbf{x},t)$ in (46) for the finite temperature field, we reach

$$A'(\mathbf{x},t) = \int \frac{d^3k d^3k'}{(2\pi)^6} \frac{\sqrt{\omega\omega'}}{2} \left(a_k a_{k'} e^{\beta} + a_k^{\dagger} a_{k'}^{\dagger} e^{-\beta} \right)$$
$$\cdot \cos\left(k + k'\right) x,$$
$$\quad (54)$$
$$B'(\mathbf{x},t) = \int \frac{d^3k d^3k'}{(2\pi)^6} \frac{\sqrt{\omega\omega'}}{2} \left(a_k^{\dagger} a_{k'}^{\dagger} e^{-\beta} - a_k a_{k'} e^{\beta} \right)$$
$$\cdot \sin\left(k + k'\right) x.$$

Using the approximation $\omega \approx m_{\text{eff}}$, in this case, we reach

$$\langle \dot{\phi}\dot{\phi} \rangle = m_{\text{eff}}^2 G_R. \quad (55)$$

Then plugging (53) and (55) into (15), we obtain the equation for the scale factor:

$$\frac{\ddot{a}}{a} = \frac{8\pi G}{3} \left(-\frac{1}{2} m_{\text{eff}}^2(T) G_R + \frac{\lambda}{4!} G_R^2 + \frac{3\mu^4}{2\lambda} \right). \quad (56)$$

To solve this equation, the relation between the temperature and the scale factor is needed. Due to the total entropy conservation, the relation is given as $T \propto a^{-1}$. In (56), because the amplitude of G_R is negligibly small, the last term $V(0) = (3\mu^4)/(2\lambda)$ dominates the equation. Therefore, it is not hard to predict that the scale factor a increases exponentially before the temperature is below the critical temperature.

6. A New Inflationary Scenario

In this section, we mainly discuss a new inflationary scenario which is built based on our model. At the beginning, in this new inflationary scenario, we investigate the idea that the Universe is created from nothing [12, 13]. Hence, in our model, the curvature is greater than zero or, equivalently, we take $k = 1$ in the FLRW metric. From the tunneling theory, before tunneling through the barrier, the "Universe" was in Euclidean space. After penetrating the potential barrier, the Universe was "created" and began expanding. At this stage,

the vacuum energy drove the Universe expanding exponentially. Following the previous section, the symmetry was restored because the field was at a very high temperature which is much higher than the critical temperature where phase transition of the field occurs. Therefore, ϕ oscillates at the origin with a tiny amplitude which can almost be negligible. By omitting the terms containing G_R in (56), during this period, the equation for the scale factor becomes

$$\frac{\ddot{a}}{a} \approx \frac{8\pi G}{3} \frac{3\mu^4}{2\lambda} = \frac{4\pi G\mu^4}{\lambda} = H^2. \quad (57)$$

Taking the initial condition when $t \approx 0$, we reach $a(x,t) = a(t) = H^{-1}\cosh(Ht)$. This also gives the solution to the Friedmann equation for homogeneous and isotropy space-time with positive curvature [13]. In this case, we have the same solution to (57):

$$a \approx H^{-1}\cosh(Ht). \quad (58)$$

In fact, following the Friedmann equations, besides the 00 component of Einstein's field equation as (15), the other ones are derived from the first one and the trace of Einstein's field equations. Similarly, we can derive the second equation for our model.

$$\text{LHS.} = \frac{1}{6} \left(\frac{R_{00}}{g_{00}} - \frac{R_{11}}{g_{11}} - \frac{R_{22}}{g_{22}} - \frac{R_{33}}{g_{33}} \right)$$
$$= \frac{4\left(\left(3r^2 - 2\right)a' + r\left(r^2 - 1\right)a''\right)a - 2r\left(r^2 - 1\right)a'^2}{6ra^4}$$
$$+ \frac{\dot{a}^2 + 1}{a^2},$$
$$\quad (59)$$
$$\text{RHS.} = \frac{1}{6} \left(\frac{T_{00}}{g_{00}} - \frac{T_{11}}{g_{11}} - \frac{T_{22}}{g_{22}} - \frac{T_{33}}{g_{33}} \right)$$
$$= \frac{8\pi G}{6} \left(\langle \dot{\phi}\dot{\phi} \rangle + \frac{1 - r^2}{a^2} \langle \phi'\phi' \rangle + 2V(\phi) \right)$$
$$\approx \frac{8\pi G}{3} V(0) = H^2.$$

On the left hand side of the second Friedmann equation, it separates into two parts. One part comes from the spatial dependence of the scale factor, and the other part is a common term. Because the right hand side is approximately a constant, we can also make the approximation so that $a(r,t) \approx a(t)$. Then the first part on the left hand side disappears. Hence, a much more simplified equation is derived:

$$\dot{a}^2 + 1 \approx H^2 a^2. \quad (60)$$

It is obvious that the solution to this equation is the same as that of (57).

At the first stage, the Universe expanded exponentially, so the temperature of the entire Universe decreased rapidly, due to the relation of temperature and entropy [1], $T \propto s^{-1}$. Once the temperature becomes lower than the critical temperature, the Universe switched to the next stage. Recalling Section 4
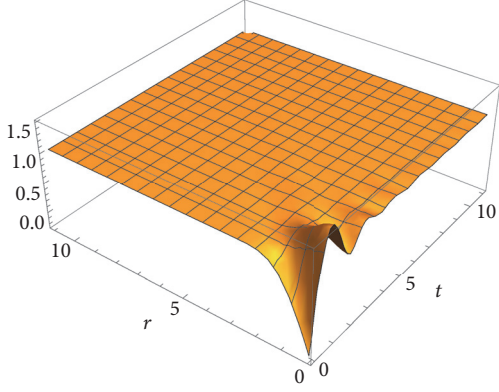
FIGURE 7: Numerical result of $G_R(r,t)$ in 3D.

and considering that $\langle \dot{\phi}\dot{\phi} \rangle$ goes to zero and G_R reaches the stable point extremely fast, these terms make very limited contributions. Therefore, they can be neglected in the large scale space-time. However, if we want to solve the second Friedmann equation, (59), for the scale factor during this period, there is still an issue: how the spatial dependence of the scale factor influences the result. Ideally, if the spatial factor has no significant effects, we can also drop those terms involving a' and a'' and obtain a simple equation as (60). To check this assumption, both two variables should be considered for G_R. To illustrate how the spatial part influences the modified Green's function, we plot a 3D figure for $G_R(r,t)$. In Figure 7, except the very little area where t is small, the surface in the figure is almost flat. This means that the spatial fluctuations of the variables are very small and can be omitted when t is not too small. Thus, it is fine to get rid of the part which contains a' or a'' in (59) and obtain a new equation:

$$\dot{a}^2 + 1 \approx \frac{8\pi G}{3} a^2 V(\phi, T)\Big|_{\min}$$
$$= \frac{8\pi G}{3}\left(\frac{c^2 T^2}{8} - \frac{\lambda T^4}{384}\right)a^2. \tag{61}$$

Because the expansion of the Universe is adiabatic, the total entropy of the Universe is conserved and set $aT = S$; then T can be replaced in (61):

$$\dot{a}^2 + 1 \approx \frac{8\pi G}{3}\left(\frac{\mu^2 S^2}{8a^2} - \frac{\lambda S^4}{384a^4}\right)a^2. \tag{62}$$

In this switching period, (62) could be rewritten as

$$\dot{a} \approx \left[\left(\frac{\pi G\mu^2 S^2}{3a^2} - 1\right) - \frac{\pi G\lambda S^4}{144a^2}\right]^{1/2} = \sqrt{P - Q/a^2}. \tag{63}$$

Therefore, it is easy to find that when scale factor grew larger, the second term Q/a^2 became smaller and $a' \approx$ constant, which means the Universe expanded approximately in a fixed speed at this stage. In this case, the expansion of the Universe was linearly in time. Meanwhile, during this period, the acceleration of the expansion kept on decreasing (in fact, the

acceleration cannot be zero, but, at a very small value, we will explain this effect next).

After the switching period, the Universe cooled down. due to the coupling with other fields, the bosons of the scalar field would decay into other particles. Thus, the $P = P(t)$ and $Q = Q(t)$ in (63) dropped down, so the speed of linear expansion in the last period also decreased rapidly. Moreover, at this stage, the vacuum energy of the scalar field contributed to the Universe's expansion decreases, so the speed of expansion continued decreasing. However, this does not mean that the Universe stopped expanding. In fact, the expansion of the Universe was still accelerating because of one element that we neglect in the previous stage, which became more important. In Section 3, the behavior of G_R shows that the field ϕ falls into the minimal of the potential very fast. However, once it reaches that point, it will oscillate at that point with a tiny amplitude. The oscillation makes a tiny shift, which is quite small compared to the right hand side of (61). To calculate the tiny shift caused by the oscillations of ϕ, the two approximations in Section 3 which are applied to calculate G_R should be both considered; when t is large, we reach

$$G_R(\mathbf{x}, t) = \sqrt{A_1^2(\mathbf{x}, t) + A_2^2(\mathbf{x}, t)}$$
$$+ \sqrt{B_1^2(\mathbf{x}, t) + B_2^2(\mathbf{x}, t)} - \sqrt{A_1^2(0, 0) + A_2^2(0, 0)}$$
$$- \sqrt{B_1^2(0, 0) + B_2^2(0, 0)} \approx \left(\sqrt{A_1^2(\mathbf{x}, t)}\right.$$
$$+ \sqrt{B_1^2(\mathbf{x}, t)} - \sqrt{A_1^2(0, 0)} - \sqrt{B_1^2(0, 0)}\right) \tag{64}$$
$$+ \frac{1}{2}\left(\frac{A_2^2(\mathbf{x}, t)}{\sqrt{A_1^2(\mathbf{x}, t)}} + \frac{B_2^2(\mathbf{x}, t)}{\sqrt{B_1^2(\mathbf{x}, t)}}\right) \approx \nu(T) + \frac{1}{36\pi^2}$$
$$\cdot \frac{\Lambda_0^6}{\Lambda^2(T)\mu^2(T)},$$

where $\Lambda(T)$ is the ultraviolet cutoff which is related to temperature. $\mu^2(T) = \mu^2 - \lambda T^2/4!$ is the square of the effective mass in this temperature. $\nu(T) = 6\mu^2(T)/\lambda$ indicates the minimal point of the potential. Thus, we can define the shift of the scalar field ϕ:

$$(\Delta\phi)^2 = \lim_{t\to\infty} G_R(\mathbf{x}, t) - \nu(T) = \frac{1}{36\pi^2}\frac{\Lambda_0^6}{\Lambda^2(T)\mu^2(T)}. \tag{65}$$

Then, the tiny shift of the potential can also be obtained

$$\Delta V = V(\phi_0 + \Delta\phi) - V(\phi_0) \approx \frac{V''(\phi_0)}{2}(\Delta\phi)^2, \tag{66}$$

where $\phi_0 = \sqrt{\nu(T)}$, which indicates the minimal point, and $V'' = \partial^2 V/\partial\phi^2$. Substituting (65) and the Lagrangian into (66), here we have

$$\Delta V = \frac{\Lambda_0^6}{36\pi^2\Lambda^2(T)}. \tag{67}$$

Currently, in the case that $T \approx 2.7k$, we have $\Lambda^2(T) \approx \Lambda^2(0) \approx (48\pi^2\mu^2)/((2 - \sqrt{2})\lambda) \gg \Lambda_0$, so the energy shift ΔV is a very small constant.

Besides the energy shift began playing a role in the Universe expansion; after the particles of the scalar field decayed into other particles, the density of particle ϕ kept decreasing. According to the radiation thermodynamics, the density of particle is proportional to T^4 [14]. Therefore, in this period, the particle density is given as

$$\rho = \rho_0 e^{-\Gamma t} \propto T^4 e^{-\Gamma t}, \tag{68}$$

where Γ is the decay rate which is dependent on the coupling constants of ϕ and other fields. Therefore, equivalently, we can replace the original temperature by $T \to T\exp(-\Gamma t/4)$. Now, we are able to establish the equation for the last stage of the inflation evolution:

$$\dot{a}^2 + 1$$
$$\approx \frac{8\pi G}{3} \left(\frac{\mu^2 S^2}{8a^2} e^{-\frac{\Gamma t}{2}} - \frac{\lambda S^4}{384a^4} e^{-\Gamma t} + \frac{\rho}{a^3} + \Delta V \right) a^2, \tag{69}$$

where ρ indicates the density of nonrelativistic matter. Now, we have established the equation which can explain the scenario of the Universe nowadays. In this equation, the first term which is proportional to a^{-2} decreases rapidly. The next term is negligible when t is large. The third term comes from the nonrelativistic matter which is created by the energy that the scalar field dissipates. The last term, which is approximately a constant, plays the role of vacuum energy or, in other words, the cosmological constant.

According to the observations, now, the Universe is still expanding, and the expansion is accelerating. Using the observational data, one can check which factor dominates the current Universe evolution. To describe the behavior of the current Universe, a general evolution equation is introduced:

$$\dot{a}^2$$
$$= H_0^2 \left[\Omega_\Lambda + \Omega_K \left(\frac{a_0}{a} \right)^2 + \Omega_M \left(\frac{a_0}{a} \right)^3 + \Omega_R \left(\frac{a_0}{a} \right)^4 \right], \tag{70}$$

where H_0 is the current Hubble's parameter and a_0 is the current scale factor. Meanwhile, the energy densities of nonrelative matter, radiation, and vacuum are, respectively,

$$\rho_{M0} = \frac{3H_0^2 \Omega_M}{8\pi G},$$

$$\rho_{R0} = \frac{3H_0^2 \Omega_R}{8\pi G}, \tag{71}$$

$$\rho_{\Lambda 0} = \frac{3H_0^2 \Omega_\Lambda}{8\pi G}.$$

By fitting with the observed data of the supernova [15, 16], the ratio of each component which sustains the expansion of the Universe can be obtained. One of the results obtained is that

$\Omega_K = \Omega_R = 0$, $\Omega_\Lambda + \Omega_M = 1$, and $\Omega_\Lambda \approx 0.7$. In (69), because at this stage t is large, the first term is small. To match the current statue of the Universe, an approximate formula can be laid down.

$$\frac{c^2 S^{2/3}}{8} e^{-\Gamma t/2} \approx \frac{3}{8\pi G}. \tag{72}$$

Thus, the curvature constant is effectively equal to zero. Then, by neglecting the second term on the right hand side of (69), we reach the equation which describes the current Universe as

$$\dot{a}^2 \approx \frac{8\pi G}{3} \left(\frac{\rho}{a^3} + \Delta V \right) a^2. \tag{73}$$

In this case, the expansion of the Universe is dominated by vacuum energy which is from the energy shift caused by the oscillations of the scalar field ϕ around the potential minimal and nonrelativistic matter, while other effects are ruled out. Meanwhile, plugging the current observed Hubble constant [17] in (71), we obtain the energy density of vacuum energy (cosmological constant):

$$\rho_{\Lambda 0} \approx 2.57 \times 10^{-47} \, (\text{GeV})^4. \tag{74}$$

This result is much smaller than the energy scales of various theories of QFT. Since ΔV in (67) is also much smaller than the energy that QFT can predict, this result can be used to explain why the current energy density of the vacuum energy is so small [6]. In our model, the density of effective vacuum energy caused by ΔV is

$$\rho_\Lambda = \Delta V \propto \Lambda^{-2}. \tag{75}$$

In this case, the Hubble parameter $H \propto \Lambda^{-1} \to 0$. Compared to another resolution to the cosmological constant problem [6], the effective Hubble parameter approaches zero, $H \propto \Lambda e^{-\beta\sqrt{G}\Lambda} \to 0$. Although both two models draw a conclusion that the Hubble parameter $H \to 0$ when the ultraviolet cutoff is taken as infinity, $\Lambda \to \infty$, the results in the two models are still different. This is because, in our model, the quantum vacuum fluctuations have direct impacts on the scalar field ϕ. Thus we obtain the effective density of vacuum energy ΔV. In [6], the vacuum fluctuations have direct impacts on the space-time structure, but not on the field itself. To summarize, there are three main stages of this new inflation scenario (shown in Figure 8): At the first stage (curve (I) in Figure 8), the scalar field had no symmetry breaking at the very high temperature and the Universe expanded exponentially. Meanwhile, the temperature kept decreasing rapidly and once it dropped below the critical point, the scenario switched to the next stage. At this transient period (curve (II) in Figure 8), the expansion was no longer exponential, but the acceleration of the expansion decreased, and finally the expansion was approximately linearly in time. Next, along the decrease of the temperature, the P and Q in (63) can no longer be constants but went down quickly. Therefore, in this stage (curve (III) in Figure 8), the speed of the expansion became slower and slower, and finally $P(t) \approx 0$. However, one effect buried
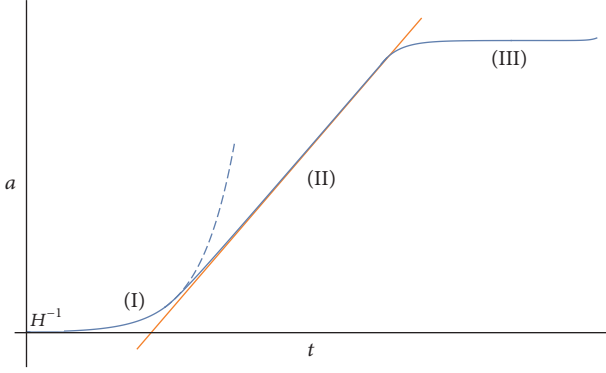
FIGURE 8: The scale factor of the new scenario. Notice that there are three stages of the evolution of the scale factor.

in previous stages became important now. After $P(t)$ being approximately zero, the effective potential in (67) leads to the acceleration of the expansion of the current Universe.

Compared to the standard inflationary scenario, the new scenario proposed here has no issue of how the Universe quits the inflationary stage from the exponential expansion. The acceleration of expansion decreased smoothly from the first stage to the second stage, and finally the expansion was almost linearly in time. This smooth transition is guaranteed by the behavior of the modified Green's function which shows that the scalar field at each point of the whole Universe can reach the local minimum on the effective potential landscape. Therefore, the new inflationary scenario does not have to quit through bubble collisions.

7. Tunneling Amplitude: How the Inhomogeneous Vacuum Influences the Creation of the Universe

After establishing the model describing the evolution of the Universe, let us go back to the moment where the Universe has not been created. Due to the tunneling theory [12, 13], the Universe can be created from "nothing" by tunneling through the potential barrier. It is therefore useful to estimate the tunneling amplitude in our model and the influence of the inhomogeneous vacuum on the tunneling amplitude. To compute the amplitude, we followed the following step. First find the minimal coupling action. Then derive the Wheeler–DeWitt (WD) equation. Finally solve the WD equation, then find the outgoing wavefunction, and calculate the tunneling amplitude.

The minimal coupling of Einstein–Hilbert action and the scalar field action is given as

$$S = \int \left[-\frac{R}{16\pi G} + \frac{1}{2} g^{\mu\nu} \partial_\mu \phi \partial_\nu \phi - V(\phi) \right] \sqrt{-g} d^4 x, \quad (76)$$

where the potential $V(\phi)$, based on our model, is given as

$$V(\phi) = \frac{1}{2} \mu^2 \phi^2 + \frac{1}{4!} \lambda \phi^4 + \frac{3\mu^4}{2\lambda}. \quad (77)$$

By setting $r = \sin\chi$, the metric becomes $ds^2 = dt^2 - a^2(t, \chi)[d\chi^2 + \sin^2\chi(d\theta^2 + \sin^2\theta d\phi^2)] = dt^2 - a^2(t, \chi)d\Omega_3^2$. Then after direct calculation, the Ricci scalar in our model is given as

$$R = -\frac{2}{a^4} \left[a'^2 - 2a \left(2\cot(\chi) a' + a'' \right) + 3 \left(1 + \dot{a}^2 \right) \right. \\ \left. + 3a^3 \ddot{a} \right], \quad (78)$$

where $\dot{a} = \partial a / \partial t$ and $a' = \partial a / \partial \chi$. Substituting the potential and Ricci scalar into action and writing out the action explicitly, we have

$$S = \int dt L \left(a, \dot{a}, a'; \phi, \dot{\phi}, \phi' \right), \quad (79)$$

where the Lagrangian reads

$$L = \int \left[\frac{1}{8\pi G a^4} \left(a'^2 - 2a \left(2\cot(\chi) a' + a'' \right) \right. \right. \\ \left. + 3 \left(1 + \dot{a}^2 \right) a^2 + 3a^3 \ddot{a} \right) + \dot{\phi}^2 - \frac{\phi'^2}{a^2} - V(\phi) \right] \\ \cdot a^3 \sin^2 \chi \sin \theta \, d\chi \, d\theta \, d\varphi. \quad (80)$$

There is an issue involving the difficulty in evaluating the integrations in (80). To evaluate the integral, we make the approximation that ϕ and a are approximately constants when integrating over χ. In fact, this approximation is acceptable. Recalling Figure 7, the spatial variation of ϕ is small, and because a is determined by ϕ, the spatial variation of a is also small. Then we have the approximate Lagrangian

$$L = 2\pi^2 \left[\frac{1}{8\pi G a} \left(a'^2 + 3 \left(1 - \dot{a}^2 \right) a^2 \right) + a^3 \dot{\phi}^2 - a \phi'^2 \right. \\ \left. - a^3 V(\phi) \right]. \quad (81)$$

Then, following the same idea, we can make further approximations that neglect a'. Therefore, now we have a simpler Lagrangian

$$L = 2\pi^2 \left[\frac{3}{8\pi G} \left(1 - \dot{a}^2 \right) a + a^3 \dot{\phi}^2 - a \phi'^2 - a^3 V(\phi) \right]. \quad (82)$$

Now, we can derive the WD equation. Firstly, the canonical momenta should be obtained:

$$P_a = \frac{\partial L}{\partial \dot{a}} = \frac{3\pi a \dot{a}}{2G}, \\ P_\phi = \frac{\partial L}{\partial \dot{\phi}} = 2\pi^2 a^3 \dot{\phi}. \quad (83)$$

By Legendre transform and substituting the canonical momenta into (82), we have the Hamiltonian:

$$H = -\frac{G}{3\pi a} P_a{}^2 + \frac{1}{4\pi^2 a^3} P_\phi{}^2 \\ - \frac{3\pi}{4G} a \left[1 - \frac{8\pi G}{3} \left(\phi'^2 + a^2 V(\phi) \right) \right]. \quad (84)$$

To obtain Wheeler–DeWitt equation, introduce canonical quantization by replacing $P_a \to -i\partial/\partial a$, $P_\phi \to -i\partial/\partial\phi$; then we have the WD equation:

$$\left[\frac{\partial^2}{\partial a^2} + \frac{p}{a}\frac{\partial}{\partial a} - \frac{1}{a^2}\frac{\partial^2}{\partial\widetilde{\phi}^2} - U(a,\phi)\right]\psi = 0, \qquad (85)$$

and here, $\widetilde{\phi}^2 = 4\pi G\phi^2/3$, the parameter p represents the ambiguity:

$$P_a{}^2 \sim a^2\dot{a}^2 = \frac{1}{a^p}(a\dot{a})\,a^p\,(a\dot{a}). \qquad (86)$$

In this case, it is not appropriate to just write $P_a{}^2$ as $\partial^2/\partial a^2$, but

$$P_a{}^2 = -\frac{1}{a^p}\frac{\partial}{\partial a}\left(a^p\frac{\partial}{\partial a}\right) = \frac{\partial^2}{\partial a^2} + \frac{p}{a}\frac{\partial}{\partial a}. \qquad (87)$$

In the WD (85), the potential U is given as

$$U(a,\phi) = \left(\frac{3\pi}{2G}\right)^2 a^2\left[1 - \frac{8\pi G}{3}\left(\phi'^2 + a^2 V(\phi)\right)\right]. \qquad (88)$$

Based on the tunneling approach, before the Universe was created, everything was formulated in Euclidean space. To know the behavior of the Universe before tunneling through the potential barrier, gravitational instanton solution should be considered. At this stage, ϕ is assumed not to change with time. Therefore, it is possible to set $\phi = 0$. This is because, in the inflationary scenario that we discussed in the previous section, the scalar field ϕ starts at the extremum, $\phi = 0$. We assume that before tunneling through the barrier, in Euclidean space, the Universe preserved the highest symmetry. Therefore, we assume that the Universe was homogeneous and the scale factor was not related to r. Therefore, in Euclidean region, $\phi = 0$. Now we have Freedman equation in Euclidean space as

$$-\dot{a}^2 + 1 = H^2 a^2, \qquad (89)$$

where $H = (8\pi G V(0)/3)^{1/2}$, $V(0) = 3c^4/2\lambda$. The solution to this simple equation is

$$a(t) = H^{-1}\cos(Ht). \qquad (90)$$

This solution shows that, before the Universe "penetration" through the potential barrier in Euclidean space, it expanded and contracted periodically. In this case, when we analyze the wave function of the WD equation, the region $a < H^{-1}$ is in Euclidean space representation. Meanwhile, the region $a > H^{-1}$ is in Lorentz space representation. At the very early time after the Universe has been created, $t \ll 1$, following the Lorentz space representation, we have

$$\dot{a}^2 + 1 \approx H^2 a^2. \qquad (91)$$

The solution is

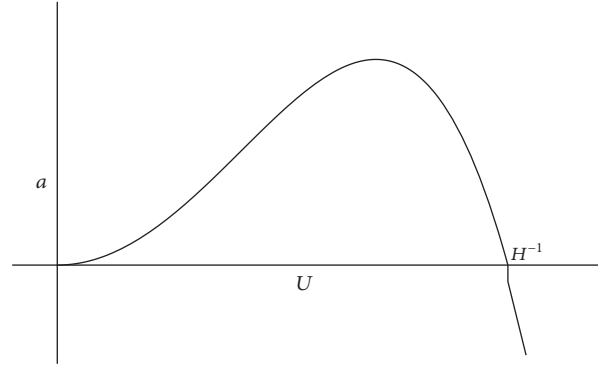$$a(r,t) \approx H^{-1}\cosh(Ht), \qquad (92)$$

FIGURE 9: Potential $U(a)$ for WD equation. Notice the step at $a = H^{-1}$.

and this is also the initial condition that we used for our model.

Following the same approach by which we obtained the WD equation for Lorentz region, in $a < H^{-1}$, the WD equation for Euclidean region is simpler:

$$\left[\frac{\partial^2}{\partial a^2} + \frac{p}{a}\frac{\partial}{\partial a} - \frac{1}{a^2}\frac{\partial^2}{\partial\widetilde{\phi}^2} - U_0(a,\phi)\right]\psi = 0, \qquad (93)$$

where the potential U_0 is

$$U_0(a,\phi) = \left(\frac{3\pi}{2G}\right)^2 a^2\left[1 - H^2 a^2\right]. \qquad (94)$$

After the WD equation is obtained, we can calculate the tunneling amplitude, which is proportional to $\psi(H^{-1})/\psi(0)$. WKB approximation can be used to derive the amplitude:

$$\begin{aligned}\frac{\psi(H^{-1})}{\psi(0)} &= \exp\left[-\int_0^{H^{-1}}\sqrt{U_0(a)}\,da\right]\\&= \exp\left[-\frac{3}{16G^2 V(0)}\right].\end{aligned} \qquad (95)$$

Because of ϕ'^2, the potential $U(a)$ is a little bit different from before. In Figure 9, we can see clearly that there is a clear sharp step at $a = H^{-1}$, which means the tunneling amplitude should be greater than the conventional result $\exp(-3/[16G^2 V(0)])$. This reflects the influence caused by the inhomogeneous vacuum. Meanwhile, the sharp step caused by ϕ'^2 and ϕ is also a spatial function. Therefore, the size of the sharp step at H^{-1} is also related to spatial variable r. This means that the tunneling probabilities vary at different spatial locations. Therefore, in our model, each spatial point of the Universe is not expected to tunnel through the barrier at the same time due to the different tunneling probability. The WD equation can be solved exactly with the choice of $p = -1$. The choice of the factor-ordering factor p dose not influence the probabilities. Now introducing a new variable,

$$z = -\left(1 - a^2 H^2\right). \qquad (96)$$

Thus, the potential U_0 becomes

$$U_0 = \left(\frac{3\pi}{2G}\right)^2 a^2 z. \tag{97}$$

Setting $p = -1$, we have

$$\left[\frac{\partial^2}{\partial z^2} + \left(\frac{3\pi}{2G}\right)^2 \frac{z}{4H^2}\right]\psi = 0. \tag{98}$$

After introducing the new variable, we can rewrite the WD equation in $a < H^{-1}$. Similarly, we can also introduce another variable for the WD equation in the region $a > H^{-1}$ [12]:

$$z' = -\left(1 - \frac{8\pi G}{3}\phi'^2 - a^2 H^2\right). \tag{99}$$

At the very early times, $\phi \approx 0$. Therefore, here, $8\pi V(\phi)/3 \approx H^2$ and ϕ'^2 are irrelevant to a. The equation can be rewritten once again as

$$\left[\frac{\partial^2}{\partial z'^2} + \left(\frac{3\pi}{2G}\right)^2 \frac{z'}{4H^2}\right]\psi = 0. \tag{100}$$

The solution to these equations are Airy functions:

$$\psi = \begin{cases} C_1 \mathrm{Ai}\left(-\sqrt[3]{A}z\right) + C_2 \mathrm{Bi}\left(-\sqrt[3]{A}z\right), & a < H^{-1} \\ C_1' \mathrm{Ai}\left(-\sqrt[3]{A}z'\right) + C_1' \mathrm{Bi}\left(-\sqrt[3]{A}z'\right), & a > H^{-1}, \end{cases} \tag{101}$$

where $A = (3\pi/4HG)^2$. Next, we should find the coefficients in the solution. The continuities of ψ and $\partial\psi/\partial a$ should be considered. Meanwhile, based on the tunneling theory, only an outgoing wave should be considered outside the barrier, which means $i\psi^{-1}\partial\psi/\partial a > 0$ for $a > H^{-1}$. For large z, we reach the asymptotic formulas for Ai and Bi:

$$\mathrm{Ai}(-z) \sim \frac{\sin\left((2/3)z^{3/2} + \pi/4\right)}{\sqrt{\pi}z^{1/4}},$$
$$\mathrm{Bi}(-z) \sim \frac{\cos\left((2/3)z^{3/2} + \pi/4\right)}{\sqrt{\pi}z^{1/4}}. \tag{102}$$

Due to the asymptotic formulas and Euler's formula, it is easy to find out that the proper form of ψ for $a > H^{-1}$ is

$$\psi = C\left(\mathrm{Ai}\left(-z'\right) + i\mathrm{Bi}\left(-z'\right)\right). \tag{103}$$

Then we can obtain the coefficients C_1 and C_2 related to C by two continuity equations. Now, we are able to calculate the tunneling amplitude:

$$\frac{\psi\left(H^{-1}\right)}{\psi(0)} = \frac{2 \cdot 3^{3/2} X}{\left(3^{4/3}\Gamma(2/3)X - 3\Gamma(1/3)Y\right)\mathrm{Ai}\left(\sqrt[3]{A}\right) + \left(3^{5/6}\Gamma(2/3)X + 3^{1/2}\Gamma(1/3)Y\right)\mathrm{Bi}\left(\sqrt[3]{A}\right)}, \tag{104}$$

where X and Y inside (104) are

$$X = \mathrm{Ai}\left(-\frac{8\pi G\sqrt[3]{A}\phi'^2}{3}\right) + i\mathrm{Bi}\left(-\frac{8\pi G\sqrt[3]{A}\phi'^2}{3}\right),$$
$$Y = \mathrm{Ai}'\left(-\frac{8\pi G\sqrt[3]{A}\phi'^2}{3}\right) + i\mathrm{Bi}'\left(-\frac{8\pi G\sqrt[3]{A}\phi'^2}{3}\right). \tag{105}$$

Compared to the conventional solution (95), the result in (104) is much more complicated, and we can see that not only H but also ϕ' plays an important role in tunneling process, which means the quantum vacuum fluctuation also affects the creation of the Universe.

8. Conclusion

In this paper, we analyzed the inhomogeneous vacuum in the Universe and come up with a new method for introducing the inhomogeneity by modifying Green's function. Meanwhile, substituting the modified Green's function in Friedmann equation, we obtained a new inflationary scenario which can explain why the Universe is still expanding and where the vacuum energy comes from which leads to the accelerated expansion. At last, we also applied our inhomogeneous model to find the tunneling amplitude of the Universe from

nothing. We found that the spatial fluctuations caused by the inhomogeneous vacuum lead to faster tunneling while the tunneling amplitude is dependent on the spatial locations.

There are still some issues that we have not addressed with our model in this paper. First, in our model, we take the simplest potential for the scalar field. However, our method which describes the inhomogeneity by modifying Green's function is general. Therefore, an improvement on our model is to consider more complicated cases, such as grand unified theory. Second, no higher order correlations, such as one-loop correlations, are considered here in our model. Thus, the loop correction should be involved in our model and then more accurate effective potential can be obtained. Third, it would be interesting to consider the cosmological consequences of the new inflation scenario suggested here, especially the density fluctuations, as the seed of the large scale structure formation and the related fluctuation power spectrum. These are closely associated with the current observations of the microwave background radiation and large scale density map.

Conflicts of Interest

The authors declare that they have no conflicts of interest.

Acknowledgments

References

 [1] A. H. Guth, "Inflationary universe: a possible solution to the horizon and flatness problems," *Physical Review D: Particles, Fields, Gravitation and Cosmology*, vol. 23, no. 2, pp. 347–356, 1981.

 [2] A. Linde, "Chaotic inflation," *Physics Letters B*, vol. 129, no. 3-4, pp. 177–181, 1983.

 [3] S. W. Hawking, I. G. Moss, and J. M. Stewart, "Bubble collisions in the very early universe," *Physical Review D: Particles, Fields, Gravitation and Cosmology*, vol. 26, no. 10, pp. 2681–2693, 1982.

 [4] A. H. Guth and E. J. Weinberg, "Could the universe have recovered from a slow first-order phase transition?" *Nuclear Physics B*, vol. 212, no. 2, pp. 321–364, 1983.

 [5] S. Weinberg, "The cosmological constant problem," *Reviews of Modern Physics*, vol. 61, no. 1, pp. 1–23, 1989.

 [6] Q. Wang, Z. Zhu, and W. G. Unruh, "How the huge energy of quantum vacuum gravitates to drive the slow accelerating expansion of the Universe," *Physical Review D: Particles, Fields, Gravitation and Cosmology*, vol. 95, no. 10, Article ID 103504, 2017.

 [7] R. M. Wald, *General Relativity*, University of Chicago Press, 1984.

 [8] T. S. Bunch and L. Parker, "Feynman propagator in curved spacetime: A momentum-space representation," *Physical Review D: Particles, Fields, Gravitation and Cosmology*, vol. 20, no. 10, pp. 2499–2510, 1979.

 [9] In fact, here, $\phi 4$ should be replaced by 4-point correlation function, which includes at least one four-point interaction. However, once $O(\lambda)$ and higher order diagrams are omitted, GR2 is still good enough to be used for the approximation.

[10] D. Ashok, *Finite Temperature Field Theory*, World Scientific Publishing Company, 1997.

[11] Strictly speaking, the imaginary time method should be applied to discuss the modification of A and B, but it makes no difference to our result. For details of the imaginary time, see Ref. [10].

[12] A. Vilenkin, "Birth of inflationary universes," *Physical Review D: Particles, Fields, Gravitation and Cosmology*, vol. 27, no. 12, pp. 2848–2855, 1983.

[13] A. Vilenkin, "Creation of universes from nothing," *Physics Letters B*, vol. 117, no. 1-2, pp. 25–28, 1982.

[14] S. Weinberg, *Cosmology*, Oxford University Press, New York, NY, USA, 2008.

[15] A. G. Riess, P. E. Nugent, R. L. Gilliland et al., "The farthest known supernova: Support for an accelerating universe and a glimpse of the epoch of deceleration," *The Astrophysical Journal*, vol. 560, no. 1, pp. 49–71, 2001.

[16] A. G. Riess, "Type Ia supernova discoveries at $z > 1$ from the *Hubble Space Telescope*: evidence for past deceleration and constraints on dark energy evolution," *The Astrophysical Journal*, vol. 607, pp. 665–687, 2004.

[17] Planck Collaboration, Ade, P. A. R., et al. Planck 2015 results - xiii. cosmological parameters. *AA*, 594:A13, 2016.

Research Article
Searches for Massive Graviton Resonances at the LHC

T. V. Obikhod [ID] and I. A. Petrenko

Institute for Nuclear Research, National Academy of Sciences of Ukraine, 47 Prosp. Nauki, Kiev 03028, Ukraine

Correspondence should be addressed to T. V. Obikhod; obikhod@kinr.kiev.ua

The Standard Model problems lead to the new theories of extra dimensions: Randall-Sundrum model, Arkani-Hamed-Dimopoulos-Dvali model, and TeV^{-1} model. In the framework of these models, with the help of computer program Pythia8.2, the production cross sections for Kaluza-Klein particles at various energies at the LHC were calculated. The generation of monojet events from scalar graviton emission was considered for number of extra dimensions ($n = 2$, 4, and 6) for the energy at the LHC 14 TeV. The graviton production processes through the gluon-gluon, quark-gluon, and quark-quark fusion processes are also studied and some periodicity was found in the behavior of the graviton mass spectrum. Production cross sections multiplied by branching fractions were calculated for the massive graviton, G, within Randall-Sundrum scenario and the most probable processes of graviton decay at 13 TeV, 14 TeV, and 100 TeV were counted.

1. Introduction

The problems with theoretical explanation of vacuum energy as well as dark energy, dark matter, and cosmological constant problems are only the tip of the iceberg of problems in the modern theoretical physics. Some of them are

  (i) ordinary matter accounting for about 5% of mass energy in the Universe and no dark matter candidate in the Standard Model (SM),

  (ii) hierarchy problem,

  (iii) fine tuning of SM Higgs mass,

  (iv) no explanation for fermion masses and mixings and three family structures,

  (v) unification of strong, electroweak, and gravitational forces,

  (vi) compositeness of leptons and quarks,

It is an experimental fact that there is something we cannot explain within the SM.

As is known, vacuum is produced in the processes of phase transitions in Early Universe and the space-time structure of the physical vacuum exhibits the connection to the structure formation in our Universe. So, the understanding of

Universe formation is deeply connected with the conception of the space-time. According to hierarchy formula [1], Plank energy can be reduced to the energy of about 10 TeV that is achieved at the LHC. So, the phenomena of the Universe formation at the early stages and the accompanying processes of particle physics could be studied at modern colliders. In spite of the fact that no new physics beyond the SM is discovered at the LHC at 13 TeV, the planned upgrading of the LHC to high luminosities and energies up to 100 TeV gives the possibility for the discovery of new physics. Among such searches for new physics, the most popular are the experimental searches for the Kaluza-Klein (KK) particles.

Historically, KK theory appeared as the unification of gravitational and electromagnetic interactions due to the proposition of a fifth dimension in addition to the usual four-dimensional space-time [2–4], which leads to the consideration of the concept of deformation of Riemannian geometry defined by extrinsic curvature of the space-time. The conclusions of this result are based, in particular, on the five-dimensional space from the paper [5]. Arkani-Hamed et al. proposed the solution to the hierarchy problem on the basis of the existence of new compact spatial dimensions. KK excitations in this extra dimensional space through the combined effect of all the gravitons became observable.
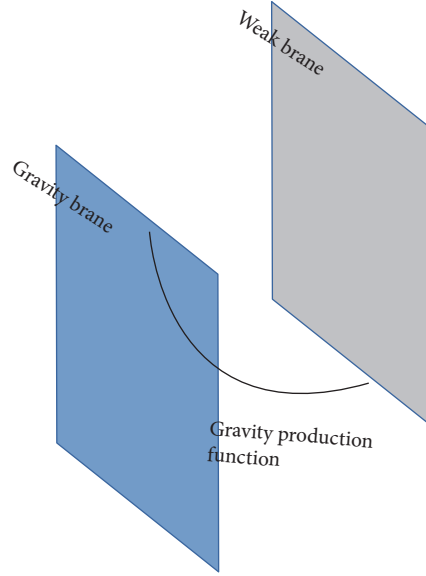
FIGURE 1: RS theory presented by the gravity and weak branes as the 4-dimensional boundaries of the extra dimension (from [12]).

Today, the idea of additional space as the instrumentation of the unification of all four interactions is of interest not only in theoretical physics [6–8] but also in experimental searches at the LHC for exotic matter that deviates from normal matter [9].

Our paper is devoted to the searches for KK particles in three models of extra dimensions: Arkani-Hamed-Dimopoulos-Dvali (ADD) model, [6], Randall-Sundrum (RS) model [7, 8], and TeV^{-1} model [10]. Using computer program Pythia8.2 [11], within these three extra dimensional models, we have calculated

(i) the production cross section of KK modes of massive gravitons and gauge bosons at energies from 14 TeV to planned 100 TeV,

(ii) the graviton mass spectrum for three graviton, G, emission processes: (a) gg → Gg, (b) qg → Gq, and (c) $q\bar{q}$ → Gg at 14 TeV at the LHC,

(iii) the graviton mass spectrum at 14 TeV at the LHC for numbers of extra dimensions ($n = 2, 4$, and 6) (for simplicity and brevity). Since the maximum of n is equal to 6 for ADD model, it was of interest to look at the behavior of graviton mass spectrum at the extreme values of n, from $n = 2$ to $n = 6$,

(iv) the production cross section of graviton, $gg \rightarrow G$, multiplied by branching ratios, Br($G \rightarrow gg$) (gluon-gluon (gg) pair), Br($G \rightarrow ll$) (leptons, l are of any type, e, μ, τ), and Br($G \rightarrow hh$) (h, Higgs boson) of the most probable processes of decay within RS model at 13 TeV, 14 TeV, and 100 TeV.

2. Models of Extra Dimensions

In this section, we will observe three models of extra dimensions, ADD, RS, and TeV^{-1}, which are the base for our further

calculations of KK particle properties. In the framework of M-theory [13], the metric of ADD model is as follows:

$$G_{MN}(x, y) = \eta_{MN} + \frac{2}{M^{1+n/2}} h_{MN}(x, y), \qquad (1)$$

where $G_{MN}(x, y)$ is the metric of $(4 + n)$-dimensional space-time with compact extra dimensions, where the gravitational field propagates and the SM localized on a 3-brane embedded into the $(4 + n)$-dimensional space-time, η_{MN} is $(4 + n)$-dimensional Minkowski background and $h_{MN}(x, y)$ is the deviation of Minkowski metrics, M is the fundamental mass scale, and n is the number of extra dimensions. Masses of KK modes for ADD model are given by

$$m_n = \frac{1}{R} \sqrt{n_1^2 + n_2^2 + \cdots + n_d^2} = \frac{|n|}{R}. \qquad (2)$$

Five-dimensional metric of RS model with one extra dimension compactified to the orbifold, S^1/Z_2, is with nonfactoriz-able geometry:

$$ds^2 = e^{-2\sigma(y)} \eta_{\mu\nu} dx^\mu dx^\nu + dy^2. \qquad (3)$$

Two 3-branes are located at points $y = 0$ and $y = \pi R$ of the orbifold with radius, R, of S^1. x^μ, $\mu = 0, 1, 2, 3$, and $\eta_{\mu\nu}$ are four-dimensional coordinates and Minkowski metrics; the function $\sigma(y)$ inside the interval $-\pi R < y < \pi R$ is equal to $\sigma(y) = k|y|$. ($k > 0$, dimensional parameter). In Figure 1 a nonfactorizable geometry with one spatial extra dimension is presented as a line segment between two four-dimensional branes, known as Planck and TeV brane.

Masses of KK particles for RS model are given by

$$m_n = \beta_n k e^{-\pi k R}, \qquad (4)$$

where $\beta_n = 3.83, 7.02, 10.17, 13.32, \ldots$ for $n = 1, 2, 3, 4, \ldots$. The metric of TeV^{-1} model for ten-dimensional string theory
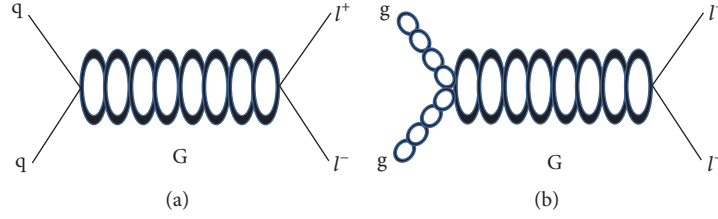
FIGURE 2: Processes for the graviton resonance production through (a) quark-quark and (b) gluon-gluon fusion.

is determined by the conditions on Calabi-Yau manifold: Ricci-flatness of metric, vanishing first Chern class, and SU(n) holonomy. Low-energy effective action has much smaller scale than Planck mass related to an internal compactification radius. In these scenarios, the SM fields as well as Z_{KK} and W_{KK} resonances are allowed to propagate in the bulk, but gravity is not included in the model. Masses of KK modes for TeV^{-1} model are given by

$$m_n = \left(m_0^2 + \frac{n \cdot n}{R_c^2} \right)^{1/2}, \qquad (5)$$

where $n \cdot n$ is scalar production of $n = (n_1, n_2, \ldots)$ which labels KK excitation levels, and m_0 is the mass of gauge zero-mode, which corresponds to SM gauge field.

The advantage of the presented models of extra dimensions lies in the possibility of the observation of the physics of Planck scales, M_{Pl}, at the energies achievable at modern colliders, M, due to the presence of extra dimensions, n. This result is possible due to the hierarchy formulas for the presented models:

ADD model: $M_{Pl}^2 \sim R^n M^{2+n}$

RS model: $M_{Pl}^2 = (M^3/k)(e^{2k\pi R} - 1)$

TeV^{-1} model: hierarchy formula is determined by the low-energy effective action

3. Results of Computer Modeling for Properties of KK Particles

RS resonances, connected with production of KK graviton, G, are described in [14]. Experimental searches for massive Graviton production are carried out at the LHC by ATLAS and CMS Collaborations and the latest data on the lower limit on graviton mass are presented in [15]. The production of narrow graviton resonances in the TeV range at the LHC as well as the decays into fermion and boson pairs was studied in this paper. For the discovering of graviton resonance, G, the parton showering formalism was used, which agrees with the NLO matrix element calculations. The partonic subprocesses are demonstrated in Figure 2.

The ADD graviton emission and virtual graviton exchange processes are described in [16]. Within model with large extra dimensions (LED), the processes that could give rise to new phenomena at LHC due to emission or exchange of gravitons were considered. The implementation

of these processes in the Monte Carlo generator Pythia8.2 was presented in this paper. The considered processes are connected with monojet, diphoton, and dilepton final states. It is also possible to generate monojet events from scalar graviton emission as described in [17].

TeV^{-1} sized extra dimensional KK production processes involve the production of electroweak KK gauge bosons, Z_{KK} and W_{KK}, in one TeV^{-1} sized extra dimension. The processes are described in [18, 19] and allow the specification of final states. In this article, the observation of a certain KK hard process in pp interactions at the LHC was presented within the S^1/Z_2, TeV^{-1} extra dimensional theoretical framework. The analytic form for the hard process cross section has been calculated and has been implemented within the Pythia8.2 Monte Carlo generator.

3.1. The Production Cross Section of KK Particles at Different Energies. With the help of computer program Pythia8.2 for three models of extra dimensions, we have calculated the production cross sections of KK particles at energies varying from 14 to 100 TeV. According to the latest experimental data presented in [15], we reconstructed jets with the anti-k_t clustering algorithm, transverse momenta, $p_T^{jet} > 20$ GeV, and rapidity $|\eta| < 2.4$ of jets to drop data connected with missing transverse momentum. Events were produced with Monte Carlo event sample using the NNPDF23LO parton distribution function (PDF) for the proton beam and scales of renormalizations and factorizations. The results are presented in Figure 3.

From Figure 3(a), we can see the significant predominance of production for dijet final states above monojet final states within LED model. Figure 3(b) shows that RS KK particles are produced at much higher values than Z_{KK} and W_{KK} bosons in TeV^{-1} extra dimensional model.

Within TeV^{-1} model with parameters $n = 10$ and $m^* = 2$–10 TeV, we calculated the production cross sections at 20 TeV, 60 TeV, and 100 TeV at the center of mass energies as a function of KK mass, $M_{Z_{KK}}$, presented in Figure 4. As the decay of Z_{KK} to muon pair is the dominant one, we decided to calculate, namely, this process of KK particle decay.

From Figure 4, we can see the sharp drop in the curve for 20 TeV compared with other curves at 60 TeV and 100 TeV at the center of mass energies. This result emphasizes the most important result for the further searches of new physics at high energies. As the last two curves (60 TeV and 100 TeV) are almost parallel, it is preferable to search for new
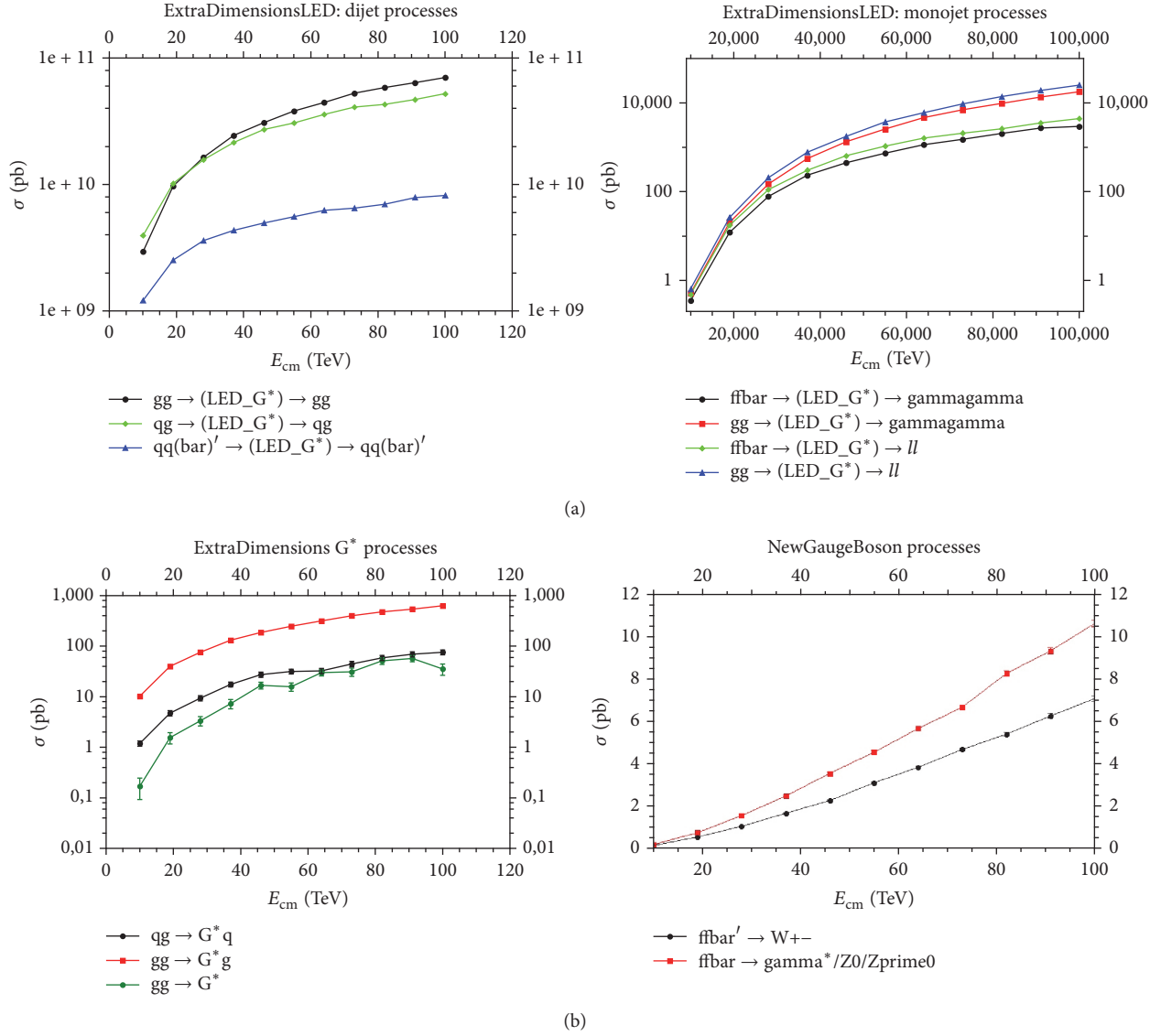
(a)

(b)

Figure 3: The production cross section at the center of mass energies varying from 14 to 100 TeV for (a) LED model: left panel, dijet final state; right panel, monojet final state; (b) left panel, RS model; right panel, TeV^{-1} model.
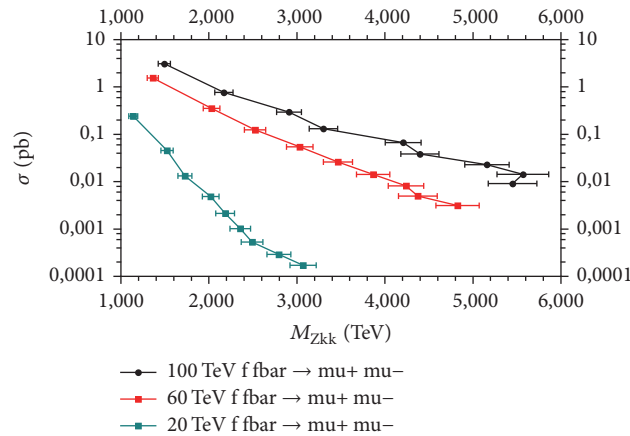

Figure 4: Production cross sections at 20 TeV, 60 TeV, and 100 TeV at the center of mass energies as a function of KK mass for TeV^{-1} model.
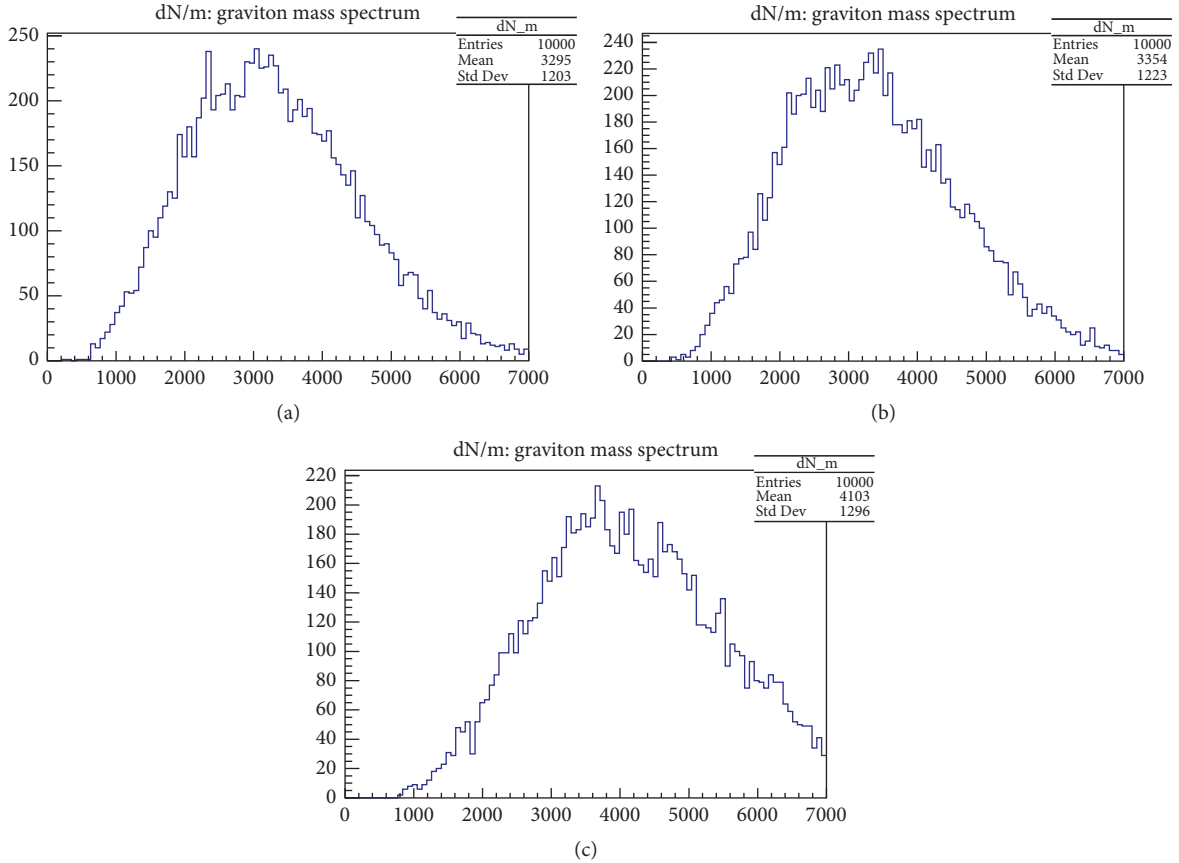
Figure 5: Graviton mass spectrum within monojet LED model for three graviton, G, emission processes: (a) gg → Gg, (b) qg → Gq, and (c) $q\bar{q}$ → Gg at the center of mass energies of 14 TeV.

phenomena at energies up to 30 TeV, when the production cross sections of KK particles can be varied in the wide range.

3.2. The Graviton Mass Spectrum at 14 TeV at the LHC. We will apply large-extra-dimensional (ADD-type) models in production processes for virtual extra dimensional scalars of graviscalar type. With the help of Pythia8.2, it is possible to generate monojet events from scalar graviton emission as described in [17].

The group of lowest-order G jet emission processes within monojet model was considered with the following parameters: ExtraDimensionsLED: $n = 6$; ExtraDimensionsLED: $M = 10000$. Three graviton, G, mass spectra for G jet emission processes, gg → Gg (gluon-gluon fusion (gg) with emission of graviton, G, and gluon, g), qg → Gq (quark-gluon fusion (qg) with emission of graviton, G, and quark, q), and $q\bar{q}$ → Gg (quark-antiquark fusion ($q\bar{q}$) with emission of graviton, G, and gluon, g) at the center of mass energies of 14 TeV at the LHC, are presented in Figure 5.

From Figure 5, the peak of the graviton mass spectrum distribution is viewed depending on the process of monojet emission. Although this dependence is insignificant, nevertheless, for the process $q\bar{q}$ → Gg of monojet graviton, G, emission, it is shifted by almost 1 TeV.

As LED model depends on the number of extra dimensions, n, it was important to study the graviton mass spectrum distributions for $n = 2$, 4, and 6. The results of our calculations of G jet emission process, gg → Gg, at the center of mass energies of 14 TeV is presented in Figure 6.

From Figure 6, substantial dependence of G jet emission process in the LED model on the number of extra dimensions is seen. Moreover, we can see clear periodicity of dependence, when peaks are shifted by 1 TeV with an increase of the number of extra dimensions by 2. According to the hierarchy formula of ADD model, this shifting is connected with the change in the radius of compactification, R. As n increases, R must decrease. Therefore, the mass shift to the right of 1 TeV indicates the decreasing of compactification radius.

3.3. The Production Cross Section of Graviton Emission Multiplied by Branching Ratio in RS Model. As is known, the discovery of a Higgs boson, h, at the LHC motivates the searches for physics beyond SM in channels involving Higgs boson. Higgs pair production is predicted by RS model with KK graviton, G_{KK}, emission that may decay to a pair of Higgs bosons. Such experimental searches were performed by ATLAS Collaboration, [20] at 13 TeV, presented in Figure 7.

From [12], branching fractions of graviton decay to SM particles are taken, presented in Figure 8. The predictions
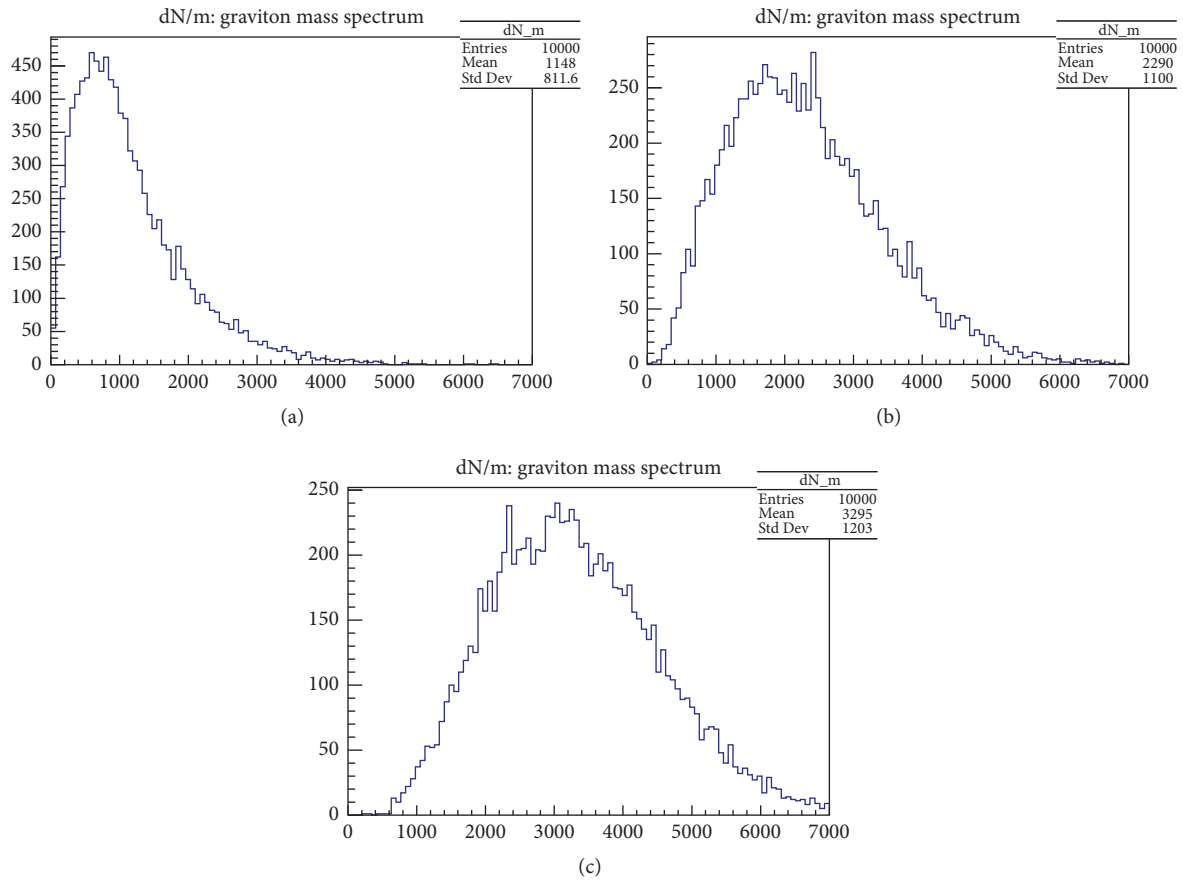
FIGURE 6: Graviton mass spectrum within monojet LED model for G jet emission process gg → Gg for (a) $n = 2$, (b) $n = 4$, and (c) $n = 6$ at the center of mass energies of 14 TeV.
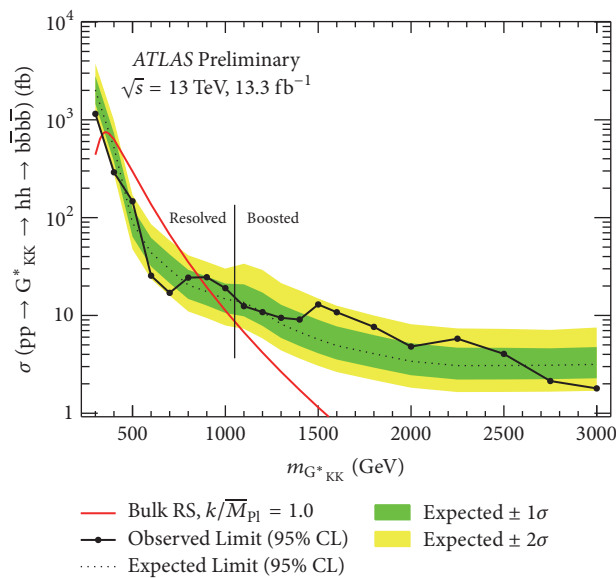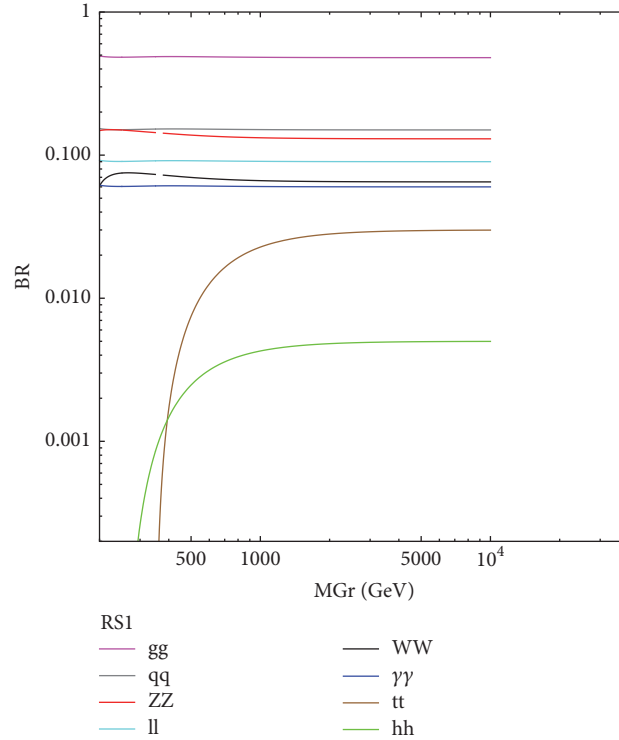

FIGURE 7: The expected and observed upper limit for pp → G_{KK} → hh → $b\bar{b}b\bar{b}$ in the bulk RS model with $k/M = 1$ at the 95% confidence level.

FIGURE 8: Branching fractions of graviton, G (from [12]).

for decay were updated using state-of-the-art computation tools with the highest branching fraction to dijet final states.

We will consider three processes of graviton decay, G $\rightarrow$ gg, G $\rightarrow$ ll, and G $\rightarrow$ hh, for further $\sigma \times Br$ calculations within RS scenario for graviton production process gg $\rightarrow$ G at 13 TeV, 14 TeV, and 100 TeV at the center of mass energies. In Figure 9, our calculations performed with the help of Pythia8.2 are presented, with parameters $k/M = 1$ and 0.1.

From Figure 9, we see the dependence of the $\sigma \times Br$ calculations on the parameter k/M and on the energy at the center of mass. Comparison of Figure 9(a) and 9(b) shows that the resonance peak shifts from 5 TeV to 7 TeV with increasing of energy at the collider. This mass shift of 2 TeV for case (b) indicates decreasing of the compactification radius of RS model according to hierarchy formula. In the case of Figure 9(c), we can see that there is no peak at 100 TeV and that the cross section for the formation of the resonance as a function of energy is observed to decrease.

4. Conclusion

The modern high energy physics is connected with experimental searches of new physics beyond the SM. These searches are connected not only with new possibilities of modern accelerating technics but also with problems of SM physics. The SM problems are not only of theoretical

character but also of experimental one, which is confirmed by modern experiments on the Higgs boson. Our work is dedicated to the studying of the properties of the new particles predicted by the theories of extra dimensions. Within three models, ADD, RS, and TeV^{-1}, we have calculated the production cross sections of massive graviton formation as well as the production of KK modes of gauge bosons depending on the energies of the modern and future colliders. Within LED model, the behavior of graviton mass spectrum for G jet emission processes for different numbers of extra dimension ($n = 2, 4$, and 6) was studied and clear periodicity of peaks shifted by 1 TeV was seen with an increase in the number of extra dimensions by 2. The graviton mass spectrum for three graviton, G, emission processes was also investigated: (a) gg $\rightarrow$ Gg, (b) qg $\rightarrow$ Gq, and (c) $q\bar{q}$ $\rightarrow$ Gg at 14 TeV at the LHC. The experimental searches for KK graviton emission and decay to a pair of Higgs bosons, performed by ATLAS Collaboration at 13 TeV, stimulated us to perform calculations at different parameters and energies within RS model. Our calculations of $\sigma \times Br$ shows that the resonance peak shifts from 5 TeV to 7 TeV with increasing of energy at the colliders from 13 TeV to 14 TeV as well as the absence of peak at energy of 100 TeV at the center of mass energies.

Conflicts of Interest

The authors declare that there are no conflicts of interest regarding the publication of this paper.

(a)

(b)

(c)
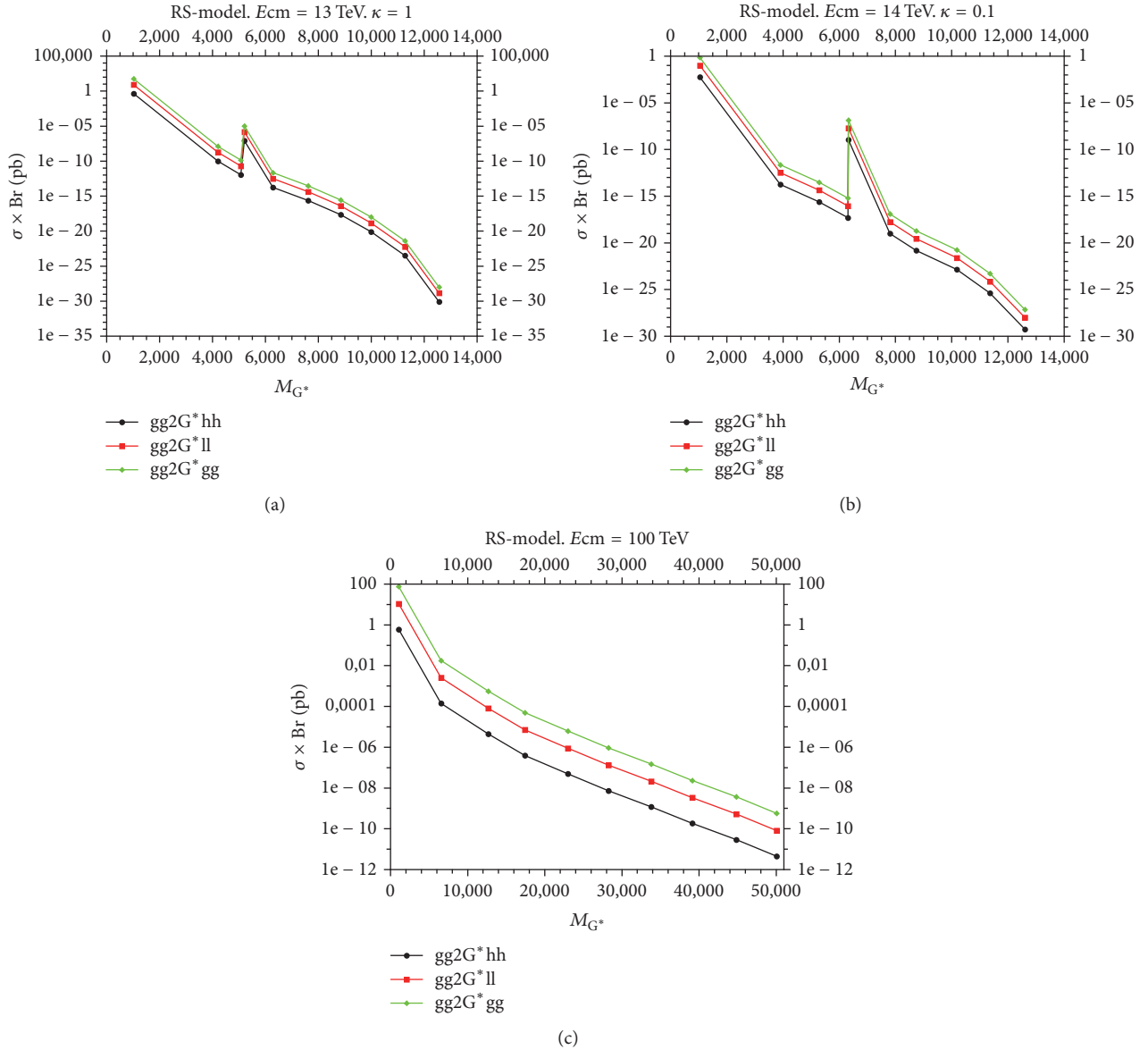
FIGURE 9: $\sigma \times Br$ for graviton production and decay as the function of graviton mass, M_G, at (a) 13 TeV, $k/M = 1$; (b) 14 TeV, $k/M = 0.1$; and (c) 100 TeV, $k/M = 0.1$.

References

[1] Y. A. Kubyshin, *Models with Extra Dimensions and Their Phenomenology*, 2001.

[2] T. Kaluza, "Zum Unitatsproblem in der Physik," *Sitzungsberichte der Koniglich Preußischen Akademie der Wissenschaften (Mathematical Physics)*, pp. 966–972, 1921.

[3] O. Klein, "Quantentheorie und fünfdimensionale Relativitäts-theorie," *Zeitschrift für Physik*, vol. 37, no. 12, pp. 895–906, 1926.

[4] M. D. Maia, "The Poincare conjecture and the cosmological constant," *International Journal of Modern Physics: Conference Series*, vol. 03, pp. 195–202, 2011.

[5] N. Arkani-Hamed, S. Dimopoulos, and G. Dvali, "The hierarchy problem and new dimensions at a millimeter," *Physics Letters B*, vol. 429, no. 3-4, pp. 263–272, 1998.

[6] N. Arkani-Hamed, S. Dimopoulos, and G. Dvali, "Phenomenology, astrophysics and cosmology of theories with sub-millimeter dimensions and TeV scale quantum gravity," *Physical Review D*, vol. 59, article 086004, 1999.

[7] L. Randall and R. Sundrum, "A large mass hierarchy from a small extra dimension," *Physical Review Letters*, vol. 83, no. 17, pp. 3370–3373, 1999.

[8] L. Randall and R. Sundrum, "An alternative to compactification," *Physical Review Letters*, vol. 83, no. 23, pp. 4690–4693, 1999.

[9] S. Maruyama, for the ATLAS, and CMS Collaborations, "Searches for Exotic Phenomena at ATLAS and CMS," *High Energy Physics - Experiment*, 2014.

[10] I. Antoniadis, "A possible new dimension at a few TeV," *Physics Letters B*, vol. 246, no. 3-4, pp. 377–384, 1990.

[11] T. Sjöstrand, S. Ask, J. R. Christiansen et al., "An introduction to PYTHIA 8.2," *Computer Physics Communications*, vol. 191, no. 1, pp. 159–177, 2015.

[12] A. Carvalho, *Gravity Particles from Warped Extra Dimensions, Predictions for LHC*, 2017.

[13] P. Hořava and E. Witten, "Heterotic and Type I String Dynamics from Eleven Dimensions," *Nuclear Physics B*, vol. 460, no. 3, pp. 506–524, 1996.

[14] J. Bijnens, P. Eerola, M. Maul, A. Månsson, and T. Sjöstrand, "QCD signatures of narrow graviton resonances in hadron colliders," *Physics Letters B*, vol. 503, no. 3-4, pp. 341–348, 2001.

[15] The ATLAS Collaboration, "Search for diboson resonances with boson-tagged jets in pp collisions at $s = 13$ TeV with the ATLAS detector," *Physics Letters B*, vol. 777, no. 91, 2017.

[16] S. Ask, I. V. Akin, L. Benucci, A. De Roeck, M. Goebel, and J. Haller, "Real emission and virtual exchange of gravitons and unparticles in Pythia8," *Computer Physics Communications*, vol. 181, no. 9, pp. 1593–1604, 2010.

[17] G. Azuelos, P.-H. Beauchemin, and C. P. Burgess, "Phenomenological constraints on extra-dimensional scalars," *Journal of Physics G: Nuclear and Particle Physics*, vol. 31, pp. 1–20, 2005.

[18] G. Bella, E. Etzion, N. Hod, and M. Sutton, "Introduction to the MCnet Moses project and Heavy gauge bosons search at the LHC," *High Energy Physics - Experiment*, 2010.

[19] G. Bella, E. Etzion, N. Hod, Y. Oz, Y. Silver, and M. Sutton, "A search for heavy Kaluza-Klein electroweak gauge bosons at the LHC," *Journal of High Energy Physics*, vol. 2010, no. 9, article no. 025, 2010.

[20] The ATLAS Collaboration, "Search for pair production of Higgs bosons in the $bbbb$ final state using proton-proton collisions at $s = 13$ TeV with the ATLAS detector," *ATLAS-CONF-049*, 2016.

Research Article
Electroweak Phase Transitions in Einstein's Static Universe

M. Gogberashvili [1,2]

[1]*Javakhishvili Tbilisi State University, 3 Chavchavadze Avenue, 0179 Tbilisi, Georgia*
[2]*Andronikashvili Institute of Physics, 6 Tamarashvili Street, 0177 Tbilisi, Georgia*

Correspondence should be addressed to M. Gogberashvili; gogber@gmail.com

We suggest using Einstein's static universe metric for the metastable state after reheating, instead of the Friedman-Robertson-Walker spacetime. In this case, strong static gravitational potential leads to the effective reduction of the Higgs vacuum expectation value, which is found to be compatible with the Standard Model first-order electroweak phase transition conditions. Gravity could also increase the CP-violating effects for particles that cross the new phase bubble walls and thus is able to lead to the successful electroweak baryogenesis scenario.

According to standard cosmology at the electroweak scale, our universe is in radiation dominated phase where all Standard Model particles are massless [1]. Once the temperature drops below the critical value, $T \sim 170$ GeV, the electroweak phase transition has occurred and the Higgs boson, gauge bosons, and fermions (except neutrinos) acquire masses through the Higgs mechanism. The order of this phase transition depends on the details of the Higgs potential with the temperature dependent terms [2–5]. To have a first-order phase transition effective Higgs potential of the model should have several minima. Of special importance is the cubic term in effective potential, which is essential to generate a potential barrier between the symmetric and broken phases and thus can provide the phase transition to be of the first order. In the Standard Model the cubic term, ET^3, is contributed only by the electroweak gauge bosons. If at zero temperature the Higgs field at the minimum of the potential has the value

$$v \approx 246 \, \text{GeV}, \tag{1}$$

the parameter E is the cubic term of the effective potential of order of

$$E \approx \frac{2M_W^3 + M_Z^3}{4\pi v^3} \approx 0.01, \tag{2}$$

where M_W and M_Z are the gauge bosons masses. Then the condition that the Higgs effective potential has two minima

leads to the very small value for the Higgs self-coupling parameter,

$$\lambda \approx 2E \approx 0.02, \tag{3}$$

which according to (1) is incompatible with the observed Higgs boson mass,

$$m_H = \sqrt{2\lambda} v \simeq 125 \, \text{GeV}. \tag{4}$$

This means that within the minimal Standard Model the electroweak phase transition is a smooth crossover, or of the second order [4, 5].

On the other hand, the first-order electroweak phase transitions may solve some cosmological problems, like the generation of the baryon asymmetry of the universe (see recent reviews [6, 7]). A first-order cosmological phase transition proceeds through the formation and expansion of cosmic bubbles. In this scenario spacetime is separated into two manifolds with their own distinct metrics, which are typically joined across a thin wall (domain wall). The dynamics of such objects can be very complicated, depending on the matter content of the interior (true vacuum) and exterior (false vacuum) regions as well as the tension on the bubble walls and how they interact with the surrounding plasma [8]. In bubble models matter-antimatter asymmetry can be generated at the electroweak scale, because all three Sakharov conditions

(baryon number violation, C and CP-violation, and departure from the thermal equilibrium) are fulfilled. Baryon production is a bubble surface effect but can be used to explain the observed matter-antimatter asymmetry, since the entire universe is swept out during the first-order phase transition and we may live in one bubble today [9, 10]. However, in traditional approach not only is the electroweak phase transition not of first order, but the CP-violation from the Cabibbo-Kobayashi-Maskawa matrix is too small, and to obtain the observed baryon asymmetry various extensions of the Standard Model have been proposed [4–7].

We want to emphasize that the conventional scenario of electroweak baryogenesis does not take into account gravitational effects. It is assumed that at the electroweak scale the universe was radiation dominated (filled with relativistic particles in thermal equilibrium) and the Friedmann-Robertson-Walker scale factor was unimportant for the particle reactions [1]. However, details of the anticipated periods (inflation and reheating) and conditions at the moment of transition to the radiation dominated phase, with the normal expansion of spacetime, are still poorly understood. For instance, if one assumes the existence of black holes in the early universe, the gravitational effects in their static fields are able to modify parameters of the effective Higgs potential and lead to the first-order phase transitions [11–14].

It is known that the Cosmological Principle for the uniform matter distribution not only leads to the Friedmann-Robertson-Walker nonstatic solution, but gives the Einstein's static universe as well [15]. Einstein's static universe refers to the homogenous and isotropic universe with the positive cosmological constant and positive spatial curvature. In the framework of General Relativity this model has been widely investigated for several kinds of matter sources (see [16, 17] and references therein). The metric of Einstein's universe can be written in the form:

$$ds^2 = dt^2 - \frac{dr^2}{1 - \Phi(r)} - r^2 \left(d\theta^2 + \sin^2\theta d\phi^2\right), \quad (5)$$

where

$$\Phi(r) = \frac{8\pi}{3} G\rho r^2 \quad (6)$$

denotes the gravitational potential and ρ is the uniform cosmic fluid density. In (5), it has been set $g_{tt} = 1$, since in cosmological case there must be a universal proper time for all fundamental observers. Introducing the radial coordinate transformation,

$$r = \frac{R}{1 + 2\pi G\rho R^2/3}, \quad (7)$$

the metric (5) can be written also in terms of Cartesian coordinates [18, 19]:

$$ds^2 = dt^2 - \frac{1}{\left(1 + 2\pi G\rho R^2/3\right)^2} \left(dx^2 + dy^2 + dz^2\right). \quad (8)$$

It was found that Einstein's static universe (5) is critically unstable to gravitational collapse or expansion and in modern

cosmological models usually is considered only as the initial state for the inflationary phase [20].

In our opinion, the short metastable period with $\ddot{a} = \dot{a} = 0$, in course of transition of the inflation ($\ddot{a} > 0$) into the deceleration stage ($\ddot{a} < 0$), that is, during or after the reheating epoch, when our universe was a spherule with the homogenous cosmic fluid of all kinds of ultrarelativistic particles, is natural to be described by Einstein's static solution (5), with the later transition to the nonstationary radiation dominated phase with the Friedmann-Robertson-Walker metric. This can be achieved by introducing a dark energy like substance, presence of which at early times is a quite generic feature of several dynamical dark energy models [21, 22], for example, $f(R)$ modification of gravity [23, 24], or the decaying scalar field (quintessence) [25], rather than a large fixed value classical cosmological constant. One can also assume that the higher-energy degrees of freedom of the quantum vacuum during reheating do not cancel the contribution of the zero-point motion of the quantum fields and the nullification of vacuum energy in the equilibrium vacuum is not acquired at this stage.

Introduction of Einstein's static metric (5) for our spherule-universe can radically change the common view that for the observed large Higgs mass the cosmological electroweak phase transition is of the second order [4, 5]. In a static island of space we can expect appearance of large gravitational potential in the Standard Model Lagrangian, similar to the case with a static black hole background [11–14]. Indeed, introducing the density function, $\Omega = \rho/\rho_c$, where

$$\rho_c = \frac{3}{8\pi Gd^2}, \quad (9)$$

is the critical density parameter and d is the horizon distance at the electroweak scale, and the gravitational potential (6) can be written in the form:

$$\Phi(r) = \Omega \frac{r^2}{d^2}. \quad (10)$$

A preferred location in the universe is absent and for uniform matter distribution we expect the existence of a constant average gravitational potential, $\langle\Phi(r)\rangle$, and the radial dependence will disappear. The total matter density of our universe at all stages of its evolution is assumed to be close to unity [26],

$$\Omega \lesssim 1.005. \quad (11)$$

Then the average gravitational potential (10) in the Einstein static universe (5) is estimated to reach the value:

$$\langle\Phi(r)\rangle = \frac{1}{V} \int dV \Phi(r) = \frac{3\Omega}{d^5} \int_0^d dr\, r^4 \approx 0.6. \quad (12)$$

Thus the factor which would multiply spatial components of the metric in matter Lagrangian will be of the order of

$$S^2 = \frac{1}{1 - \langle\Phi(r)\rangle} \approx 2.5. \quad (13)$$

Unlike the case of Friedmann-Robertson-Walker scale factor, one cannot hide the function S in the definitions of the spatial

coordinates, which are already set by the assumption to have the asymptotical Minkowski (or de Sitter) metric.

In the case of static, isotropic metrics (5), one can apply the well-established effective potential technique to particle models. The optical-mechanical analogy leads to a remarkable simplification of the equations of motion of particles and general-relativistic problems become formally identical to the classical ones with the effective index of refraction [27, 28],

$$n(r) = \sqrt{\frac{g_{rr}}{g_{tt}}} = \frac{1}{S} \approx 0.6. \tag{14}$$

In addition to the gravitational refraction index (14), in the Standard Model Lagrangian one can take into account the constant gravitational factor (13) by introduction of the new time parameter, $t \rightarrow St$, and conducting the conformal transformation of the Minkowski metric,

$$\eta_{\mu\nu} \longrightarrow \frac{1}{S^2}\eta_{\mu\nu},$$
$$\sqrt{-\eta} \longrightarrow \frac{1}{S^4}\sqrt{-\eta}. \tag{15}$$

It is known that it is possible to bring the conformally equivalent matter Lagrangian to the Minkowskian form by the rescaling,

$$A^{\nu} \longrightarrow A^{\nu},$$
$$\phi \longrightarrow S\phi, \tag{16}$$
$$\psi \longrightarrow S^{3/2}\psi,$$

of the gauge, scalar, and spinor fields, respectively [29, 30].

In general, the gravitational field affects strongly the symmetry behaviors of all quantum-field models, including scalar field Lagrangian [29, 30]. Currently, we do not have a standard theory of massive scalar bosons in curved spacetime, and several models exist with the minimal or conformal couplings with curvature. Nonminimal couplings usually are supposed in inflation models [31]. Investigations of the minimal case are important as well, since massive vector mesons and gravitons satisfy equations of this type [29], and also for nonminimal couplings in general it is impossible to conserve conformal invariance not only of the effective action (the conformal anomaly) but of the action itself [30].

To explore properties of cosmological phase transitions in the presence of static external gravitational field, one should evaluate the expectation value of the Higgs field over the lowest energy state. To find an energy spectrum it is important construction of the Hamiltonian of the system, which in general is difficult problem in the presence of gravitational field. However, in stationary conformal metric there exist some eligible models, even for massive scalar fields [32]. It was found that, in most situations, in regions where the conformal factor is almost constant, the conformal transformations finally amount to rescaling of a scalar boson mass in this region [29, 30, 32]. Our situation with the static gravitational field in some finite region of bulk spacetime differs with the cases where the parameters of cosmological phase transitions

were investigated in the infinite universe at the one-loop level [33, 34].

Since a solution of the Higgs equation in the metric $\eta_{\mu\nu}$ is the solution of the similar equation with an effective mass (for simplicity, we consider minimal coupling of the Higgs field to gravity) in the conformal metric, then under the transformation (15) the Standard Model Lagrangian obtains the ordinary form, but with the modified Higgs mass,

$$m_H \longrightarrow \frac{1}{S}m_H \approx 0.6m_H. \tag{17}$$

This means that in the early universe at the electroweak scale (in the symmetric phase) the effective vacuum expectation value (1) probably was smaller than in the present broken phase,

$$v \longrightarrow 0.6v \approx 156\,\text{GeV}. \tag{18}$$

Under the conformal rescaling (15), other parameters of the Standard Model are unchanged (including gauge boson masses), and in the perturbative analysis on the static background the modification of the vacuum expectation value (18) leads to the alteration of the parameter (2),

$$E \longrightarrow \frac{E}{0.2} \approx 0.05. \tag{19}$$

Then from the condition to have the first-order electroweak phase transition in the early universe (3), we obtain the acceptable value for the Higgs self-coupling constant,

$$\lambda \simeq 0.1. \tag{20}$$

This means that for the minimal Standard Model in the Einstein static universe background (5), the electroweak phase transitions can be of the first order. After the expansion of new phase bubbles and the passage to the Friedman-Robertson-Walker expansion of spacetime in the broken phase, the gravitational potential in the universe (6) will tend to zero and all parameters of the Standard Model will get the present values.

Note that, together with the allowance of electroweak phase transition to be of the first order, gravitational effects are able to solve another problem of the Standard Model baryogenesis—the smallness of CP-violating parameters.

It is known that, in general, gravitation can induce CP-violation processes [35–44]. Since antimatter can be interpreted as an ordinary matter propagating backward in time, for nonstationary spacetime (like an expanding new phase bubble) the time and thus CP-violation could be accrued in a CPT preserving framework [45]. To explore gravitational CP-violations for static backgrounds as well, one can use the fact that some quantum mechanical effects depend upon the gravitational potential themselves, not only to its gradient. Equations of quantum particles with a gravitational interaction terms contain inertial and gravitational mass separately. If within a model inertial and gravitational masses are not equal then in fermions wavefunctions there can appear the mass dependent gravitationally induced CP-violating phases [46, 47].

It is known that topological defects could violate the Week Equivalence Principle and exhibit nontrivial gravitational features [48]. Since it is impossible to surround any topological object by a spatial boundary, one cannot define their gravitational mass, M, by the integral from the zero-zero component of energy-momentum tensor, T_{00}, but needs to use the Tolman formula,

$$M = \int \sqrt{-g}dV \left(T_0^0 - T_1^1 - T_2^2 - T_3^3 \right). \tag{21}$$

From this formula it follows that, in spite of having large tensions, cosmic strings do not produce any gravitational force on the surrounding matter locally, while global monopoles, global strings, and planar domain walls exhibited repulsive nature [48].

In the bubble scenario spacetime is separated into two manifolds by a specific topological object—a spherical domain wall [8]. Spherical domain walls with the outer Schwarzschild metric can be gravitationally repulsive as well (with the negative mass parameter), when the time coordinate changes its direction on the bubble surface [49], or if one assumes that the asymptotic metric is non-Minkowskian [50]. Having written the interior/exterior metrics in a static form (Einstein's static universe (5) inside and the Schwarzschild outside), we must allow for the time coordinate to be different in each region, and it need not match across the bubble. On the other hand, the radial coordinate measures the proper size of the spheres of a spherically symmetric spacetime and therefore has to vary continuously across the bubble. Note that the reversion of time direction is equivalent to the introduction of a new family of negative tension bubbles [51, 52].

Due to the violation of the Weak Equivalence Principle, particles penetrating a topological object undergo strong jump in the gravitational potential, [Φ], and pick up the addition phases in their wavefunctions [53]. The gravitationally induced phases ϕ_{ij} can be approximated by [54, 55],

$$\phi_{ij} \sim [\Phi] \Delta m_{ij}^2, \tag{22}$$

where Δm_{ij} are the mass differences between different flavors. So the large jump of the gravitational potential at the new phase bubble walls, [Φ], could significantly increase CP-violating effects within the electroweak baryogenesis scenario.

In summary, it is taken for granted that the minimal Standard Model is unable to explain the baryon asymmetry of the universe, since electroweak phase transition in the early universe appeared to be of second order (without nonequilibrium processes) and the CP-violation parameter from the Cabibbo-Kobayashi-Maskawa matrix is too small. However, if for the description of the metastable state at the electroweak scale we replace the Friedman-Robertson-Walker spacetime with the Einstein static universe model, the strong static gravitational potential leads to the effective reduction of the Higgs vacuum expectation value, which is found to be compatible with the first-order electroweak phase transition conditions. We also argue that gravitational effects could increase the CP-violating parameters for the particles crossing the new phase bubble walls, which are appearing in electroweak baryogenesis scenarios.

Conflicts of Interest

The author declares that there are no conflicts of interest.

Acknowledgments

References

[1] V. Mukhanov, *Physical Foundations of Cosmology*, Cambridge University Press, New York, NY, USA, 2005.

[2] M. Dine, R. G. Leigh, P. Huet, A. Linde, and D. Linde, "Comments on the electroweak phase transition," *Physics Letters B*, vol. 283, no. 3-4, pp. 319–325, 1992.

[3] M. Dine, R. G. Leigh, P. Huet, A. Linde, and D. Linde, "Towards the theory of the electroweak phase transition," *Physical Review D*, vol. 46, article 550, 1992.

[4] I. G. Moss, "Higgs boson cosmology," *Cosmology and Nongalactic Astrophysics*, vol. 56, article 468, 2015.

[5] A. Katz and M. Perelstein, "Higgs couplings and electroweak phase transition," *Journal of High Energy Physics*, vol. 2014, article 108, 2014.

[6] D. E. Morrissey and M. J. Ramsey-Musolf, "Electroweak baryogenesis," *New Journal of Physics*, vol. 14, Article ID 125003, 2012.

[7] T. Konstandin, "Quantum Transport and Electroweak Baryogenesis," *Physics-Uspekhi*, vol. 56, no. 8, p. 747, 2013.

[8] V. A. Berezin, V. A. Kuzmin, and I. I. Tkachev, "Dynamics of bubbles in general relativity," *Physical Review D: Particles, Fields, Gravitation and Cosmology*, vol. 36, no. 10, pp. 2919–2944, 1987.

[9] A. G. Cohen, D. B. Kaplan, and A. E. Nelson, "Weak scale baryogenesis," *Physics Letters B*, vol. 245, no. 3-4, pp. 561–564, 1990.

[10] A. G. Cohen, D. B. Kaplan, and A. E. Nelson, "Baryogenesis at the weak phase transition," *Nuclear Physics B*, vol. 349, no. 3, pp. 727–742, 1991.

[11] P. Burda, R. Gregory, and I. G. Moss, "Gravity and the stability of the Higgs vacuum," *Journal of High Energy Physics*, vol. 2015, article 115, 2015.

[12] P. Burda, R. Gregory, and I. Moss, "Vacuum metastability with black holes," *Journal of High Energy Physics*, vol. 2015, article 114, 2015.

[13] P. Burda, R. Gregory, and I. G. Moss, "The fate of the Higgs vacuum," *Journal of High Energy Physics*, vol. 2016, article 025, 2016.

[14] N. Tetradis, "Black holes and Higgs stability," *Journal of Cosmology and Astroparticle Physics*, vol. 2016, no. 09, article 036, 2016.

[15] S. W. Hawking and G. F. R. Ellis, *The Large Scale Structure of Space-Time*, Cambridge University Press, London, UK, 1973.

[16] J. D. Barrow and C. G. Tsagas, "On the stability of static ghost cosmologies," *Classical and Quantum Gravity*, vol. 26, no. 19, 195003, 10 pages, 2009.

[17] J. D. Barrow and K. Yamamoto, "Instabilities of Bianchi type IX Einstein static universes," *Physical Review D: Particles, Fields,*

Gravitation and Cosmology, vol. 85, no. 8, Article ID 083505, 2012.

[18] R. C. Tolman, "On the use of the energy-momentum principle in general relativity," *Physical Review A: Atomic, Molecular and Optical Physics*, vol. 35, no. 8, pp. 875–895, 1930.

[19] R. C. Tolman, *Relativity, Thermodynamics and Cosmology*, Oxford University Press, Oxford, UK, 1962.

[20] G. Ellis and R. Maartens, "The emergent universe: inflationary cosmology with no singularity," *Classical and Quantum Gravity*, vol. 21, p. 223, 2004.

[21] C. Wetterich, "Cosmology and the fate of dilatation symmetry," *Nuclear Physics B*, vol. 302, no. 4, pp. 668–696, 1988.

[22] A. Friedland, C. Lunardini, and C. Peña-Garay, "Solar neutrinos as probes of neutrino–matter interactions," *Physics Letters B*, vol. 594, no. 3-4, pp. 347–354, 2004.

[23] A. De Felice and S. J. Tsujikawa, "f(R) theories," *Living Reviews in Relativity*, vol. 13, p. 3, 2010.

[24] S. Capozziello and M. de Laurentis, "Extended Theories of Gravity," *Physics Reports*, vol. 509, no. 4-5, pp. 167–321, 2011.

[25] E. J. Copeland, M. Sami, and S. Tsujikawa, "Dynamics of dark energy," *International Journal of Modern Physics D: Gravitation, Astrophysics, Cosmology*, vol. 15, no. 11, pp. 1753–1935, 2006.

[26] P. A. R. Ade, N. Aghanim, M. Arnaud et al., "Planck 2015 results. XIII. Cosmological parameters," *Astronomy & Astrophysics*, vol. 594, article A13, 2016.

[27] J. Evans, P. M. Alsing, S. Giorgetti, and K. K. Nandi, "Matter waves in a gravitational field: An index of refraction for massive particles in general relativity," *American Journal of Physics*, vol. 69, no. 10, pp. 1103–1110, 2001.

[28] L. B. OKUN, "Photons and static gravity," *Modern Physics Letters A*, vol. 15, no. 31, pp. 1941–1947, 2000.

[29] A. A. Grib, S. G. Mamayev, and V. M. Mostepanenko, *Vacuum Quantum Effects in Strong Fields*, Friedmann Lab. Publ, St. Petersburg, Russia, 1994.

[30] N. D. Birrell and P. C. W. Davies, *Quantum Fields in Curved Space*, Cambridge Monographs on Mathematical Physics, Cambridge University Press, Cambridge, UK, 1984.

[31] A. Linde, *Particle Physics and Inflationary Cosmology*, Harwood Academic, New York, NY, USA, 1990.

[32] A. J. Silenko, "Scalar particle in general inertial and gravitational fields and conformal invariance revisited," *Physical Review D: Particles, Fields, Gravitation and Cosmology*, vol. 88, no. 4, Article ID 045004, 2013.

[33] L. H. Ford and D. J. Toms, "Dynamical symmetry breaking due to radiative corrections in cosmology," *Physical Review D*, vol. 25, p. 1510, 1982.

[34] V. G. Lapchinsky, V. I. Nekrasov, V. A. Rubakov, and A. V. Veryaskin, in *Quantum Gravity*, M. A. Markov and P. C. West, Eds., Plenum Press, New York, NY, USA, 1984.

[35] S. W. Hawking, "Black hole explosions?" *Nature*, vol. 248, no. 5443, pp. 30-31, 1974.

[36] S. W. Hawking, "Particle creation by black holes," *Communications in Mathematical Physics*, vol. 43, no. 3, pp. 199–220, 1975.

[37] S. W. Hawking, "Black holes and thermodynamics," *Physical Review D: Particles, Fields, Gravitation and Cosmology*, vol. 13, no. 2, pp. 191–197, 1976.

[38] S. H. Aronson, G. J. Bock, H.-Y. Cheng, and E. Fischbach, "Energy dependence of the fundamental parameters of the K0-K0 system. II. Theoretical formalism," *Physical Review D: Particles, Fields, Gravitation and Cosmology*, vol. 28, no. 3, pp. 495–523, 1983.

[39] D. B. Cline, "Possible Observation Of Gravitational Effects For Vertical And Horizontal K0(s) / K0(l) Events At A Phi Factory," *Modern Physics Letters A*, vol. 5, pp. 1951–1956, 1990.

[40] I. R. Kenyon, "A recalculation on the gravitational mass difference between the K0 and K0 mesons," *Physics Letters B*, vol. 237, no. 2, pp. 274–277, 1990.

[41] G. Chardin, "CP violation and antigravity (revisited)," *Nuclear Physics A*, vol. 558, pp. 477–495, 1993.

[42] D. V. Ahluwalia and M. Kirchbach, "Primordial space-time foam as an origin of cosmological matter-antimatter asymmetry," *International Journal of Modern Physics D*, vol. 10, no. 6, artice 811, 2001.

[43] G. Lambiase, S. Mohanty, and A. R. Prasanna, "Neutrino coupling to cosmological background: a review on gravitational baryo/leptogenesis," *International Journal of Modern Physics D*, vol. 22, no. 12, Article ID 1330030, 2013.

[44] G. Amelino-Camelia, "Quantum-spacetime phenomenology," *Living Reviews in Relativity*, vol. 16, article 5, 2013.

[45] A. Barnaveli and M. Gogberashvili, "Cosmological "arrow of time" and baryon asymmetry of the universe," *Physics Letters B*, vol. 316, no. 1, pp. 57–60, 1993.

[46] M. Gasperini, "Testing the principle of equivalence with neutrino oscillations," *Physical Review D: Particles, Fields, Gravitation and Cosmology*, vol. 38, no. 8, pp. 2635–2637, 1988.

[47] A. Halprin and C. N. Leung, "Can the Sun shed light on neutrino gravitational interactions?" *Physical Review Letters*, vol. 67, no. 14, pp. 1833–1835, 1991.

[48] A. Vilenkin and E. P. S. Shellard, *Cosmic Strings and Other Topological Defects*, Cambridge University Press, Cambridge, UK, 1994.

[49] A. Barnaveli and M. Gogberashvili, "Antigravitating bubbles," *General Relativity and Gravitation*, vol. 26, p. 1117, 1994, https://arxiv.org/abs/hep-ph/9505412.

[50] A. Barnaveli and M. Gogberashvili, "Asymptotically non-minkowskian" bubbles with gravitational repulsion," *Theoretical and Mathematical Physics*, vol. 113, article 1491, 1997.

[51] K. Marvel and D. Wesley, "Tunneling with negative tension," *Journal of High Energy Physics*, vol. 2008, no. 12, article 034, 2008.

[52] B. Lee, C. H. Lee, W. Lee, S. Nam, and C. Park, "Dynamics of false vacuum bubbles with nonminimal coupling," *Physical Review D: Particles, Fields, Gravitation and Cosmology*, vol. 77, no. 6, Article ID 063502, 2008.

[53] L. Stodolsky, "Matter and light wave interferometry in gravitational fields," *General Relativity and Gravitation*, vol. 11, no. 6, pp. 391–405 (1980), 1979.

[54] D. V. Ahluwalia and C. Burgard, "Interplay of gravitation and linear superposition of different mass eigenstates," *Physical Review D: Particles, Fields, Gravitation and Cosmology*, vol. 57, pp. 4724–4727, 1998.

[55] D. V. Ahluwalia and C. Burgard, "Gravitationally induced neutrino-oscillation phases," *General Relativity and Gravitation*, vol. 28, pp. 1161–1170, 1996.

Research Article

Moving Unstable Particles and Special Relativity

Eugene V. Stefanovich 🔵

1763 Braddock Court, San Jose, CA 95125, USA

Correspondence should be addressed to Eugene V. Stefanovich; eugenev@synopsys.com

In Poincaré-Wigner-Dirac theory of relativistic interactions, boosts are dynamical. This means that, just like time translations, boost transformations have a nontrivial effect on internal variables of interacting systems. In this respect, boosts are different from space translations and rotations, whose actions are always universal, trivial, and interaction-independent. Applying this theory to unstable particles viewed from a moving reference frame, we prove that the decay probability cannot be invariant with respect to boosts. Different moving observers may see different internal compositions of the same unstable particle. Unfortunately, this effect is too small to be noticeable in modern experiments.

1. Introduction

Time dilation is one of the most spectacular predictions of special relativity. This theory predicts that any time-dependent process slows down by the universal factor of $1/\sqrt{1 - v^2/c^2} \equiv \cosh\theta$ when viewed from a reference frame moving with the speed v (and rapidity θ). The textbook example of such a time-dependent process is the decay law $\Upsilon(0, t)$ of an unstable particle at rest. The function $\Upsilon(0, t)$ is the probability of finding the unstable particle at time t, if it was prepared with 100% certainty at time $t = 0$. Then, according to special relativity, the decay law of a moving particle should be exactly $\cosh\theta$ times slower:

$$\Upsilon^{SR}(\theta, t) = \Upsilon\left(0, \frac{t}{\cosh\theta}\right). \tag{1}$$

Indeed, this prediction was confirmed in numerous measurements [1–4]. The best accuracy of 0.1% was achieved in experiments with relativistic muons [5, 6].

However, the exact validity of (1) is still a subject of controversy. One point of view [7–9] is that special-relativistic time dilation was derived in the framework of classical theory and may not be directly applicable to unstable particles, which are fundamentally quantum systems without well-defined masses, velocities, positions, and so on.

However, such a quantum clock as an unstable particle cannot be at rest (i.e., cannot have zero velocity or zero momentum) and simultaneously be at a definite point (due to the quantum uncertainty relation). So, the standard derivation of the moving clock dilation is inapplicable for the quantum clock. The related quantum-mechanical derivation must contain some reservations and corrections. Shirokov [10]

Indeed, detailed quantum-mechanical calculations [8, 10–12] suggest that (1) is not accurate, and that corrections to this formula should be expected, especially at large times, exceeding multiple lifetimes. Although these corrections are too small to be observed in modern experiments, their presence casts doubt on the limits of applicability of Einstein's special relativity.

Unfortunately, the corrections to (1) were derived in [8, 10–12] under certain assumptions and approximations. So, the question remains whether one can design a relativistic model in which the decay slowdown will acquire exactly the form (1) demanded by special relativity [13, 14]?

In order to answer this question we will analyze the status of interactions in special relativity from a more general point of view. We are going to prove that under no circumstances the decay law transforms with respect to boosts exactly as in (1).

TABLE 1: Inertial transformations.

Transformation	Type	Parameter	Generator	Meaning of generator
Space translation	Kinematical	Distance $\mathbf{a}$	$\mathbf{P} = \mathbf{P}_0$	Total momentum
Rotation	Kinematical	Angle $\boldsymbol{\varphi}$	$\mathbf{J} = \mathbf{J}_0$	Total angular momentum
Time translation	Dynamical	Time t	$H = H_0 + V$	Total energy (Hamiltonian)
Boost	Dynamical	Rapidity $\boldsymbol{\theta}$	$\mathbf{K} = \mathbf{K}_0 + \mathbf{Z}$	Boost operator

2. Materials and Methods

2.1. Inertial Transformations. The theory of relativity tries to connect views of different inertial observers. The principle of relativity says that all such observers are equivalent; that is, two inertial observers performing the same experiment will obtain the same results.

There are four classes of inertial transformations, space translations, time translations, rotations, and boosts, and their actions on observed systems differ very much (see Table 1). For example, it is easy to describe the results of space translations and rotations. An observer displaced by the 3-vector $\mathbf{a}$ sees all atoms in the Universe simply shifted in the opposite direction $-\mathbf{a}$. This shift is absolutely exact and universal. It applies to all systems, however complicated. The same can be said about rotations. One can switch to the point of view of the rotated observer by simply rotating all atoms in the Universe. For example, rotation through the angle φ about the z-axis results in the transformation of coordinates

$$x' = x \cos\varphi - y \sin\varphi$$

$$y' = y \cos\varphi + x \sin\varphi \qquad (2)$$

$$z' = z$$

which is independent on the composition of the observed system and on its interactions. Due to this exact universality, we can regard space translations and rotations as purely geometrical or *kinematical* transformations.

Time translation is also an inertial transformation, because repeating the same experiment at different times will not change the outcome. However, this transformation is by no means kinematical. Time evolutions of interacting systems can be very complicated. Their description requires intimate knowledge of the system's composition, state, and interactions acting between system's parts. We will say that time translations are *dynamical* inertial transformations.

Now, what about boosts? Are they kinematical or dynamical? In nonrelativistic classical physics boosts are definitely regarded as kinematical, they simply change velocities of all atoms in the Universe. However, things become more complicated in relativistic physics, as we shall see below.

2.2. Boosts in Special Relativity. Description of boost transformations is the central subject of special relativity. Einstein based his approach on the already mentioned relativity postulate and on his second postulate about the invariance of the speed of light. It is remarkable how all results of special relativity can be derived from these two simple and undeniable statements.

Consider the light clock shown in Figure 1(a). It consists of two parallel mirrors and the light pulse reflecting back and forth between them. The period of the clock at rest is equal to $\tau = 2t = 2l/c$. If the clock is moving, as in Figure 1(b), the distance traveled by the light pulse increases to $l' = 2ct' = 2\sqrt{l^2 + (vt')^2}$. Solving this system of equations with respect to the clock period, we obtain

$$\tau' = 2t' = \frac{\tau}{\sqrt{1 - v^2/c^2}} = \tau \cosh\theta. \qquad (3)$$

So, the moving clock runs $\cosh\theta$ times slower than the clock at rest. This is the time dilation effect that we used in (1).

Let us now consider the same clock oriented parallel to its velocity, as in Figure 2. The clock's rate should not depend on its orientation, so we already know the period of this clock in motion (3). Taking into account the invariance of the speed of light, this result can be achieved only if the distance between the two mirrors decreases. The corresponding system of equations is

$$\tau' = t_1 + t_2 = \frac{(l' + vt_1)}{c} + \frac{(l' - vt_2)}{c}. \qquad (4)$$

Solving with respect to l', we obtain the familiar length contraction formula:

$$l' = l\sqrt{1 - \frac{v^2}{c^2}} = \frac{l}{\cosh\theta}. \qquad (5)$$

Formulas (3) and (5) already imply that no material object can move faster than the speed of light. Otherwise, the factor $\sqrt{1 - v^2/c^2}$ would become imaginary, which is absurd.

We can also make a clock, in which, instead of the light pulse, we have a massive steel ball bouncing between the two mirrors. The ball's speed w is less than c, and the speed invariance postulate does not apply to w. Nevertheless, we expect this clock to obey the same time dilation and length contraction rules as derived above. Then, for consistency, we have to modify the classical velocity transformation law. For example, if the resting clock in Figure 2(a) had ball's velocities $\pm w$, then the moving clock in Figure 2(b) should have velocities

$$w_1 = \frac{w + v}{1 + wv/c^2} \qquad (6)$$

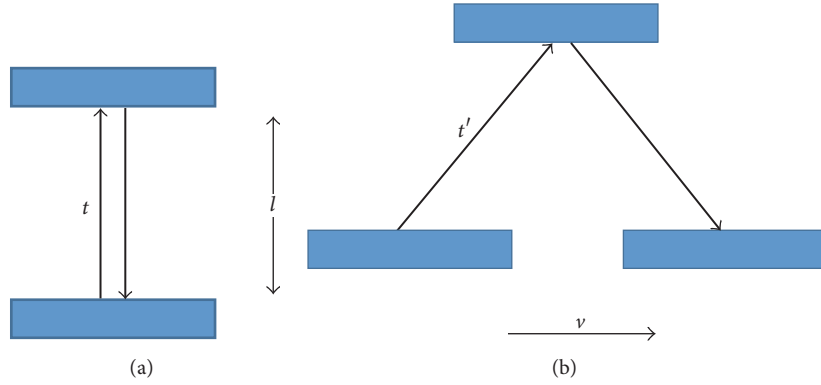$$w_2 = \frac{-w + v}{1 - wv/c^2}. \qquad (7)$$

FIGURE 1: Light clock: (a) at rest and (b) in motion perpendicular to the clock's axis.
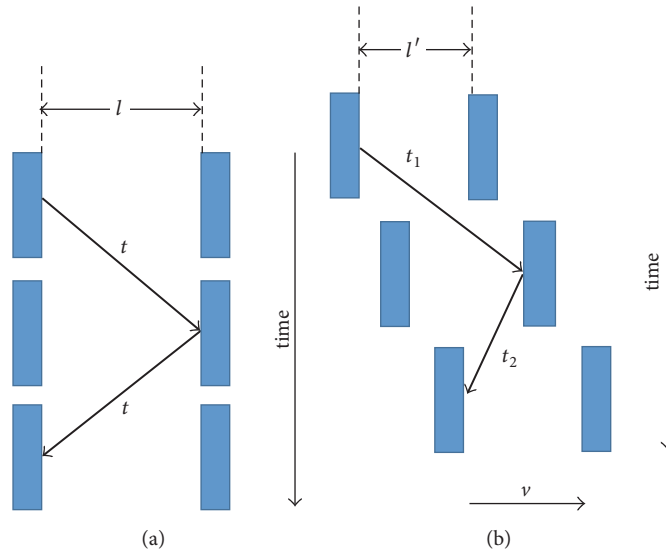

FIGURE 2: Light clock: (a) at rest and (b) in motion parallel to the clock's axis. The time evolution is shown in three frames stacked up vertically.

Indeed, it is not difficult to verify that these values solve the system of equations

$$
\begin{aligned}
w_1 t_1 &= l' + v t_1 \\
-w_2 t_2 &= l' - v t_2 \\
t_1 + t_2 &= \left(\frac{2l}{w} \right) \cosh \theta
\end{aligned}
\tag{8}
$$

that describe the movement of the ball during one clock period.

As a consistency check, by applying the velocity addition law (6) to the photon moving with the speed of light ($w = c$), we return back to Einstein's light speed invariance postulate

$$
w_1 = \frac{c + v}{1 + v/c} = c.
\tag{9}
$$

Special relativity explains how all these particular results can be generalized into Lorentz transformations for the times and positions of events. For example, any event having 4-coordinates (t, x, y, z) in the rest frame will have other 4-coordinates

$$
\begin{aligned}
t' &= t \cosh \theta - \left(\frac{x}{t} \right) \sinh \theta \\
x' &= x \cosh \theta - ct \sinh \theta \\
y' &= y \\
z' &= z
\end{aligned}
\tag{10}
$$

in the frame moving with velocity $v = c \tanh \theta$ along the x-axis. The linear character and the exact universality of these formulas are similar to transformations of 3-coordinates under rotations (2). So, it is tempting to continue this analogy and to introduce the idea of the 4D Minkowski space-time, whose points constitute physical events, and where boosts are represented by purely geometrical (kinematical) pseudo-rotations.

However, it is important to note that all the above derivations used model systems without interactions. The second Einstein postulate is formally applicable only to light pulses and events associated with them. So, strictly speaking, we are not allowed to extend results of special relativity

beyond corpuscular optics. In addition, one can show [15] that Lorentz transformations (10) can be extended to special events, such as intersections of particle trajectories, involving massive noninteracting particles, for example, our steel ball and mirrors. (Of course, reflections of light pulses or steel balls from the mirrors do involve interactions, but in our idealized thought experiments we can assume that these processes take negligibly short times.)

How can we be confident that the same conclusions apply to interacting systems? For example, what if the steel ball is bouncing between plates of a charged capacitor? Can we be sure that Lorentz formulas (10) still apply?

Here we meet the following fork in the road. On the one hand, we can choose to postulate that the laws of special relativity established above are valid independent of interactions. Then boosts should be rigorously kinematical, just as space translations and rotations. This nonobvious postulate is tacitly assumed in all textbooks. In particular, it was used in numerous attempts [16–22] to derive Lorentz transformations from the first Einstein postulate only.

Alternatively, we can assume that, similar to time translations, boosts are dynamical; that is, they involve interactions, and their actions cannot be expressed by simple universal formulas, like (10). We will discuss these two possibilities in Section 3. However, before doing that, in the rest of this section, we are going to recall the fundamentals of relativistic quantum theory pioneered by Wigner and Dirac. This theory is based on the extremely important fact that inertial transformations form the Poincaré group.

2.3. Representations of the Poincaré Group in Quantum Mechanics.

We are interested in application of inertial transformations to quantum systems. Properties of such systems are described by objects in the Hilbert space $\mathcal{H}$, such as state vectors and Hermitian operators of observables. So, we have to define the action (a.k.a. representation) of inertial transformations in $\mathcal{H}$. Operators of this representation U_g must preserve quantum-mechanical probabilities, so these operators have to be unitary [23]. This brings us to the classical mathematical problem of constructing unitary representations of the Poincaré group in the given Hilbert space $\mathcal{H}$ [24].

Important role is played by the so-called "infinitesimal transformations" or generators. They are represented by Hermitian operators in $\mathcal{H}$ (see Table 1). Unitary representatives U_g of finite transformations can be expressed by exponential functions of the Hermitian generators. For example, a general inertial transformation g is a composition of (boost $\boldsymbol{\theta}$) × (rotation $\boldsymbol{\varphi}$) × (space translation $\mathbf{a}$) × (time translation t). It is represented by the following product of unitary exponents:

$$U_g = e^{-(ic/\hbar)\mathbf{K}\cdot\boldsymbol{\theta}} e^{-(i/\hbar)\mathbf{J}\cdot\boldsymbol{\varphi}} e^{-(i/\hbar)\mathbf{P}\cdot\mathbf{a}} e^{(i/\hbar)Ht}. \tag{11}$$

Commutators of the Hermitian generators are fully determined by the structure of the Poincaré group [25, 26]

$$\left[J_i, P_j\right] = i\hbar \sum_{k=1}^{3} \epsilon_{ijk} P_k \tag{12}$$

$$\left[J_i, J_j\right] = i\hbar \sum_{k=1}^{3} \epsilon_{ijk} J_k \tag{13}$$

$$\left[J_i, K_j\right] = i\hbar \sum_{k=1}^{3} \epsilon_{ijk} K_k \tag{14}$$

$$\left[P_i, P_j\right] = \left[J_i, H\right] = \left[P_i, H\right] = 0 \tag{15}$$

$$\left[K_i, K_j\right] = -\frac{i\hbar}{c^2} \sum_{k=1}^{3} \epsilon_{ijk} J_k \tag{16}$$

$$\left[K_i, P_j\right] = -\frac{i\hbar}{c^2} H \delta_{ij} \tag{17}$$

$$\left[K_i, H\right] = -i\hbar P_i. \tag{18}$$

2.4. Hilbert Space of Unstable Particle.

According to Wigner and Weinberg [24, 26], the Hilbert space $\mathcal{H}^{(i)}$ of each stable elementary particle carries an unitary irreducible representation $U_g^{(i)}$ of the Poincaré group. The Hilbert space of an N-particle system is constructed as a tensor product (with proper (anti)symmetrization) of one-particle spaces

$$\mathcal{H}^N = \mathcal{H}^{(1)} \otimes \mathcal{H}^{(2)} \otimes \cdots \otimes \mathcal{H}^{(N)}. \tag{19}$$

In the formalism with varied numbers of particles (e.g., in quantum field theory), one builds the Fock space as a direct sum of spaces (19). For example, in a good approximation one can describe the unstable particle α with one decay channel $\alpha \rightarrow \beta + \gamma$, in the part of the Fock space, which includes the particle α itself and its decay products $\beta + \gamma$

$$\mathcal{H} = \mathcal{H}^{(\alpha)} \oplus \left(\mathcal{H}^{(\beta)} \otimes \mathcal{H}^{(\gamma)}\right). \tag{20}$$

Each normalized state vector $|\Psi\rangle$ in the Hilbert space $\mathcal{H}$ can be represented as a sum of two orthogonal components

$$|\Psi\rangle = |\Psi\rangle_\alpha + |\Psi\rangle_{\beta\gamma}, \tag{21}$$

where the component

$$|\Psi\rangle_\alpha \equiv T |\Psi\rangle \in \mathcal{H}^{(\alpha)} \tag{22}$$

lies entirely in the subspace of the unstable particle, while the other component

$$|\Psi\rangle_{\beta\gamma} \equiv (1 - T) |\Psi\rangle \in \mathcal{H}^{(\beta)} \otimes \mathcal{H}^{(\gamma)} \tag{23}$$

is in the subspace of decay products. Here we denoted by T the Hermitian projection on the subspace $\mathcal{H}^{(\alpha)}$

$$T\mathcal{H}^{(\alpha)} = \mathcal{H}^{(\alpha)}. \tag{24}$$

According to basic rules of quantum mechanics, the norms of these two components have simple physical interpretations:

$$\Upsilon \equiv \left\| |\Psi\rangle_\alpha \right\|^2 \tag{25}$$

is the probability of finding the unstable particle α in the state $|\Psi\rangle$, and $\left\| |\Psi\rangle_{\beta\gamma} \right\|^2 = 1 - \left\| |\Psi\rangle_\alpha \right\|^2$ is the probability of finding its decay products.

Observations of the unstable particle can be also described in the quantum-logical language of yes-no questions, like "Do we see the unstable particle?" and an observable, which can take two values 1 or 0, corresponding to the possible answers "yes" or "no." Obviously, the Hermitian operator of this observable is the projection T introduced above. Its eigensubspaces $\mathcal{H}^{(\alpha)}$ and $\mathcal{H}^{(\beta)} \otimes \mathcal{H}^{(\gamma)}$ correspond to the eigenvalues 1 and 0, respectively. Then the probability of finding the particle α can be written as the expectation value of the projection T. Taking into account the property $T^2 = T$, we see that this definition is in full agreement with (25)

$$\langle \Psi | T | \Psi \rangle = (\langle \Psi | T) (T | \Psi \rangle) = \| T | \Psi \rangle \|^2 = \big\| | \Psi \rangle_\alpha \big\|^2$$
$$= \Upsilon. \tag{26}$$

2.5. Interacting Representation of the Poincaré Group. Next we should find out how the quantity Υ depends on the observer. To obtain the formula for the decay law (i.e., the time evolution of the probability Υ), we can use either the Schrödinger representation, where state vectors depend on time

$$\Upsilon(0, t) = \left(\langle \Psi | e^{(i/\hbar)Ht} \right) T \left(e^{-(i/\hbar)Ht} | \Psi \rangle \right), \tag{27}$$

or, equivalently, the Heisenberg picture, where observables are time-dependent

$$\Upsilon(0, t) = \left\langle \Psi \left| \left(e^{(i/\hbar)Ht} T e^{-(i/\hbar)Ht} \right) \right| \Psi \right\rangle. \tag{28}$$

To perform these calculations, we have to specify the Hamiltonian H in the Hilbert space $\mathcal{H}$. In order to keep the relativistic invariance, this Hamiltonian should be consistent with other Poincaré generators: that is, commutation relations (12)–(18) have to be satisfied.

Using available 1-particle irreducible representations $U_g^{(\alpha)}$, $U_g^{(\beta)}$, $U_g^{(\gamma)}$, one can easily construct one valid representation of the Poincaré group in $\mathcal{H}$

$$U_g^0 \equiv U_g^{(\alpha)} \oplus \left(U_g^{(\beta)} \otimes U_g^{(\gamma)} \right). \tag{29}$$

It is appropriate to call this representation "noninteracting," because its generators $\{ \mathbf{P}_0, \mathbf{J}_0, \mathbf{K}_0, H_0 \}$ take the forms corresponding to free particles. Apparently, in this case, the subspace $\mathcal{H}_\alpha$ remains invariant with respect to all inertial transformations. In particular, noninteracting translation generators commute with the projection T

$$[T, H_0] = 0 \tag{30}$$

$$[T, \mathbf{P}_0] = 0. \tag{31}$$

According to Dirac and Weinberg [25, 26], one can introduce relativistic interaction by defining in $\mathcal{H}$ a new unitary representation $U_g \neq U_g^0$ of the Poincaré group with generators $\{ \mathbf{P}, \mathbf{J}, \mathbf{K}, H \}$. Referring to our understanding of the

kinematical/dynamical character of inertial transformations from Section 2.1, we can immediately conclude that generators of space translations and rotations coincide with their noninteracting counterparts

$$\mathbf{P} = \mathbf{P}_0 \tag{32}$$

$$\mathbf{J} = \mathbf{J}_0, \tag{33}$$

while the generator of time translations contains a nontrivial interaction term V

$$H = H_0 + V \tag{34}$$

(see Table 1). It is important to note that the Hermitian projection T cannot commute with this interaction and with the total Hamiltonian H

$$[T, H] = [T, V] \neq 0. \tag{35}$$

Indeed, only in this case, the decay law is a nontrivial function of time

$$\Upsilon(0, 0) = \langle \Psi | T | \Psi \rangle = 1$$

$$e^{-(i/\hbar)Ht} | \Psi \rangle \notin \mathcal{H}_\alpha, \quad \text{if } t \neq 0 \tag{36}$$

$$\Upsilon(0, t > 0) = \left\langle \Psi \left| e^{(i/\hbar)Ht} T e^{-(i/\hbar)Ht} \right| \Psi \right\rangle < 1$$

as required for any unstable particle prepared at time $t = 0$.

A Poincaré-Wigner-Dirac relativistic quantum description of any isolated interacting system is constructed in a similar manner. In the Hilbert space $\mathcal{H}$ of the system one defines 10 Hermitian generators $\{ \mathbf{P}_0, \mathbf{J}_0, \mathbf{K}_0 + \mathbf{Z}, H_0 + V \}$ with commutators (12)–(18). These operators not only specify the basic total observables of the system, but also determine how the results of observations transform from one inertial system to another. Moreover, one can switch to the classical relativistic description by taking the limit $\hbar \rightarrow 0$ and considering only states describable by localized quasiclassical wave packets, which can be approximated by points in the phase space. In this limit, observables are replaced by real functions on the phase space, quantum commutators are represented by Poisson brackets, and time evolution is approximated by trajectories in the phase space [27, 28].

3. Results and Discussion

3.1. Kinematical Boosts. As we mentioned at the end of Section 2.2, Einstein's special relativity assumes that boost transformations can be represented by exact Lorentz formulas (10), which are valid universally for all events and physical systems, independent on their state, composition, and involved interactions. In other words, in special relativity boosts are kinematical.

In classical relativistic physics, this hypothesis is known as the condition of "invariant trajectories" or "manifest covariance." The well-known Currie-Jordan-Sudarshan theorem [29] states that this condition is not compatible with

the Hamiltonian description of dynamics presented in the previous section. In other words, a Poincaré-invariant theory with invariant trajectories can exist only in the absence of interactions. This explains the name "no-interaction theorem" often used for the Currie-Jordan-Sudarshan result. Several options were tried in the literature for explaining this paradox.

One idea was that Hamiltonian dynamics is not suitable for describing relativistic interactions. Instead, various non-Hamiltonian theories were developed [30–35], which deviated from the Poincaré-invariant Wigner-Dirac approach. So far, the predictive power of these theories remains rather limited.

Another idea is to abandon particles and replace them by (quantum) fields [36–39], because *"there are no particles, there are only fields"* [40]. This approach goes as far as claiming that there is no point in discussing observables (positions and momenta) of interacting particles, their wave functions, and also their time evolutions in the interacting regime.

> *The foregoing discussion suggests that the theory will not consider the time dependence of particle interaction processes. It will show that in these processes there are no characteristics precisely definable (even within the usual limitations of quantum mechanics); the description of such a process as occurring in the course of time is therefore just as unreal as the classical paths are in non-relativistic quantum mechanics. The only observable quantities are the properties (momenta, polarizations) of free particles: the initial particles which come into interaction, and the final particles which result from the process (L. D. Landau and R. E. Peierls, 1930). Berestetskii et al. [41]*

> *The more one thinks about this situation, the more one is led to the conclusion that one should not insist on a detailed description of the system in time. From the physical point of view, this is not so surprising, because in contrast to non-relativistic quantum mechanics, the time behavior of a relativistic system with creation and annihilation of particles is unobservable. Essentially only scattering experiments are possible, therefore we retreat to scattering theory. One learns modesty in field theory. Scharf [42]*

We cannot accept this point of view, because it has nothing to say about such interacting time-dependent system as the unstable particle.

3.2. Dynamical Boosts. Our preferred way to resolve the Currie-Jordan-Sudarshan controversy is to abandon the hypothesis of "invariant trajectories" and admit that boost transformations are dynamical. Actually, even in the original Dirac's paper [25], it was mentioned that, in a theory with kinematical space translations (32) and rotations (33), boosts

must depend on interactions. Indeed, if we assume that boosts are kinematical ($\mathbf{Z} = 0$), then we obtain from (17)

$$H = \frac{ic^2}{\hbar} [K_x, P_x] = \frac{ic^2}{\hbar} [(K_0)_x, (P_0)_x] = H_0 \qquad (37)$$

the absurd proposition that interaction in the Hamiltonian must vanish ($V \equiv H - H_0 = 0$).

Therefore, we should have $V \neq 0$, $\mathbf{Z} \neq 0$, which means that we are working in the *instant form* of dynamics, according to Dirac's classification [25].

3.3. Decays Caused by Boosts. Our conclusion about the dynamical character of boosts disagrees with the usual special-relativistic "geometrical" view on boosts. In particular, we can no longer claim that

> *Any event that is "seen" in one inertial system is "seen" in all others. For example if observer in one system "sees" an explosion on a rocket then so do all other observers. Polishchuk [21]*

Returning to our example of unstable particle, we can say that when the observer at rest sees the pure unstable particle α, moving observers may see also its decay products $\beta+\gamma$ with some probability. We can prove an even stronger statement: if all (both resting and moving with different rapidities θ) observers see the particle α at $t = 0$ with 100% probability

$$\Upsilon(\theta, 0) = 1 \qquad (38)$$

then this particle is stable with respect to time translations as well.

Suppose that (38) is true; that is, for any $|\Psi\rangle \in \mathscr{H}_\alpha$,

$$\Upsilon(\theta, 0) \equiv \left\langle \Psi \left| e^{-(ic/\hbar)K_x\theta} T e^{(ic/\hbar)K_x\theta} \right| \Psi \right\rangle = 1. \qquad (39)$$

This means that all boosts leave the subspace $\mathscr{H}_\alpha$ invariant

$$e^{(ic/\hbar)K_x\theta} |\Psi\rangle \in \mathscr{H}_\alpha, \quad \forall \theta \qquad (40)$$

and that the interacting boost operator K_x commutes with the projection T. Then commutators (17) and (31) and the Jacobi identity imply

$$[T, H] = -\frac{ic^2}{\hbar} [T, [K_x, P_{0x}]]$$

$$= \frac{ic^2}{\hbar} [K_x, [P_{0x}, T]] + \frac{ic^2}{\hbar} [P_{0x}, [T, K_x]] = 0 \qquad (41)$$

which contradicts the fundamental property (35) of unstable particles. To resolve this contradiction, we have to admit that the boosted state $e^{(ic/\hbar)K_x\theta}|\Psi\rangle$ does not correspond to the particle α with 100% probability. This state must contain an admixture of decay products even at the initial time $t = 0$

$$e^{(ic/\hbar)K_x\theta} |\Psi\rangle \notin \mathscr{H}_\alpha, \quad \text{if } \theta \neq 0. \qquad (42)$$

This means that, from the point of view of the moving observer, the state vector's projection on the subspace of decay products is nonzero

$$
\begin{aligned}
0 &< \left\| (1 - T) \, e^{(ic/\hbar)K_x\theta} \, |\Psi\rangle \right\|^2 \\
&= \left\langle \Psi \left| e^{-(ic/\hbar)K_x\theta} \, (1 - T) \, (1 - T) \, e^{(ic/\hbar)K_x\theta} \right| \Psi \right\rangle \\
&= \left\langle \Psi \left| e^{-(ic/\hbar)K_x\theta} \, (1 - T) \, e^{(ic/\hbar)K_x\theta} \right| \Psi \right\rangle \\
&= 1 - \left\langle \Psi \left| e^{-(ic/\hbar)K_x\theta} T e^{(ic/\hbar)K_x\theta} \right| \Psi \right\rangle
\end{aligned}
\tag{43}
$$

and that the nondecay probability is less than unity

$$
\Upsilon(\theta, 0) = \left\langle \Psi \left| e^{-(ic/\hbar)K_x\theta} T e^{(ic/\hbar)K_x\theta} \right| \Psi \right\rangle < 1. \tag{44}
$$

This is the "decay caused by boost" [11, 12, 43], which means, among other things, that special-relativistic formulas (1) and (38) are inaccurate, and that boosts have a nontrivial effect on the internal state of the unstable particle.

It is important that (44) describes decays viewed from a moving reference frame, that is, by a moving detector. This is completely different from the more familiar experimental setup in which a stationary detector looks at a moving particle. In the latter case, the state vector of the moving unstable particle lies entirely in the subspace $\mathscr{H}_\alpha$, and there is no "decay caused by boost."

3.4. Discussion. Here we discussed the dynamical effect of boosts on unstable particles (44). However, similar nontraditional effects should be visible also in other interacting systems, even in classical (nonquantum) ones [44–46]. In order to verify these predictions, one has to look at composite interacting systems, where interaction acts for a sufficiently long time. Unfortunately, most experimental checks of special relativity [47–49] do not satisfy these criteria. For example, dynamical boosts do not change the relativistic kinematics (the relationships between momenta, velocities, and energies of free particles) in collisions, reactions, and decays. Likewise, dynamical boosts do not affect Doppler type experiments [50, 51], which measure the frequency (energy) of light and its dependence on the motion of the source or the observer. Michelson-Morley type experiments [52–54], studying the invariance of the speed of light, are not affected as well.

The time dilation experiments with unstable particles [1–4] are exceptional, because they study systems that are under the action of interaction during sufficiently long time interval. Unfortunately, predicted deviations from the special-relativistic time dilation formula (1) are too small to be observed. One can see that the "decay caused by boost" effect is also very small and beyond the sensitivity of modern experiments [12].

Perhaps, the most convincing evidence for the dynamical character of boosts was obtained in the Frascati experiment [55–57], which established the superluminal dynamics of the electric field of relativistic charges. This observation was explained from the point of view of the Poincaré-Wigner-Dirac theory in [27, 58, 59].

4. Conclusions

We applied Poincaré-Wigner-Dirac theory of relativistic interactions to unstable particles. In particular, we were interested in how the same particle is seen by different moving observers. We proved that the decay probability cannot be invariant with respect to boosts. Different moving observers may see different internal compositions of the same particle. In spite of being very small, this effect is fundamentally important as it sets the limit of applicability for special relativity.

Conflicts of Interest

The author declares no conflicts of interest.

References

[1] B. Rossi and D. B. Hall, "Variation of the rate of decay of mesotrons with momentum," *Physical Review A: Atomic, Molecular and Optical Physics*, vol. 59, no. 3, pp. 223–228, 1941.

[2] D. H. Frisch and J. H. Smith, "Measurement of the relativistic time dilation using μ-mesons," *American Journal of Physics*, vol. 31, no. 5, article 342, 1963.

[3] D. S. Ayres, A. M. Cormack, A. J. Greenberg et al., "Measurements of the lifetimes of positive and negative pions," *Physical Review D: Particles, Fields, Gravitation, and Cosmology*, vol. 3, article 1051, 1971.

[4] C. E. Roos, J. Marraffino, S. Reucroft et al., "$\sigma^\pm$ lifetimes and longitudinal acceleration," *Nature*, vol. 286, pp. 244-245, 1980.

[5] J. Bailey, K. Borer, F. Combley et al., "Measurements of relativistic time dilatation for positive and negative muons in a circular orbit," *Nature*, vol. 268, pp. 301–305, 1977.

[6] F. J. M. Farley, "The CERN (g-2) measurements," *Zeitschrift für Physik C Particles and Fields*, vol. 56, supplement 1, pp. S88–S96, 1992.

[7] L. A. Khalfin, *Quantum Theory of Unstable Particles and Relativity*, 1997, preprint of Steklov Mathematical Institute, St. Petersburg Department, PDMI-6/1997, http://www.pdmi.ras.ru/preprint/1997/97-06.html.

[8] K. Urbanowski, "The true face of quantum decay processes: unstable systems at rest and in motion," *Acta Physica Polonica B*, vol. 48, no. 10, article 1411, 2017.

[9] G. N. Fleming, "Observations on unstable quantons, hyperplane dependence and quantum fields," *Studies in History and Philosophy of Science. Part B. Studies in History and Philosophy of Modern Physics*, vol. 42, no. 2, pp. 136–147, 2011.

[10] M. Shirokov, "Decay law of moving unstable particle," *International Journal of Theoretical Physics*, vol. 43, no. 6, pp. 1541–1553, 2004.

[11] E. V. Stefanovich, "Quantum effects in relativistic decays," *International Journal of Theoretical Physics*, vol. 35, no. 12, pp. 2539–2554, 1996.

[12] E. V. Stefanovich, "Violations of Einstein's time dilation formula in particle decays," 2006, https://arxiv.org/abs/physics/0603043.

[13] P. Exner, "Representations of the Poincaré group associated with unstable particles," *Physical Review D: Particles, Fields, Gravitation and Cosmology*, vol. 28, no. 10, pp. 2621–2627, 1983.

[14] S. A. Alavi and C. Giunti, "Which is the quantum decay law of relativistic particles?" *Europhysics Letters*, vol. 109, no. 6, article 60001, 2015.

[15] E. V. Stefanovich, "Is Minkowski space-time compatible with quantum mechanics?" *Foundations of Physics. An International Journal Devoted to the Conceptual Bases and Fundamental Theories of Modern Physics*, vol. 32, no. 5, pp. 673–703, 2002.

[16] A. R. Lee and T. M. Kalotas, "Lorentz transformations from the first postulate," *American Journal of Physics*, vol. 43, no. 5, article 434, 1975.

[17] J.-M. Lévy-Leblond, "One more derivation of the Lorentz transformation," *American Journal of Physics*, vol. 44, no. 3, pp. 271–277, 1976.

[18] D. A. Sardelis, "Unified derivation of the Galileo and the Lorentz transformations," *European Journal of Physics*, vol. 3, no. 2, article 96, 1982.

[19] H. M. Schwartz, "Deduction of the general Lorentz transformations from a set of necessary assumptions," *American Journal of Physics*, vol. 52, no. 4, article 346, 1984.

[20] J. H. Field, "A new kinematical derivation of the Lorentz transformation and the particle description of light," *Helvetica Physica Acta*, vol. 70, pp. 542–564, 1997, https://arxiv.org/abs/physics/0410262.

[21] R. Polishchuk, "Derivation of the Lorentz transformations," 2001, https://arxiv.org/abs/physics/0110076.

[22] A. Galiautdinov, "Derivation of the Lorentz transformation without the use of Einstein's second postulate," 2017, https://arxiv.org/abs/1701.00270.

[23] E. P. Wigner, *Group Theory and its Application to the Quantum Mechanics of Atomic Spectra*, Academic Press, New York, NY, USA, 1959.

[24] E. Wigner, "On unitary representations of the inhomogeneous Lorentz group," *Annals of Mathematics*, vol. 40, no. 1, pp. 149–204, 1939.

[25] P. A. M. Dirac, "Forms of relativistic dynamics," *Reviews of Modern Physics*, vol. 21, article 392, 1949.

[26] S. Weinberg, *The Quantum Theory of Fields*, vol. 1, Cambridge University Press, Cambridge, UK, 1995.

[27] E. V. Stefanovich, "Relativistic quantum dynamics: a non-traditional perspective on space, time, particles, fields, and action-at-a-distance," 2005, https://arxiv.org/abs/physics/0504062.

[28] E. Stefanovich, *Relativistic Quantum Theory of Particles*, vol. I, Lambert Academic Publishing, Saarbrücken, Germany, 2015.

[29] D. G. Currie, T. F. Jordan, and E. C. Sudarshan, "Relativistic invariance and Hamiltonian theories of interacting particles," *Reviews of Modern Physics*, vol. 35, pp. 350–375, 1963.

[30] H. Van Dam and E. P. Wigner, "Classical relativistic mechanics of interacting point particles," *Physical Review A: Atomic, Molecular and Optical Physics*, vol. 138, no. 6B, pp. B1576–B1582, 1965.

[31] H. Van Dam and E. P. Wigner, "Instantaneous and asymptotic conservation laws for classical relativistic mechanics of interacting point particles," *Physical Review A: Atomic, Molecular and Optical Physics*, vol. 142, no. 4, pp. 838–843, 1966.

[32] E. C. G. Sudarshan and N. Mukunda, "Forms of relativistic dynamics with world line condition and separability," *Foundations of Physics*, vol. 13, no. 3, pp. 385–393, 1983.

[33] W. N. Polyzou, "Manifestly covariant, Poincaré-invariant quantum theories of directly interacting particles," *Physical Review D: Particles, Fields, Gravitation and Cosmology*, vol. 32, no. 4, pp. 995–1003, 1985.

[34] B. D. Keister, "Forms of relativistic dynamics: what are the possibilities?" *AIP Conference Proceedings*, vol. 334, no. 1, article 164, 1995.

[35] S. N. Sokolov, "Mechanics with Retarded Interactions," 1997, preprint IHEP Protvino, IHEP 97-84, http://web.ihep.su/library/pubs/prep1997/ps/97-84.pdf.

[36] D. B. Malament, "In defense of dogma: why there cannot be a relativistic quantum mechanics of (localizable) particles," in *Perspectives on Quantum Reality*, R. Clifton, Ed., Springer, Dordrecht, Netherlands, 1996.

[37] F. Wilczek, "Quantum field theory," *Reviews of Modern Physics*, vol. 71, no. 2, pp. S85–S95, 1999.

[38] H. Halvorson and R. Clifton, "No place for particles in relativistic quantum theories?" in *Ontological Aspects of Quantum Field Theory*, pp. 181–213, 2002.

[39] F. Strocchi, "Relativistic quantum mechanics and field theory," *Foundations of Physics*, vol. 34, no. 3, pp. 501–527, 2004.

[40] A. Hobson, "There are no particles, there are only fields," *American Journal of Physics*, vol. 81, no. 3, article 211, 2013.

[41] V. B. Berestetskii, E. M. Livshitz, and L. P. Pitaevskii, *Quantum Electrodynamics*, Elsevier, Oxford, UK, 1982.

[42] G. Scharf, *Finite Quantum Electrodynamics. The Causal Approach*, Texts and Monographs in Physics, Springer-Verlag, Berlin, Germany, 2nd edition, 1995.

[43] F. Giacosa, "Decay law and time dilation," *Acta Physica Polonica B*, vol. 47, no. 9, pp. 2135–2150, 2016.

[44] W. Glöckle and Y. Nogami, "Relativistic dynamics and Lorentz contraction," *Physical Review D: Particles, Fields, Gravitation and Cosmology*, vol. 35, no. 12, pp. 3840–3846, 1987.

[45] B. Hamme and W. Glöckle, "Relativistic two-body bound state in motion," *Few-Body Systems*, vol. 13, no. 1, pp. 1–10, 1992.

[46] B. T. Shields, M. C. Morris, M. R. Ware, Q. Su, E. V. Stefanovich, and R. Grobe, "Time dilation in relativistic two-particle interactions," *Physical Review A: Atomic, Molecular and Optical Physics*, vol. 82, no. 5, Article ID 052116, 2010.

[47] D. Newman, G. W. Ford, A. Rich, and E. Sweetman, "Precision experimental verification of special relativity," *Physical Review Letters*, vol. 40, no. 21, pp. 1355–1358, 1978.

[48] D. W. MacArthur, "Special relativity: understanding experimental tests and formulations," *Physical Review A: Atomic, Molecular, and Optical Physics and Quantum Information*, vol. 33, no. 1, 1986.

[49] C. M. Will, "Special relativity: a centenary perspective," in *Einstein, 1905–2005*, T. Damour, O. Darrigol, B. Duplantier, and V. Rivasseau, Eds., vol. 47 of *Progress in Mathematical Physics*, Birkhäuser, Basel, Switzerland, 2005.

[50] M. Kaivola, O. Poulsen, E. Riis, and S. A. Lee, "Measurement of the relativistic doppler shift in Neon," *Physical Review Letters*, vol. 54, no. 4, pp. 255–258, 1985.

[51] D. Hasselkamp, E. Mondry, and A. Scharmann, "Direct observation of the transversal Doppler-shift," *Zeitschrift füur Physik A Atoms and Nuclei*, vol. 289, no. 2, pp. 151–155, 1979.

[52] H. Müller, C. Braxmaier, S. Herrmann, A. Peters, and C. Lämmerzahl, "Electromagnetic cavities and Lorentz invariance violation," *Physical Review D: Particles, Fields, Gravitation and Cosmology*, vol. 67, no. 5, Article ID 056006, 2003.

[53] P. Wolf, S. Bize, A. Clairon, A. N. Luiten, G. Santarelli, and M. E. Tobar, "Tests of Lorentz invariance using a microwave resonator," *Physical Review Letters*, vol. 90, no. 6, Article ID 060402, 2003.

[54] T. Alväger, F. J. M. Farley, J. Kjellman, and L. Wallin, "Test of the second postulate of special relativity in the GeV region," *Physics Letters*, vol. 12, no. 3, pp. 260–262, 1964.

[55] R. de Sangro, G. Finocchiaro, P. Patteri, M. Piccolo, and G. Pizzella, "Measuring propagation speed of Coulomb fields," *The European Physical Journal C*, vol. 75, no. 3, 2015.

[56] R. de Sangro, G. Finocchiaro, P. Patteri, M. Piccolo, and G. Pizzella, "Why the interpretation of "Measuring propagation speed of Coulomb fields" stands," *The European Physical Journal C*, vol. 77, no. 2, 2017.

[57] R. de Sangro, G. Finocchiaro, P. Patteri, M. Piccolo, and G. Pizzella, "Experimental result on the propagation of Coulomb fields," *Journal of Physics: Conference Series*, vol. 845, Article ID 012015, 2017.

[58] E. Stefanovich, *Relativistic Quantum Theory of Particles*, vol. II, Lambert Academic Publishing, Saarbrücken, Germany, 2015.

[59] E. V. Stefanovich, "Does Pizzella's experiment violate causality?" *Journal of Physics: Conference Series*, vol. 845, Article ID 012016, 2017.